Exploring the phases of 2+1 dimensional gauge theories through bosonization, holography & more

Andrew Baumgartner

A dissertation
submitted in partial fulfillment of the
requirements for the degree of

Doctor of Philosophy

University of Washington

2020

Reading Committee:

Andreas Karch, Chair

Laurence Yaffe

Stephen Sharpe

Jason Detwiler

Program Authorized to Offer Degree:
Physics

University of Washington

Abstract

Exploring the phases of 2+1 dimensional gauge theories through bosonization, holography & more

Andrew Baumgartner

Chair of the Supervisory Committee:
Professor Andreas Karch
Department of Physics

The dynamics of 2+1 dimensional gauge theories offer insight into the exciting interplay between topology and physics. With the addition of Chern-Simons terms to the action, one can engineer conformal field theories which are related by a myriad of dualities. Understanding these dualities offers insight into the phases and behavior of these theories, and allows one to explore the phase diagram from many different points of view. In this thesis, we will use these dualities to i) amass evidence for their validity, ii) derive new dualities for exotic gauge theories, and iii) explore the symmetry breaking patterns of QCD_3 with product flavor groups.

TABLE OF CONTENTS

Page

List of Figures iii

Chapter 1: Introduction and Review 1
1.1 Chern-Simons Theory–Where Physics Becomes Topological 6
1.2 Dualities: Things Are Not Always What They Seem 14
1.3 Symmetry Breaking in 2+1 Dimensions 26

Chapter 2: Dualities at the Boundary 30
2.1 Review of Abelian dualities 31
2.2 Theories on half-space 36
2.3 Dualities including boundaries 45
2.4 Lattice construction 58
2.5 Discussion 66

Chapter 3: Deriving New Dualities: Quiver Gauge Theories 68
3.1 Review of 3d Bosonization 71
3.2 Non-Abelian Linear Quiver Dualities 73
3.3 Theta Wall Dualities 95
3.4 Adding Flavors to Quivers 110
3.5 Orthogonal and Symplectic Gauge Groups 146
3.6 Discussion 150
3.7 Supplementary: Building Non-Abelian Linear Quivers 156
3.8 Supplementary: Background Terms and Flavor Violation 166
3.9 Supplementary: Quivers and Spin$_c$ 173

Chapter 4: Breaking the Flavor Symmetry 175
4.1 Constructing the Phase Diagram 176

4.2 Comments on Scalar Potentials 191
4.3 Taking the Large N Limit 194
4.4 Symmetry Breaking in QCD_3 and Vacuum Structure at Large N 196
4.5 Vacuum Structure With an Explicitly Broken Flavor Group 203
4.6 Scalar Potentials and Double Condensation 215
4.7 Numerical Evidence for the Phase Diagram 218
4.8 Discussion 219

Chapter 5: Conclusion 225

LIST OF FIGURES

Figure Number Page

1.1 Measurements of the Hall (curve with plateaus) and longitudinal (curve with intermittent peaks) resistances by von Klitzing, Dorda and Pepper [79] . . . 3

3.1 Parent Chern-Simons matter theory at the phase transition for the special case $n = 5$. 70

3.2 Derivation of the bosonic particle-vortex duality as a duality between two node linear quiver theories. On the left-hand side, we have represented each side of Aharony's Abelian dualities as a two-node quiver. The filled yellow circle represents the color gauge group while the empty circle represents promoted global symmetries (which for the case of $SU(1)$ are placeholders). The equation numbers corresponding to the two-node quivers are shown in red. Since the two fermionic theories are the same, one can perform a matching to arrive at a duality between three two-node quiver theories, the top and bottom of which are the XY and Abelian Higgs models, respectively. 74

3.3 Dualizing a linear quiver. Red nodes are SU gauge groups and black nodes are U groups. Black (red) links are bifundamental bosons (fermions). Applying Aharony's duality to the leftmost link turns the scalar into a fermion. Then, applying the master duality repeatedly moves said fermion across the quiver until it reaches the final link where Aharony's duality can again be used to turn the fermion into a boson. 81

3.4 Configuration of D6 branes. 108

3.5 Expected behavior of the vacuum energy as a function of θ in a large N gauge theory. Distinct branches are shown in different colors. 111

3.6 SU and U sides of the flavor-violated master duality for $N > N_s$. On the SU side, the critical lines in green are well-described by the corresponding SU theory. The critical lines in black are best described by the U duals. 118

3.7 SU and U sides of the flavor-violated master duality for $N = N_s$ and $|k| < N_f < N_*$. 123

3.8 Flavored quiver with fermions on the SU side and scalars on the U side. The red/black nodes correspond to U and SU gauge groups, respectively. The red and black links are fermions and scalars. The white nodes are background flavor symmetries. 130

3.9 Flavored quiver with fermions on the SU side and scalars on the U side. This is an alternate theory in the flavor extended case. Here we have introduced the notation $\ell_i \equiv F_i - k_i$. 136

3.10 Explanation of interaction and enhanced flavor symmetries which arise due to the flavor-violated master duality and its finite interaction terms. We are using green/blue arrows to denote the (unidirectional) interactions. The green arrows represent finite interactions between the flavor degrees of freedom and adjacent bifundamentals. The light blue arrows represent interactions between bifundamental scalars, which were also present in the pure YM case of [9]. We assume they take the very same form they did there. The right-hand side shows how one arrives at enhanced flavor symmetries on the adjacent node at each step of the duality. 143

3.11 How the matching occurs on a generic internal link, which for the purposes of concreteness we have labeled C' and C". 159

3.12 Example case of properly dualizing interaction terms. This is for the second node of the four node case considered in the main text in Sec. 3.2.2 and also pictures in Figure 3.3. 161

4.1 Symmetry breaking of QCD_3 according to [80] 176

4.2 Phases when $f + F < k$ 178

4.3 Phase diagram for flavor broken QCD_3 with $f, F < k$. The phases are described in Sec. 4.1.2. The stars denote the bosonic duals given in [80]. 181

4.4 Phase diagram for flavor broken QCD_3 with $f < k$, $F > k$. These phases are laid out in Sec. 4.1.2. 182

4.5 Phase diagram for flavor broken QCD_3 with $f, F > k$. These phases are laid out in Sec. 4.1.2. 184

4.6 Phase diagram for flavor broken QCD_3 with $f < k$, $F = k$. These phases are described in Sec. 4.1.2. 186

4.7 Phase diagram for flavor broken QCD_3 with $f = k$, $F > k$. These phases are laid out in Sec. 4.1.2. 187

4.8 Phase diagram for flavor broken QCD_3 with $f = k$, $F = k$. These pahses are described in Sec. 4.1.2. This symmetry breaking pattern was first conjectured by Vafa and Witten [110]. 189

4.9 Phases as a function of f and F. 192
4.10 Resolution of critical points into a series of first order phase transitions. The different colored regions represent distinct Grassmannians 196
4.11 Various phase diagrams for the scenarios discussed in sec. 4.4.1, where m is on the y axis and M is on the x-axis. 199
4.12 Leading (a) and subleading (b) diagrams in the large N limit. Blue represents arbitrary gluon loops and stars are insertions of $\mathcal{M}$. 202
4.13 Phase diagrams for QCD_3 with an explicitly broken flavor symmetry. The various TFTs shown are $SU(N)$ Chern-Simons gauge theory with level $k + \frac{1}{2}(\text{sgn}(m)f + \text{sgn}(M)(N_f - f))$. The shaded regions represent the Grassmannians as explained in eq. (4.67) 213
4.14 Diagram associated to the $U(f)\times U(N_f - f)$ invariant term discussed in section 4.6 216
4.15 Phase diagram for $N_f = 6, f = 4$ with $k = 0$. Various effective potential at the indicated points along trajectories 1,2 and 3 shown are given in tables 4.1, 4.2 and 4.3. 220

ACKNOWLEDGMENTS

The author wishes to express sincere appreciation to my advisor Andreas Karch for never giving up on me and answering all my dumb questions and to my collaborators/friends Kyle Aitken, Brandon Robinson and Changha Choi for engaging in these interesting topics with me.

DEDICATION

To Karolyn and Peter

I can still taste the Wine Sap
sitting halfway up the hill.
Do the ebbs and flows still
smell as sweet as they once did?
Or do the breaths of time need one last refill?

I can still see the Apple Trees and
the Apple Woods from whence they came.
Greens and yellows and reds and browns,
this "house of God" is not yet different
but somehow not the same.

I can still smell the Pound Sweet
adjoined to the Walnut Hill.
A climb, descent, and climb again, and again
until at the top, formless and familiar,
enters a mother's beckoning will.

I can still hear the Rockwell and
the clang of wood being freshly chopped.
Yet as the smoke that fills the room wains,
our lives, be they here or there, stop.

I am home.

Chapter 1

INTRODUCTION AND REVIEW

Quantum field theory is a strange beast. On one hand it offers a relatively simple, elegant framework by which one can understand the most fundamental aspects of the universe. This relative simplicity, however, gets drowned out by difficult-to-calculate path integrals, subtle issues of renormalization and anomalies, nonperturbative solutions and other interesting topics. Still, the basic tenets of the path integral are straightforward to understand – integrate over all possible field configurations weighted by an integral measure which favors classical solutions (and small perturbations around such solutions). Thus it is no surprise that there has been much effort in finding physical systems which become analytically tractable that mimic aspects of our messy, 3+1 dimensional world. There are many ways this can be done, of course, but one method that has proved fruitful, especially in the context of strongly coupled and nonperturbative physics, has been studying theories in different dimensions. Understanding how the dimensionality effects the physics gives a unique type of insight and intuition about our own universe.

One good example of this comes from the Schwinger model [100]. This 1+1 dimensional model is (almost[1]) the simplest gauge theory one can write down: an Abelian gauge theory coupled to fermions. Surprisingly this solvable model shares two important characteristics with 3+1 dimensional quantum chromodynamics – it is confining and anomalous. To see the former one must only note that the Coloumb interaction between charged particles is linear in their separation, a hallmark feature of confinement in 3+1D QCD. To see the latter one must do more work, but indeed this simple gauge theory has a chiral anomaly, again like QCD. One can then study this simplified, Abelian model to gain more understanding and

[1]It is the author's belief that scalars are easier to deal with than fermions.

intuition for the more difficult and interesting non-Abelian case.

Still, the linear nature of the Coulomb force in 1+1 d does not entirely capture the effects of confinement. A slightly better model comes instead from Polyakov [97]. Polyakov's model slightly improves upon Schwinger's by studying a non-Abelian theory, specifically an $SU(2)$ theory, in 2+1D coupled to a real scalar field. The fact that this theory is defined in 2+1D allows the photon to be rewritten in a dual representation as a compact, real scalar. One can then compute the instanton contribution to the effective potential and find that the theory is confining. It is important to note that this is possible precisely because of the dimensionality – the photon can be dualized into a scalar.

Aside from providing toy models for difficult concepts in higher dimensions, low dimensional physics has its own physical significance, specifically in the realm of condensed matter physics. As experimental techniques grow more and more sophisticated, exotic 2+1 dimensional systems can be engineered and studied to their full extent. Oftentimes, the strongly coupled nature of these theories leads to strange collective behaviors and degrees of freedom which can be modeled by gauge theories. And while it is true that a vast majority of these gauge theories are Abelian, it is not out of the realm of possibility to create a system in which these emergent gauge fields are non-Abelian. Thus the study of 2+1D non-Abelian gauge theories, in addition to being theoretically very interesting, could potentially help uncover some yet-to-be-discovered exotic materials.

The canonical manifestations of 2+1D gauge theories in real life are the integer and fractional quantum Hall effect. The classical Hall effect refers the phenomenon in which a 2+1 dimensional sample of electrons is immersed in a transverse magnetic field with an externally applied voltage. When the electrons in the sample move with the external electric field, their trajectories bend, giving rise to a transverse current. This current is characterized, through Ohm's law, by a resistance known as the Hall resistance. This resistivity, in the classical regime, increases linearly with the strength of the magnetic field.

In the 1980's von Klitzing, Dorda and Pepper [79] set out to measure this Hall resistance in the quantum regime using an ultra-pure 2d electron gas from the inversion layer of a

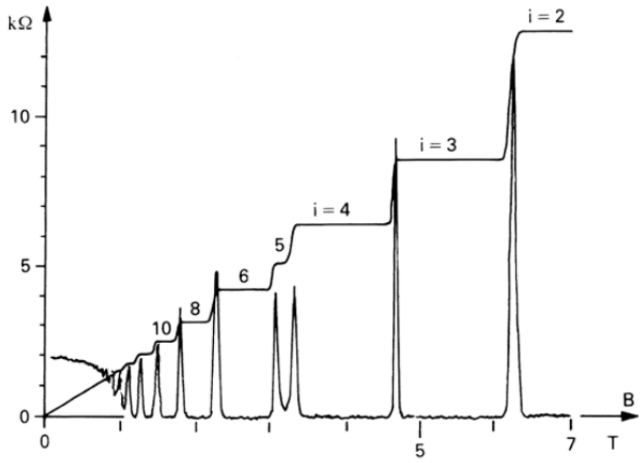

Figure 1.1: Measurements of the Hall (curve with plateaus) and longitudinal (curve with intermittent peaks) resistances by von Klitzing, Dorda and Pepper [79]

metal-oxide-semiconductor field-effect transistor. They found that, contrary to the classical picture, the Hall resistance is quantized, jumping to different discrete values[2] at special values of the magnetic field strength. Additionally, the longitudinal resistance drops to zero, becoming nonzero only when the Hall resistance jumps (see fig 1.1). This peculiar quantized hall resistance is not the only hallmark of quantum Hall states. Additionally, these transport properties are both chiral[3] and confined to the edge of the sample. These "chiral edge modes" have since been realized as the signature of a new phase of matter – topological phases of matter – which has spawned a whole new direction in condensed matter research.

The peculiar properties of quantum Hall states mentioned above can be derived from the microscopic physics in the usual manner: placing many electrons in a magnetic field, guessing a many body wave function for the low energy physics, deriving transport properties via Kubo formula etc... This approach, however, can be quite painful. Indeed, anyone familiar with

[2]In appropriate units

[3]Charge only flows in one direction.

quantum mechanics knows that dealing with many body quantum states quickly devolves into chaos[4]. Fortunately there is another way to study the low energy physics of the quantum Hall states without mention of electrons in strong magnetic fields and annoying many body wave functions. One can instead construct an *effective field theory* to study these properties. An effective field theory is a quantum field theory which is meant to capture the low energy/macroscopic physics of complicated physical systems. While the microscopic physics may involve complicated interactions between many particles, the macroscopic physics simplifies dramatically. As one probes the physics at lower and lower energies, the high energy degrees of freedom – be they massive particles, vorticies, what have you – decouple, and one is left with gapless[5] (or nearly gapless) degrees of freedom. To construct such a macroscopic theory one must write down all the terms in the Lagrangian which are consistent with the symmetries of the system, which scale in the appropriate way with the energy, and capture the physics at the scale which you are interested in. This translates to writing down all symmetric[6], relevant operators with the fewest number of derivatives.

The effective field theory which describes the quantum Hall effect is known as an Abelian Chern-Simons gauge theory (see [44] for a comprehensive review) . We will discuss this gauge theory in (mostly) all of its gory detail in the following subsection, but we wish only to make a few comments about it here. First of all, it is a topological field theory. That means its action is a topological invariant of the manifold on which it is defined and so the degrees of freedom are non-local and non-propagating, just like the ground state in the bulk of a quantum Hall system. Second of all it is anomalous. Specifically it has a chiral anomaly. This means that the theory is not well defined when placed on a manifold with boundaries unless there are extra, chiral degrees of freedom at the boundary. This gives rise to the edge states of the quantum Hall effect. Third of all, the coefficient in front of the action is quantized to preserve gauge invariance. This coefficient enters into electronic transport

[4]Sometimes literally!

[5]By gapless we mean there exists energy differences between the ground state and the first excited state

[6]Symmetric with respect to whatever global and gauge symmetries are present.

calculations as a part of the Hall resistance, thus giving rise to the quantized Hall coefficient. Thus, all the important properties of quantum Hall states can effectively be captured by this simple topological field theory.

The Abelian Chern-Simons theory is not the end of the story. Indeed one can complicate matters by studying non-Abelian Chern-Simons theories, or coupling the gauge field to gapless matter. There are many variants which can be studied which lead to interesting physics. In this thesis, we study a subset of these variants, primarily non-Abelian Chern-Simons theories coupled to gapless fermionic and scalar matter. These theories are subject to dualities–known as bosonization–which relate seemingly disparate theories to each other at some energy scale. The dualities, along with other properties which we will review below, allow for a rich phase structure that can be explored through a number of lenses.

First, we will explore the nature of these dualities when placed on a manifold with boundaries. As mentioned above, a pure Chern-Simons theory admits gapless, chiral edge modes. When coupled to gapless matter, the theory on a boundary will have boundary conditions for the matter as well as the edge modes. How must the boundary conditions of the matter be related to the Chern-Simons edge modes? Additionally, how do these edge modes map under the aforementioned dualities? We will explore these questions in the context of Abelian bosonization dualities by carefully examining the role boundary conditions play in these Chern-Simons-Matter theories. The non-Abelian story has been worked out by collaborators of the author in [13], but since the author has only contributed to the Abelian story, the non Abelian analog will not be included.

Next we derive dualities for a certain type of Chern-Simons matter theory known as a quiver gauge theory. This theory contains certain, exotic types of matter which can interact via two different types of forces. Using known bosonization and holographic dualities, one can derive a dual theory which, in certain parameter regimes, greatly simplifies. The phase structure of this theory is rich and requires special attention in parameter regimes where symmetry breaking can occur, and to the coefficients of certain background terms which are required to make the theory anomaly free. These dualities are then applied to 3+1

dimensional QCD where they represent the low energy effective theories living on domain walls when one continuously changes the θ-angle.

Finally, we end with an exploration of the phase diagram of 2+1 dimensional QCD – that is non-Abelian Chern-Simons theory coupled to light, fermionic matter – as a function of two distinct mass deformations. This phase diagram is required for a full mapping of the phases of the aforementioned quiver gauge theory, but is also interesting in its own right. We find that the symmetry breaking scenarios which lead to mesonic and baryonic degrees of freedom heavily depend on the size of the groups of fermions involved relative to the Chern-Simons level, gauge group rank and other parameters of interest. We map out these scenarios and provide phase diagrams for a multitude of parameter regimes, both at finite and large N[7].

In the rest of this introduction we will review some of the necessary background for this thesis. First we will take a more extensive look at Chern-Simons gauge theory. This special type of gauge theory plays a pivotal role in the work presented here. Next we turn to the various dualities which will be employed throughout. This includes 2+1 bosonization dualities and holographic duality. Finally, we will review various aspects of spontaneous symmetry breaking in QCD. The most pertinent information will be reviewed again as needed throughout the bulk of the text. This introduction is only to provide a broad overview of the important concepts and tools used extensively throughout.

1.1 Chern-Simons Theory–Where Physics Becomes Topological

In 2+1 dimensions there is a special Lorentz invariant, single derivative action known as the Chern-Simons action. For an Abelian gauge theory, where the gauge potential A_μ is valued in $U(1)$ or some other compact Abelian group, the action is given by

$$S_{CS} = \frac{k}{4\pi} \int d^3x \epsilon^{\mu\nu\rho} A_\mu \partial_\nu A_\rho \tag{1.1}$$

[7]N here, and throughout, refers to the rank of the gauge group, i.e. $SU(N)$.

while for non-Abelian gauge theories the gauge field A_μ becomes an $N \times N$ Hermitian matrix valued in the Lie algebra associated to the gauge group, and the action becomes

$$S_{CS} = \frac{k}{4\pi} \int d^3x \epsilon^{\mu\nu\rho} \mathrm{Tr} \left(A_\mu \partial_\nu A_\rho - \frac{2i}{3} A_\mu A_\nu A_\rho \right). \tag{1.2}$$

The equations of motion derived from these actions require the field strength to vanish. In other words, the space of classical solutions to Chern-Simons gauge theory is flat connections. This might indicate that the theory is trivial, but as we will see this is not the case.

The coefficient k is known as the level of the Chern-Simons theory and is often times denoted as a subscript when specifying the gauge group i.e. $SU(N)_k$ or $U(1)_k$[8]. The actions presented in (1.1) and (1.2) are not, strictly speaking, gauge invariant, although they do lead to gauge invariant theories. This is not obvious since the action depends on the gauge field A_μ and not the gauge-invariant field strength $F_{\mu\nu}$. To see this, let us perform a gauge transformation by some element of the gauge group $U(x)$:

$$A_\mu \to U A_\mu U^\dagger + \frac{i}{g} U \partial_\mu U^\dagger. \tag{1.3}$$

Under this transformation, the action becomes (up to a total derivative)

$$S_{CS} \to S_{CS} + \frac{k}{12\pi} \int d^3x \epsilon^{\mu\nu\rho} \mathrm{Tr} \left(U \partial_\mu U^\dagger \, U \partial_\nu U^\dagger \, U \partial_\rho U^\dagger \right). \tag{1.4}$$

This new term has a nice topological meaning. It is simply 2π times the winding number of the gauge transformation! To understand this better, consider Wick rotating to Euclidean space so our spacetime manifold becomes 3d Euclidean space. In doing so we must specify boundary conditions on our gauge field at spatial infinity. To skirt this slight complication, we could instead consider a compactification of Euclidean space and regard our spacetime as S^3. In doing so, we find that U is a map from our spacetime S^3 into our gauge group. Since the gauge groups we will be doing this are sem-simple Lie groups, they com equipped with a manifold structure as well as a group structure. These manifolds can have non-trivial

[8]Here, we will only be concerned with unitary gauge groups, although there is some discussion on generalizations to orthogonal and symplectic groups in chapter 3.

S^3 submanifolds around which the spatial S^3 can wind. From the group perspective, these S^3 submanifolds are $SU(2)$ subgroups of the gauge group. The winding number tells us how many times our spacetime S^3 wraps around some $S^3 \simeq SU(2)$ subgroup of our gauge group So under this type of gauge transformation, the action changes as

$$S_{CS} \to S_{CS} + 2\pi kn$$

where

$$n = \frac{1}{24\pi^2} \int d^3x \epsilon^{\mu\nu\rho} \mathrm{Tr} \left(U\partial_\mu U^\dagger \, U\partial_\nu U^\dagger \, U\partial_\rho U^\dagger \right) \in \mathbb{Z}. \tag{1.5}$$

Still, this does not look gauge invariant! But we are saved by the fact that it is only $e^{iS_{CS}}$ which must remain single valued under a gauge transformation, since it is in this form that the action enters the path integral measure. For this to be the case, we must take $k \in \mathbb{Z}$. Thus, the Chern-Simons action leads to a physical theory which is perfectly gauge invariant so long as k is an integer. In addition, the Chern-Simons action also breaks both time reversal and parity. In 2+1 dimensions these act as

$$\mathcal{P} : x_0 \to x_0, \ x_1 \to -x_1, \ x_2 \to x_2 \quad A_0 \to A_0, \ A_1 \to -A_1, \ A_2 \to A_2 \tag{1.6}$$

$$\mathcal{T} : x_0 \to -x_0, \ x_1 \to x_1, \ x_2 \to x_2 \quad A_0 \to -A_0, \ A_1 \to A_1, \ A_2 \to A_2. \tag{1.7}$$

This differs from how we think of parity in 3+1 dimensions, where the x_2 coordinate would also flip signs. This means that the Chern-Simons action can only arise in systems where parity and time reversal are broken such as electrons in a large magnetic field like in the quantum Hall effect.

At low energies the Chern-Simons action, when present, dominates the dynamics due to the single derivative. The reason for this is due to the inverse relationship of energy scales and length scales in relativistic physics: low energies correspond to large distances. Let L be the length scale at which we are probing out theory. A single derivative term in the action will be order $1/L$ while a two derivative term is on the order of $1/L^2$. As $L \to \infty$ the latter tends to zero more quickly than the former. As $L \to 0$ the opposite occurs.

This is not the only reason, however. Consider the Chern-Simons-Maxwell theory (or Chern-Simons-Yang-Mills if the gauge group is non-Abelian) defined by

$$S = -\frac{1}{4g^2}\int d^3x F_{\mu\nu}F^{\mu\nu} + \frac{k}{4\pi}\int d^3x \epsilon^{\mu\nu\rho}A_\mu \partial_\nu A_\rho. \tag{1.8}$$

The equations of motion for this action are

$$\partial_\mu F^{\mu\nu} + \frac{kg^2}{8\pi}\epsilon^{\nu\mu\rho}F_{\nu\rho} = 0 \tag{1.9}$$

which defines the propagation of a single massive degree of freedom with mass $m = kg^2/4\pi$. To see this, we define a new field related to the field strength by $\tilde{F}^\mu = \epsilon^{\mu\nu\rho}F_{\nu\rho}$. Then eq. (1.9) becomes the equation of motion for a massive pseudo-vector. Because of this Chern-Simons theory is sometimes called *topologically massive gauge theory*. When probing the theory at low energies, i.e. when going down the RG flow, the coupling constant tends to infinity, since the Maxwell term is an irrelevant operator, and the photon/gluon becomes infinitely massive. This suppresses the dynamics associated to the Maxwell term since $g^2 \to \infty$ implies $1/g^2 \to 0$. Thus, the low energy dynamics is completely determined by the Chern-Simons action.

A rather important aspect of Chern-Simons gauge theory is its topological nature. Simply stated this means that the partition function of a Chern-Simons gauge theory is a topological invariant for whatever 2+1D (or 3D if you are dealing with the Euclidean theory) manifold you are studying. This manifests itself in a myriad of ways, but the most obvious is the lack of dependence on the metric. When defining an action on a curved spacetime manifold, one must include a factor of $\sqrt{-|g|}$ in the integration measure and change the derivative to a covariant derivative. The Chern-Simons action, however, also contains a factor of the Levi-Civita tensor. When defined on a curved manifold, this tensor includes a factor of $1/\sqrt{-|g|}$ which cancels the analogous term in the integration measure. Additionally, due to the symmetric properties of the Christofell symbols hiding in the covariant derivative, the contraction with the antisymmetric Levi-Civita tensor gives zero. The resulting action doesn't depend on the metric and so small changes in the metric have no bearing on the

dynamics associated to the Chern-Simons term. This is one hallmark feature of topological field theories. This has important consequences, most notably that there is no stress-energy tensor associated to the Chern-Simons gauge theory, which in turn applies that there are no propagating local degrees of freedom. After all, how is one supposed to propagate when there are no generators of spacetime translation?

If there are no local degrees of freedom in Chern-Simons theory, then what are the degrees of freedom? To understand this, let us briefly discuss the canonical structure of the Abelian CS theory. Consider the structure of the CS action (1.1). The temporal component of the gauge field does not have a kinetic term, so the "coordinates" of our gauge theory are the spatial components of the gauge field A_1 and A_2. This means the space of classical solutions is the space of all A_1 and A_2 such that $F_{\mu\nu} = 0$. However, due to the Levi-Civita tensor, these "coordinates" are also canonically conjugate to each other! Thus, the space of classical solutions is also the phase space of the theory. We must therefore find a gauge invariant way to parameterize such a space, thereby giving us our gauge invariant degrees of freedom. But what are these objects? The answer, perhaps unsurprisingly, are non-local degrees of freedom known as Wilson loops i.e. holonomies of the gauge field along closed 1-cycles:

$$W_{\mathcal{C}} = \mathrm{Tr}_R \left(e^{i \oint_{\mathcal{C}} A_\mu dx^\mu} \right) \tag{1.10}$$

where $\mathcal{C}$ is a closed 1-cycle and the trace is taken in the representation R. These gauge invariant Wilson loops take on values in S^1 which is a compact manifold. This means that the phase space is compact and therefore the Hilbert space should be finite. When defined on a spacetime manifold of genus g, these loops can wrap the $2g$ nontrivial cycles leading to a degeneracy of ground states. Upon deriving the algebra of observables (a task we will not undertake in this brief introduction) ones finds that the lowest dimensional representation allowable is k^g. This shows that the ground state of Chern-Simons that has a degeneracy of k^g. This type of degeneracy is now known as topological order and plays a special role in modern condensed matter physics, especially in studies of topological phases of matter. Additionally, as discovered by Witten in the 80's [117], expectation values of Wilson loops

in Chern-Simons theory are interesting topological invariants related to knot invariants on three manifolds. These invariants offer a vast generalization of known knot invariants that have been studied by mathematicians, and contains detailed information about the linking and winding of the various knots considered.

Another important aspect of Chern-Simons theories we will review is the relation between Chern-Simons theories and fermions in 2+1D. Fermions in odd dimension are distinct from fermions in even dimension in the sense that there is i) no sense of chirality since the analog of the γ_5 matrix, which defines chirality in even dimensions, becomes part of the Clifford algebra and ii) mass terms break parity since fermions transform under parity as $\psi \to \gamma^1 \psi$ which implies $\bar{\psi}\psi \to -\bar{\psi}\psi$. Consider a fermion in 2+1D coupled to a background Abelian[9] gauge field:

$$S[A_\mu] = i \int d^3x \bar{\psi} \left(\not{\partial} + i \not{A} + m \right) \psi. \tag{1.11}$$

If we wish to study the dynamics at energies much below the mass of the fermion, we must first integrate out the fermion. Standard guidance from 3+1D quantum field theories would tell us that the massive fermion decouples from the low energy physics and should not effect the resulting theory. This, however, is not the case in 2+1D. The path integral of the fermion field contributes terms to the effective action which look like

$$S_{eff} = \log \det \left(\not{\partial} + i \not{A} + m \right) \tag{1.12}$$

If we expand this in powers of the gauge field, one finds that the first nontrivial contribution comes at quadratic order:

$$S_{eff} \sim \text{const} + \frac{1}{2} \text{Tr } \log \left(\frac{1}{\not{\partial} + i \not{A} + m} \not{A} \frac{1}{\not{\partial} + i \not{A} + m} \not{A} \right) + ... \tag{1.13}$$

To compute the trace, we pass to momentum space. The resulting integral is equivalent to performing a 1-loop fermion correction to the gauge field propagator. We will not perform this integral here, but when the dust settles one finds the contribution to the effective action

[9] an equivalent calculation is possible for non-Abelian gauge fields

is

$$S_{eff} = \frac{i}{4\pi}\frac{\text{sgn}(m)}{2}\int d^3x \epsilon^{\mu\nu\rho} A_\mu \partial_\nu A_\rho \tag{1.14}$$

which is nothing more than an Abelian Chern-Simons theory at level $\frac{\text{sgn}(m)}{2}$! Integrating out, say, N_f massive fermions would then contribute one such term per fermion, leading to, for example, a Chern-Simons theory at level $N_f\frac{\text{sgn}(m)}{2}$ if all the masses are the same sign. Thus, integrating out N_f such fermions, all with the positive mass deformations, serves to shift the level as:

$$k \to k + N_f\frac{\text{sgn}(m)}{2}.$$

This answer is 1-loop exact

So integrating out massive fermions in 2+1D in a background gauge field leads to Chern-Simons theories at level $\frac{\text{sgn}(m)}{2}$. Although the computation is 1-loop exact it is still a little bit problematic since, as discussed above, Chern-Simons theory is only gauge invariant when the level is an integer, not a half integer. How do we reconcile these facts? One may think that there are some higher order corrections when integrating out the fermion, but this is not the case. Instead, the answer lies in how we regularize the theory. Recall that, in general, quantum field theories often suffer from UV divergences. As such, we will need a gauge invariant way to deal with such divergences. In 2+1D, (arguably) the best way to go about this is include a Pauli-Villars regulator for the fermions. This regulator is a very massive boson which obeys the Dirac equation [122], so the calculation of the effective action will go through in exactly the same way as the above. Integrating out the Pauli-Villars regulator will also generate a Chern-Simons term at level $sgn(M)/2$, where M now refers to the mass of the regulator. It is conventional to give this Pauli-Villars mass a sign opposite to the current CS level, although either sign is appropriate so long as one is consistent.

This argument, although good enough for our purposes, is not the entire story. To gain a better understanding, one can phrase this issue of regulator contributions to the level in terms of anomalies. Simply stated, massless fermions in odd dimensions suffer from something known as the "parity anomaly", which implies that the theory cannot be quantized

in a parity-invariant way. This has many consequences, one of which being that it is only the magnitude of the parition function that is well defined. To get a feel for this consider a single, massless fermion in 2+1D. Formally, the partition function will be a determinant of the kinetic term:

$$Z_\psi = \det i\not{D} = \prod_{k\in\mathbb{N}} \lambda_k \tag{1.15}$$

where $i\not{D}\psi = \lambda_k\psi$. This quantity is real since $i\not{D}$ is Hermitian, but the sign is ill-defined. The sign will be determined by the relative number of positive and negative eigenvalues, and since $k \in \mathbb{N}$ there is no clear way to determine how many λ's are positive and how many are negative. In particular, it is possible to perform a gauge transformation that leaves the entire spectrum unchanged but changes the sign of a finite number of eigenvalues! This has the effect of changing the sign of the partition function [122]. One can account for this change of sign by including a parity violating, but still gauge invariant, regulator such as a Pauli-Villars regulator. If one includes this regulator, upon integrating it out one obtains the shifted Chern-Simons level as described above. But one can also treat this at the level of the eigenvalues as in eq. (1.15). Denoting the mass of this Pauli-Villars field to be $|M| \gg 0$, the regularized parition function becomes

$$Z_\psi = \prod_k \frac{\lambda_k}{\lambda_k + iM}. \tag{1.16}$$

For large M, we see that

$$Z_\psi = \prod_k \frac{\lambda_k}{\lambda_k + iM} \approx \prod_k (-i)\frac{\lambda_k}{M} = \prod_k (-i)\mathrm{sgn}(\lambda_k)\frac{|\lambda_k|}{|M|} = |Z_\psi|(-i)^{\#_{pos}-\#_{neg}} = |Z_\psi|e^{-i\frac{\pi}{2}\eta} \tag{1.17}$$

where $\eta = \sum_k sgn(\lambda_k)$ is known as the Atiyah-Padoti-Singer (APS) invariant, or eta-invariant. Changing the sign of the regulator's mass will simply take $\eta \to -\eta$, but give an equally acceptable regularization. When squared, the η invariant is equivalent to a Chern-Simons term, and so we often think of it as a half-integer level Chern-Simons term. Strictly speaking, such a half integer term is nonsensical due to it's lack of gauge invariance, but

viewing it as such leads to a nice physical interpretation of the offset as due to the integrating out of infinitely massive Pauli-Villars fields. Formally, this half-integer shift takes into account how the sign of the partition function changes when the signs of the eigenvalues change. See [101] for more details.

Chern-Simons theory underlies every aspect of the work done in this thesis. Here we have outlined just a few of the many interesting properties of such theories and yet already we see a rich interplay between physics and topology. This interplay will continue to give interesting phenomena as we couple such theories to different types of matter, exotic or not. The robustness of this interplay may also allow insight into the relationships between the different types of Chern-Simons theories. Exploring these relationships, using them to map out phase diagrams and derived new relationships, is the main subject of this work. Broadly, we refer to such relationships as dualities. We now turn to examine some of the various dualities that arise in this work and their relationship to Chern-Simons gauge theory.

1.2 Dualities: Things Are Not Always What They Seem

A large portion of this thesis is devoted to the study and use of *dualities*. A duality is an equivalence between two seemingly disparate physical theories, equipped with a duality dictionary for mapping observables between them. These maps are usually very difficult to construct, except in a select few cases [30]. Still, one can amass evidence of these dualities through phase matching, anomaly matching and, if you are lucky, explicit computation of partition functions. This work will primarily employ three such dualities: i) level/rank duality between pure Chern-Simons theories, ii) bosonization dualities between Chern-Simons-Matter theories and iii) holographic duality between quantum gravity and quantum field theory. Each of these dualities comes equipped with a range of validity. That is, there may be certain energy scales at which these dualities are valid. For example, the level/rank dualities and bosonization dualities are both defined in the infrared, i.e. at low energies. Holography, on the other hand, is valid at all energy scales. Understanding these regions of validity is an important part in understanding these dualities and how to use them. We will

begin our review of these dualities by first discussing these regimes of validity in the context of renormalization group flows.

Primer on Renormalization Group Flows

Interacting field theories[10], such as those considered in the bosonization dualities to be discussed below, come equipped with a variety of parameters which characterize the strength of interactions, as well as a cutoff scale Λ to regularize UV divergences. Since we will primarily be concerned with physics in the infrared, we will focus our attention to energy scales which are much below this cutoff scale. Equivalently, we can consider zooming out of our system to macroscopically large distances. Such a zooming out is equivalent to a rescaling of the cutoff $\Lambda \to \tilde{\Lambda}$ and then integrating out the modes between Λ and $\tilde{\Lambda}$ to bring the cutoff back to Λ. This process is know as "following the renormalization group (RG) flow" and is equivalent to rescaling the parameters of the theory in a well-defined way.

Following the RG flow from high energies to low energies is generally an intractable task. If the theory is weakly coupled, one can compute loop integrals to find the equations which govern how these parameters change. If the theory is strongly coupled you are likely out of luck. Luckily there is a small set of guiding principles from which some conclusions can be made. For instance, each term in the Lagrangian comes equipped with a "mass dimension" which tells us the first order approximation for how these parameters will flow. These are generally grouped into three categories: relevant, irrelevant and marginal. Classically this means that relevant parameters will grow as the energy is lowered, irrelevant parameters will decrease and marginal terms do neither. This classical dependence will be modified, possibly very dramatically, when one includes quantum corrections. Still, the classical dependence is a necessary first step to understanding how these theories will behave at low energies.

This RG flow is governed by a system of differential equations and can be thought of as a trajectory in parameter space. As the energy approaches zero, this trajectory must

[10] And also massive free theories.

end at some specific values which renders the theory scale-invariant. This can happen in a number of ways, such as gapping everything in sight and leaving behind a trivial theory. A more interesting scenario is when the trajectory tends to some non-trivial fixed-point of the RG equations. By non-trivial, we mean an interacting fixed point, otherwise we would be left with a free theory. Such non-trivial fixed points host non-trivial conformal field theories which describe quantum critical points.

When we say we have a duality between two theories in the IR what we really mean is that the two theories tend to the same RG fixed point in the IR. Deforming these theories away from the fixed points also leads to dual theories, so long as these deformations map to each other under the duality map. Matching these deformed phases is a crucial piece of evidence for the duality that we will use many times in the work below.

1.2.1 Level/Rank Duality

Before diving into the more complicated bosonization dualities which constitutes a majority of this work, we will review another important duality which will serve as benchmark by which the bosonization dualities can be checked. This is level/rank duality between pure Chern-Simons theories.

There are three such level rank dualities [58] :

$$SU(N)_k \leftrightarrow U(k)_{-N} \tag{1.18}$$

$$U(N)_{k,k\pm N} \leftrightarrow U(k)_{-N,-N\mp k} \tag{1.19}$$

where $U(N)_{K,L} = \left(SU(N)_K \times U(1)_{NL}\right)/\mathbb{Z}_N$. One can also act with a time reversal operator on the defining actions on either side of the duality to generate the time-reversed level/rank dualities. This just amounts to flipping the sign of the level, and slightly modifying the observable map between the two sides. Both the level/rank duality stated above and their time reversed cousins will be utilized in the work below.

This level/rank duality can be rigorously derived and proved using methods from 1+1 d conformal field theories. As reviewed above, Chern-Simons theory (Abelian and non-Abelian

alike) are anomalous when placed on a manifold with boundary. We saw a reason for this near (1.4), where we ignored the boundary term in deriving the transformation properties of the Chern-Simons action under large gauge transformations. Generally this boundary term does not disappear and so pure Chern-Simons theories are ill-defined on such manifolds. One can rectify this by adding extra degrees of freedom to the boundary of the manifold to "cancel off" this lack of gauge invariance. These extra degrees of freedom take the form of a chiral boson in the Abelian theory, and the so-called Wess-Zumino-Witten model in the non-Abelian theory.

A full review of these boundary theories and their relation to level/rank duality would take us too far afield. We only wish to say that these special 1+1 d conformal field theories are simple enough that explicit computations can be made [87]. One important such computation uncovered a bijection between the space of conformal blocks of two very different WZW modesl–one defined for a WZW model associated to a $SU(N)_k$ theory and the other for a $U(k)_{-N}$ theory. This duality between the boundary theories can then be lifted to 2+1D as a duality between the Chern-Simons gauge theories. This is precisely level/rank duality. One can go further, as in [58] and construct the Lagrangians to both theories and show this equivalence by gauging certain global symmetries and performing the path integrals over restricted sectors of the theory. One can then transform one such CS Lagrangian into the other. The rigorous nature of level/rank duality makes it perfect check for the more complicated bosonization dualities, which we will now review.

1.2.2 Bosonization

Matter coupled to Chern-Simons gauge theories has a number of peculiar properties. For the purposes of understanding the 2+1D bosonization dualities the most important property is that of flux attachment. To see this, consider an Abelian Chern-Simons theory coupled to some type of matter with a current $J^\mu = (\rho, J^i)$. In a minimal coupling scheme one must

simply add a term $A_\mu J^\mu$ to the Lagrangian. The full theory then becomes

$$\mathcal{L} = \frac{k}{4\pi}\epsilon^{\mu\nu\rho}A_\mu\partial_\nu A_\rho + A_\mu J^\mu + \mathcal{L}_{\text{mat}}. \tag{1.20}$$

The equations of motion for the gauge field become

$$\frac{k}{4\pi}\epsilon^{\mu\nu\rho}F_{\nu\rho} = J^\mu \tag{1.21}$$

which, in components, becomes

$$F_{ij} = \frac{4\pi}{k}\rho \tag{1.22}$$

$$\epsilon^{ij}E_j = \frac{4\pi}{k}J^i \tag{1.23}$$

where $E_i = \partial_0 A_j$ is the ith component of the electric field. The second of these offers a clear explanation as to why Abelian Chern-Simons theory is used as an effective field theory for the quantum Hall effect–Ohm's law $J^i = \sigma^{ij}E_j$ implies $\sigma^{ij} = \frac{k}{4\pi}\epsilon^{ij}$, and since k is quantized we obtain a quantum Hall conductance! This is not extremely pertinent to 2+1 bosonization, however. We are more interested in the implications of the first line, which, when written in conventional electricity and magnetism language says $B \sim \rho$. In other words, where there is density, there is magnetic field. Consider, for instance, the simplest non-relativistic case of a point particle with $\rho \sim \delta(\mathbf{x})$. The CS equations of motion then say that wherever this point particle is, there is also magnetic flux attached to the particle! This *flux attachment* procedure does not change too much when passing to the relativistic quantum field theories we are interested in. The only difference is that the charge densities are a little more difficult to interpret, but still the equations of motion are clear: when there exists non-zero density, there exits magnetic field flux.

To better understand this consider the following object:

$$J^\mu_{top} = \frac{1}{4\pi}\epsilon^{\mu\nu\rho}\partial_\nu A_\rho. \tag{1.24}$$

This current, known as a topological current, and its non-Abelian generalization is automatically conserved in any 2+1 gauge theory (Chern-Simons or not) due to the properties of the

Levi-Civita tensor. Noether's theorem tells us that associated with some conserved current is some continuous symmetry under which the theory is invariant. Moreover, objects charged under this symmetry, i.e. objects which transform in some specified way under the action of this symmetry, give rise to the associated current. The question then becomes: what types of objects are charged under this symmetry? Additionally, what is the symmetry group? Well, since the current is known as the topological current, it stands to reason that the symmetry which generates its is known as topological symmetry and is denoted by $U(1)_{\text{top}}$. To understand what types of object are charged under this symmetry, consider the total charge associated with this current:

$$Q = \int d^2x J^0 = \frac{1}{4\pi} \int d^2x B. \tag{1.25}$$

This is nothing more than the magnetic flux! This current should then be associated to some type of point-like objects which produce magnetic flux. But such objects are known field configurations in gauge theory: magnetic monopoles! The topological current is due to the presence of monopoles in the theory. Further, standard Dirac quantization type arguments imply that this flux is quantized. Strictly speaking these objects are more like vorticies with magnetic flux, similar to the type of vorticies one obtains in a superconductor. However, the larger bosonization community has deemed these objects "magnetic monopoles" and so we will refer to them for the rest of this work.

This interpretation helps us get a slightly more physical picture into the nature of the flux attachment conditions: attaching magnetic flux to a point-like particle is, in a sense, equivalent to forming a bound state between the particle and a magnetic monopole. In fact, this is more than just an interpretation, but is required by gauge invariance! That is, in these types of Chern-Simons matter theories, the flux attachment conditions comes from coupling the gauge field to the matter in a gauge invariant way. Thus, if we want to have a perfectly gauge invariant CS-matter theory, then these types of bound states must be formed! For the moment let us specialize to $k = 1$. The properties of the resulting bound state depends on a lot of factors, the most important of which is the statistics of the resulting particle. In

fact, one can show that when a particle moves in a background of magnetic flux, the angular momentum of the particle shifts by 1/2! So the monopole-particle bound state described above will have a different spin than the original particle.

We can now understand the nomenclature “bosonization": consider a scalar coupled to a CS gauge theory. Particle excitations will come dressed with monopole operators which will shift the angular momentum by 1/2. Thus a spin-0 particle will be come a spin-1/2 particle! Effectively, we have turned a scalar boson into a fermion! Equivalently we can do the opposite, couple a fermion to the CS gauge theory and obtain a boson. The turning of these bosons into fermions and vice versa is what garnered this relationship “bosonization". Fermionization, while also appropriate, just does not roll of the tongue as well. The next step is to ask if the dynamics of the resulting monopole-particle type bound state is describable through any classical quantum field theory techniques. Do the dynamics simply? Can we write down a Lagrangian for it? The answer is, in some cases, yes! But only for very particular types of conformal field theories.

As stated before, these bosonization dualities are only valid at low energies, when the two theories flow to the same IR fixed point and thus to conformal field theories. So what exactly are these theories? For a fermion the answer is simple: a massless, free Dirac fermion governed by the Lagrangian

$$\mathcal{L} = i\bar{\psi}\not{D}\psi \tag{1.26}$$

where $\not{D} = \gamma^{\mu}(\partial_{\mu} - iA_{\mu})$ is the covariant derivative. Clearly this theory is conformally invariant, since there is no mass or interaction terms. The bosonic side of things is a little more complicated. The correct theory to which this flows is known as a Wilson-Fisher fixed point. Conventionally, the Wilson-Fisher actions contains with a single trace, quartic interaction, but recent work has shown that an extra, double trace quartic interaction term is necessary to obtain the correct symmetry breaking patterns [16, 17]. The Lagrangian is

$$\mathcal{L} = \frac{1}{2}\left(D_{\mu}\phi\right)^{\dagger}\left(D_{\mu}\phi\right) + \lambda \mathrm{Tr}\left(|\phi|^{4}\right) + \tilde{\lambda}\left(\mathrm{Tr}\,|\phi|^{2}\right)^{2}. \tag{1.27}$$

We are now in a position to state the bosonization dualities as first written down by Aharony

[2][11]:

$$SU(k)_N \text{ with } N_f \ \phi \qquad \leftrightarrow \qquad U(N)_{-k+\frac{N_f}{2}} \text{ with } N_f \ \psi, \tag{1.28a}$$

$$U(k)_N \text{ with } N_f \ \phi \qquad \leftrightarrow \qquad SU(N)_{-k+\frac{N_f}{2}} \text{ with } N_f \ \psi \tag{1.28b}$$

where ψ and ϕ refer to the actions in (1.26) and (1.27) respectively. These are subject to the "flavor bound" $N_f \leq k$. It is possible to extend these beyond the flavor bound, as we will review below.

An interesting thing happens when you take $N_f = k = N = 1$ in the above dualities [76, 101]. One winds up with a set of Abelian dualities and due to the lack of the A^3 term in the Abelian CS action, one can integrate out the gauge fields relatively easily. By constantly coupling the dualities to various background fields, gauging them and integrating them out, one can generate an infinite web of dualities. Contained in this web are well known dualities such as the well known bosonic particle/vortex duality and it's younger sister, fermionic particle vortex duality [112, 107]. In chapter 2 we will perform an important consistency check for these dualities by examining the behavior of these Abelian dualities on manifolds with boundaries.

One can go further with the dualities in (1.28a) and (1.28b) and couple both fermions and bosons to a single gauge field, with interactions between them! Such a "master duality" was discovered independently by Benini and Jensen [24, 64] and states

$$SU(N)_{-k+\frac{N_f}{2}} \text{ with } N_s \ \phi \text{ and } N_f \ \psi \qquad \leftrightarrow \qquad U(k)_{N-\frac{N_s}{2}} \text{ with } N_f \ \Phi \text{ and } N_s \ \Psi. \tag{1.29}$$

One can then obtain the dualities in (1.28a) and (1.28b) by setting $N_s = 0$. With the addition of a new matter comes an additional flavor bound. These are now subject to $N_f \leq k$ and $N_s \leq N$. We will use these master dualities in deriving the quiver dualities of chapter 3. In doing so, we will extend the range of validity of the master duality past the first flavor bound and find an incredibly rich phase diagram with many interesting properties. It would

[11] Work has been done prior to the publication of Aharony's work, but he gets the credit work working through the annoying subtleties.

be interesting to find a doubly extended master duality, but that is be beyond the scope of this work.

Even though the dualities above are all different, they behave in exactly the same way. By this I mean the mapping of operators on either side of the duality is the same for the non-Abelian, Abelian and master dualities. A crucial part of this story is the matching of global symmetries across the dualities. After all, if these theories are equivalent then they should both have the same global symmetries. Clearly the flavor symmetry will match since there are the same number of bosons and fermions on either side. The more difficult symmetries to deal with are the Abelian global symmetries. As we said earlier each of these theories comes equipped with a $U(1)$ topological symmetry which couples to monopoles. In addition, there is a baryon number $U(1)$ associated with conservation of baryons, i.e. bound states of N different fermions of differing gauge (color) charge. Under these dualities, the topological symmetry is mapped to the baryon symmetry and vice versa. This gives the interpretation that the nonperturbative objects in one theory (be they monopoles, vortices, etc...) are mapped to baryons in the other and vice versa. Evidence for this mapping can be sees by computing the anomalous dimensions of these operators in the large N limit and verifying that they match.

Bosonization in 2+1 dimensions is not the only example of this type of duality. Long before the canonical works on 2+1D bosonization, physicists in the condensed matter and string theory communities discovered a similar relationship between a free boson and a free fermion in 1+1 d. Contrary to the 2+1 case, the 1+1 case does not involve flux attachment. Similar to the 2+1 case is the fact that it does not hold for all bosonic or fermionic theories, just a special, select few. The canonical example of this is the compact boson in 1+1 d. One can construct an operator called a vertex operator $\mathcal{V}(\phi) \sim e^{i\phi}$ which is fermionic. This operator is important for, among other things, constructing asymptotic states in string theory to compute scattering amplitudes. This relationship has also been used to study the Luttinger liquid [**?**], a simple model for interacting electrons in 1+1 d.

1.2.3 Holography

The last duality we will use in this work is gauge/gravity duality, or holography, or AdS/CFT. To fully understand this duality one must first understand the behavior of D-branes–nonperturbative charged objects in string theory on which open strings can end. In string theory, the bosonic degrees of freedom are simply the coordinates of the string embedded in some auxiliary spacetime. To parameterize this string, one introduces the string coordinates: (σ, τ), often denoted by σ for convenience. The action is then the area of the string embedded in spacetime. Let $X^\mu(\sigma)$ denote these embedding coordinates. The action for the bosonic string, known as the Polyakov action, is

$$S_P = -\frac{1}{4\pi\alpha'}\int d^2\sigma h_{\alpha\beta}(\sigma)\partial^\alpha X^\mu(\sigma)\partial^\beta X_\mu \tag{1.30}$$

where $h_{\alpha\beta}(\sigma)$ is the world sheet metric. This action exhibits full conformal symmetry in 1+1 d. As with any theory defined by an action, in deriving the equations of motion one winds up with a boundary term which defines the boundary conditions of the theory. They are:

$$\text{Dirichlet: } X^\mu(\sigma)_{\text{bdry}} = 0 \tag{1.31a}$$

$$\text{Neumann: } \partial^\perp X_\mu = 0 \tag{1.31b}$$

where $\partial^\perp$ refers to the derivative perpendicular to the boundary. One must choose such boundary conditions for each direction in the embedding space. By choosing the Dirichlet boundary conditions for $D-p-1$ directions, one restricts the motion of the string endpoints to lie on some $p+1$ submanifold of the embedding space. This submanifold gives rise to a classical view of Dp-branes. These can of course fluctuate in all sorts of interesting ways.

Even though they are defined in terms of strings, D-branes can be studied in their own right. In analogy to (1.30), the D-brane action, known as the DBI action, is the area of the D-branes:

$$S_{DBI} = -T\int d^{p+1}\xi\sqrt{-\det(P[g]_{ab})} \tag{1.32}$$

where $P[g]_{ab}$ is the pullback of the embedding space metric onto the $p+1$ submanifold and T is the tension of the D-brane. These objects carry charges associated to the modes of the

string endpoints. The facts together imply that the dynamical D-branes carry energy and thus they couple to gravity and bend the ambient spacetime. This gives rise to a curved background in which closed strings (the strings which don't need these types of boundary conditions) can propagate.

Upon quantizing the open string one finds massless modes which give rise to, among other things, an Abelian gauge field. Since this is associated to the movement of the string endpoints along the directions defined by the Neumann boundary conditions, this gauge field is interpreted as "living on the D-brane". One can include this in (1.32) by adding $2\pi\alpha F_{ab}$ in the determinant. When there are N D-branes stacked on top of each other, strings have the option of ending on any of one of these D-branes. This gives rise to extra charges known as *Chan-Paton factors* which lift the Abelian gauge modes to a $U(N)$ gauge theory. Similarly when quantizing the closed string one finds, among other things, massless symmetric tensors which can be interpreted as gravitons. As stated before, these gravitons can couple to the D-branes since they have energy. Additionally, they can propogate in the curved background created by these D-branes. This gives rise to two complementary views of D-branes–one in which they are surfaces on which closed strings end, hosting the massless modes of the open string, and one in which they create backgrounds in which closed strings can propagate. At high energies there are complicated interactions between the open strings and the closed strings, but at low energies they completely decouple from one another. Thus, these complementary views gives rise to two equivalent dynamical theories–one living on the D-brane and the other propagating in the gravitational background created by the D-branes.

One can do this for a lot of different D-branes and obtain a lot of different theories which are equivalent by these complementary views. The most famous of these types of dualities, however, comes from focusing on D3-branes. The gauge theory which lives on the D3 branes is $\mathcal{N} = 4$ super Yang-Mills, a maximally supersymmetric version of our favorite non-Abelian gauge theory. On the other hand, the gravitational background which the D-branes create, in the appropriate low energy limit, is $AdS_5 \times S^5$, i.e. a product of 5-dimensional anti-de

Sitter space and a 5 sphere[12]. We are then left with a closed string theory propagating on this exotic background. The difference in dimensionality, coupled with the fact that AdS space has a time-like boundary, gives rise to the nomenclature "holography"–we have two equivalent theories one defined in 5 dimensions[13] and one defined in 4 dimensions, where the 4 dimensional theory is interpreted as living on the boundary of the 5 dimensional AdS space. Much like a hologram stores information about a 3d image in a 2d setting, the 3+1 SYM theory contains information about the 3+2 string theory.

The duality in this form does not give us much. Indeed, closed string theory on AdS_5 is notoriously difficult to construct, let alone calculate anything. To make this duality more useful, one takes some limits where the string theory simplifies. First, one takes the strength of the string coupling to zero. This brings us into the classical regime of string theory, which makes calculations *slightly* simpler since now one does not need to quantize anything. On the field theory side, this is equivalent to taking the large N limit in the 't Hooft sense–that is we take $N \to \infty$ while keeping $g^2N = \text{const}$. Next, we take the length of the string to be much smaller than the radius of AdS. This washes out the "stringiness" of the theory and we are left with point particle limit of string theory–supergravity. On the field theory side, this is equivalent to taking the strongly coupled limit of the field theory. Thus, we have a weak/strong duality between supergrvaity on a weakly curved spacetime (which, in the absence of other fields, is simply Einstein gravity) to a strong coupled conformal field theory–something that is infamously difficult to study. In this way we can use gravity to draw conclusions about very complicated types of field theories–a huge deal in the theoretical physics world!

There is an issue here: how can a duality involving a 3+1 d conformal field theory help

---

[12]The dimensionality comes from requirements of conformality of the 1+1 d field theories associated to the string modes.

[13]The 5-sphere plays an important role, but one can perform a Kaluza-Klein type compactification of closed string degrees of freedom, generating an infinite tower of massive modes and leaving behind a massless 5 dimensional theory on AdS. These massive modes are related to composite operators in the field theory, where the masses map to the scaling dimension of the operators.

us understand to the dynamics of 2+1D gauge theories? We will provide a more detailed answer to this procedure in chapter 3 when we use holography to derived dualities between quiver gauge theories. For now, we simply sketch two ways this can be done. Both of these processes involve compactifying the theory along one direction, breaking supersymmetry by giving fermions different boundary conditions than the bosons, and taking the radius of the resulting circle to be very small. This gives mass to most of the matter content of the theory, leaving behind massless gauge fields. In one approach, one starts with a 3+1-dimensional quantum field theory, compactified down to 2+1 dimensions with fundamental matter added back in by placing a small amount of "flavor" branes so as to not warp the background away from AdS. This procedure was carried out by Karch and Jensen in [65] and leads to a purely 2+1 dimensional gauge theory. The holographic duality becomes the bosonization dualitiy. In the other approach, one can go from a 5-dimensional theory down to a 4 dimensional one and embed the flavor branes in such a way so that they are living on some 2+1D submanifold. This was first suggested by Witten in [120] and will be important for studying the quiver gauge theories which arise from varying the QCD θ angle along a given direction. Either approach is useful and the choice depends on the problems we want to solve.

1.3 Symmetry Breaking in 2+1 Dimensions

As mentioned in section 1.2.2, the bosonization dualities (1.28a), (1.28b) and their "master" extensions, are subject to the flavor bound $N_f \leq k$. To understand why this is so, consider the scalar gauge theory of (1.28b). This is a $U(k)_N$ gauge field coupled to N_f scalars. If the flavor bound is satisfied, we give all of the scalars a negative mass, and we assume the resulting theory is "maximally Higgsed"[14] the scalars would obtain a vacuum expectation value of the form

$$\langle \phi \rangle^{aI} = \begin{pmatrix} \mathbb{1}_{N_f \times N_f} \\ 0 \end{pmatrix}. \tag{1.33}$$

[14] An assumption which requires both the single and double trace quartic terms in eq. (1.27)

where the 0 represents an $(k - N_f) \times N_f$ block of zeros. This breaks the gauge group as:

$$U(k)_N \to U(k - N_f)_N \tag{1.34}$$

leading to the usual Higgs mechanism effects such as massive gauge bosons. From (1.34) we can see the origins of the flavor bound: if $k \leq N_f$ the gauge group gets completely broken down. Further, the flavor group breaks down too, at least for $k < N_f$. To see why this occurs, consider the vev in the Higgs phase when the flavor bound is broken:

$$\langle \phi \rangle^{aI} = \begin{pmatrix} \mathbb{1}_{k \times k} & 0 \end{pmatrix} \tag{1.35}$$

where now the 0 represents an $k \times N_f - k$ block of zeros. The resulting symmetry of the ground state is given by the transformations which leave this vacuum expectation value invariant. Clearly this breaks the entirety of the gauge group. To see if there is any residule symmetry breaking in the flavor group, one can then perform a flavor transformation by multiplying on the right by some $U \in U(N_f)$. Due to the form of (1.35), we can bring this flavor transformation into a block diagonal form

$$U = \begin{pmatrix} U_1 & 0 \\ 0 & U_2 \end{pmatrix} \tag{1.36}$$

where $U_1 \in U(k)$ and $U_2 \in U(N_f - k)$. This implies that the flavor symmetry is broken as

$$U(N_f) \to U(k) \times U(N_f - k). \tag{1.37}$$

In other words, the flavor group is spontaneously broken, and Goldstone's theorem tells us that the low energy theory contains massless scalars valued in the coset known as the complex Grassmannian

$$\mathcal{M}(N_f, k) = \frac{U(N_f)}{U(k) \times U(N_f - k)}. \tag{1.38}$$

In the corresponding regime in the fermion theory, such symmetry breaking does not occur. Thus, the duality is lost.

There are some observations to be made, though. First and foremost, one of the mass deformed phases, the one where the scalar has a positive mass and the fermion has a negative

mass, still matches in the flavor violating regime. Moreover, the other mass deformed phase in which the fermion has a positive mass (which does not match the symmetry broken phase of the scalar) can be matched by a *different* scalar theory under a positive mass deformation, namely

$$U(N_f - k)_{-N} \text{ with } N_f\, \phi \tag{1.39}$$

Interestingly enough, when this theory enters its Higgsed regime, it leads to the same Grassmannian (1.38). This lead the authors of [80] to conjecture a new duality which leads to spontaneous symmetry breaking for the fermion in a finite range of masses about the origin. Their conjecture states the following duality:

$$SU(N)_{-k+N_f/2} \text{ with } N_f\, \psi \qquad \leftrightarrow \qquad \begin{cases} U(k)_N \text{ with } N_f\, \Phi_1 & m_\psi = -m_* \\ U(N_f - k)_{-N} \text{ with } N_f\, \Phi_2 & m_\psi = m_* \end{cases}, \tag{1.40}$$

where m_* is just some yet-to-be-known value of the fermion mass where the dual theories become massless. In contrast to the dualities in section 1.2.2, (1.40) requires two scalar duals which overlap on some finite range about the origin where symmetry breaking occurs.

Our main objective in the latter half of chapter 3 will be to extend this duality to the master duality by coupling it to scalar matter and tracking how the various interactions will effect the symmetry broken phases. This will be a necessary step in constructing duals to quiver gauge theories which host fundamental matter on the nodes. Part of this requires a breaking of the flavor group, since in constructing the quiver some fermions will be fundamental and some will be bifundamental. We turn to the question of the phase diagrams of these types of flavor broken, flavor bound violating fermions in chapter 4.

This concludes our brief review of the pertinent topics explored in this thesis. We will review these topics again in more detail as needed.

Notation

An annoying part of this line of work is the question of conventions for the Chern-Simons level when coupled to fermions. Some authors like to explicitly display the half-integer

contribution to the level from the η-invariant, while some like to absorb it in a redefinition of the level. In chapters 2 and 3 and the first half of chapter 4 we will do the former, but when switching to the large N limit in the last half of chapter 4 we will do the latter.

Chapter 2

DUALITIES AT THE BOUNDARY

Disclaimer: *This work [10] was done in collaboration with Kyle Aitken, Andreas Karch and Brandon Robinson. The author contributed to most aspects of the work discussed here, with the exception of the lattice construction which was primarily done by Kyle.*

One aspect of both the Abelian and non-Abelian bosonization dualities that had previously received little attention is the role that boundaries in the duality. If there is any testable prediction to come from the duality, it is necessary to understand how to describe the behavior of systems with dual bulk theories in the presence of a boundary in order to make contact with quantities measurable on a finite sample. After all, the physics of edge modes is the most easily accessible physical manifestation in quantum Hall samples. Furthermore, including boundaries gives us one more check of the dualities which to some extent remain conjectural, even though there has been recent progress on providing a proof of the basic "seed duality" by realizing it via a lattice construction in [27]. To understand both these points, we will study how Abelian theories on flat, half space $\mathbb{R}^{2,1}_{+}$ are related by bosonization. In particular, we will restrict our investigation to flux attachment between IR descriptions of free fermions and scalars with quartic self-coupling near or at the conformal fixed point. We note that while we will be considering bosonization and particle-vortex duality as in [76, 101] throughout, the results obtained should be easily generalizable to include, say, non-trivial flavor symmetries [75]. Despite our restriction to $\mathbb{R}^{2,1}_{+}$, we believe our results generalize to curved manifolds with arbitrary boundaries so long as they are topologically trivial.

An ambitious program considering boundary conditions in 2+1 dimensional dualities has been outlined by Gaiotto in a talk in honor of Nathan Seiberg's birthday [48]. In that talk, he conjectures dual pairs of boundary conditions based on constructing interfaces between

a theory and its dual. Assuming that at low energies the theories decouple across the interface, an interesting web of Abelian and non-Abelian dualities emerges with subtle, non-trivial interplay of boundary conditions imposed on scalars and gauge fields. In this work, we construct a duality that agrees with one of the examples in [48] and gives evidence that these conjectures – which are based on the decoupling assumption – are possibly true more broadly. While not attempted in the following work, it would be very interesting to flesh out the details of Gaiotto's program.

In § 2.1, we review the status of the web of dualities in $d = 2 + 1$ including conventions, notation, and descriptions of the theories participating in the dualities for use in all of the subsequent sections. In § 2.2, we construct the appropriate theories participating in bosonization on $\mathbb{R}^{2,1}_+$ including possible boundary conditions and requirements for the theory to be non-anomalous. Joining the concepts from the previous section, in § 2.3 we formulate the role of boundary conditions and self-consistency in describing dual theories on $\mathbb{R}^{2,1}_+$. Further, in § 2.4, we will give evidence for the continuum duality by writing down the microscopic theory on a Euclidean three-dimensional cubic lattice. Finally, we will conclude with an overview of the results and a discussion of future directions.

2.1 Review of Abelian dualities

To begin the analysis of Abelian dualities with boundaries, we will give a brief review of the basic players and the mechanisms that relate them [76, 101]. Our starting point will be the two basic forms of bosonization relating a Wilson-Fisher (WF) scalar, a free Dirac fermion, and level-k $U(1)$ Chern-Simons theories ($U(1)_k$ CS) living on $\mathbb{R}^{2,1}$. Specifically, we begin with the "seed" dualities

$$\text{WF scalar} \;+\; U(1)_1 \text{ CS} \quad \longleftrightarrow \quad \text{Free Fermion}, \tag{2.1}$$

$$\text{WF scalar} \quad \longleftrightarrow \quad \text{Free Fermion} \;+\; U(1)_{-1} \text{ CS}. \tag{2.2}$$

These schematic relations are understood at the level of equating the partition functions as a function of background fields of the theories across the arrows.

In the following, we use uppercase letters to denote background gauge fields, and lowercase for a dynamical gauge fields, φ for scalar fields, ψ for Dirac fermions, and λ for heavy Pauli-Villars regulator fields. In what will be a necessary distinction for later application, we will denote dynamical (background) spin$_c$ valued connections with a (A), while ordinary U(1) connections will be denoted with b (B), c (C), and so on. The background and dynamical gauge fields are coupled through a BF-term that is defined below. With these conventions, eqs. (2.1) and (2.2) are more precisely written respectively as

$$\begin{aligned}\mathcal{Z}_{\mathrm{WF+flux}}[A] \equiv \int \mathcal{D}\varphi\, \mathcal{D}b\; e^{iS_{\mathrm{WF}}[\varphi,\, b]+iS_{CS}[b]+iS_{BF}[b,A]} \\ \leftrightarrow \int \mathcal{D}\psi\mathcal{D}\lambda\; e^{iS_f[\psi,\lambda,\, A]} \equiv \mathcal{Z}_{\mathrm{f}}[A],\end{aligned} \tag{2.3}$$

and

$$\begin{aligned}\mathcal{Z}_{\mathrm{WF}}[B] \equiv \int \mathcal{D}\varphi\; e^{iS_{\mathrm{WF}}[\varphi,\, B]} \\ \leftrightarrow \int \mathcal{D}\psi\mathcal{D}\lambda\, \mathcal{D}a\; e^{iS_f[\psi,\lambda,\, a]-iS_{BF}[a,B]-iS_{CS}[B]} \equiv \mathcal{Z}_{\mathrm{f+flux}}[B].\end{aligned} \tag{2.4}$$

The actions for the various matter fields participating in the above dualities are given by

$$S_{\mathrm{WF}}[\varphi,\, B] = \int d^3x\; |(\partial_\mu - iB_\mu)\varphi|^2 - \alpha|\varphi|^4, \tag{2.5a}$$

$$S_f[\psi, \lambda,\, A] = \lim_{m_\lambda \to -\infty} \int d^3x\; i\bar{\psi}\gamma^\mu(\partial_\mu - iA_\mu)\psi + i\bar{\lambda}\gamma^\mu(\partial_\mu - iA_\mu)\lambda - m_\lambda\bar{\lambda}\lambda\,. \tag{2.5b}$$

It is well known that a single Dirac fermion in $d = 3$ has a parity anomaly, which necessitates the inclusion of the Pauli-Villars regulator in eq. (2.5b) to yield a well defined fermion determinant. Even though we are ultimately interested in the case where the regulator mass is parametrically heavy ($|m_\lambda| \to \infty$), its effect on the theory by shifting topological terms must always be tracked – even when λ is integrated out. In the literature it is common to forego writing down the regulator and instead add a $k = -\frac{1}{2}$ Chern-Simons term to the

action to account for the effects of λ.[1] We prefer to explicitly keep the regulator field around as it makes the accounting of edge modes clearer.

The actions for the level-k Chern-Simons and BF-terms are

$$kS_{CS}[A] = \frac{k}{4\pi}\int d^3x\ \epsilon^{\mu\nu\rho}A_\mu\partial_\nu A_\rho, \tag{2.6a}$$

$$kS_{BF}[b, A] = \frac{k}{2\pi}\int d^3x\ \epsilon^{\mu\nu\rho}b_\mu\partial_\nu A_\rho. \tag{2.6b}$$

The normalizations in eqs. (2.6a) and (2.6b) are chosen such that the theories with arbitrary $k \in \mathbb{Z}$ are gauge invariant in the absence of a boundary. Taking inspiration from the microscopic description of bosonization [27], the coupling of the dynamical field b to the background field A can alternatively be written

$$S_{CS}[b] + S_{BF}[b,\, A] = S_{CS}[b + A] - S_{CS}[A]. \tag{2.7}$$

We will see in later sections that rewriting eqs. (2.3) and (2.4) with only Chern-Simons terms will be useful in understanding edge modes.

A few remarks are warranted before proceeding. The statements of eqs. (2.3) and (2.4) should to be understood at the IR fixed point. Thus, the absence of a Maxwell term for a, i.e. $\frac{1}{4e^2}(da)^2$, can easily be seen because the IR limit requires $e^2 \to \infty$. Moreover, the action for the Wilson-Fisher scalar is obtained by tuning the scalar mass $m_\varphi^2 \to 0$ and quartic coupling $\alpha \to \infty$. Alternatively, one can think of the Wilson-Fisher scalar by introducing an auxiliary scalar (Hubbard-Stratonovich) field, σ, such that

$$S_{WF}[\varphi,\, \sigma,\, B] = \int d^3x\ \Big(|(\partial_\mu - iB_\mu)\varphi|^2 - \sigma|\varphi|^2 + \frac{\sigma^2}{2\alpha}\Big). \tag{2.8}$$

Integrating out σ produces eq. (2.5a). Treating σ as a background field, it functions as a mass-term source. Relating the operator insertion sourced by σ through either of the dualities yields the map: $\sigma \leftrightarrow -\bar{\psi}\psi$. The way that we will interpret this map for mass

[1] More precisely, we should note that this topological effect is the η-invariant coming from the Atiyah-Patodi-Singer index theorem [19, 92]. The precise definition will be discussed more thoroughly when the distinction is important in Sec. § 2.3.2.

deformed theories is that the scalar and fermion mass terms are mapped into one another under the duality as

$$\pm m_\varphi^2 |\varphi|^2 \qquad \leftrightarrow \qquad \mp m_\psi \bar{\psi}\psi. \tag{2.9}$$

Consistency of the dualities (2.3) and (2.4) for positive and negative mass deformations will be a guiding principle in what follows.

Another useful map between dualities will be between global symmetry currents. Since we identify the global $U(1)$ symmetries on either side of the duality, it is natural to also identify the conserved currents associated with said symmetries. For example, the duality eq. (2.3) implies the identification of

$$j^\mu_{\text{WF+flux}}(x) \equiv \frac{\delta S_{\text{WF+flux}}[A]}{\delta A_\mu(x)} \qquad \leftrightarrow \qquad j^\mu_f(x) \equiv \frac{\delta S_f[A]}{\delta A_\mu(x)}. \tag{2.10}$$

For the side of the duality with a dynamical $U(1)$ gauge field, the global $U(1)$ is associated with a flux current. Meanwhile, the side with just matter has a global $U(1)$ that is associated with particle number.

Spin Considerations

A large portion of the subtleties involved in extending these dualities to include manifolds with boundaries comes from the differences between spin and spin$_c$ valued $U(1)$ connections. We will now take a brief detour to review some of these concepts. The discussion here will be largely heuristic, while more mathematically oriented treatments can be found in [102, 101, 84].

Consider an arbitrary manifold, $\mathcal{M}$, and turn on a background gauge field, i.e. a $U(1)$ connection $\mathcal{A}$. Suppose that we want to ask questions about the dynamics of a system of fermions on $\mathcal{M}$ that couple to $\mathcal{A}$. We first must ensure that it is sensible to define the Dirac operator on $\mathcal{M}$. This requires us to define an appropriate connection, $\omega_\mu{}^{ab}$, that consistently parallel transports a local Lorentz frame over all of $\mathcal{M}$, allowing us to meaningfully talk about placing a spinor anywhere on $\mathcal{M}$. An $\mathcal{M}$ that admits a global definition of $\omega_\mu{}^{ab}$ is

called a spin manifold. On a spin manifold the full covariant Dirac operator is given by

$$D_\mu = \partial_\mu + \frac{1}{4}\omega_\mu{}^{ab}\gamma_a\gamma_b + i\mathcal{A}_\mu. \tag{2.11}$$

However, certain topological constraints imply that not every manifold admits a global definition of $\omega_\mu{}^{ab}$. The topological obstruction to defining ω everywhere on $\mathcal{M}$ can be compensated by a non-standard choice for quantization of $\mathcal{A}$:

$$\frac{1}{2\pi}\int_\Sigma d\mathcal{A} \in 2\mathbb{Z}, \tag{2.12}$$

where Σ is an oriented co-dimension 2 surface in $\mathcal{M}$. Within this quantization scheme, the covariant Dirac operator

$$D^{(n)}_\mu = \partial_\mu + \frac{1}{4}\omega_\mu{}^{ab}\gamma_a\gamma_b + in\mathcal{A}_\mu \tag{2.13}$$

is well defined for odd n. An $\mathcal{M}$ whose topological obstruction to a global definition of the Dirac operator is compensated by the unusual quantization of $\mathcal{A}$ is called a spin$_c$ manifold, and the $\mathcal{A}$ obeying eq. (2.12) will be referred to as a spin$_c$ valued connection.

Further, we can impose eq. (2.12) even if the manifold admits a global definition of $\omega_\mu{}^{ab}$, which implies that spin and spin$_c$ valued connections can be defined spin manifolds . Thus since $\mathbb{R}^{2,1}$ and $\mathbb{R}^{2,1}_+$ are spin manifolds, the distinction that we must make is at the level of fermions being coupled to either a spin or spin$_c$ valued connection.

The restriction to odd n gives rise to the spin-charge relation of condensed matter physics; particles with integer spin have even charge and half-integer spin have odd charge. While this does not appear to be a fundamental law of nature, it is believed to be valid for systems made up of protons, electrons and other charged (quasi-)particles. This motivates the distinction between spin and spin$_c$ valued connections in our notation and further implies that our background field appearing in eq. (2.3) is spin$_c$ [102].

As an example of how this distinction can enter into the seed dualities, consider pure a $U(1)_1$ theory with spin valued connection, b, on $\mathcal{M} = T^3$.[2] Further, consider that $\mathcal{M}$ is the

[2]This discussion follows Appendix B of [101] where more details can be found.

boundary of a four-dimensional manifold X. Upon quantization, we find that there is just one state such that the path integral is

$$\mathcal{Z} = \int \mathcal{D}b \; e^{iS_{CS}[b]} = e^{-i\Omega} \tag{2.14}$$

where Ω denotes "framing anomaly"

$$\Omega = 2\int_{\partial X} \mathrm{CS}_{\mathrm{g}} = \frac{1}{96\pi}\int_X \mathcal{R}\wedge\mathcal{R}, \tag{2.15}$$

and CS_{g} is the gravitational Chern-Simons term.

If the same $U(1)$ theory with dynamical gauge field b is defined with respect to a background spin$_c$ structure with connection A on $\mathcal{M}$, we must couple our dynamical $U(1)$ field b to the background connection A through a BF term. As with the previous case, there is only one state, and the theory is uniquely determined. The difference is that the partition function evaluates to

$$\mathcal{Z}[A] = \int \mathcal{D}b \; e^{iS_{CS}[b]+iS_{BF}[b,A]} = e^{-i\Omega - i\frac{1}{4\pi}\int AdA}. \tag{2.16}$$

Accounting for these extra terms will prove to be a useful guiding principle for keeping track of edge modes across the duality.

2.2 Theories on half-space

Now that we have reviewed the basics of the standard Abelian dualities, we are in a position to address the subtleties associated with the theories on the half-space, $\mathbb{R}^{2,1}_+$. We will explore the space of boundary conditions consistent with eqs. (2.5b) or (2.5a) defined on $\mathbb{R}^{2,1}_+$.

To do so, we must remind ourselves of how to be honest about boundary conditions in field theories. Consider a theory with action S defined on the manifold $\mathcal{M}$ with boundary $\partial\mathcal{M}$. By taking the variation δS we will find two classes of terms

$$\delta S = \delta S_{\mathrm{bulk}} + \delta S_{\mathrm{bdry}} = \int_{\mathcal{M}} \delta\mathcal{L}_{\mathrm{bulk}} + \int_{\partial\mathcal{M}} \delta\mathcal{L}_{\mathrm{bdry}}. \tag{2.17}$$

The bulk part of the action is still extremized by the classical equations of motion, and consistency of the variation amounts to choosing conditions on the field configurations such

that δS_{bdry} vanishes as well. In the classical limit of the theory, the field configuration that satisfies the equations of motion should also satisfy boundary conditions. In the full quantum theory this is not necessarily the case. One way to proceed is by manually restricting the space of allowed field configurations by inserting delta funtions in the path integral which impose the desired boundary conditions. This method excludes fluctuations where $\delta S_{\text{bdry}} \neq 0$. Alternatively, we could do the path integral over all boundary field configurations. In that case the boundary conditions would only be obeyed by the dominant field configurations in the path integral–those which extremize the action. Below we will see that for all fields we consider there will be multiple boundary conditions which satisfy $\delta S_{\text{bdry}} = 0$. The boundary conditions will be chosen such that the theory remains non-anomalous and we keep the global symmetries on either side of the duality consistent.

In addition to the field conventions listed above, we will take coordinates on $\mathbb{R}^{2,1}_+$ to be $\{t, x, y\}$ where $t, x \in (-\infty, \infty)$ and $y \geq 0$. The boundary of $\mathbb{R}^{2,1}_+$ is the surface at $y = 0$. Indices i, j will be used to denote coordinates on the boundary and μ, ν in the bulk.

2.2.1 Boundary conditions

Applying the above approach to eq. (2.5a), we take the theory defined on $\mathbb{R}^{2,1}_+$ by fiat and vary such that

$$\delta S_{WF}[\varphi, B] = \ldots + \int_{y=0} d^2x \left(\delta\varphi^\dagger D_y\varphi + \delta\varphi D_y\varphi^\dagger\right) \tag{2.18}$$

where "..." contains bulk terms which vanish on-shell. This implies that both Dirichlet $\delta\varphi|_{y=0} = 0$ and Neumann $D_y\varphi|_{y=0} = 0$ are valid boundary conditions.

Now consider the boundary conditions for a Dirac fermion. We write the Dirac fermion eq. (2.5b) evaluated on $\mathbb{R}^{2,1}_+$ in terms of left and right handed components:

$$\psi = \begin{pmatrix}\psi_+\\ \psi_-\end{pmatrix}, \qquad \text{i.e.} \quad \psi_\pm = P_\pm\psi \qquad \text{with} \qquad P_\pm = \frac{\mathbb{1} \pm \gamma^y}{2}, \tag{2.19}$$

and γ^y is the gamma matrix in the direction perpendicular to the boundary. $\gamma^y = i\gamma^t\gamma^x$ is the 'γ_5' in the boundary theory. Now, on $\mathbb{R}^{2,1}_+$ the terms in eq. (2.5b) that depend on ψ in

this language read

$$S_f[\psi, \lambda, A] = \int_{\mathbb{R}^{2,1}_+} d^3x \, \Big(i\bar{\psi}_+ \not{D}_{A_i} \psi_+ + i\bar{\psi}_- \not{D}_{A_i} \psi_- + \bar{\psi}_- A_y \psi_+ - \bar{\psi}_+ A_y \psi_- \\ + \frac{i}{2}(\bar{\psi}_- \partial_y \psi_+ - \partial_y \bar{\psi}_- \psi_+ + \partial_y \bar{\psi}_+ \psi_- - \bar{\psi}_+ \partial_y \psi_-) \Big) + \dots \tag{2.20}$$

where the ellipses denote the terms that only depend on the Pauli-Villars regulator field and $\not{D}_{A_i} \equiv \gamma^i(\partial_i - iA_i)$.

The boundary terms generated by the variation of eq. (2.20) are

$$\delta S_f[\psi, A] = \dots + \int_{y=0} d^2x \, \big(\psi_- \delta\bar{\psi}_+ - \psi_+ \delta\bar{\psi}_- + \bar{\psi}_- \delta\psi_+ - \bar{\psi}_+ \delta\psi_- \big). \tag{2.21}$$

We can consistently impose Dirichlet boundary conditions on *either* of the chiral components,[3]

$$\psi_+|_{y=0} = 0 \qquad \text{or} \qquad \psi_-|_{y=0} = 0. \tag{2.22}$$

However, choosing *both* $\psi_+|_{y=0} = 0$ and $\psi_-|_{y=0} = 0$ over-constrains the equations of motion at the boundary [39]. Either choice in eq. (2.22) leaves behind a chiral edge mode as seen in the current running parallel to the boundary, $j^i_\psi = \bar{\psi}\gamma^i\psi$. In § 2.3.1, we will explore how requiring a non-anomalous theory forces us to choose one boundary condition over the other.

Since the action for the Pauli-Villars regulator fields is identical to that for the Dirac fermions, the analysis above applies in kind. In particular, we apply chiral boundary conditions on the Pauli-Villars regulator as well, i.e.

$$\lambda_+|_{y=0} = 0 \qquad \text{or} \qquad \lambda_-|_{y=0} = 0. \tag{2.23}$$

In what follows, we will show boundary condition of the Dirac fermion and Pauli-Villars field are related. In order to keep track of which boundary condition we are imposing on the two fields, we introduce a superscript $S^{\pm}_f[\psi, \lambda, A]$ to indicate imposing the boundary conditions $\psi_\mp|_{y=0} = \lambda_\pm|_{y=0} = 0$.

---

[3] We will always take $P_\pm\psi|_{y=0}$ to imply the corresponding relation on the conjugate field, namely $\bar{\psi}P_\mp|_{y=0} = 0$.

We will use similar notation for the time reversed fermion actions $\bar{S}_f^{\mp}[\psi, \lambda, A]$ with the superscript indicating the type of boundary conditions imposed. Note that the time reversed version of S_f^+ is $\bar{S}_f^-$ and vice versa. In addition, we should keep in mind that $S_f^{\pm}$ itself was defined with a large negative Pauli-Villars mass, and since fermion mass terms are time-reversal odd, $\bar{S}_f^{\pm}$ is defined with a large positive Pauli-Villars mass. This means that $\bar{S}_f$ can be thought of as coming with a $k = +\frac{1}{2}$ Chern-Simons term rather than $k = -\frac{1}{2}$.

Next, consider the possible boundary conditions for our dynamical gauge fields. To constrain such fields, we will consider the action at the level of the microscopic description in which the Maxwell term is still dominant. Upon variation, we find

$$\delta S_{\text{Maxwell}}[b] = \ldots - \frac{1}{e^2} \int_{y=0} d^2x \; F^{yi} \delta b_i, \tag{2.24}$$

with $F_{yi} = \partial_y b_i - \partial_i b_y$. Once more, we see we can impose either Dirichlet or Neumann boundary conditions. The former requires the variation along the boundary to vanish, i.e. $b_i = 0$. Neumann boundary conditions require the field strength adjacent and oriented perpendicular to the boundary be flat, $F_{iy} = 0$.

Lastly, we will consider the boundary conditions for a level-k Chern-Simons term. Such terms will only come up in the IR limit of the dualities. Varying eq. (2.6a) gives

$$k \; \delta S_{\text{CS}}[b] = \ldots + \frac{k}{4\pi} \int_{y=0} d^2x \; \epsilon^{ij} b_i \delta b_j. \tag{2.25}$$

While we could impose $b_t = 0$ or $b_x = 0$ at the boundary, requiring the general, sufficient condition that

$$(b_t - v_b b_x)|_{y=0} = 0, \tag{2.26}$$

makes the boundary physics clear in the context of eqs. (2.3) and (2.4). That is, we maintain a chiral edge mode with velocity v_b and chirality set by $\text{sgn}(v_b)$. In order for the boundary kinetic term to be positive definite, the velocity must be chosen such that $v_b k > 0$ [45]. In what follows we will be mostly interested in relativistic theories fixing the magnitude $|v_b| = 1$. Since a gauge transformation of eq. (2.6a) also produces a boundary term, any gauge choice

that we make must be consistent with eq. (2.26). The simplest solution is to promote the boundary condition to a gauge fixing condition, i.e. we let $(b_t - v_b b_x) = 0$ in the bulk as well. As we will see in the next section, the freedom to choose v_b is actually tied to the choice of fermionic boundary conditions. The consistency requirement on the sign of v_b will then pick a preferred fermionic boundary condition, which we will hardwire into the path integral.

In this section, we have seen that there are multiple choices of boundary conditions for all of the fields in our theories. However, the choices will be constrained by requiring the theory to be non-anomalous and that the global symmetries on either side of the duality match.

2.2.2 Boundary modes and anomalies

The discussion of the previous subsection will prove sufficient to study the duality between the conformal field theories related by bosonization. However, to check the consistency of our dualities under deformations, we will also be interested in adding mass gaps to the theories on $\mathbb{R}^{2,1}_+$. Before formulating dualities like eqs. (2.3) and (2.4) with boundary conditions, we will highlight additional subtleties in gapped phases in the presence of a boundary.

Our main concern in this section is the possible existence of domain wall fermions (DWFs) and their interplay with anomalies.[4] DWFs are typically discussed in the context of Dirac fermions defined on $\mathbb{R}^{2,1}$ with a spatially varying mass term – specifically, a mass term that changes sign across an interface. But the same basic construction also allows us to look for the existence of massless boundary modes on $\mathbb{R}^{2,1}_+$. A massless chiral mode localized on the boundary will exist when the mass profile leaves

$$\xi(y) = e^{\pm \int_0^y dy'\, m(y')} \tag{2.27}$$

finite for all $y \in \mathbb{R}^{2,1}_+$ [70]. Unlike the DWF descending from the construction on $\mathbb{R}^{2,1}$, any constant, non-zero mass profile ($m(y) = m$) in eq. (2.27) yields a normalizable zero mode for a fermionic theory on $\mathbb{R}^{2,1}_+$. The chirality of the DWF is set by the sign of the mass:

[4] Strictly speaking, our "domain wall" is really the boundary of our material, but we will continue to use this slight abuse of vocabulary.

$\text{sgn}(m) = +1$ gives a left-mover and $\text{sgn}(m) = -1$ a right-mover. In either case, the chiral current is not conserved, and so the boundary theory on its own is anomalous. While this is not necessarily an inconsistency in the case when the fermion number is not gauged, we are only interested in theories in which our global symmetry currents are in fact conserved and so can be consistently coupled to background fields.[5]

It has long been known that a level-k Chern-Simons in the bulk can precisely account for the anomalous chiral modes living on the defect so long as they satisfy the relation

$$k = n_+ - n_-, \tag{2.28}$$

where (n_+) n_- are the number of (right-) left-moving modes. More precisely, the nonzero anomaly of the bulk Chern-Simons term under gauge transformations of its associated gauge field can be exactly compensated by the axial anomaly of chiral edge movers on the boundary. This is know as the Callan-Harvey mechanism [26].

In addition to the chiral anomaly, there is also a framing anomaly of such edge theories which arises under diffeomorphism transformations. There is a condition analogous to the Callan-Harvey mechanism which accounts for anomalies associated with diffeomorphism transformations of the gravitational Cherm-Simons terms we will consider. In particular, a manifold $\mathcal{M}$ with a boundary will not be diffeomorphism invariant unless the theory satisfies

$$k_\Omega = \frac{1}{2}\left(n_+^{\text{MW}} - n_-^{\text{MW}}\right) \tag{2.29}$$

where k_Ω is the coefficient of gravitational Chern-Simons term, $i\Omega$ of eq. (2.15), and $n_\pm^{\text{MW}}$ the number of right- and left-moving Majorana-Weyl fermions, respectively. Fortuantely, a single chiral Dirac fermion is equivalent to two Majorana-Weyl fermions, i.e. $n_\pm = 2n_\pm^{\text{MW}}$ [101]. Hence, so long as $k = k_\Omega = \pm 1$, a single chiral fermion can render the theory non-anomalous for both the chiral and framing anomalies. In what follows, our calculations will be organized such that keeping track of eq. (2.28) is completely equivalent to eq. (2.29).

[5]Dualities between theories which have non-vanishing boundary anomalies for global symmetries can also be formulated, as long as the anomalies on both sides of the duality agree. We do not consider such dualities in this work, but they have been outlined in [48] along with the theories we consider.

We will see that requiring our theories to be non-anomalous – such that eq. (2.28) is satisfied – arranges for us the pieces laid out above into a working conjecture for Abelian dualities with a boundary. Furthermore, this counting will naturally appear as an organizational tool in the lattice construction in later sections.

Let us now take account of the possible edge modes that can appear in the context of bosonization dualities. To start, we will only consider matter fields. The scalars will never give rise to a chiral edge mode. For gapped fermions, we naturally get DWFs subject to the boundary conditions of eq. (2.22), which select any possible surviving edge mode. As hinted by eq. (2.28) these DWFs are intimately connected to Chern-Simons terms.

By the same reasoning that our gapped fermions give rise to DWFs, so too do the Pauli-Villars fields. We will always take the boundary conditions on the Pauli-Villars regulators to kill off the would-be DWF. If we do not kill off the Pauli-Villars DWF, this would give us massless ghosts localized to the boundary. This would be orthogonal to the Pauli-Villar's field original purpose, which was to regulate high energy degrees of freedom giving rise to the parity anomaly.

Consider a spin$_c$ valued connection, A, coupled to a heavy Dirac fermion, χ, and a heavy Pauli-Villars regulator, λ, with positive masses. Here we will take A to be a background field, but analogous results hold for dynamical spin$_c$ valued connections up to potential boundary conditions which we will discuss later. The effective action generated by integrating out a heavy Dirac fermion is $iS_{CS}[A] + i\Omega$. Furthermore from eq. (2.27), χ gives rise to a DWF of positive chirality, and so we can satisfy eq. (2.28) by imposing $\chi_-|_{y=0} = 0$ to leave the DWF unaffected. The same DWF is precisely the edge mode we also need to account for the framing anomaly. To remove the DWF associated with the Pauli-Villars regulator, we impose $\lambda_+|_{y=0} = 0$. Analogous results follow choosing negative mass Dirac fermions and Pauli-Villars regulators with a flipped Chern-Simons level and the opposite boundary conditions. Choosing the signs of the fermion and Pauli-Villars masses to be anti-aligned, the Chern-Simons terms cancel. Furthermore, both the fermion and Pauli-Villars boundary conditions prevent any DWFs from arising. As promised, for $k = \pm 1$ only one of the two

possible fermionic boundary conditions yields a theory consistent with eq. (2.28).

Returning to the IR boundary conditions on the gauge fields, we saw the Chern-Simons term gave us a chiral edge mode whose handedness was set by the sign by the velocity in eq. (2.26) and hence by k. If this Chern-Simons term is generated by integrating out a massive fermion, the bosonic chiral edge mode from the gauge field can be understood as a $1+1$-dimensional bosonized DWF. Thus, the IR physics still retains some memory of the microscopic picture due to the gapless chiral edge mode furnished by the underlying DWF, which appropriately accounts for the anomalies. Together the massive fermions, Maxwell term for the gauge field, and chiral edge mode give a complete microscopic picture of the theory. This implies that eq. (2.26) emerges from the boundary conditions imposed on the microscopic fermions.

In fact, we would like to promote this to an operating principle for how to deal with Chern-Simons terms when analyzing theories in the presence of boundaries. We want to view *all* spin$_c$ and gravitational Chern-Simons terms as being generated by integrating out massive fermions. This is the easiest way to get a consistent microscopic picture accounting for all the resulting boundary modes and anomaly inflows. In particular, this means we will have the following view of the Chern-Simons terms appearing in Abelian bosonization:

> $+iS_{CS}[A]+i\Omega$ **Chern-Simons terms:** Pauli-Villars regulator and a free fermion with m_λ, $m_\chi > 0$ and the $\chi_-|_{y=0} = 0$ and $\lambda_+|_{y=0} = 0$ boundary conditions.
>
> $-iS_{CS}[A]-i\Omega$ **Chern-Simons terms:** Pauli-Villars regulator and a free fermion with m_λ, $m_\chi < 0$ and the $\chi_+|_{y=0} = 0$ and $\lambda_-|_{y=0} = 0$ boundary conditions.

The signs of the masses of the fermion and Pauli-Villars fields and their appropriate boundary conditions are completely determined by the sign of the Chern-Simons level. We will use this microscopic description both for Chern-Simons terms for dynamical spin$_c$ fields and for Chern-Simons terms associated with background spin$_c$ valued connections. For clarity, we will denote the fermions that appear in eqs. (2.3) and (2.4) as ψ and refer to them as

"dynamical", while "fiducial" fermions χ refer to the microscopic description of the Chern-Simons term. More explicitly, we will view every Chern-Simon terms as arising from

$$e^{\pm iS_{CS}[A]\pm i\Omega} = \int \mathcal{D}\chi\, \mathcal{D}\lambda\; e^{iS^{\pm}_{ff}[\chi,\,\lambda,A]}, \tag{2.30}$$

where

$$S^{\pm}_{ff}[\chi,\lambda,A] = \lim_{|m_\chi|,|m_\lambda|\to\infty} \int_{\mathbb{R}^{2,1}_{+}} d^3x\, \Big(i\bar{\chi}\not{D}_A\chi \mp |m_\chi|\bar{\chi}\chi + i\bar{\lambda}\not{D}_A\lambda \mp |m_\lambda|\bar{\lambda}\lambda\Big). \tag{2.31}$$

The superscript on fiducial fermion action denotes the sign of the fermion and Pauli-Villars masses[6] as well as the corresponding boundary conditions, $\chi_{\mp}|_{y=0} = \lambda_{\pm}|_{y=0} = 0$. As usual, we have chosen the convention that the fermionic mass term appears generically as $V(\psi) = +m_\psi\bar{\psi}\psi$.

The only difference between dynamical and background spin$_c$ valued connections is the possibility of imposing boundary conditions on the former. Since Dirichlet boundary conditions set the gauge field at the boundary to zero, imposing them will eliminate anomalous current flow onto the boundary from a dynamical Chern-Simons term. Hence, we do not need to put any additional chiral boundary modes to compensate for such currents. However, employing Dirichlet boundary conditions changes the boundary gauge symmetry to a global symmetry; thus, introducing a second global $U(1)$ symmetry into the theory. On the dual side, new boundary localized matter has to be added to account for this enhanced global symmetry. In this work, we will only consider Neumann boundary conditions on the dynamical gauge fields so that eq. (2.28) needs to be satisfied for all types of gauge fields. Additional dualities with Dirichlet boundary conditions on gauge fields have been outlined in [48].

We will see that the boundary modes associated with the fiducial fermions will be crucial in developing a consistent picture of boundary modes. This is particularly interesting when the Chern-Simons terms involved describe only background fields. In this case the fiducial

[6]This is to be contrasted with our definition of $S^{\pm}_{f}[\psi,\lambda,A]$ for the dynamical fermions. The latter were massless to begin with and we always took the Pauli-Villars mass to be negative and large. The superscript in that case only referred to the boundary conditions.

fermion still can contribute massless boundary modes, even though the Chern-Simons term does not involve any fluctuating fields. From the point of view of the low energy theory it appears that these fermionic boundary modes have to be added “by hand" in order for the duality to hold.

2.3 Dualities including boundaries

We now turn to establishing three-dimensional bosonization and particle-vortex duality in the presence of a boundary. Our starting point is the conjecture that dualities (2.1) and (2.2) are valid on $\mathbb{R}^{2,1}_{+}$ provided the boundary conditions are correctly applied to dynamical and fiducial fermions. From this conjecture, we will also be able to establish a web of Abelian dualities – i.e. scalar-vortex and fermion-QED$_3$ – in the presence of boundaries. The derivation will give us a setting to establish checks between chiral degrees of freedom on the boundary and Chern-Simons levels such that eq. (2.28) is satisfied at every step of the way. All partition functions in this and subsequent sections are understood to be defined on the half-space and distinct from their full-space equivalents.

2.3.1 Bosonization

Scalar+Flux = Fermion

Our conjecture for the form of the seed duality with a boundary starts with rewriting the flux attachment to Wilson-Fisher scalars using eq. (2.7),

$$\mathcal{Z}_{\text{WF+flux}}[A] = \int \mathcal{D}\varphi\, \mathcal{D}b\, e^{iS_{WF}[\varphi,b]+iS_{CS}[b+A]-iS_{CS}[A]}. \tag{2.32}$$

In this form, the coupling of the statistical gauge field b to the background A can be understood entirely in terms of the microscopic fiducial description via heavy fermions:

$$\mathcal{Z}_{\text{WF+flux}}[A] = \int \mathcal{D}\varphi\, \mathcal{D}b \prod_{j=1,2} \mathcal{D}\chi_j \mathcal{D}\lambda_j\, e^{iS_{WF}[b]+iS^{+}_{ff}[\chi_1,\lambda_1,b+A]+iS^{-}_{ff}[\chi_2,\lambda_2,A]}, \tag{2.33}$$

where once again the superscripts are chosen such that they generate the corresponding Chern-Simons terms appearing in eq. (2.32). Implicit in the above expression is the fact the

	Scalar + flux	**Fermion**
Boundary conditions	$\varphi = 0$	$\psi_+ = 0$
	$\partial_y b_i - \partial_i b_y = 0$	
Additional edge modes	Left-mover coupled to A	None
	Right-mover coupled to $b + A$	

Table 2.1: Summary of boundary conditions and additional edge movers for eq. (2.35).

gravitational Chern-Simons terms coming from each of the fiducial fermions cancel,

$$(iS_{CS}[b+A] + i\Omega) + (-iS_{CS}[A] - i\Omega) = iS_{CS}[b+A] - iS_{CS}[A]. \tag{2.34}$$

This particular combination of Chern-Simons terms will be used many times in what follows.

We should reemphasize that this rewriting has actual content in the case of a theory with boundary: Even though A is a non-dynamical background gauge field, $S^-_{ff}[\chi_2,\, \lambda_2,\, A]$ will give rise to massless chiral boundary modes associated with the fiducial fermion χ_2 despite working in the $|m_{\chi_2}| \to \infty$ limit. As noted above, from the perspective of the coarse-grained, Chern-Simons formulation of the theory in eq. (2.32) these gapless edge modes appear to be added by hand.

The fermionic side of the duality eq. (2.3) does not need any additional work: It is already in a form that makes the chiral edge modes obvious. We can simply apply the chiral boundary conditions on dynamical fermions ($\psi_+|_{y=0} = 0$) and Pauli-Villars regulator ($\lambda_-|_{y=0} = 0$). Our conjecture is then that

$$\begin{aligned}\mathcal{Z}_{\mathrm{WF+flux}}[A] \equiv \int \mathcal{D}\varphi\ \mathcal{D}b \prod_{j=1,2} \mathcal{D}\chi_j\, \mathcal{D}\lambda_j\ e^{iS_{WF}[b]+iS^+_{ff}[\chi_1,\,\lambda_1,b+A]+iS^-_{ff}[\chi_2,\,\lambda_2,\,A]} \\ \leftrightarrow \int \mathcal{D}\psi\ \mathcal{D}\lambda\, e^{iS^-_f[\psi,\lambda,\,A]} \equiv \mathcal{Z}_{\mathrm{f}}[A]\end{aligned} \tag{2.35}$$

holds as an equivalence at the conformal point. Additionally, we choose the dynamical gauge field to obey Neumann boundary conditions, $(\partial_y b_i - \partial_i b_y)|_{y=0} = 0$, and the scalar to obey the Dirichlet condition, $\varphi|_{y=0} = 0$. These results are summarized in Table 2.1.

In order to establish some guiding principle for the conjectured duality of CFTs, we can gap both theories and track whether our putative equivalence holds for positive and negative mass deformations. We will see the boundary conditions in our conjecture naturally arise by requiring the theory to be non-anomalous and have consistent global symmetries. With the correspondence of signs between fermion and scalar mass terms in the original bosonization duality in eq. (2.9) and the convention we've already chosen for fermions, the potential for the scalars is $V(\varphi) = -m_\varphi^2|\varphi|^2 + \alpha|\varphi|^4$. We should find consistent dualities between theories in the bulk and on the boundary for positive and negative mass deformations away from the CFT.

Let us start with the free fermion side of eq. (2.3). Making the mass deformation explicit, the action is given by the replacement

$$S_f^+[\psi, \lambda, A] \to S_f^+[\psi, \lambda, A] - m_\psi \bar{\psi}\psi \tag{2.36}$$

where $\psi_+|_{y=0} = 0$. In the IR limit of the theory, integrating out the massive degrees of freedom of the fermion yields

$$S_f = -\frac{1}{2}\left(1 - \mathrm{sgn}(m_\psi)\right)\left(iS_{CS} + i\Omega\right) \qquad \text{(IR Limit)}. \tag{2.37}$$

When the Pauli-Villars field and the fermion have the same sign of mass, corresponding to a $-iS_{CS}[A] - i\Omega$ Chern-Simons term, we need a single left-moving chiral edge mode to account for the anomalous term in order for this to be consistent with eq. (2.28). Since $m_\psi < 0$, the DWF which arises from our analysis of § 2.2.2 is exactly the anomaly cancelling edge mode we need. If instead we had imposed the condition $\psi_-|_{y=0} = 0$, then this would have suppressed the DWF. Hence, if we demand a non-anomalous theory, we are forced into choosing $\psi_+|_{y=0} = 0$.

We should now check to make sure everything is consistent for $m_\psi > 0$. In this case we get no ordinary or gravitational Chern-Simons terms and ψ's mass profile naturally gives rise to a right-moving DWF. It seems like we are in trouble. Fortunately, applying $\psi_+|_{y=0} = 0$ prevents any right-movers on the boundary. We are thus left with no chiral edge modes and eq. (2.28) is satisfied for both signs of m_ψ.

For the Wilson-Fisher scalar with flux, introducing a mass deformation $m_\varphi^2 < 0$ with our conventions for $V(\varphi)$ gives an overall positive mass term that corresponds to a gapped scalar. Flowing to the IR, the only term with b dependence is $iS_{CS}[b + A]$. As reviewed in above and in appendix B of [101], this theory is completely determined by its framing anomaly and thus equal to $-i\Omega$. This results in an overall $-iS_{CS}[A] - i\Omega$ Chern-Simons term, consistent with the fermionic side when $m_\psi < 0$.

We should also check that the anomaly inflow condition eq. (2.28) is still satisfied on this side of the duality. It is here where our microscopic description of the Chern-Simons term in eq. (2.33) will be important. Integrating out b caused the first Chern-Simons term to vanish leaving behind $-iS_{CS}[A] - i\Omega$. From the micrscopic perspective, this can be viewed as the condition

$$\int \mathcal{D}\chi\ \mathcal{D}\lambda\ \mathcal{D}b\ e^{iS_{ff}^{\pm}[\chi,\lambda,b+A]} = 1. \tag{2.38}$$

That is, the fiducial fermions provide no ordinary or gravitational Chern-Simons terms as well as no corresponding edge movers. Per our prescription, the remaining fiducial fermion associated with $-iS_{CS}[A] - i\Omega$ has the correct mass profile and boundary condition such that it contains a left-moving DWF. Thus, eq. (2.28) is satisfied.

To complete our discussion of massive phases we need to check that everything is consistent when $m_\varphi^2 > 0$. This gives a negative mass squared term in $V(\varphi)$, spontaneously breaking the emergent $U(1)$ in the scalar theory. This kills off the Chern-Simons term for b, and so integrating out φ and b leave behind no Chern-Simons terms. As expected, this means that the IR theory in the Higgs phase is identical to the 'vacuum' region. When $b = 0$, the edge modes of the fiducial fermions associated with $iS_{CS}[b + A]$ and $-iS_{CS}[A]$ have the same gauge coupling but opposite chiralities, and hence cancel one another. Since no Chern-Simons terms or fermions are left behind, there are no possible chiral modes that can arise and make this theory anomalous. Hence, we have found a consistent story for the duality on either side of the mass deformation.

That last step is to see if the scalar boundary conditions is constrained. To do so, we rely on our identification of global symmetry currents on either side of the duality, eq. (2.10). For

this purpose, it becomes useful to reinterpret the cancellation of the anomaly from eq. (2.28) in a slightly different, but equivalent, language. The Chern-Simons term of the bulk is anomalous on its own under the global $U(1)$ topological symmetry because the corresponding current has a nonzero divergence at the boundary. This seems to imply that the symmetry is broken at the boundary. However, the Chern-Simons anomaly is compensated via the axial $U(1)$ symmetry of the DWFs, and hence the theory is non-anomalous under a simultaneous topological $U(1)$ transformation in the bulk and the axial $U(1)$ transformation on the DWFs. If the two symmetries are identified, the global topological $U(1)$ symmetry is restored on the boundary by the transformation of the DWFs and is unbroken everywhere. This is in agreement with the fermion side of the duality where the global $U(1)$ symmetry of particle number is unbroken in the bulk and on the boundary.

Returning to the constraints on the boundary condition of the scalar, recall that the equations of motion for the scalar and Chern-Simons term tie the matter current to the topological current,

$$j^\mu_{\text{flux}} \equiv \frac{k}{2\pi}\epsilon^{\mu\nu\rho}\partial_\nu b_\rho = -j^\mu_{\text{scalar}}. \tag{2.39}$$

Here, j^μ_{scalar} is the usual scalar matter current and we have temporarily set the background fields to zero. However, as we have argued above, on the boundary it is not the flux which accounts for the topological $U(1)$ symmetry, but the DWFs. Hence, we should have $j^i_{\text{flux}}|_{y=0} = 0$ and by eq. (2.39) should also take $j^i_{\text{scalar}}|_{y=0} = 0$. Such a condition on the scalar current can only be achieved by Dirichlet boundary conditions, $\varphi|_{y=0} = 0$. Dirichlet boundary conditions are usually referred to as the "ordinary transition" boundary conditions of the $O(2)$ Wilson-Fisher fixed point. See [81] for a recent discussion.

The above constructions leads us to conjecture what happens to the DWFs at the conformal fixed point: As the mass deformation becomes smaller, according to eq. (2.27) the DWF becomes less and less localized to the boundary. In the massless limit, the DWF recombines with a DWF of opposite chirality living on – in the case of a finite interval $y \in [0, L]$ – the other boundary. Note that on the semi-infinite interval that we have used for $\mathbb{R}^{2,1}_+$, the

	Fermion + flux	**Scalar**
Boundary conditions	$\psi_- = 0$	$\varphi = 0$
	$\partial_y a_i - \partial_i a_y = 0$	
Additional edge modes	Left-mover coupled to $a + B$	None
	Right-mover coupled to a	

Table 2.2: Summary of boundary conditions and additional edge movers for eq. (2.40).

oppositely chiral fermion is not explicitly seen as the boundary condition at $y = L$ is replaced by a condition on the asymptotic behavior of the matter fields. At the conformal fixed point, we then have an ordinary Dirac fermion which lives in the bulk.

Fermion+Flux = Scalar

Having established a set of conventions in the first seed duality in the presence of a boundary, we can carry the above notation through into the second seed duality. Our conjecture is that

$$\begin{aligned}\mathcal{Z}_{\text{f+flux}}[B] \equiv \int \mathcal{D}\psi\ \mathcal{D}a\ \mathcal{D}\lambda_0 \prod_{j=1,2} \mathcal{D}\chi_j\, \mathcal{D}\lambda_j\ e^{iS_f^+[\psi,\lambda_0,a]+iS_{ff}^-[\chi_1,\lambda_1,a+B]+iS_{ff}^+[\chi_2,\lambda_2,a]} \\ \leftrightarrow \int \mathcal{D}\varphi\ e^{iS_{WF}[\varphi,B]} \equiv \mathcal{Z}_{\text{WF}}[B]\end{aligned} \tag{2.40}$$

holds as an equivalence at the conformal point. Once more, we have imposed Neumann boundary conditions on the dynamical gauge field a and Dirichlet boundary conditions on the scalar. These results are summarized in Table 2.2. We should recall the procedure that maps from eq. (2.3) to eq. (2.4) and make sure that it is consistent with our boundary picture.

In the bulk, this duality can be derived from the first seed duality by promoting the background spin_c valued connection A to a dynamical field, a, introducing an ordinary background $U(1)$ field B, and adding $-iS_{BF}[a, B] - iS_{CS}[B]$ to the action. Looking first at the scalar side of this procedure and starting with eq. (2.32), it becomes useful to define a new recipe for moving from the first seed duality to the second in the presence of a boundary by

rewriting the BF term:

> **New Promotion:** Promote A to a dynamical field, a, introduce a new background field B, and add $iS_{CS}[a] - iS_{CS}[a+B]$ to the action.

The Chern-Simons terms should be understood throughout the process in their microscopic descriptions with appropriate boundary conditions such that they give rise to chiral modes on the boundary to satisfy eq. (2.28). Once more, we have introduced the combination whose gravitational Chern-Simons terms cancel one another. Note the old and new promotions are completely equivalent in the bulk where there are no surface terms from integration by parts or chiral modes to consider on the boundary.

Applying this procedure to eq. (2.32) gives

$$\int \mathcal{D}\varphi \mathcal{D}a \mathcal{D}b \; e^{iS_{WF}[\varphi,b]+iS_{CS}[b+a]-iS_{CS}[a+B]}. \tag{2.41}$$

For brevity, we will leave the process of rewriting Chern-Simons terms as fermion and Pauli-Villars fields as implied moving forward. When integrating out the dynamical fields, we find in the absence of holonomies, an assumption we will always make from now on, $0 = b + a$, $0 = a + B$, and thus $b = -a = B$.

With the methods we used in the first seed duality, it is straightforward to establish a duality between non-anomalous theories in the second. After integrating out the dynamical fields, there are no ordinary or gravitational Chern-Simons terms left over for either mass deformation. This is easiest to understand on the scalar side. There are no Chern-Simons terms present regardless of the mass deformation, and hence, there are no edge movers required for the theory to be non-anomalous. Since the scalar fields give rise to no chiral edge modes, we are consistent with eq. (2.28).

Following our process for promotion for the free fermion gives

$$\mathcal{Z}_{\text{fermion+flux}}[B] = \int \mathcal{D}\psi \mathcal{D}a \; e^{iS_f[\psi,a]+iS_{CS}[a]-iS_{CS}[a+B]}. \tag{2.42}$$

In the IR limit, integrating out the fermion gives

$$S_{\text{fermion+flux}} = -\frac{1}{2}\left(1 - \text{sgn}(m_\psi)\right)\left(iS_{CS}[a] + i\Omega\right) - iS_{CS}[a+B] + iS_{CS}[a]. \tag{2.43}$$

For $m_\psi > 0$, integrating out the fermion gives no Chern-Simons terms, and the equations of motion for a imply $B = 0$; leaving behind no Chern-Simons terms and the edge modes of the fiducial fermions exactly cancel. For $m_\psi < 0$, the first and last Chern-Simons terms and DWFs cancel and we are left with a $-iS_{CS}[a + B] - i\Omega$. Here we can again find a theory completely determined by its framing anomaly and hence it can be replaced by $+i\Omega$.[7] Microscopically, this amounts to

$$\int \mathcal{D}\chi \; \mathcal{D}\lambda \; \mathcal{D}a \; e^{iS^{\pm}_{ff}[\chi,\lambda,a+B]} = 1. \tag{2.44}$$

This leaves behind no ordinary or gravitational Chern-Simons terms and hence no edge modes are left behind. Thus, we find that after integrating out the dynamical degrees of freedom requiring the absence of anomalies for each of the Chern-Simons terms individually gives us a consistent theory.

Note that the fiducial fermion picture may not seem strictly necessary in this duality since there are no nonzero Chern-Simons terms from mass deformations and hence no edge movers are necessary to make the theory non-anomalous. However, the fiducial fermions *do* play an integral role in the above analysis since they cancel the would-be dynamical DWF, which cannot be eliminated without additional edge movers.

As with the first duality, imposing boundary conditions on the scalar requires a closer look at the global symmetry currents. Choosing Neumann boundary conditions on the dynamical gauge field a implies a constraint to field configurations which obey $(\partial_y a_i - \partial_i a_y)|_{y=0} = 0$. This also means the topological current parallel to the boundary vanishes, since $j^i_{\text{flux}} \propto \partial_y a_i - \partial_i a_y$. Since this topological current should be identified with the particle number current on the scalar side of the duality, consistency requires $j^i_{\text{scalar}}|_{y=0} = 0$. Again, this can only be achieved by imposing Dirichlet boundary conditions on the scalar.

Lastly, one can easily check consistency of the above prescriptions by applying the promotions again to get back to the first seed duality. The only subtlety is the sign of all the

[7] This follows in an analogous manner to eq. (2.38). To see this, rewrite the dynamical spin$_c$ valued connection as the sum of a background spin$_c$ valued connection and a dynamical $U(1)$ connection $a = b + A$. Then, we can simply shift away the extra B to recover the usual expression.

Chern-Simons terms in the promotion need to be flipped. This means that our prescription is to promote B to a dynamical field in eq. (2.40), introduce a new background field A, add $+iS_{CS}[b+A] - iS_{CS}[A]$ to the action, and integrate out the dynamical fields. Following this through, we are left with the appropriate chiral modes for the remaining Chern-Simons terms to satisfy eq. (2.28).

Time-reversed dualities

The time-reversed version of the seed dualities follow in a completely analogous manner. Since the Chern-Simons terms are time-reversal odd, in order to satisfy eq. (2.28) we also need to swap the chiralities of the fermionic boundary terms. Other than the minor consistency check required by the fermionic and Pauli-Villars boundary conditions, the time-reversed analogs of eq. (2.3) and eq. (2.4) are

$$\begin{aligned}\bar{\mathcal{Z}}_{\text{WF}+\text{flux}}[A] \equiv \int \mathcal{D}\varphi\ \mathcal{D}b\ e^{iS_{WF}[\varphi,b]-iS_{CS}[b+A]+iS_{CS}[A]} \\ \leftrightarrow \int \mathcal{D}\psi\ \mathcal{D}\lambda\ e^{i\bar{S}_f^+[\psi,\lambda,A]} \equiv \bar{\mathcal{Z}}_{\text{f}}[A],\end{aligned} \tag{2.45}$$

and

$$\begin{aligned}\bar{\mathcal{Z}}_{\text{f}+\text{flux}}[B] \equiv \int \mathcal{D}\psi\ \mathcal{D}\lambda\ \mathcal{D}a\ e^{i\bar{S}_f^-[\psi,\lambda,a]+iS_{CS}[a+B]-iS_{CS}[a]} \\ \leftrightarrow \int \mathcal{D}\varphi\ e^{iS_{WF}[\varphi,B]} \equiv \bar{\mathcal{Z}}_{\text{WF}}[B].\end{aligned} \tag{2.46}$$

As in the previous versions of the dualities, we can simply identify the correct number of boundary modes needed to ensure the absence of anomalies by looking at the sign and level of the Chern-Simons term directly.

2.3.2 Particle-Vortex duality

Scalar-Vortex duality

Moving deeper into the web of dualities in [76, 101], we will start with finding the influence of a boundary on

$$\overline{\mathcal{Z}}_{\text{WF}}[C] \leftrightarrow \mathcal{Z}_{\text{scalar-QED}}[C]. \tag{2.47}$$

Beginning with eq. (2.40), this duality is derived by promoting B to be dynamical, introducing a new background field C, and adding $-iS_{CS}[b] + iS_{CS}[b+C] - iS_{CS}[C]$ to both sides of the duality. Note these terms are equivalent to $iS_{BF}[b, C]$ in the absence of boundaries. However, there would appear to be an issue of applying our fiducial fermion prescription to this duality. That is we have Chern-Simons terms of ordinary $U(1)$ – rather than spin$_c$ valued – connections.[8] The coupling of the fiducial fermions to such fields violates the relation forced by eq. (2.12) discussed in § 2.1. However, we can work around that by rewriting the BF term including a spin$_c$ valued connection as [58]

$$S_{BF}[b, C] = S_{CS}[b + C + A] - S_{CS}[b + A] - S_{CS}[C + A] + S_{CS}[A]. \tag{2.48}$$

Note that all of the gravitational Chern-Simons terms that would have accompanied each S_{CS} on the right hand side of eq. (2.48) cancel and have thus been ignored. Now, the promotion of the ordinary background connection, $B \to b$, and the subsequent coupling to another ordinary background connection C can be realized as a system of four fiducial fermions in the usual way.

Proceeding with the prescription, the scalar side of the duality becomes

$$\mathcal{Z}_{\text{scalar-QED}}[C] = \int \mathcal{D}\varphi \mathcal{D}b \, e^{iS_{WF}[\varphi,b]+iS_{CS}[b+C+A]-iS_{CS}[b+A]-iS_{CS}[C+A]+iS_{CS}[A]}. \tag{2.49}$$

The analysis of Chern-Simons terms and edge modes follows in a similar fashion to the WF + flux case. In the phase where the scalar is massive, the equations of motion for b imply

[8] Recall, a $U(1)$ Chern-Simons term is well defined modulo $\pi\mathbb{Z}$ in general. It is only picking a spin structure that makes it well defined modulo $2\pi\mathbb{Z}$.

$C = 0$, which causes the four Chern-Simons terms and associated edge modes cancel. In the Higgsed phase, $b = 0$, and once more all Chern-Simons terms cancel and there are no edge modes.

The modified fermionic theory is

$$\mathcal{Z}_{\mathrm{f}'}[C] = \int \mathcal{D}\psi\mathcal{D}\lambda\mathcal{D}a\,\mathcal{D}b\, e^{iS_f^+[\psi,\lambda,a]+iS_{CS}[a]-iS_{CS}[a+b]+iS_{CS}[b+C+A]-iS_{CS}[b+A]-iS_{CS}[C+A]+iS_{CS}[A]}. \tag{2.50}$$

Integrating out b implies $b = C - a$ and plugging this back into the above expression yields

$$\mathcal{Z}_{\mathrm{f}'}[C] = \int \mathcal{D}\psi\mathcal{D}\lambda\,\mathcal{D}a\, e^{iS_f^+[\psi,\lambda,a]+iS_{CS}[a-C]}. \tag{2.51}$$

Up to the sign of the mass terms, the two terms in the action of eq. (2.51) are exactly the time-reversed alternate seed duality, eq. (2.46), with $B \to -C$, so that[9]

$$\mathcal{Z}_{\mathrm{f}'}[C] = \overline{\mathcal{Z}}_{\mathrm{f+flux}}[-C] \leftrightarrow \overline{\mathcal{Z}}_{\mathrm{WF}}[C]. \tag{2.52}$$

This confirms the desired relation in eq. (2.47). This is consistent with the scalar-QED side of the duality.

There is one caveat to the use of the time reversed duality connected to our use of $\overline{\mathcal{Z}}_{\mathrm{WF}}$ rather than $\mathcal{Z}_{\mathrm{WF}}$. The time reversal operation changes the sign on the fermion mass term. This has the effect of flipping the relationship between the way mass deformations in the two scalar theories are mapped to one another: positive mass deformations in $\overline{\mathcal{Z}}_{\mathrm{WF}}$ correspond to *negative* mass deformations in $\mathcal{Z}_{\text{scalar-QED}}$. However, at the conformal fixed point $\overline{\mathcal{Z}}_{\mathrm{WF}}$ is completely equivalent to $\mathcal{Z}_{\mathrm{WF}}$. This is a nice check, since it reproduces the equivalence $m_\varphi^2 \leftrightarrow -m_{\varphi'}^2$ on the two sides of the bosonic particle-vortex duality.

Fermion-Vortex duality

The last duality we will consider in the presence of a boundary is the fermionic particle-vortex duality, which has some additional nuances. This duality,

$$\overline{\mathcal{Z}}_{\mathrm{f}}[A]e^{-\frac{i}{2}S_{CS}[A]} \leftrightarrow \mathcal{Z}_{\mathrm{QED}_3}[A], \tag{2.53}$$

[9]The $-iS_{CS}[a]$ term is hidden in our difference of Pauli-Villars masses in S_f and $\bar{S}_f$.

was originally formulated with theories which are $\mathcal{T}$-invariant on both sides, similar to the bosonic case [107].

Recall that with our definition of $\mathcal{Z}_f$ in eq. (2.5b) this partition function contains the contribution of the negative mass, heavy Pauli-Villars field λ. Often the regulator is treated as producing a level -$\frac{1}{2}$ Chern-Simons term when integrated out. More precisely, we get the η-invariant of A. This factor means that $\mathcal{Z}_\text{f}$ is not time reversal invariant: $m_\lambda \to -m_\lambda$. The purpose of the $e^{-\frac{i}{2}S_{CS}[A]}$ in eq. (2.53) is to cancel the η-invariant and produce a time-reversal invariant fermionic partition function. However, from our normalization in eq. (2.6a) we require that $k \in \mathbb{Z}$ for the Chern-Simons term to be gauge-invariant. Thus, multiplying with half-integer Chern-Simons terms is not a consistent procedure in a purely $2+1$ dimensional theory. To avoid this issue, this term can be viewed as arising as a boundary insertion in a theory on a $3+1$ dimensional bulk manifold, X [85, 112, 101]. More precisely, one promotes A to a spin$_c$ valued connection on X and adds

$$\frac{1}{8\pi}\int_X dA \wedge dA \tag{2.54}$$

to the Lagrangian. This promotion of A to a spin$_c$ valued connection is possible for any (orientable) choice of bulk X as all such $3+1$ dimensional manifolds admit a spin$_c$ structure. This cancels the contribution of the regulator; rendering the fermionic partition function real and both sides of the duality time-reversal invariant. All of this is perfectly valid in the $2+1$ dimensional bulk, but in the present context – where $\mathbb{R}^{2,1}_+$ would need to be realized as a boundary surface – this prescription fails. Indeed, had we proceeded through with multiplying $\mathcal{Z}_\text{f}$ in with $e^{\frac{i}{2}S_{CS}[A]}$ as in [76], we would have found the Chern-Simons levels of $\pm\frac{1}{2}$ on either side of the mass deformation. This is a clear contradiction with the assertion that the boundary is non-anomalous: We cannot generate "half" a DWF to satisfy eq. (2.28).

Thus we find that in order to have a purely $2+1$ dimensional description of fermionic particle-vortex duality, we must either abandon time-reversal invariance at the conformal fixed point or find some other means of canceling the η-invariant of A.

Let us first explore what happens when we give up time reversal invariance. It is no

longer necessary to transfer the $k = \frac{1}{2}$ Chern-Simons term from one side of the duality to the other. In this case, it will be convenient to begin our derivation with eq. (2.40). We then promote the background field to be dynamical, $B \to b$, and couple to a new background spin$_c$ valued connection A via $-iS_{CS}[b + A] + iS_{CS}[A]$, the fermion+flux side is

$$\mathcal{Z}_{\mathrm{QED}_3'}[A] = \int \mathcal{D}\psi\ \mathcal{D}\lambda\ \mathcal{D}a\ \mathcal{D}b\, e^{iS_f^+[\psi,\lambda,a] - iS_{CS}[a+b] + iS_{CS}[a] - iS_{CS}[b+A] + iS_{CS}[A]}. \tag{2.55}$$

where the prime is being used to distinguish this from $\mathcal{T}$-invariant QED$_3$. We proceed as usual in the IR limit and integrate out the dynamical fields a and b.[10] For $m_\psi > 0$ we find no Chern-Simons terms, while for $m_\psi < 0$ we find $iS_{CS}[A] + i\Omega$. The fiducial fermion associated with $iS_{CS}[A]$ provides the necessary right-mover.

Meanwhile, the scalar side yields

$$\mathcal{Z}_{\mathrm{scalar}'}[A] = \int \mathcal{D}\varphi\ \mathcal{D}b\ e^{iS_{\mathrm{WF}}[\varphi, b] - iS_{CS}[b+A] + iS_{CS}[A]}. \tag{2.56}$$

However, we recognize this as the time-reversed first seed duality, eq. (2.45). This ultimately gives

$$\mathcal{Z}_{\mathrm{QED}_3'}[A] \leftrightarrow \overline{\mathcal{Z}}_{\mathrm{f}}[A]. \tag{2.57}$$

Again, we end up with level-0 and 1 ordinary and gravitational Chern-Simons terms on either side of the mass deformation. This time, the dynamical fermion can provide consistent chiral edge modes satisfying eq. (2.28).

The other way to proceed is to insist on time-reversal invariance at the fixed point and doubly quantize the fields to avoid issues associated with half-integer Chern-Simons terms. With this redefinition of our fields, cancelling the $\mathcal{T}$-violating η-invariant term can be achieved with a term which meets the quantization requirements of eq. (2.6a). However, taking $A = 2A'$ for some new spin$_c$ valued connection A' is in violation of the spin-charge relation, which would mean such an effective theory is not relevant to usual condensed matter systems [101, 102].

[10] More precisely, we must integrate out a before b to avoid imposing conditions which violate the spin-charge relation of our connections, i.e. imposing $2b = -a - A$ [101]. The same condition prevents us from simplifying eq. (2.55) by integrating out b.

Following similar steps to that above, we find

$$\mathcal{Z}_{\mathrm{QED}_3''}[A] \equiv \int \mathcal{D}\psi\ \mathcal{D}\lambda\ \mathcal{D}a\ e^{iS_f^+[\psi,\lambda,2a]-2iS_{CS}[a]+2iS_{CS}[a+A]-2iS_{CS}[A]} \\ \leftrightarrow \int \mathcal{D}\psi\mathcal{D}\lambda\ e^{i\bar{S}_f^+[\psi,\lambda,\,2A]} = \bar{\mathcal{Z}}_{\mathrm{f}}[2A]. \tag{2.58}$$

It is straightforward to show edge movers are consistent with eq. (2.28) with an ordinary $U(1)$ connection fiducial fermion prescription, analogous to eq. (2.30),

$$e^{\pm iS_{CS}[B]} = \int \mathcal{D}\chi\,\mathcal{D}\lambda\ e^{iS_{ff}^{\pm}[\chi,\,\lambda,B]}. \tag{2.59}$$

One needs to keep in mind the double gauge field coupling causes the edge modes to contribute double the anomalous current, but this is still compensated by the Chern-Simons current inflow.

2.4 Lattice construction

In this section, we will build on recent work that realized the Abelian dualities in [76, 101] using exact techniques. We will consider the complex XY model on a Euclidean cubic lattice in $d = 3$ as in [27]. We will introduce a boundary to this formalism in order to find the microscopic description of one of the dualities described in § 2.3, the claim that scalars with flux are equivalent to a theory of fermions.

Our conventions for the lattice will be that the matter living at lattice sites are denoted by a subscript n and the link variables are labeled by $n\mu$ designated to mean pointing from site n in the direction $\hat{\mu}$. A boundary will be implemented by simply truncating the lattice in the y-direction, rendering it semi-infinite. We use the index β for sites on the boundary. Link variables transverse and parallel to the boundary will be denoted by βy and $\beta i \in \{\beta t,\, \beta x\}$, respectively.

To realize the scalar + flux theory, we start with the XY model for a complex scalar living at lattice site n, $\Phi_n \sim e^{i\theta_n}$ given in terms of a set of phase variables $\theta_n \in [0,\, 2\pi)$ and background $U(1)$ gauge fields living on links $A_{n\mu}$ by

$$\mathcal{Z}_{\mathrm{XY}}[A] = \Big(\prod_n \int_{-\pi}^{\pi} \frac{d\theta_n}{2\pi}\Big)\ \exp\Big\{\frac{1}{T}\sum_{n\mu}\cos(\theta_{n+\hat{\mu}} - \theta_n - A_{n\mu})\Big\} \equiv \int \mathcal{D}\theta\ e^{-\frac{1}{T}H_{XY}[A]}. \tag{2.60}$$

To generate the necessary Chern-Simons term, we will employ the trick of coupling eq. (2.60) to two-component Grassmann fields χ_n and $\bar{\chi}_n$. This is equivalent to our fiducial fermion prescription in the continuum case. The fermionic sector of the theory is given by

$$\mathcal{Z}_{\mathrm{W}}[A] = \prod_n \int d^2\bar{\chi}_n d^2\chi_n \; e^{-H_W[A](M) - H_{\mathrm{int}}(U)}, \tag{2.61}$$

where the Wilson action H_W and hopping-hopping interaction H_{int} are

$$-H_W[A](M) = \sum_{n\mu} \left(D_{n\mu} e^{-iA_{n\mu}} + D^*_{n\mu} e^{iA_{n\mu}} \right) + \sum_n (M - R)\bar{\chi}_n \chi_n, \tag{2.62a}$$

$$-H_{\mathrm{int}}(U) = U \sum_{n\mu} D_{n\mu} D^*_{n\mu}. \tag{2.62b}$$

with $D_{n\mu}$ and $D^*_{n\mu}$ the fermionic forward and backward hopping terms, respectively

$$D_{n\mu} \equiv \left(\bar{\chi}_n \frac{\sigma^\mu + R}{2} \chi_{n+\hat{\mu}} \right), \qquad D^*_{n\mu} \equiv \left(\bar{\chi}_{n+\hat{\mu}} \frac{-\sigma^\mu + R}{2} \chi_n \right). \tag{2.63}$$

This particular form of H_{int} is chosen in [27] to reproduce the known continuum results. Similar to the continuum theory, integrating out these Wilson fermions will produce the Chern-Simons term. However, as a consequence of fermion doublers, the level of the resulting Chern-Simons theory is dependent on the relative magnitudes of M and the Wilson term, R, as well as the sign of R. Compiling the above components of the theory and including the analog of the dynamical $U(1)$ gauge field present in the continuum theory, the scalar coupled to flux is

$$\mathcal{Z}[A] = \int \mathcal{D}a \; \mathcal{Z}_{\mathrm{XY}}[a] \, \mathcal{Z}_{\mathrm{W}}[A - a], \qquad \int \mathcal{D}a \equiv \prod_{n\mu} \int_{-\pi}^{\pi} \frac{da_{n\mu}}{2\pi}. \tag{2.64}$$

For the remainder of this section, we will assume $|R| = 1$, which is motivated by reflection positivity. Additionally, we assume we have chosen T, $U \lesssim 0$, and $M \lesssim 6$ in order to hit the IR critical point, as explained in [27].[11] That is, these values are tuned such the theory eq. (2.64) flows in the IR to

$$\mathcal{Z}_{\mathrm{W}}[A] = \prod_n \int d^2\bar{\chi}_n d^2\chi_n \; e^{-H_W[A](M') - H_{\mathrm{int}}(U')}, \tag{2.65}$$

[11] We have chosen to define eqs. (2.62a) and (2.62b) such that it matches [54, 63, 104, 70] and thus differs slightly from that of [27]. To translate back, take $(M - 3R) \to M$ and then $R \to -R$.

with $M' = 6$ and $U' = 0$.

Boundary conditions

To study the effect of the presence of a boundary on eq. (2.64), we need to understand how boundary conditions come about on the site and link variables. We will start with the scalar fields, Φ_β. Ideally, we would have a direct analogy to the continuum case where either Neumann or Dirichlet boundary conditions are possible. The former can be implemented by requiring the scalar hopping terms perpendicular to the boundary vanish. However, due to our construction of scalar fields as having magnitude one, $\Phi_n \sim e^{i\theta_n}$, it is not actually possible to enforce Dirichlet boundary conditions, i.e. $\Phi_\beta = 0$. Instead, we will enforce Dirichlet boundary conditions by requiring the scalar current along the boundary to be zero.

The fermionic boundary conditions are such that either

$$P_+\chi_\beta = \bar{\chi}_\beta P_- = 0, \qquad \text{or} \qquad P_-\chi_\beta = \bar{\chi}_\beta P_+ = 0, \tag{2.66}$$

extremize the boundary variation term [106]. We will use as our convention $\sigma^{\hat{y}} = \begin{pmatrix} 1 & 0 \\ 0 & -1 \end{pmatrix}$ such that the chiral projectors in eq. (2.66) are $P_\pm = \frac{1}{2}(1 \pm \sigma^{\hat{y}})$. From the assumption that $|R| = 1$ and up to a sign, the chiral projectors are equivalent to the matrices $\frac{1}{2}(\pm\sigma^{\hat{y}} - R)$ appearing in the fermionic hopping terms perpendicular to the boundary in eqs. (2.62a) and (2.62b). Either of the conditions in eq. (2.66) will remove one chiral mode worth of degrees of freedom, while the other chiral mode is left unconstrained. These conditions can be compared to those in eq. (2.22) and be seen to agree – albeit by construction [106].

Lastly, we need to consider the link variables. We again draw inspiration for the appropriate boundary conditions from the continuum case. That is, Neumann boundary conditions correspond to the condition that plaquettes perpendicular and adjacent to the boundary must vanish. On the lattice, this will correspond to the constraint

$$a_{\beta i} + a_{(\beta+\hat{i})y} - a_{(\beta+\hat{y})i} - a_{\beta y} = 0. \tag{2.67}$$

Alternatively, we could choose Dirichlet boundary conditions which simply require $a_{\beta i} = 0$. We would like to reproduce the results of the continuum duality eq. (2.35) and this will guide us in choosing the corresponding boundary conditions on the lattice.

Implementation

The main results of ref. [27] – following the choice of hopping-hopping interaction H_{int} – are contained in the identification of a suitable UV map for the conserved currents built out of θ_n and $a_{n\mu}$ into a theory of free fermions. Those theories are then flowed to the IR where one can then compare to continuum results. Following these general principles, we identify the effects of truncating the lattice at some arbitrary boundary site. We will show the derivation of [27] holds in the presence of a truncated boundary and is non-anomalous for $M > 0$ so long as $R = 1$ and the $P_- \chi_\beta = \bar{\chi}_\beta P_+ = 0$ boundary condition is chosen. We will also verify mass deformations away from the conformal fixed point yield equivalent results to the continuum case.

Recall the existence of a DWF at the boundary was of particular importance in our continuum picture for self-consistency checks away from the conformal point. A truncated lattice also gives rise to massless chiral modes localized to the boundary [104]. In particular, there are fermionic modes obeying

$$\Psi_\pm(x, y, t) = \xi(y)(1 \pm \sigma^{\hat{y}})\psi_\pm, \qquad \xi(y) \equiv [1 - F^2(k_\mu)]^{\frac{1}{2}}[F(k_\mu)]^y \tag{2.68}$$

with $\psi_\pm$ a right/left helicity eigenstate and

$$F(k_i) = R - M + R \sum_{i=t,x} (1 - \cos k_i). \tag{2.69}$$

For a given k_i, this solution can be normalized only if $|F(k_i)| < 1$ [104]. At the limit $|F(k_i)| = 1$ the DWF becomes a continuum eigenstate.

Now let's turn to the derivation of the duality. We will follow the derivation of ref. [27] and point out where subtleties of the boundary come into play. To begin, rewrite the bosonic

hopping term to make the bosonic currents explicit

$$e^{\frac{1}{T}\cos(\theta_{\beta+\hat{\mu}}-\theta_\beta-a_{\beta\mu})} = \sum_{j_{\beta\mu}=-\infty}^{\infty} I_{\beta_\mu}(T^{-1})\Phi_\beta\Phi^*_{\beta+\hat{\mu}}e^{-ia_{\beta\mu}j_{\beta\mu}}, \tag{2.70}$$

where I_j is the j^{th} modified Bessel function. As mentioned in the previous section, we will enforce Dirichlet boundary conditions on the scalar by requiring the scalar current in the boundary to vanish, i.e. $j_{\beta i} = 0$. The bosonic degrees of freedom can be integrated out explicitly and this simply enforces Gauss's law for the scalar currents at the boundary sites. By current conservation, this implies current onto the boundary also vanishes, $j_{\beta y} = 0$.

The implementation of boundary conditions for the Grassmann variable and their effect on eqs. (2.62a) and (2.62b) is more subtle. In the continuum case, one of these boundary conditions will kill off the DWF on the boundary, while the other will leave it untouched. This had important implications relating to the anomalous nature of the theory. Is this feature also realized in the lattice? To see this is still consistent with the Callan-Harvey mechanism on either side of the mass deformation, we need to take a closer look at the interplay between Chern-Simons terms and DWFs on the semi-infinite lattice.

On the lattice, the Chern-Simons term is determined by the masses of the $2^3 = 8$ chiral Dirac fermion modes in the continuum. These correspond to the eight extrema of the Brillouin zone at $k_{t,x,y} = \{0, \pi\}$. The effective masses of these eights modes are determined by [54, 27]

$$m_{\text{eff}}(k_\mu) = M - R\sum_\mu(1 - \cos k_\mu). \tag{2.71}$$

Since the value of R is important in eqs. (2.69) and (2.71), we should see if we can first fix its sign. Recall that it is the current of the Chern-Simons term flowing onto the boundary which renders the theory non-anomalous. This current is nonzero only when the R and M in eq. (2.62b) have the same sign [54]. Hence, given our choice of $M > 0$ we must take $R = 1$ to allow for anomaly inflow.

From eq. (2.63), the choice of $R = 1$ has the effect of projecting onto the right-moving chiral mode for hopping terms perpendicular to the boundary. For reasons that will become

Brillouin Zone	**Chirality**	**Mass Parameter**		
Extremum, k_μ		$M = 6 - \epsilon$	$M = 6$	$M = 6 + \epsilon$
$(0, 0, 0)$	R	$+$	$+$	$+$
$(0, 0, \pi)$	L	$-$	$-$	$-$
$(0, \pi, 0)$	L	$-$	$-$	$-$
$(\pi, 0, 0)$	L	$-$	$-$	$-$
$(0, \pi, \pi)$	R	$+$	$+$	$+$
$(\pi, \pi, 0)$	R	$+^*$	$+$	$+$
$(\pi, 0, \pi)$	R	$+$	$+$	$+$
(π, π, π)	L	$+^*$	0	$-$
Total CS Level		1	$\frac{1}{2}$	0
Total DWF		one R, one L	none	none

Table 2.3: Chirality, mass, and existence of a DWF for the eight modes at the extremum of the Brillouin zone, $k_\mu = (k_t, k_x, k_y)$, as calculated using eqs. (2.69) and (2.71). Positive and negative masses are denoted by a $+$ and $-$, respectively and an astrix denotes a mode which meets the condition to be a DWF.

clear shortly, the correct fermionic boundary condition to choose in this case is $P_- \chi_\beta = \bar{\chi}_\beta P_+ = 0$. Together with the choice of R, this implies $D^*_{\beta y} \neq 0$ and $D_{\beta y} \neq 0$ in general. Had we chosen the opposite boundary conditions or $R = -1$ we would have found no current flow onto the boundary.

With R fixed, the value of M – or equivalently, M' of eq. (2.61) – determines both the Chern-Simons level and the existence of DWFs for each of the k_μ. For our present purposes, we will only be concerned with the behavior of the theory in the vicinity of the critical mass, $M = 6$, and so we will check the behavior of the k_μ extrema for these values.

Our results are summarized in Table 2.3. For $M = 6$, corresponding to the IR fixed point,

the Chern-Simons term is level-$\frac{1}{2}$ and there are no DWFs. More precisely, the would-be DWF is at the limit where $|F(k_i)| = 1$ and has become a continuum eigenstate. This is consistent with the proposed continuum behavior at the conformal fixed point. For $M' = 6 + \epsilon$, the Chern-Simons level is zero and we have no DWFs since eq. (2.69) is not satisfied for any k_i. Again, this is in agreement with eq. (2.28).

$M' = 6 - \epsilon$ is slightly more subtle. This value corresponds to the UV sector of the theory where we need to level-1 Chern-Simons to generate the $e^{iS_{CS}[A-a]}$ term as well as negative mass deformations at the IR fixed point. For this case we find a Chern-Simons level of 1 and two DWFs, since both $k_\mu = (\pi, \pi, 0)$ and $k_\mu = (\pi, \pi, \pi)$ satisfy eq. (2.69). However, this is where our fermionic boundary conditions we enforced earlier come back into play. Since we have a Chern-Simons level of 1, we have chosen our boundary condition to kill off the left-mover, namely $P_- \chi_\beta = \bar{\chi}_\beta P_+ = 0$. This gives the correct chiral modes on the boundary to satisfy eq. (2.28). Interestingly, since they supply a level-$\frac{1}{2}$ Chern-Simons term with no DWF, it is the fermion doublers that play the role of the Pauli-Villars regulator on the lattice. Thus, we are self-consistent with the Callan-Harvey mechanism all the way through. This analysis follows similarly for $M < 0$ in which case we would need to choose $R = -1$ and kill off right-movers with the fermionic boundary condition.

Note that by imposing the fermionic boundary conditions, we have fixed two of the Grassmann variables we would normally integrate over on the boundary sites. The fermionic current conservation imposed by Grassmann integration will still hold for such links, but now each site has only two Grassmann degrees of freedom instead of four. The contribution of the double hopping/interaction term with any boundary site is very limited in such cases, since it already contains both Grassmann degrees of freedom. To have a non-vanishing contribution it must be isolated from any other links.

Finally, we need to understand the effect of the Neumann boundary conditions on the dynamical gauge field, i.e. eq. (2.67). The bulk integration over the link variables tied the bosonic and fermionic currents together. From the above construction, the boundary scalar current vanishes, which would seem to imply the boundary fermionic current does as well.

This would present a problem for satisfying eq. (2.28) if not for the gauge field boundary conditions. Enforcing eq. (2.67) on, e.g., the βi link kills off the link integration along the boundary and transforms the fermionic current terms as

$$D_{\beta i} e^{-i(A_{\beta i} - a_{\beta i})} \qquad \rightarrow \qquad D_{\beta i} e^{-i(A_{\beta i} + a_{(\beta+\hat{i})y} - a_{(\beta+\hat{y})i} - a_{\beta y})}. \tag{2.72}$$

Hence, there is no tying of the fermionic current to the vanishing scalar current, but we should still verify that is possible to get a non-vanishing fermionic current on the boundary so our DWFs are still allowed solutions.

First, consider $e^{ia_{\beta y}}$, which naïvely would be problematic for the survival of terms like eq. (2.72) upon integration over the corresponding link variable unless it is canceled by $e^{-ia_{\beta y}}$ from somewhere else in the path integral. With no scalar current flowing onto the boundary, we could use fermionic current term such as $D^*_{\beta y} e^{i(A_{\beta y} - a_{\beta y})}$ to cancel $e^{ia_{\beta y}}$. However, such a term means the fermionic current flows off the boundary. Since the number of Grassmann variables at the site β is saturated by the two fermionic currents due to our fermion boundary conditions, a double-hopping term to return the fermionic current to the same site is forbidden. Relying on such a cancellation would mean the boundary fermionic current is only supported for a single link.

Fortunately, there are additional contributions that work to cancel $e^{ia_{\beta y}}$. Consider the form of eq. (2.72) for neighboring boundary links. The $(\beta - \hat{i})i$ link contains an exponential of the form $e^{-ia_{\beta y}}$ which can cancel $e^{ia_{\beta y}}$. This has the interpretation of a fermionic current flowing from the $(\beta - \hat{i})i$ link to the βi link. The cancellation generalizes over a chain of adjacent boundary links with nonzero fermionic current and causes all exponentials with dynamical gauge links perpendicular to the boundary to vanish.

The only remaining term the needs to be cancelled in eq. (2.72) is $e^{-ia_{(\beta+\hat{y})i}}$. This can easily be achieved by either the fermionic or bosonic currents living on the $(\beta+\hat{y})i$ link. Combining this with the cancellation of $e^{ia_{\beta y}}$ and $e^{-ia_{(\beta+\hat{i})y}}$, it is possible to have an uninterrupted fermionic current flowing along the boundary in spite of having chosen scalar boundary

conditions which set bosonic currents on the boundary to zero.[12] Furthermore, the chirality of this boundary current is set by our choice of fermionic boundary conditions. This is completely analogous to the continuum case.

2.5 Discussion

In this chapter, we presented a generalization of Abelian bosonization that remains valid in the presence of a boundary. Our main finding is that, for the duality to be valid in the presence of boundaries, one carefully needs to account for edge modes that are associated with Chern-Simons terms. Most importantly, we require edge modes even for Chern-Simons terms in the action that only involve non-dynamical fields. We implemented this consistently by replacing all Chern-Simons terms with heavy "fiducial" fermions.

Given the fact that even the $S_{BF}[b, C]$ term of eq. (2.48) can be rewritten using our fiducial fermion prescription to yield a consistent theory, a natural question one might ask if this is always the case. In other words, can we ever run into some combination of Chern-Simons terms which is consistent with the spin-charge relation of a spin$_c$ but cannot be rewritten in terms of our fiducial building blocks? Reassuringly, the answer appears to be no. In [58] it was shown that any consistently quantized Chern-Simons term which can be put on a spin$_c$ manifold can be rewritten as

$$S_{BF}[B, C] = S_{CS}[B + C + A] - S_{CS}[B + A] - S_{CS}[C + A] + S_{CS}[A], \tag{2.73a}$$

$$S_{CS}[B] + S_{BF}[B, A] = S_{CS}[A + B] - S_{CS}[A], \tag{2.73b}$$

$$16\mathrm{CS}_{\mathrm{g}} = 9S_{CS}[A] - S_{CS}[3A]. \tag{2.73c}$$

All such terms lend themselves to a description in terms of fiducial fermions.

From a condensed matter perspective, the fermionic particle/vortex was originally proposed as a $\mathcal{T}$-symmetric UV completion of the half-filled lowest Landau level. However, the

[12] It is also possible to have a nonzero fermionic current on the boundary with Dirichlet boundary conditions on the gauge field. This is still consistent with the continuum case, but would require killing off edge movers in order to get a non-anomalous theory.

need to view it as the surface of a $3+1$ dimensional topological insulator lead the authors of [112, 114] to conclude that there is no strictly $2+1$ dimensional UV completion for this system. Our analysis suggests such a completion does exist so long as one is willing to lose the spin-charge relation of a spin_c valued connection or $\mathcal{T}$-invariance. One can ask whether the projection onto the lowest Landau level is somehow inconsistent with formulating the theory on a spin_c manifold. If such inconsistencies arise, then the doubly quantized theory would provide a purely $2+1$ dimensional UV completion that is manifestly $\mathcal{T}$ invariant. This would require a rigorous study of lowest Landau level projectors on spin_c manifolds – a problem we leave to future work.

Since there have been other microscopic descriptions of the bulk Abelian dualities, e.g. [90, 89], one could wonder how those models realize the boundary physics as presented above. In [90], a discrete 2+1 dimensional lamination of 1-dimensional quantum wires was used to derive the Abelian bosonization and particle-vortex duality. Each wire supporting a 1+1-dimensional continuum theory suggests a natural microscopic realization of the above results; the study of which is also left for future work.

Obvious questions we have not addressed in this work are generalizations to the non-Abelian case or to theories with interfaces rather than boundaries. The former has been explored by some authors of this work in [13]. Lastly, left unexplored in this analysis among the transitions enumerated in [81] are the "extraordinary" type where the boundary scalar gets a vev and drives a surface transition in addition to gapping the bulk. That the extraordinary transition is believed to admit no relevant boundary deformations sets it apart from the boundary conditions studied in this work and warrants further study in the context of the $2+1$ dimensional dualities studied here. A rich network of dualities making along these lines has been laid out in [48] based on conjectures about the infrared behavior of "duality walls". It would be very interesting to generalize our work to these other options as well.

Chapter 3

DERIVING NEW DUALITIES: QUIVER GAUGE THEORIES

Disclaimer: *This work was done in collaboration with Kyle Aitken, Andreas Karch and Changha Choi. The author conceived and contributed to most aspects of the work discussed here.*

Prior to the publication of the work discussed in this section, the pool of bosonization dualities was limited to the original duality laid out by Aharony [2]:

$$SU(k)_N \text{ with } N_f \ \phi \qquad \leftrightarrow \qquad U(N)_{-k+\frac{N_f}{2}} \text{ with } N_f \ \psi, \tag{3.1a}$$

$$U(k)_N \text{ with } N_f \ \phi \qquad \leftrightarrow \qquad SU(N)_{-k+\frac{N_f}{2}} \text{ with } N_f \ \psi \tag{3.1b}$$

and the "master" duality of Benini and Jensen [24, 64] where each side of the duality has fermions and scalars which interact through a quartic interaction:

$$SU(N)_{-k+\frac{N_f}{2}} \text{ with } N_s \ \phi \text{ and } N_f \ \psi \qquad \leftrightarrow \qquad U(k)_{N-\frac{N_s}{2}} \text{ with } N_f \ \Phi \text{ and } N_s \ \Psi. \tag{3.2}$$

Both of these are subject to the "flavor bound" $N_f \leq k$. In this work we deepen this pool by using the master duality and holographic methods similar to those developed in [65] to derive novel Bose-Bose dualities between non-Abelian linear quivers. We argue that these dualities can be viewed as a natural generalization of the bosonic particle-vortex duality to non-Abelian gauge groups since the quivers share many of the qualitative features present in the particle-vortex duality.

Of particular interest is the application of these dualities to $2+1$-dimensional defects in Yang-Mills theory on $\mathbb{R}^4$, which will be the focus of the latter half of this paper. It has recently been shown that there is a mixed 't Hooft anomaly between time-reversal symmetry and center symmetry at $\theta = \pi$ [49]. This is rooted in the fact that $SU(N)$ YM theory is

believed to have N distinct vacua associated to N branches of the theory. Such branches are individually $2\pi N$ periodic and correspond to $SU(N)/\mathbb{Z}_N$ gauge theories. This seems to contradict the long held belief that θ is 2π periodic in $SU(N)$ YM theory, but the conflict is resolved since the vacua interchange roles under a 2π transformation. More specifically, if one tracks the true ground state of the theory, one changes branches in a single 2π period. Thus, as theta is varied from, say $\theta = 0$ to $2\pi n$, the theory traverses several vacua. However, this changes when one couples the one-form center symmetry to a background (two-form) gauge field. In this case one cannot consistently choose the coefficient of the counterterm, sometimes referred to as the "discrete theta angle", to make the theory non-anomalous. Since this counterterm changes as one traverses branches, a spatially varying θ angle gives rise to domain walls separating regions with distinct discrete theta angle. Using anomaly inflow arguments, the effective field theory living on the interface is found to be a Chern-Simons gauge theory (see [49, 50] for more details).

Although anomaly considerations require a non-trivial theory to live on the interface, they alone do not fully fix the theory. Among others, $[SU(N)_{-1}]^n$ or $SU(N)_{-n}$ would be consistent choices.[1] The authors of [50] argue that, at least at $n \ll N$, $[SU(N)_{-1}]^n$ is the appropriate description for slowly varying theta (meaning that $|\nabla\theta| \ll \Lambda$ where Λ is the strong coupling scale of the confining gauge theory), whereas $SU(N)_{-n}$ is appropriate for a sharp interface such as a discrete jump by $2\pi n$ at a given location. If these are indeed the correct descriptions this suggests that there is a phase transition as one smooths out a given jump in θ. If this phase transition is second order, the transition point would be governed by a CFT which is most easily realized as a Chern-Simons-matter theory. In any case, this CFT can serve as a parent theory from which topological field theories, describing either the slowly varying as well as the sharp step, can be realized as massive deformation.

[1] Note that we are changing the direction of the θ gradient relative to [50] and so have negative levels for our Chern-Simons theories. This is in order to conform to the conventions of [66] for the stringy embeddings.

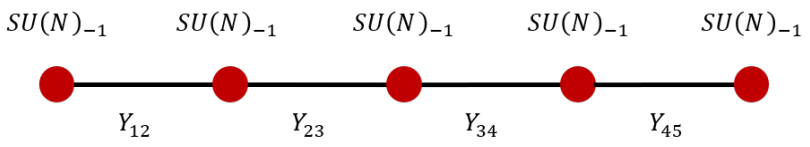

Figure 3.1: Parent Chern-Simons matter theory at the phase transition for the special case $n = 5$.

The conjectured CFT between the two extreme phases is schematically

$$[SU(N)_{-1}]^n + \text{bifundamental scalars} \tag{3.3}$$

which was used in ref. [50] to explain the transition between two different vacua of $(3+1)$-dimensional Yang-Mills. This parent CFT is based on a quiver gauge theory as displayed in Fig. 3.1. Each node depicts a $SU(N)_{-1}$ Chern-Simons gauge theory, the links connecting them represent bifundamental scalar fields, Y. The theory has two obvious massive deformations: we can give all the scalars a positive or a negative mass squared. In the former case the scalars simply decouple and we are left with the $[SU(N)_{-1}]^n$ TFT appropriate for slowly varying theta, in the latter case the gauge group factors get Higgsed down to the diagonal subgroup and we find the $SU(N)_{-n}$ associated with the steep defect. There are also mixed phases, where some of the Y have negative and some positive mass squared.

In this work, we propose a theory dual to (3.3) which is supported by both 3d bosonization of non-Abelian linear quivers and holographic duality. The proposed "theta wall" duality is

$$[SU(N)_{-1}]^n + \text{bifundamental scalars} \qquad \leftrightarrow \qquad U(n)_N + \text{adjoint scalars.} \tag{3.4}$$

We will see that this is a special case of the more general quiver dualities derived in Sec. 3.4 which do not include matter in the adjoint. This is a special feature of (3.4), owed to the fact that when all ranks of the SU quiver theory are equal, the U quiver contains nodes which are confining. With the careful addition of interactions in the proposed theories, mass deformations on either side of the duality yield TFTs which are level-rank dual to each other.

The paper is outlined as follows. In Sec. 3.1 we review the master duality and establish the conventions we use for the rest of the paper. Sec. 3.4 contains our derivation of the non-Abelian linear quiver dualities, including the details of how such dualities should be viewed as generalization of the particle-vortex duality. We then specialize to quivers applicable to theta interfaces in $3+1$-dimensional $SU(N)$ Yang-Mills theory in Sec. 3.3. Subsections 3.3.1 and 3.3.2 contain the 3d bosonization and holographic support for such dualities, respectively. In Sec. **??** we discuss our results and conclude. The appendix contains several details of our construction of the non-Abelian quivers.

As we were finalizing this work, we were made aware of [15] which studies domain walls in different phases of the Witten-Sakai-Sugimoto model. This has some overlap with Sec. 3.3.2, particularly regarding the nature of domain walls in the pure YM sector.

3.1 Review of 3d Bosonization

We begin by reviewing 3d bosonization and establish conventions we will use throughout this paper. The most general form of 3d bosonization, the so-called master bosonization duality [24, 64], is a conjecture that the following two Lagrangians share the same IR fixed point[2]

$$\begin{aligned}\mathcal{L}_{SU} &= \left|D_{b'+B+\tilde{A}_1+\tilde{A}_2}\phi\right|^2 + i\bar{\psi}\not{D}_{b'+C+\tilde{A}_1}\psi + \mathcal{L}_{\text{int}} - i\left[\frac{N_f-k}{4\pi}\text{Tr}_N\left(b'db' - i\frac{2}{3}b'^3\right)\right] \\ &\quad - i\left[\frac{N}{4\pi}\text{Tr}_{N_f}\left(CdC - i\frac{2}{3}C^3\right) + \frac{N(N_f-k)}{4\pi}\tilde{A}_1 d\tilde{A}_1\right], \qquad (3.5a)\\ \mathcal{L}_U &= |D_{c+C}\Phi|^2 + i\bar{\Psi}\not{D}_{c+B+\tilde{A}_2}\Psi + \mathcal{L}'_{\text{int}} - i\left[\frac{N}{4\pi}\text{Tr}_k\left(cdc - i\frac{2}{3}c^3\right) - \frac{N}{2\pi}\text{Tr}_k(c)d\tilde{A}_1\right] \qquad (3.5b)\end{aligned}$$

with the mass identifications $m_\psi \leftrightarrow -m_\Phi^2$ and $m_\phi^2 \leftrightarrow m_\Psi$. Our definitions of fields are shown in Table 3.1. We will use uppercase letters for background gauge fields, lowercase for dynamical gauge fields, and Abelian fields carry a tilde. This duality is subject to the

[2]Here we follow the conventions outlined in ref. [13]. We have dropped all gravitational Chern-Simons terms since they are not relevant for our purposes. Note there is a slight difference in convention in the sign of the BF term and the $\tilde{A}_2$ coupling on the U side of the duality. However since the difference always amounts to an even number of sign changes the TFTs still match under mass deformations. Additionally, the flux attachment procedure picks up two minus signs from this effect as well, meaning the quantum numbers of the baryon and monopole operators still match.

	Gauge Fields		Background Fields			
Symmetry	$SU(N)$	$U(k)$	$SU(N_s)$	$SU(N_f)$	$U(1)_{m,b}$	$U(1)_{F,S}$
Field	b'_μ	c_μ	B_μ	C_μ	$\tilde{A}_{1\mu}$	$\tilde{A}_{2\mu}$

Table 3.1: Various gauge fields used in the master duality. Dynamical fields are denoted but uppercase letters while background fields by lowercase. $\tilde{A}_{1\mu}$ is associated with the monopole/baryon number $U(1)$ symmetry also present in Aharony's dualities. $\tilde{A}_{2\mu}$ is associated to the $U(1)$ symmetry which couples to the additional fermion/scalar matter in the master duality.

flavor bound $(N_f, N_s) \leq (k, N)$, but excludes the case $(N_f, N_s) = (k, N)$.[3] Our notation for covariant derivatives is

$$\left(D_{b'+B+\tilde{A}_1+\tilde{A}_2}\right)_\mu \phi = \left[\partial_\mu - i\left(b'_\mu \mathbb{1}_{N_s} + B_\mu \mathbb{1}_N + \tilde{A}_{1\mu}\mathbb{1}_{NN_s} + \tilde{A}_{2\mu}\mathbb{1}_{NN_s}\right)\right]\phi, \tag{3.6a}$$

$$\left(D_{b'+C+\tilde{A}_1}\right)_\mu \psi = \left[\partial_\mu - i\left(b'_\mu \mathbb{1}_{N_f} + C_\mu \mathbb{1}_N + \tilde{A}_{1\mu}\mathbb{1}_{NN_f}\right)\right]\psi, \tag{3.6b}$$

$$\left(D_{c+C}\right)_\mu \Phi = \left[\partial_\mu - i\left(c_\mu \mathbb{1}_{N_f} + C_\mu \mathbb{1}_k\right)\right]\Phi, \tag{3.6c}$$

$$\left(D_{c+B+\tilde{A}_2}\right)_\mu \Psi = \left[\partial_\mu - i\left(c_\mu \mathbb{1}_{N_s} + B_\mu \mathbb{1}_k + \tilde{A}_{2\mu}\mathbb{1}_{kN_s}\right)\right]\Psi. \tag{3.6d}$$

The interaction terms are

$$\mathcal{L}_{\text{int}} = \alpha\left(\phi^{\dagger a_c a_s}\phi_{a_c a_s}\right)^2 - C\left(\bar{\psi}^{a_c a_f}\phi_{a_c a_s}\right)\left(\phi^{\dagger b_c a_s}\psi_{b_c a_f}\right) \tag{3.7a}$$

$$\mathcal{L}'_{\text{int}} = \alpha\left(\Phi^{\dagger a_c a_f}\Phi_{a_c a_f}\right)^2 + C'\left(\bar{\Psi}^{a_c a_s}\Phi_{a_c a_f}\right)\left(\Phi^{\dagger b_c a_f}\Psi_{b_c a_s}\right) \tag{3.7b}$$

where a_c, b_c are indices associated with the color symmetries; a_f, b_f with the $SU(N_f)$ symmetry; and a_s, b_s with the $SU(N_s)$ symmetry.

As mentioned in the introduction, Aharony's dualities (3.1) can be found by taking the $N_s = 0$ and $N_f = 0$ limits of (3.5). For example, Aharony's duality (3.1a) is the $N_f = 0$

[3]There are proposals for dualities describing the phase structure of these theories slightly beyond the bounds [80], but such cases will not be relevant for this work.

limit and is an IR duality between Lagrangians of the

$$\mathcal{L}_{SU} = \left|D_{b'+B+\tilde{A}_1}\phi\right|^2 - i\left[-\frac{k}{4\pi}\mathrm{Tr}_N\left(b'db' - i\frac{2}{3}b'^3\right) - \frac{Nk}{4\pi}\tilde{A}_1 d\tilde{A}_1\right], \tag{3.8a}$$

$$\mathcal{L}_U = i\bar{\Psi}\not{D}_{c+B}\Psi - i\left[\frac{N}{4\pi}\mathrm{Tr}_k\left(cdc - i\frac{2}{3}c^3\right) - \frac{N}{2\pi}\mathrm{Tr}_k(c)d\tilde{A}_1\right] \tag{3.8b}$$

which are subject to the flavor bounds $N_s \leq k$.

We will use the η-invariant convention where a positive mass deformation for the fermion will not change the level of the Chern-Simons term. When compared to the often employed convention where an ill defined naive Dirac operator gets augmented with an half integer Chern-Simons term this means we replace [122, 123]:

$$i\bar{\psi}\not{D}_A\psi - i\left[-\frac{N_f}{8\pi}\mathrm{Tr}_N\left(AdA - i\frac{2}{3}A^3\right)\right] \qquad \rightarrow \qquad i\bar{\psi}\not{D}_A\psi. \tag{3.9}$$

We will continue to denote fermion half-levels when specifying the Chern-Simons theory.

3.2 Non-Abelian Linear Quiver Dualities

We now turn to constructing linear quivers using the master duality. As explained in the introduction, we are ultimately motivated by the theta wall construction that leads to (3.4), but we will derive dualities for a far more general case. We will begin with recasting the 3d bosonization derivation of bosonic particle-vortex duality in a way that highlights the relation to the non-Abelian quivers.

3.2.1 Bosonic Particle-Vortex Duality

To derive the bosonic particle-vortex duality we will use 3d bosonization techniques similar to those used in refs. [76, 101]. We then show how one can reinterpret the derivation in terms of a two-node quiver. This will be the simplest non-trivial case of the far more general quivers we derive in Sec. 3.2.2. We will drop tildes from Abelian gauge fields in this subsection since the distinction is not necessary.

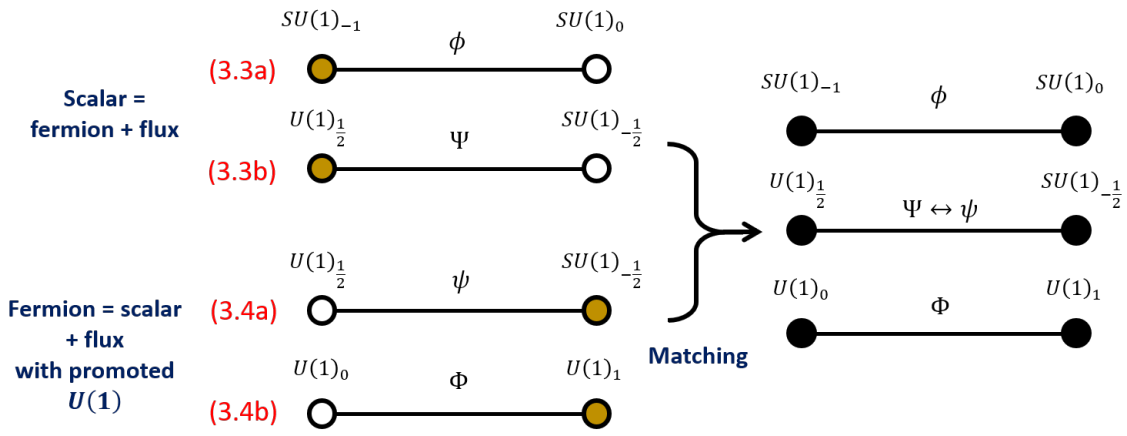

Figure 3.2: Derivation of the bosonic particle-vortex duality as a duality between two node linear quiver theories. On the left-hand side, we have represented each side of Aharony's Abelian dualities as a two-node quiver. The filled yellow circle represents the color gauge group while the empty circle represents promoted global symmetries (which for the case of $SU(1)$ are placeholders). The equation numbers corresponding to the two-node quivers are shown in red. Since the two fermionic theories are the same, one can perform a matching to arrive at a duality between three two-node quiver theories, the top and bottom of which are the XY and Abelian Higgs models, respectively.

Recall the bosonic particle-vortex duality states that, at low energies, the XY model is dual to the Abelian Higgs model [95, 42],

$$\mathcal{L}_{\text{XY}} = |D_{A_1}\phi|^2 \qquad \leftrightarrow \qquad \mathcal{L}_{\text{AH}} = |D_c\Phi|^2 - i\left[-\frac{1}{2\pi}cdA_1\right]. \tag{3.10}$$

The mapping of the phases is such that positive mass deformations on one end maps to a negative deformation on the other end, $m_\Phi^2 \leftrightarrow -m_\phi^2$.

In order to derive (3.10) we start by taking the Abelian limit of Aharony's dualities, (**??**). In particular, take the $N = k = N_f = 1$ and $N_s = 0$ limit of (3.5), which yields the "scalar + $U(1)_1 \leftrightarrow$ free fermion" duality,

$$\mathcal{L}_{SU} = i\bar{\psi}\not{D}_{A_1}\psi \tag{3.11a}$$

$$\mathcal{L}_{U} = |D_c\Phi|^2 - i\left[\frac{1}{4\pi}cdc - \frac{1}{2\pi}cdA_1\right], \tag{3.11b}$$

with $m_\psi \leftrightarrow -m_\Phi^2$. Meanwhile, the "fermion + $U(1)_{-1/2} \leftrightarrow$ WF scalar" duality is obtained by taking the $N = k = N_s = 1$ and $N_f = 0$ limit,

$$\mathcal{L}_{SU} = |D_{A_1}\phi|^2 - i\left[-\frac{1}{4\pi}A_1dA_1\right], \tag{3.12a}$$

$$\mathcal{L}_{U} = i\bar{\Psi}\not{D}_c\Psi - i\left[\frac{1}{4\pi}cdc - \frac{1}{2\pi}cdA_1\right], \tag{3.12b}$$

with $m_\phi^2 \leftrightarrow m_\Psi$.

Deriving the bosonic particle-vortex duality from the above two dualities is straightforward. Note that we already have the XY model in (3.12a) up to the additional background Chern-Simons term. Hence, we should look for another bosonic theory dual to (3.12b). To do so, add $-i\left[\frac{1}{4\pi}A_1dA_1 - \frac{1}{2\pi}A_1dB_1\right]$ to each side of (3.11) and promote the $U(1)$ background field to be dynamical, $A_1 \to a_1$. This gives the dual theories

$$\mathcal{L}'_{SU} = i\bar{\psi}\not{D}_{a_1}\psi - i\left[\frac{1}{4\pi}a_1da_1 - \frac{1}{2\pi}a_1dB_1\right] \tag{3.13a}$$

$$\mathcal{L}'_{U} = |D_c\Phi|^2 - i\left[\frac{1}{4\pi}cdc - \frac{1}{2\pi}cda_1 + \frac{1}{4\pi}a_1da_1 - \frac{1}{2\pi}a_1dB_1\right]. \tag{3.13b}$$

Since the action is quadratic in the newly promoted a_1 field we can integrate it out, which imposes the constraint $a_1 = c + B_1$. Plugging this in, we find

$$\mathcal{L}'_U = |D_c\Phi|^2 - i\left[-\frac{1}{2\pi}cdB_1 - \frac{1}{4\pi}B_1dB_1\right]. \tag{3.14}$$

After relabeling the dynamical field in (3.13a) as $a_1 \to c$ and changing the background field $B_1 \to A_1$, we see (3.13a) matches (3.12b), and thus (3.14) is dual to (3.12a). Canceling the common background Chern-Simons term, we arrive at the usual particle-vortex duality, (3.10). Note we get the relative mass flipping between the two ends of the duality since there is only a relative sign flip between ψ and Φ masses.

We would now like to recast the derivation we just performed to motivate generalization to a two-node linear quiver. Fig. 3.2 schematically shows how we would like to view the derivation. Each of our dual theories in (3.12) and (3.13) can be viewed as a two-node linear quiver, with the matter bifundamentally charged under the two nodes which it connects.

This is motivated by the fact that in Aharony's dualities (3.1), each matter field is fundamentally charged under both a dynamical gauge field and background global flavor symmetry. If we were to promote said flavor symmetry to be dynamical, the matter becomes a bifundamental and thus admits a natural description as a two node quiver. This looks rather trivial since $SU(N)$ gauge groups for $N = 1$ are nonsensical, but will generalize nicely for $N \geq 2$. For the Abelian case we will use $SU(1)$ as a placeholder for symmetries that can be gauged in the more general case.

To see this on the Abelian Higgs side, we will first shift the dynamical gauge field, $c \to c + a_1$, so that (3.13b) becomes

$$\mathcal{L}''_U = |D_{c+a_1}\Phi|^2 - i\left[\frac{1}{4\pi}cdc - \frac{1}{2\pi}a_1dB_1\right]. \tag{3.15}$$

In this form the scalar is bifundamentally charged under two $U(1)$ gauge groups, which represent the two nodes in the quiver theory. The dual to the Abelian Higgs model, (3.13a), couples to a single dynamical $U(1)$ gauge field, a_1. This was previously the flavor symmetry but was promoted to a gauge symmetry in moving from (3.11) to (3.13). As mentioned

above, the gauge field belonging to the second node is absent only because we are working in the Abelian limit of Aharony's dualities. On the XY model end of the duality (3.12a), ϕ couples to two $SU(1)$ fields, so it has no gauge couplings at all.[4]

The upshot of recasting the derivation in this form is that it readily generalizes to more complicated two-node quivers. One can use the more general Aharony's dualities to perform very similar steps as was done in the Abelian case. We'll see particle-vortex duality generalizes to a duality of the form

$$SU(N_1)_{-k_1} \times SU(N_2)_{-k_2} + \text{bifundamental scalar} \qquad \leftrightarrow \qquad U(k_1)_{N_1-N_2} \times U(k_1+k_2)_{N_2} + \text{bifundamental scalar}. \quad (3.16)$$

The bosonic particle-vortex duality is then just the $N_1 = N_2 = k_1 = 1$ and $k_2 = 0$ case. In Sec. 3.2.3 we present further evidence of this interpretation by matching the spectrum of particles and vorticies in (3.16) in a manner similar to the Abelian case. Before we do this we demonstrate how we can systematically construct the non-Abelian quivers for an arbitrary number of nodes. This requires the use of the master duality when the number of nodes is greater than two.

3.2.2 Building Non-Abelian Linear Quiver Dualities

Following the discussion in the previous subsection, our strategy in deriving dual descriptions of quiver gauge theories is to start with the master duality and gauge global symmetries on both sides of the duality in order to arrive at a duality for the resulting product gauge group. Since in a quiver gauge theory the gauge group associated with a given node sees the gauge groups associated with the neighboring nodes as global flavor symmetries, this roughly speaking amounts to dualizing the quiver one node at a time. While not a proof, this procedure suggests the resulting theories are dual. This basic idea had previously been pursued in ref. [65] using Aharony's duality, but the flavor bounds put severe limitations on

[4]For our purposes here, we are ignoring the possibility of gauging the $U(1)$ global symmetry since its properties are well established in the particle-vortex duality as a global symmetry.

the quivers that were amendable to this analysis. In particular, the most interesting case with equal rank gauge groups on each node was out of reach. We will see that the master duality will help overcome many of these limitations.

To streamline the derivation it is helpful to follow ref. [65] and rearrange BF terms to group the $SU(N)$ and $U(1)$ global symmetries together. Additionally, a key ingredient in matching this analysis to the existing particle-vortex duality will be the global $U(1)$ symmetries on either side of the duality. As such, we will be especially careful in keeping track of the global symmetries at every step.

We start by recalling how ref. [65] derived their quiver transformations and generalize their method to the master duality. Starting from (3.8), one can use the fact the $U(k)$ field can be separated into its Abelian and non-Abelian parts, i.e. $c = c' + \tilde{c}\mathbb{1}_k$, to perform a shift on the Abelian portion, $\tilde{c} \to \tilde{c} + \tilde{A}_1$. This allows one to rewrite $\mathcal{L}_U$ as

$$\mathcal{L}_U = i\bar{\Psi}\not{D}_{c+B+\tilde{A}_1}\Psi - i\left[\frac{N}{4\pi}\mathrm{Tr}_k\left(cdc - i\frac{2}{3}c^3\right) - \frac{Nk}{4\pi}\tilde{A}_1 d\tilde{A}_1\right]. \tag{3.17}$$

Canceling the overall factor of $i\frac{Nk}{4\pi}\tilde{A}_1 d\tilde{A}_1$ on either side of the duality and defining the new $U(N_s)$ background field $G_\mu \equiv B_\mu + \tilde{A}_{1\mu}\mathbb{1}_{N_s}$, (3.8) becomes

$$\mathcal{L}_{SU} = |D_{b'+G}\phi|^2 - i\left[-\frac{k}{4\pi}\mathrm{Tr}_N\left(b'db' - i\frac{2}{3}b'^3\right)\right] \tag{3.18a}$$

$$\mathcal{L}_U = i\bar{\Psi}\not{D}_{c+G}\Psi - i\left[\frac{N}{4\pi}\mathrm{Tr}_k\left(cdc - i\frac{2}{3}c^3\right)\right]. \tag{3.18b}$$

The procedure used in [65] to derive new dualities is to promote the non-Abelian $U(N_s)$ global symmetry to be dynamical. Since both the ϕ and Ψ matter is charged under G, this turns the matter into bifundamentals. Schematically, we denote the promoted duality as

$$SU(N)_{-k} \times U(N_s)_0 \qquad \leftrightarrow \qquad U(k)_{N-N_s/2} \times U(N_s)_{-k/2}. \tag{3.19}$$

This is subject to the flavor bound $k \geq N_s$.

In promoting the $U(1)$ global symmetry to a gauge symmetry, we get another $U(1)$ global symmetry which couples to the new gauge current on either side of the duality. If we

wanted to make the coupling to the new background gauge field $\tilde{B}_1$ explicit, we would add a $-i\frac{1}{2\pi}\tilde{A}_1 d\tilde{B}_1$ term to each side of the duality. This is completely analogous to the procedure preformed in ref. [76], where a new BF term was included with each promotion to represent the new $U(1)$-monopole symmetry on each side of the duality.

Below, we will sometimes apply this duality to strictly SU gauge fields, in which case it is advantageous to only gauge the SU part of the flavor symmetry, so that (3.19) becomes

$$SU(N)_{-k} \times SU(N_s)_0 \qquad \leftrightarrow \qquad U(k)_{N-N_s/2} \times SU(N_s)_{-k/2}. \tag{3.20}$$

Note that in this form of the duality each side retains the original global $U(1)$ symmetries and we do not obtain the additional global $U(1)$ as above.

We could apply the same procedures to the case where the SU side contains the fermion and the U side contains the scalar, where we would then find

$$SU(N)_{-k+N_f/2} \times U(N_f)_{N/2} \qquad \leftrightarrow \qquad U(k)_N \times U(N_f)_0, \tag{3.21}$$

which matches the result found in ref. [65] up to an overall shift in the level of the background term. This case is considered in more detail in Appendix 3.7.1.

Now let us perform similar manipulations to the master duality in (3.5). Since the Chern-Simons terms on the U side are identical to (3.8b), performing the same manipulations, (3.5b) becomes

$$\mathcal{L}_U = \left|D_{c+\tilde{A}_1+C}\Phi\right|^2 + i\bar{\Psi}\not{D}_{c+\tilde{A}_1+B+\tilde{A}_2}\Psi + \mathcal{L}'_{\text{int}} - i\left[\frac{N_1}{4\pi}\text{Tr}_{k_1}\left(cdc - i\frac{2}{3}c^3\right) - \frac{N_1 k_1}{4\pi}\tilde{A}_1 d\tilde{A}_1\right]. \tag{3.22}$$

Again, we cancel the common $\tilde{A}_1$ Chern-Simons terms on either side of the duality. It will also be convenient to perform a shift to move the $\tilde{A}_2$ fields onto the ψ and Φ matter, so we take $\tilde{A}_1 \to \tilde{A}_1 - \tilde{A}_2$ on either side of the duality. We could now combine the $U(1)$ and $SU(N_f)$ global symmetries into the definition of $E_\mu = C_\mu + \tilde{A}_{1\mu}\mathbb{1}_{N_f}$ as we did in (3.19). However, we will hold off on doing this since it is more convenient to keep the two global

symmetries separate for our purposes. This leaves us with a duality of the form

$$\mathcal{L}_{SU} = \left|D_{b'+B+\tilde{A}_1}\phi\right|^2 + i\bar{\psi}\not{D}_{b'+C+\tilde{A}_1-\tilde{A}_2}\psi + \mathcal{L}_{\text{int}} - i\left[\frac{N_f-k}{4\pi}\text{Tr}_N\left(b'db' - i\frac{2}{3}b'^3\right)\right]$$
$$- i\left[\frac{N}{4\pi}\text{Tr}_{N_f}\left(CdC - i\frac{2}{3}C^3\right) + \frac{NN_f}{4\pi}(\tilde{A}_1-\tilde{A}_2)d(\tilde{A}_1-\tilde{A}_2)\right], \tag{3.23a}$$

$$\mathcal{L}_U = \left|D_{c+C+\tilde{A}_1-\tilde{A}_2}\Phi\right|^2 + i\bar{\Psi}\not{D}_{c+B+\tilde{A}}\Psi + \mathcal{L}'_{\text{int}} - i\left[\frac{N}{4\pi}\text{Tr}_k\left(cdc - i\frac{2}{3}c^3\right)\right]. \tag{3.23b}$$

At this point, we have two choices with how to treat the global symmetry associated with $\tilde{A}_2$. The first choice is to simply leave it as a global symmetry and gauge only the $SU(N_f)$ flavor symmetry associated with C. In this form, each side of the master duality retains the $U(1)$ global symmetries associated with $\tilde{A}_1$ and $\tilde{A}_2$. Alternatively, we could also gauge the global symmetry associated with $\tilde{A}_2$. The latter of these cases will be useful for our purposes in this paper, so we define a $U(N_f)$ gauge field $G_\mu \equiv C_\mu - \tilde{A}_{2\mu}\mathbb{1}_{N_f}$ to which ψ and Φ couple. After gauging the $U(N_f)$ and $SU(N_s)$ global symmetries, this leaves us with

$$SU(N)_{-k+N_f/2} \times U(N_f)_{N/2} \times SU(N_s)_0 \quad \leftrightarrow \quad U(k)_{N-N_s/2} \times U(N_f)_0 \times SU(N_s)_{-k/2}. \tag{3.24}$$

Similar to Aharony's duality, in gauging the $U(N_f)$ symmetry which is associated with G, we pick up an additional monopole $U(1)$ symmetry on either side of the duality which couples to the newly gauged $\tilde{A}_2$ field. We will denote the background gauge field associated with said symmetry by $\tilde{B}_2$. For completeness, we consider the master duality with all global symmetries gauged in Appendix 3.7.1.

Note that we can modify either of the above dualities by adding additional background flavor levels to either side of the duality before promotion. As a reminder, these dualities are subject to the flavor bound $N \geq N_f$ and $k \geq N_s$, but $(N,k) \neq (N_f, N_s)$. In the $N_f = 0$ and $N_s = 0$ limits, (3.24) reduces to (3.20) and (3.21), respectively, with appropriate relabeling.

Four Node Example

Let us now use the dualities we've defined to dualize a four node quiver. Walking through this construction will make generalization to the n node case straightforward. We begin with

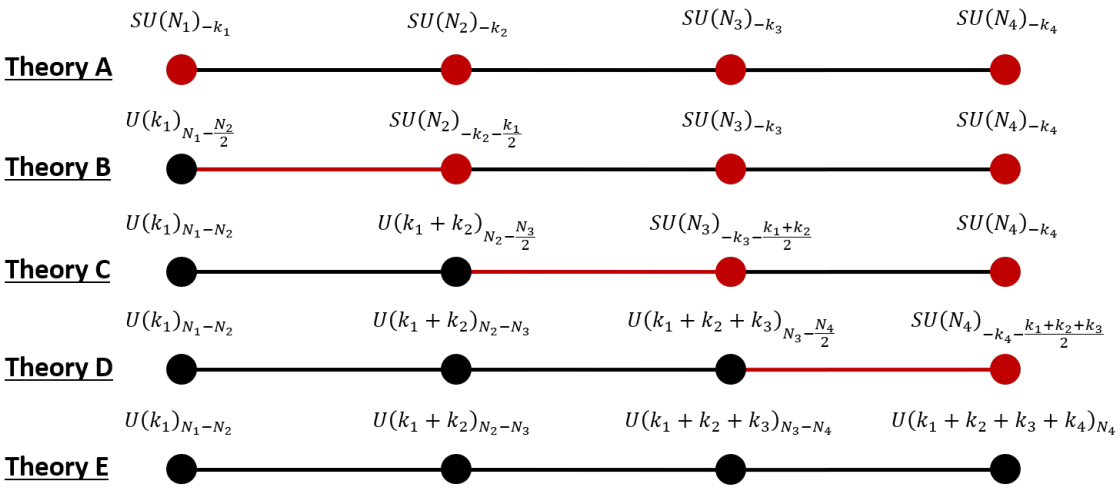

Figure 3.3: Dualizing a linear quiver. Red nodes are SU gauge groups and black nodes are U groups. Black (red) links are bifundamental bosons (fermions). Applying Aharony's duality to the leftmost link turns the scalar into a fermion. Then, applying the master duality repeatedly moves said fermion across the quiver until it reaches the final link where Aharony's duality can again be used to turn the fermion into a boson.

Theory A	$SU(N_1)_{-k_1}$	$SU(N_2)_{-k_2}$	$SU(N_3)_{-k_3}$	$SU(N_4)_{-k_4}$
$Y_{1,2}$	$\square$	$\square$	1	1
$Y_{2,3}$	1	$\square$	$\square$	1
$Y_{3,4}$	1	1	$\square$	$\square$

Table 3.2: Charges of the bifundamental matter in our linear quivers. $\square$ denotes the matter transforms in the fundamental representation of the corresponding gauge group.

the SU side of the theory

$$\text{Theory A:} \qquad SU\left(N_1\right)_{-k_1} \times SU\left(N_2\right)_{-k_2} \times SU\left(N_3\right)_{-k_3} \times SU\left(N_4\right)_{-k_4}\,. \tag{3.25}$$

This theory has the bifundamental scalars which have charges as given in Table 3.2. In what follows we will assume that $N_1 \geq N_2 \geq N_3 \geq N_4$ as well as $k_i \geq 0$ for $i = 1, 2, 3, 4$. Although this is not the most general case, below we will find this is required to avoid flavor bounds to get to the desired U theory. Each of the bifundamentals is charged under a global $U(1)$ symmetry which rotates its overall phase, giving this side of the duality a $[U(1)]^3$ global symmetry.

We will denote the bifundamental scalars living between nodes j and $j+1$ by $Y_{j,j+1}$ and $X_{j,j+1}$ on the SU and U side of the duality, respectively. The masses of the U bifundamentals are denoted by $m_{j,j+1}$ while we will use $M_{j,j+1}$ for those on the SU side.

Before embarking on deriving the duality, note that the uniform mass deformations of (3.25) are given by

$$\text{(A1)} \qquad M_{i,i+1}^2 > 0: \qquad SU\left(N_1\right)_{-k_1} \times SU\left(N_2\right)_{-k_2} \times SU\left(N_3\right)_{-k_3} \times SU\left(N_4\right)_{-k_4} \tag{3.26a}$$

$$\text{(A2)} \qquad M_{i,i+1}^2 < 0: \qquad SU\left(N_1 - N_2\right)_{-k_1} \times SU\left(N_2 - N_3\right)_{-k_1-k_2} \times SU\left(N_3 - N_4\right)_{-k_1-k_2-k_3} \times SU\left(N_4\right)_{-k_1-k_2-k_3-k_4}\,. \tag{3.26b}$$

Here we have been careful to account for which gauge group is Higgsed by each bifundamental scalar. The bifundamental scalar $Y_{i,i+1}$ has $N_i \times N_{i+1}$ components. Below we will always

view the smaller of the two gauge groups to be associated with the "flavor" symmetry of the bifundamentals. As such, if we assume the Higgsing to be maximal, the Higgsing can be thought of as acting on the "color" gauge group, i.e. the group with the larger rank, while leaving the flavor group unchanged.[5] Since to meet flavor bounds below we have assumed $N_1 \geq N_2 \geq N_3 \geq N_4$, this means vacuum expectation value takes the form

$$\langle Y_{i,i+1}^{a_i a_{i+1}} \rangle \propto \begin{pmatrix} \mathbb{1}_{N_{i+1}} \\ 0 \end{pmatrix}^{a_i a_{i+1}} \tag{3.27}$$

with a_i, b_i and a_{i+1}, b_{i+1} gauge indices to $SU(N_i)$ and $SU(N_{i+1})$, respectively. Reassuringly, no gauge group acquires a negative rank with this Higgsing pattern.

Returning to our derivation of the non-Abelian linear quiver dualities, we will now show five theories are dual to one another,

$$\text{Theory A} \quad \leftrightarrow \quad \text{Theory B} \quad \leftrightarrow \quad \cdots \quad \leftrightarrow \quad \text{Theory E}, \tag{3.28}$$

by sequentially dualizing each node from left to right, see Fig. 3.3. To begin, we apply Aharony's duality (3.20) to the first node to obtain

$$\text{Theory B:} \qquad U\left(k_1\right)_{N_1 - N_2 + \frac{N_2}{2}} \times SU\left(N_2\right)_{-k_2 - k_1 + \frac{k_1}{2}} \times SU\left(N_3\right)_{-k_3} \times SU\left(N_4\right)_{-k_4}. \tag{3.29}$$

Flavor bounds are satisfied so long as $N_1 \geq N_2$. This turns the bifundamental scalar on the link between nodes one and two into a bifundamental fermion. The $U(1)$ global symmetry of the first bifundamental becomes a monopole symmetry for the Abelian part of the gauge field which lives on the first node. This will be a common theme as we sequentially step through nodes and the details are shown in Appendix 3.7.2.

Dualizing the $SU(N_2)$ node is where we will need to use something new. We could try applying Aharony's dualities (3.19) or (3.21) to the second node. However, one will inevitably

[5]For example, for a bifundamental coupled to $SU(N_1)_c$ and $SU(N_2)_f$ with $N_1 \geq N_2$, what occurs can be best understood by first splitting $SU(N_1)_c \times SU(N_2)_f \to SU(N_1 - N_2)_c \times SU(N_2)_c \times SU(N_2)_f$. Since the bifundamental is maximally Higgsed in the $SU(N_2)$ subgroup, the unbroken part of the two $SU(N_2)$ factors is their diagonal, leaving $SU(N_1 - N_2)_c \times SU\left(N_2\right)_{\text{diag}}$. Thus, saying the flavor group is unchanged is a merely a convenient relabeling. Also note that the Chern-Simons level of the new flavor group will be the sum of the original flavor and color Chern-Simons levels.

run into flavor bound issues since nodes with links on two sides require a $SU(N_{i-1}+N_{i+1})$ flavor symmetry, which exceeds the $SU(N_i)$ color symmetry for the cases we are interested in here.

Notice that since the master duality has two types of matter it has two *separate* flavor symmetries, each subject to its own flavor bound. This is useful for dualizing the nodes with two links and, furthermore, has the correct matter content since node two in Theory B has both a bifundamental scalar and fermion attached to it. However, the master duality is quite a bit different from Aharony's original dualities in that it requires additional interactions terms between the scalars and fermions on a given side of the duality, as given in (3.7). Let us consider how we could introduce such interactions terms and how they affect the theories we are considering.

Including Bifundamental Interactions

The interaction we need in order to apply the master duality in theory B is

$$\text{Theory B:} \qquad C_2^{(B)} \left(\bar{\psi}_{1,2}^{a_2 a_1} Y_{a_2 a_3}^{2,3}\right) \left(Y_{2,3}^{\dagger b_2 b_3} \psi_{b_2 a_1}^{1,2}\right). \tag{3.30}$$

Here $C_2^{(B)}$ is the coefficient of the interaction on the second node in theory B and we have not yet committed to its sign or magnitude, but we will do so later by matching TFTs. In what follows, it will be useful to associate each interaction term with one of the interior nodes of the quiver.

In order to give rise to (3.30), we must backtrack slightly since a similar interaction should also then be present in theory A in its dualized form. The exact matching of the interactions between theories A and B is quite subtle and requires auxiliary field techniques that were originally introduced in the large N and k literature [86]. Here we will only give a schematic overview. The full details of this matching are given in Appendix 3.7.3.

Recall that the purpose of the interaction term in the master duality is to ensure that when the scalars acquire a vacuum expectation value we also gain an additional mass term for the fermions [24, 64]. This was vital for matching the phases and TFTs on either side of

the duality. Importantly, regardless of the sign of the mass deformation, the fermions never condense and thus there is no opportunity for a fermion condensate to influence the mass of the scalars through the same interaction term. If the fermions did condense, this would yield a very different looking phase diagram than that found in refs. [24, 64].

Here we identify the fermions with scalars, which *can* condense when their quadratic term goes negative. In order to match the TFT phase diagrams of theories A and B under mass deformations, we need to make sure the interaction term does not allow the $Y_{1,2}$ condensate to influence the $Y_{2,3}$ mass. In Appendix 3.7.3 we derive an interaction term which has the desired properties: this term will cause a nonzero vacuum expectation value for the $Y_{2,3}$ bifundamental to give a positive or negative mass to $Y_{1,2}$, depending on the sign of the coefficients $C_2^{(A)}$. However, the opposite effect cannot occur: $Y_{1,2}$ acquiring a vacuum expectation value *cannot* influence the mass of $Y_{2,3}$. More generally, for the SU side of the duality, the vacuum expectation value of a link can only affect nodes/links to its *left*. The interaction term is unidirectional as it is for the original master duality.

We will *schematically* denote the interactions we add to Theory A as

$$\text{Theory A:} \qquad C_2^{(A)} \left(Y_{1,2}^{\dagger a_2 a_1} Y_{a_2 a_3}^{2,3} \right) \left(Y_{2,3}^{\dagger b_2 a_3} Y_{b_2 a_1}^{1,2} \right) \tag{3.31}$$

with the understanding that the true interaction is as given in (3.139). Eq. (3.31) is equivalent to (3.139) if we simply ignore the fact that when the $Y_{1,2}$ acquires a vacuum expectation value the interaction term gives a mass to $Y_{2,3}$, so we will do so henceforth for brevity. An analogous interaction term is added to node three as well since it will be needed when stepping from theory C to D.

Having introduced the necessary interaction term, we subsequently apply the master

duality (3.24) to the second and third nodes, this gives

$$\text{Theory C:} \qquad U(k_1)_{N_1-N_2} \times U(k_1+k_2)_{N_2-\frac{N_3}{2}} \times SU(N_3)_{-k_3-k_1-k_2+\frac{k_1+k_2}{2}} \times SU(N_4)_{-k_4} \tag{3.32}$$

$$\begin{aligned}\text{Theory D:} \qquad & U(k_1)_{N_1-N_2} \times U(k_1+k_2)_{N_2-N_3} \times U(k_1+k_2+k_3)_{N_3-\frac{N_4}{2}} \\ & \times SU(N_4)_{-k_4-k_1-k_2-k_3+\frac{k_1+k_2+k_3}{2}} \,. \end{aligned} \tag{3.33}$$

These in turn require the flavor bounds $N_2 \geq N_3, k_2 \geq 0$ and $N_3 \geq N_4, k_3 \geq 0$, respectively.[6] Each application of the master duality changes a boson link to a fermion link and vice versa, effectively driving the single fermion link down the quiver, see Fig. 3.3. As with the duality relating theories A and B, the application of the master duality above changes the global $U(1)$ symmetry across the duality. Specifically, it changes the $U(1)$ global symmetry under which $Y_{2,3}$ was charged to a monopole-like symmetry which couples to the Abelian part of gauge field on the second node. A completely analogous transformation occurs for the baryon number symmetry of $Y_{3,4}$. The details of how this occurs are shown in Appendix 3.7.2.

Finally, to arrive at the desired dual theory we again apply Aharony's duality (3.21) to the last node. Flavor bounds require $k_4 \geq 0$. This ultimately gives

$$\text{Theory E:} \qquad U\left(k_1\right)_{N_1-N_2} \times U\left(k_1+k_2\right)_{N_2-N_3} \times U\left(k_1+k_2+k_3\right)_{N_3-N_4} \times U\left(k_1+k_2+k_3+k_4\right)_{N_4} \,. \tag{3.34}$$

Note that the fourth node does not pick up a monopole-like global symmetry for its Abelian gauge field. This is related to the fact we have one more node than bifundamentals and is also a feature of the dualities in ref. [65] and ABJM theory [4].

Following the mass identifications through the dualities, we see $M^2_{i,i+1} \leftrightarrow -m^2_{i,i+1}$. The

[6] More precisely, this should exclude the double saturation cases where $N_2 = N_3$ and $k_2 = 0$ or $N_3 = N_4$ and $k_3 = 0$. We will not make note of such special cases henceforth since they will not be relevant for our purposes.

uniform mass deformations of Theory E are

$$\text{(E1)} \qquad m^2_{i,i+1} < 0: \qquad U(k_1)_{N_1} \times U(k_2)_{k_2} \times U(k_3)_{N_3} \times U(k_4)_{N_4} \tag{3.35a}$$

$$\text{(E2)} \qquad m^2_{i,i+1} > 0: \qquad U(k_1)_{N_1-N_2} \times U(k_1+k_2)_{N_2-N_3} \times U(k_1+k_2+k_3)_{N_3-N_4} \times U(k_1+k_2+k_3+k_4)_{N_4} \tag{3.35b}$$

which, reassuringly, are level-rank dual to the phases considered above. Here once again some care is required for the Higgs phase. Since we are assuming all $k_i \geq 0$ in order to meet the flavor bounds above, the maximal Higgsing vacuum expectation value is, using block matrix notation,

$$\langle X^{a_i a_{i+1}}_{i,i+1} \rangle \propto \begin{pmatrix} \mathbb{1}_{K_i} & 0 \end{pmatrix}^{a_i a_{i+1}}. \tag{3.36}$$

where a_i, a_{i+1} are gauge indices to $U(K_i)$ and $U(K_{i+1})$, respectively and we have defined the shorthand

$$K_j \equiv \sum_{i=1}^{j} k_i. \tag{3.37}$$

Of course, as we apply all the aforementioned dualities the matter interaction terms are changing as well. We also end up with the interaction term (3.138) between adjacent bifundamental scalars for theory E. The interaction is such that a bifundamental scalar vacuum expectation can only affect nodes/links to its *right* now.[7] The analog of (3.31), which is a schematic stand-in for (3.138), is

$$\text{Theory E:} \qquad C_2^{(E)} \left(X^{\dagger a_2 a_1}_{1,2} X^{2,3}_{a_2 a_3} \right) \left(X^{\dagger b_2 a_3}_{2,3} X^{1,2}_{b_2 a_1} \right). \tag{3.38}$$

where now we ignore the fact that when $X_{2,3}$ acquires a vacuum expectation value it gives a mass to $X_{1,2}$.

Effect of Interactions

We would now like to show that these interaction terms are vital for a matching the mass deformed TFTs. Although we found a matching between phases for the completely gapped/Higgsed

[7] This is most obvious to see when moving from Theory C to Theory D. In theory C, the $X_{1,2}$ bifundamental can influence the mass of the fermion on the $2,3$ link, but not vice versa. Hence, in Theory D the interaction between $X_{1,2}$ and $X_{2,3}$ should obey the same rule to get a matching of TFTs.

phases above, these were very special cases. In order to observe the expected partial gapping/Higgsing behavior to apply to theta walls, we need to carefully treat the interactions.

First it will be helpful to specialize to a particular sign and magnitude of interaction terms coefficients, $C_I^{(A)}$ and $C_I^{(E)}$ for $I = 2, 3$ (i.e. all internal nodes). Specifically for the purposes of matching onto the phases of (3.3), we take $C_I^{(A)} < 0$ and $C_I^{(E)} < 0$. [8] We also assume $|C_I^{(E)}| \to \infty$ such that $|C_I^{(E)}| \gg |m_{i,i+1}^2|$. Although not considered in [24, 64], it is straightforward to check that a very large interaction term on one side of the master duality implies a very small interaction term on the other side of the duality.[9] Hence, $C_I^{(A)} \to 0$ so the hierarchy $M_{i,i+1}^2 \gg C_I^{(A)} > 0$ holds for all mass deformations. In such a limit we can effectively ignore the interaction terms on the SU side of the duality.

The choice of magnitudes above has the added effect of simplifying the analysis of the interaction terms and the TFT structure. It is possible to derive quiver theories for more general interaction coefficients and still find matching TFTs, but we leave such analysis for future work.

Let us now consider the effect of the interaction terms on the U side of the duality. The two interaction terms of theory E are given by

$$C_2^{(E)} \left(X_{1,2}^{\dagger a_2 a_1} X_{a_2 a_3}^{2,3} \right) \left(X_{2,3}^{\dagger b_2 a_3} X_{b_2 a_1}^{1,2} \right) + C_3^{(E)} \left(X_{2,3}^{\dagger a_3 a_2} X_{a_3 a_4}^{3,4} \right) \left(X_{3,4}^{\dagger b_3 a_4} X_{b_3 a_2}^{2,3} \right). \tag{3.39}$$

Consider the case when $X_{1,2}$ acquires a nonzero vacuum expectation value as in (3.36). This term breaks $U(K_2)$ down to $U(K_2 - K_1)$, which is the usual effect of the Higgsing.

---

[8] We must choose the coefficients of the interactions to be the same sign for a matching of TFTs. To see this, first note that we use the master duality once on each internal node, and under the master duality the interaction term flips sign [24, 64]. An additional sign flip comes from the application of the master duality for the node to the left of an internal node, which sign flip when changing the fermions in the interaction to bosons.

[9] To see this, let us specialize to the notation used in [64]. Here we saw that by changing the sign of c_4 and c_4', one could change the location of the "singlet critical line". Smoothly changing $c_4 \to -c_4$ causes the line to move from phase IV to phase III. Meanwhile, changing $c_4' \to -c_4'$ to move from phase IV' to phase I'. Thus, for example, we can shrink the size of region IVb and IVb' by decreasing the magnitude of c_4' and increasing the magnitude of c_4. In the limit $c_4' \to 0$, we must take $|c_4| \to \infty$.

Additionally, the first interaction term (3.39) becomes

$$-\left(X_{1,2}^{\dagger a_2 a_1} X_{a_2 a_3}^{2,3}\right)\left(X_{2,3}^{\dagger b_2 a_3} X_{b_2 a_1}^{1,2}\right) \propto -\left(\begin{array}{cc} \mathbb{1}_{K_1} & 0 \\ 0 & 0 \end{array}\right)_{b_2}^{a_2} X_{2,3}^{\dagger b_2 a_3} X_{a_2 a_3}^{2,3}. \tag{3.40}$$

Hence the vacuum expectation value of $X_{1,2}$ shows up as a negative mass deformation for the first K_1 components of $X_{2,3}$ and thus *also* breaks the $U(K_3)$ to $U(K_3 - K_1)$. As such, except for the $X_{1,2}$ link, each bifundamental can acquire a mass deformation from two different sources: its explicit mass term as well as the interaction terms to its left. As an example, let us assume $m_{2,3}^2 = m_{3,4}^2 = 0$ but $m_{1,2}^2 < 0$. Then $X_{2,3}$ acquires a vacuum expectation value from (3.40). The interaction term between $X_{2,3}$ and $X_{3,4}$ also means $X_{3,4}$ gets a negative mass shift,

$$-\left(X_{2,3}^{\dagger a_3 a_2} X_{a_3 a_4}^{3,4}\right)\left(X_{3,4}^{\dagger b_3 a_4} X_{b_3 a_2}^{2,3}\right) \propto -\left(\begin{array}{cc} \mathbb{1}_{K_1} & 0 \\ 0 & 0 \end{array}\right)_{b_3}^{a_3} X_{3,4}^{\dagger b_3 a_4} X_{a_3 a_4}^{3,4}. \tag{3.41}$$

breaking $U(K_4)$ to $U(K_4 - K_1)$ and giving the first K_1 components an additional negative mass deformation. If there are no other mass term deformations, this effect cascades to the *right* across the entire quiver.

Now let us consider how this changes if $X_{2,3}$ also had a mass deformation. A negative mass deformation would further break down the $U(K_3)$ subgroup to $U(K_3 - K_2)$, and this could also propagate down the quiver, as we just discussed. Positive mass deformations are slightly more tricky since we need to consider them in two regimes. First consider the case where the negative mass deformation from (3.40) is larger than that of the mass term for $X_{2,3}$. Then the results considered above are unchanged, $X_{1,2}$ is still partially broken. When the mass term has a larger positive mass contribution than that of (3.40), $X_{2,3}$ is completely gapped. This means none of the components have a nonzero vacuum expectation value, and thus the interaction (3.41) contributes no mass to $X_{3,4}$. In other words, if the mass term for $X_{2,3}$ is large enough, it can stop of propagation of $X_{1,2}$'s breaking down the quiver. We have avoided this case by assuming $\left|C_I^{(E)}\right| \gg \left|m_{i,i+1}^2\right|$, thereby forbidding large positive mass deformations from blocking the propagation of the breaking down the quiver.

What about when $X_{2,3}$ acquires a negative mass deformation but the $X_{1,2}$ and $X_{3,4}$ mass terms are untouched? By the same reasoning above, $X_{3,4}$ will also acquire a negative mass shift to its first K_2 components via the interaction terms, causing the breaking of $U(K_3)$ and $U(K_4)$ to $U(K_3 - K_2)$ and $U(K_4 - K_2)$, respectively. However, as we have been careful to argue in Appendix 3.7.3, $X_{2,3}$'s vacuum expectation value should not be able to influence nodes/links to its left. Hence $X_{1,2}$ is unaffected.

We are now in the position to consider mass deformations which are partially Higgsed. That is, not all bifundamental masses are taken to be the same sign. Specifically, consider the case where the bifundamentals $Y_{1,2}$ and $Y_{3,4}$ are Higgsed and $Y_{2,3}$ is gapped (corresponding via mass identifications to $X_{1,2}$ and $X_{3,4}$ being gapped and $X_{2,3}$ being Higgsed). This yields the phases

$$\text{(A3)} \quad : \quad SU(N_1 - N_2)_{-k_1} \times SU(N_2)_{-k_1-k_2} \times SU(N_3 - N_4)_{-k_3} \times SU(N_4)_{-k_3-k_4} \tag{3.42a}$$

$$\text{(E3)} \quad : \quad U(k_1)_{N_1-N_2} \times U(k_1 + k_2)_{N_2} \times U(k_3)_{N_3-N_4} \times U(k_3 + k_4)_{N_4} \tag{3.42b}$$

which are level-rank dual to one another! Note that the interactions are vital for us to reach this conclusion. We have used the fact that $X_{2,3}$ acquiring a vacuum expectation value breaks the $U(K_2)$ subgroup of $U(K_3) \to U(k_3)_{N_3-N_4} \times U(K_2)_{N_3-N_4}$ and also, due to the interaction term, $U(K_4)_{N_4} \to U(k_3 + k_4)_{N_4} \times U(K_2)_{N_4}$. Without such terms we would have found the $U(K_4)_{N_4}$ group unbroken, yielding the TFT

$$\text{(E}\bar{3}\text{)} \quad : \quad U(k_1)_{N_1-N_2} \times U(k_1 + k_2)_{N_2-N_4} \times U(k_3)_{N_3-N_4} \times U(K_4)_{N_4} \tag{3.43}$$

which is clearly not level-rank dual to (3.42a).

Generalization to n Nodes

Now let us generalize this prescription to an arbitrary number of nodes. For n nodes, there is a duality between the following two theories:

$$\text{Theory A:} \qquad SU(N_1)_{-k_1} \times \prod_{i=2}^{n} [SU(N_i)_{-k_i} \times \text{bifund } Y_{i-1,i}] \tag{3.44a}$$

$$\text{Theory B:} \qquad \prod_{i=1}^{n-1} \left[U(K_i)_{N_i - N_{i+1}} \times \text{bifund } X_{i,i+1}\right] \times U(K_n)_{N_n} \tag{3.44b}$$

where flavor bounds require $k_i \geq 0$ and $N_1 \geq N_2 \geq \ldots \geq N_n$. As with the above case, these theories can be shown to be dual by systematically applying Aharony's duality (3.1a) to the first node, the master duality to every two-link node, and then Aharony's other duality (3.1b) to the last node. The master duality is not needed for the two node case.

Implied above are interaction terms on the U side of the duality of the form of (3.138). Equivalently, we can use the schematic interaction

$$\mathcal{L}^{(B)} \supset \sum_{I=2}^{n-1} C_I^{(B)} \left(X_{I-1,I}^{\dagger a_I a_{I-1}} X_{a_I a_{I+1}}^{I,I+1}\right) \left(X_{I,I+1}^{\dagger b_I a_{I+1}} X_{b_I a_{I-1}}^{I-1,I}\right) \tag{3.45}$$

with the understanding that such interactions can only give mass terms to the link on their left. Here, a_i, b_i the gauge indices of the ith node and $C_I^{(B)} \to -\infty$ so that $|C_I^{(B)}| \gg m_{i,i+1}^2$. In this limit, on the SU side of the duality the interaction terms are very small and have no effect on the mass deformed phases, so we ignore them.

To summarize the interaction behavior on the U side: a bifundamental scalar $X_{j,j+1}$ acquiring a nonzero vacuum expectation value affects nodes/links to the right but *not* to the left. Namely, it causes all bifundamental scalars (i.e $X_{i,i+1}$ with $i > j$) to acquire a similar vacuum expectation for the first K_j components. This in turn causes a breaking of all gauge groups nodes $i > j$ to $U(K_i - K_j)$. Note this effect can compound, so if $X_{j,j+1}$ and $X_{\ell,\ell+1}$ acquire a vacuum expectation value from their respective mass deformations, the gauge group on node $i > j > \ell$ undergoes breaking $U(K_i) \to U(K_i - K_j) \times U(K_j - K_\ell) \times U(K_\ell)$.

As mentioned earlier, other dualities which flow to other TFTs can be constructed by

changing the sign/magnitude of the interaction terms, but such considerations are left for future work.

3.2.3 Self-Consistency Checks

Returning to the bosonic particle-vortex duality, it should now be clear the derivation we outlined in Sec. 3.2.1 is the two node case of the more general non-Abelian linear quivers with values

$$N_1 = N_2 = k_1 = 1, \qquad k_2 = 0, \tag{3.46}$$

which is shown in Fig. 3.2. Note this saturates all flavor bounds and carries the minimum value of parameters without being completely trivial, so the particle-vortex duality can be thought of as the simplest case of an infinite class of $2+1$ dimensional Bose-Bose dualities. Additionally, it is clear that the derivation of the two node quiver requires no master duality since there are no nodes connected to two links.

Another helpful tool in analyzing the more general non-Abelian quiver dualities as well as comparing them to the holographic dualities in Sec. 3.3.2 will be comparing the spectrum of the two theories. To this end, let us briefly review how the spectra of the particle-vortex duality match on either side of the duality.

First consider the case when Φ acquires a vacuum expectation value in (3.14) through a negative mass deformation. It is well known the breaking of the $U(1)$ gauge symmetry gives rise to vortex solutions of finite mass charged under B_1 flux. Since there is no dynamical Chern-Simons term on this end, there is no funny business with flux attachment or alternative vortex solutions. These vortices carry flux charge under the broken $U(1)$ gauge group which can be seen by looking at the asymptotic behavior of the gauge field.

Now consider the Abelian-Higgs model but instead in the form which is more amenable to matching onto the non-Abelian quivers (i.e. (3.15)). In this form we have two $U(1)$ gauge fields, one of which is redundant and can be integrated out. When $\langle\Phi\rangle \sim v$, it forces the breaking of $U(1) \times U(1) \to U(1)_A$, where $U(1)_A$ is the subgroup where the two $U(1)$

transformations act oppositely on Φ, leaving it invariant. Again, the breaking of a $U(1)$ symmetry ensures that there are vortex solutions which are charged under the flux of the broken symmetry. In this case, it corresponds to a nonzero winding of both a_1 and c at spatial infinity, since the broken $U(1)$ group is where they are set equal to one another (i.e. $U(1)_{\text{diag}}$). For the vortex solution where $a_1 = c$ energy contributions from the Chern-Simons terms drop out, as they should since they weren't present in (3.14). Since there is nonzero a_1 flux the vortex is charged under the background B_1 field. Also note that the vortex has finite mass proportional to the vacuum expectation value of the scalar. As expected, we reach the same conclusions when working from (3.14), albeit in a slightly more complicated manner.

Due to the mass identification, the phase where Φ has a vacuum expectation value should be identified with the phase where ϕ is simply gapped. The $U(1)$ global symmetry is unbroken and ϕ excitations of (3.12a) are charged under the B_1 field, which are identified with the vortices on the opposite side of the duality.

Meanwhile, for mass deformations where ϕ obtains a vacuum expectation value and Φ is gapped, the $U(1)$ global symmetry on both sides of the duality is broken. This is straightforward to see on the ϕ side of the duality and is made clear on the Φ side by rewriting the photon using the Abelian duality, $F_{\mu\nu} \sim \epsilon_{\mu\nu\rho}\partial^\rho\sigma$. Since the $U(1)$ global symmetry is broken, we expect Goldstone bosons on either side of the duality. For the ϕ field, we have massless angular excitations. In this phase the photon remains gapless and it is identified with the Goldstone boson of the Φ side.

We claim the above results completely generalize to the n-node quiver case. Across the duality we have established the fact that the global $U(1)$ symmetry of the $X_{i,i+1}$ bifundamental is identified with the monopole number symmetry of the ith node. We begin with the side of the duality where a $U(1)$ global symmetry is unbroken, which corresponds to a positive mass deformation on the SU side and a negative mass deformation on the U side. We will focus on the behavior of a single bifundamental since generalization is straightforward.

When we gap the $Y_{i,i+1}$ bifundamental on the SU side, on the U side this should cause the $X_{i,i+1}$ bifundamental to acquire a vacuum expectation value as a result of the $M^2_{i,i+1} \leftrightarrow$

$-m^2_{i,i+1}$ mass mapping.

Let's take a closer look at the breaking term to account for degrees of freedom. Schematically the interaction term can be written in the form

$$V(X_{i,i+1}) \sim \mathrm{Tr}\left[(X_{i,i+1})_{a_i a_{i+1}}\left(X^\dagger_{i,i+1}\right)^{b_i a_{i+1}} - v^2\delta^{b_i}_{a_i}\right]^2. \tag{3.47}$$

With the gauge freedom we can take $\langle X_{i,i+1}\rangle$ to be of the from of (3.36). This causing the breaking of

$$U(K_i)\times U(K_{i+1}) \to U(K_i)_{\mathrm{diag}}\times U(k_{i+1}), \tag{3.48}$$

corresponding to an overall broken $U(K_i)$ gauge symmetry. Each $X_{i,i+1}$ field has $2K_iK_{i+1}$ total degrees of freedom. Within the $U(K_i)$ subspace, there are K_i^2 flat directions corresponding to "angular" excitations, which are consumed by the broken $U(K_i)$ gauge fields to become (two-component) massive "W-bosons". The remaining K_i^2 scalar degrees of freedom represent "modulus" excitations in directions of the potential which are not flat and are thus analogous to Higgs bosons. Additionally, these modes are now adjoint particles since they are charged under $U(K_i)_{\mathrm{diag}}$. This leaves $2K_ik_{i+1}$ degrees of freedom, which acquire a mass through the double trace-like interaction term that is present for Wilson-Fisher scalars. Hence all bifundamental scalar particles are gapped, as they should be.

As with the particle-vortex duality, we would like to show vortices on the U side should be identified with the gapped particles on the SU side of the duality. The gapped $Y_{i,i+1}$ particles are charged under the unbroken $U(1)$ symmetry and carry baryon number. Meanwhile, when the $X_{i,i+1}$ particles acquire a vacuum expectation value, the breaking of the corresponding $U(1)$ subgroup mean vortices associated to that link now have finite mass and are topologically stable since [10]

$$\pi_1\left(U(K_i)\times U(K_{i+1})/U(K_i)_{\mathrm{diag}}\right) \simeq \mathbb{Z}. \tag{3.49}$$

[10]One might worry that we may be able to form other vortex solutions by winding the other broken subsets, say $U(1)_A \subset U(K_{i+1})\times U(K_{i+2})/U(K_i)_{\mathrm{diag}}$. Note however that the interactions force the vacuum expectation value of the associated $U(K_i)$ subgroup of the $X_{i+1,i+2}$ bifundamental to be effectively infinite. This is distinct from $\langle X_{i,i+1}\rangle$ which is presumed to be proportional to the mass deformation and finite. Thus such vortices are significantly heavier than the vortex formed from a winding of the $X_{i,i+1}$

Specifically, the vortex configurations correspond to a winding of the broken $U(1)_A \subset U(K_i) \times U(K_{i+1})/U(K_i)_{\text{diag}}$ gauge group as well as the phase of $\langle X_{i,i+1} \rangle$ at spatial infinity. Since the broken subgroup $U(1)_A$ contains the ith node's $U(1)$ factor, through the BF term of that node it coupled to the $\tilde{B}_2$ field.[11] This is the same symmetry the gapped $Y_{i,i+1}$ couple to, and thus the two modes should be identified in a manner analogous to what we saw for the particle-vortex duality.

Unlike the particle-vortex duality, the presence of nonzero Chern-Simons terms in the mass deformed phases means variation with respect to dynamical gauge groups imposes a flux attachment condition on the excitations. That is, particles charged under the respective symmetry must be attached to the vortex excitations. This might be modified slightly due to the breaking of the U gauge group, since the broken gauge degrees of freedom will become massive giving an extra term when varying with respect to the corresponding massive gauge degrees of freedom. We leave such analysis for future projects.

3.3 Theta Wall Dualities

In this section we consider duals to the Chern-Simons theories found on defects in $3+1$-dimensional $SU(N)$ Yang Mills theory when the θ angle varies as a function of location. Specifically, we look for a dual to (3.3).

We begin by reviewing a few essential facts about the expected theta dependence in pure $SU(N)$ gauge theories. Such gauge theories are believed to have multiple vacua related to the physics of the theta angle. In each vacuum, physical quantities are not periodic in theta

---

bifundamental and its corresponding gauge groups. Note for the $X_{i,i+1}$ vortex, no matter the mass deformations of bifundamentals to its left, its $U(k_i)$ subgroup will always have a finite vacuum expectation value, and thus the topologically stable vortex solutions can always have finite energy via a winding of this corresponding subgroup.

[11] Since the $X_{i,i+1}$ vortices contain winding under $U(1)_A$, which is a subgroup of the $U(1) \times U(1)$ gauge symmetries of the ith and $(i+1)$th nodes, one might worry that such a vortex also carries flux under the $(i+1)$th gauge group and is thus charged under the $U(1)$ symmetry of the $(i+1)$th node. However, as explained in Appendix 3.7.2, the BF coupling is such that nodes to the right of a bifundamental are only coupled via the unbroken gauge group. Hence, although the vortices carry $U(1)$ flux of the $(i+1)$th node, they are only charged under global symmetry of the ith node.

with period 2π but instead with period $2\pi N$. The physical properties of the system are nevertheless 2π periodic. As we change theta by a single 2π period, the true vacuum of the system changes and the physics in the new vacuum at $\theta = \theta_0 + 2\pi$ is the same as the physics in the original vacuum at $\theta = \theta_0$.

This picture can be most rigourously established at large N. In this limit the vacuum energy as a function of θ is expected to scale as [115, 120]

$$E(\theta) = N^2 h(\theta/N) \tag{3.50}$$

for some to be determined function h. This appears to be inconsistent with the periodicity requirement

$$E(\theta) = E(\theta + 2\pi). \tag{3.51}$$

As claimed above, a single vacuum with energy of the form (3.50) is expected to be $2\pi N$ periodic, not 2π periodic. This conundrum can easily be solved by postulating that the theory has a family of N vacua labeled by an integer K. In this case the vacuum energy in the Kth vacuum is given by

$$E_K(\theta) = N^2 h((\theta + 2\pi K)/N). \tag{3.52}$$

Most of these vacua are meta-stable, the truly stable vacuum for any given θ is given by minimizing over K:

$$E(\theta) = N^2 \min_K h((\theta + 2\pi K)/N). \tag{3.53}$$

The resulting function $E(\theta)$ has the expected 2π periodicity. While the energy of (say) the 0-th vacuum keeps increasing as we increase theta from 0 towards 2π, the energy of the $K = -1$ vacuum at $\theta = 2\pi$ is exactly the same as the energy of the 0-th vacuum was at $\theta = 0$. One expects that a transition from the 0-th to the (-1)-th vacuum is triggered at $\theta = \pi$. While physics in any given vacuum is $2\pi N$ periodic, the system as a whole, in its true vacuum, is 2π periodic.

We are now in a position to discuss the physics of theta interfaces and domain walls. Let us first turn to the case of interfaces. Starting with a confining gauge theory (pure Yang-

Mills in this case), one can introduce interfaces across which the theta angle changes by an integer multiple of 2π,

$$\Delta\theta = 2\pi n. \tag{3.54}$$

The theory is assumed to be everywhere in the true ground state. This means, in particular, that the index labeling the local vacuum state changes by $-n$ units as the theta angle changes by $2\pi n$. Since the theta angle is a parameter in the Lagrangian, translation invariance is explicitly broken in this theory and we do not expect any Goldstone bosons corresponding to fluctuations of the position of the interface.

As we explained in the introduction, a spatially varying theta gives rise to domain walls on which Chern-Simons theories live. However, anomaly inflow does not constrain the exact Chern-Simons theory. Ref. [101] has argued that for $|\nabla\theta| \ll \Lambda$ and $|\nabla\theta| \gg \Lambda$, one should expect the TFTs $[SU(N)_{-1}]^n$ and $SU(N)_{-n}$, respectively. Assuming a smooth transition, (3.3) was proposed as a possible CFT to describe the transition between these two extreme cases.

The generic phase of (3.3) is characterized by a partition $\{n_i\}$ of n, that is integers n_i with the property that $\sum_i n_i = n$. Each n_i denotes the number of gauge group factors along the quiver that have been Higgsed down to their diagonal subgroup before we encounter a positive mass squared scalar. For example, $n_1 = n$ corresponds to the completely Higgsed $SU(N)_{-n}$ phase associated with the steep wall, $n_i = 1$ for $i = 1, \ldots, n$ corresponds to the shallow wall with $[SU(N)_{-1}]^n$. The generic phase is given by a TFT based on

$$\text{Phase } \{n_i\}: \qquad \prod_i SU(N)_{-n_i}. \tag{3.55}$$

One extra subtlety that arises concerns global symmetries. The scalar fields are bifundamentals under neighboring $SU(N)_{-1}$ gauge group factors. This leaves an overall phase rotation of every single scalar as a global symmetry, for a combined $U(1)^{n-1}$ extra global symmetry from the $n-1$ scalar fields. If these indeed were global symmetries of the parent theory this would lead to unexpected consequences. Most notably, in the fully broken phase the low energy theory on the interface would not just be the topological $SU(N)_{-n}$ Chern-Simons

theory we expect, but would in addition contain $n-1$ massless Goldstone bosons as these extra global symmetries are spontaneously broken in the condensed phase. The proposal of [50] is to add extra terms to the action that break these extra global symmetries so that there are no Goldstone bosons. The simplest option to do so is a $\det(Y)$ term for each link[12], which is indeed gauge invariant under all $SU(N)_{-1}$ gauge group factors but is charged under overall phase rotations of Y. The quiver gauge theories we discussed in the last section do not have these determinant terms added to the potential. The dualities we derive will most naturally apply to the theory without the determinant terms. To connect to the theory of the theta interfaces we will have to add the extra determinant term as a deformation.

In addition to interfaces a second type of co-dimension one defect we can discuss are domain walls. These are already present in a theory with constant theta. They govern the decay of one of the meta-stable vacua of the theory to the true vacuum. In the idealized case, we can consider the theory in a state where we interpolate between two metastable vacua as we move along a single direction, which we once more chose to be the x_3 direction. For simplicity we are only interested in configurations which preserve $2+1$ -dimensional Lorentz invariance, that is we focus on flat domain walls. If the theory starts in the 0-th vacuum as $x_3 \to -\infty$, we can interpolate to the $(-n)$-th vacuum at $x_3 \to \infty$. While the state of the system at large positive x_3 is not in the true local ground state, this configuration is meta-stable. The false vacuum has to decay via bubble formation, which is governed by the domain wall tension. It has been argued [120] that the tension of the wall is of order N, a fact that is obvious in the holographic realization of these walls which we will turn to in Sec. 3.3.2. At large N this means that decay of the meta-stable vacuum is e^{-N} suppressed. In addition the difference in vacuum energies will exert a pressure on the domain wall generically causing the wall to move. But since the pressure difference is order N^0, whereas the domain wall tension is order N, the domain wall can be treated as static in the large N limit.

[12]Of course any power of $\det(Y)$ would do the job in that it is gauge invariant but charged under the global symmetry. For small values of N we need to make use of this freedom. For example, for $N=1$ $\det(Y)=Y$ and we would simply add linear potentials, whereas for $N=2$ we would be adding mass terms. Instead we should add $\det(Y)^4$ and $\det(Y)^2$ respectively in those two cases.

As far as the anomalies are concerned, the analysis of [50] generalizes to the case of walls: the gauge theory on the defect should be the same whether we are forced to jump n vacua because of a $2\pi n$ jump in θ, or whether we study a dynamical wall that interpolates between two n-separated vacua in a theory with fixed θ. The main difference appears to be that this time the wall is dynamical with a finite tension. Most notably, this implies that we should have (at large N) a massless scalar living on the wall whose expectation value gives the location of the wall. It being the Goldstone boson of broken translations, the scalar has an exact shift symmetry that protects it from becoming massive. While interfaces were characterized by a free function $\theta(x_3)$ and were only loosely characterized into shallow and steep, for walls it is much easier to characterize the moduli space of allowed configurations. We have a total of n discrete jumps from one vacuum to the next. When the walls are widely separated, we should have n separate walls connecting two neighboring vacua each. In this limit, we should have a total of n translational modes as the different basic walls can presumably move independently. The gauge theory living on these widely separated walls should be $[SU(N)_{-1}]^n$ as above together with these decoupled light translational modes. This is indeed what follows from the analysis of Acharya and Vafa in the closely related case of $\mathcal{N} = 1$ supersymmetric gauge theories [1] (see also [43]). The other extreme is when all n walls coincide and we have a single wall across which we jump by n vacua, presumably governed by a single $SU(N)_{-n}$ gauge theory and a single translational mode.

To summarize, note that we are still characterizing the phases by partitions $\{n_i\}$ of n and the gauge theory on the wall is once again governed by the topological field theory (3.55). In addition we have the decoupled translational modes. At finite N the walls no longer correspond to static configurations as they will be pushed around by the pressure differences, making them generically much harder to study than the case of interfaces. The reason we discuss them at all as that, at large N, they have a very simple holographic realization which we will employ in what follows to check our dualities.

3.3.1 Theta Wall Dualities via 3d Bosonization

We now consider possible duals to (3.3) via 3d bosonization. Fortunately, such a theory can easily be constructed from the non-Abelian linear quiver dualities.[13] Consider the n node linear quiver, (3.93), and take

$$1 = k_1 = k_2 = \cdots = k_n \tag{3.56a}$$

$$N = N_1 = N_2 = \cdots = N_n. \tag{3.56b}$$

This satisfies all flavor bounds of the derivation given above since $k_i \geq 0$ and $N = N_j \geq N_{j+1} = N$. In this case the dual quiver theories become

$$\text{Theory A:} \qquad [SU(N)_{-1}]^n \times \prod_{p=1}^{n-1} \text{bifund } Y_{p,p+1} \tag{3.57a}$$

$$\text{Theory B:} \qquad \prod_{p=1}^{n-1} [U(p)_0 \times \text{bifund } X_{p,p+1}] \times U(n)_N \tag{3.57b}$$

and the relevant mass deformations for all bifundamentals taken positive/negative are given by

$$\text{(A1)} \qquad M_{i,i+1}^2 > 0: \qquad [SU(N)_{-1}]^n \tag{3.58a}$$

$$\text{(A2)} \qquad M_{i,i+1}^2 < 0: \qquad SU(N)_{-n} \times \prod_{p=1}^{n-1} [SU(0)_{-p}] \tag{3.58b}$$

$$\text{(B1)} \qquad m_{i,i+1}^2 < 0: \qquad [U(1)_N]^n \tag{3.58c}$$

$$\text{(B2)} \qquad m_{i,i+1}^2 > 0: \qquad U(n)_N \times \prod_{p=1}^{n-1} [U(p)_0]\,. \tag{3.58d}$$

The topological sector of Theory A matches the TFTs we set to find at the outset, $SU(N)_{-n}$ and $[SU(N)_{-1}]^n$. In addition both sides have decoupled massless modes that also match. We assume that the non-Abelian part of $U(p)_0$ confines at low energies and is therefore gapped.

[13] As touched upon earlier, if one tried to derive such a quiver using only Aharony's dualities, one would inevitably run into violations of the flavor bound. Thus it appears the interactions between links which come from the master duality are a necessity.

This implies that the dynamics of the confining gauge group should have no effect on the physics at scales well below the gap. The $U(1)$ part however gives rise to a light photon for every level 0 unitary gauge group. On the SU side these light photons map to Goldstone bosons. In a theory with $N_s < N$ scalars charged under a $SU(N)$ gauge symmetry a full global $U(N_s)$ flavor symmetry is unbroken as the gauge group is broken to $SU(N - N_s)$ by a scalar vacuum expectation value. The broken gauge generators can be used to compensate any flavor rotation. In the special case of $N_s = N$, which is of interest to us here, the $U(1)$ part of the flavor symmetry however is broken and so we will get a corresponding Goldstone boson. In order to keep track of these light scalars we denote the Goldstone bosons as $SU(0)_{-p}$ theories, which continue to be "level-rank" dual to the $U(p)_0$ factors of Theory (B2); either theory denotes a decoupled light scalar mode. Including these factors we see that there is a perfect matching both between the topological sector and the decoupled light modes.

One should note that these extra massless Goldstone bosons are exactly the ones that in the theory of theta interfaces have been eliminated by the $\det(Y)$ potentials. As it stands, our quiver duality applies to (3.3) without these extra determinant terms. Since the global $U(1)$ baryon number symmetries under which $\det(Y)$ is charged map to monopole symmetries on the U side, the corresponding dual operator is a monopole operator. Adding this monopole operator to the theory should lead to confinement of the $U(1)_0$ factors together with their non-Abelian counterparts and hence remove the massless photons associated to these factors from the spectrum, just as we removed their dual Goldstone bosons on the SU side.

Given the fact that most of the gauge group factors on the U side confine, we can further simplify the low energy description of this side of the duality. The confining groups cause the bifundamental matter and antimatter to form "mesons". If the matter/antimatter is still charged under some gauge group with nonzero Chern-Simons level, the meson transforms as an adjoint under said gauge group as conjectured in (3.4). For phase (B2), there are the adjoints formed from $X^\dagger_{n-1,n}X_{n-1,n}$ since the $(n-1)$th node confines. It is difficult to say if bound states such as $X^\dagger_{n-1,n}X^\dagger_{n-2,n}X_{n-2,n}X_{n-1,n}$, which are also adjoints under the $U(n)_N$

gauge group, would be stable or if it would split into separate particles $X^\dagger_{n-2,n}X_{n-2,n}$ and $X^\dagger_{n-1,n}X_{n-1,n}$. If we assume the latter, there is only a single light adjoint scalar charged under the $U(n)$ considered above.[14] We also would want to conjecture that there are no additional neutral mesons that become light together with the adjoint; such extra light matter is not accounted for on the SU side of the duality. With these dynamical assumptions our quiver duality boils down to the one we advertised in the introduction

$$[SU(N)_{-1}]^n + \text{bifundamental scalars} \qquad \leftrightarrow \qquad U(n)_N + \text{adjoint scalars} \tag{3.59}$$

with a $\det(Y)$ potential for all the bifundamental scalars on the SU side implied.

Unlike the quiver dualities, which we derived from gauging global symmetries, the duality (3.4) only follows upon making extra dynamical assumptions regarding the confining mechanism. We can give extra evidence for this duality by, once again, looking at the phase structure. On the U side the various massive phases are realized by adding mass squared terms that give expectation values to the adjoint scalar (or remove it completely) together with $\mathrm{Tr}\, X^k$ terms in the potential. We can always chose a gauge in which the scalar expectation value is diagonal, so the generic expectation values is characterized by the n eigenvalues of the scalar expectation value. Due to the presence of the interaction terms, it is possible to have none of the eigenvalues coincide, in which case the gauge group is $[U(1)_N]^n$. But whenever two or more eigenvalues coincide, we do get an enhanced unbroken subgroup. Once again the most general phase is encoded in partitions $\{n_i\}$ of n, where each integer n_i denotes the multiplicity of a given eigenvalue. The generic phase is given by $n_i = 1$ for all i, whereas the case of n coincident eigenvalues with a single $U(n)_N$ gauge group factor corresponds to $n_1 = n$. The generic partition corresponds to

$$\text{Phase } \{n_i\}: \qquad \prod_i U(n_i)_N. \tag{3.60}$$

[14]Note that when the bifundamental scalars on the SU side acquire a negative vacuum expectation value, by assumption this breaks their gauge symmetry down to the common diagonal symmetry group and causes the Higgsed bifundamentals to become adjoint particles. Thus we get gapped adjoint particles on both sides of the duality for phase 2 considered above.

Reassuringly, this is exactly the level-rank dual gauge group of what we found for the quiver theory, (3.55). In the next section we will give further support for the validity of this duality, at least in the large N limit, using holography.

3.3.2 Theta Wall Dualities via Holography

Now we turn to the holographic proof of the duality. Our work will follow closely the stringy embedding of bosonization presented in [66] based on the earlier string theory realization of level-rank duality in [47]. In this construction the holographic duality between field theory and supergravity becomes, at low energies, the purely field theoretic bosonization duality.

One starts with a well known holographic pair. The work of [47, 66] employs the original holographic duality [83] between $\mathcal{N} = 4$ super-Yang Mills (SYM) and type IIB string theory on $\mathrm{AdS}_5 \times S^5$. We then deform the theory in such a way that all, or at least most, degrees of freedom gap out and one is left with a non-trivial topological field theory (in the case of level-rank) or conformal field theory (in the case of bosonization) in the infrared. Following the same deformations in the dual gravity solution one finds that the spectrum of most supergravity excitations also gets gapped out. The only remaining low energy excitations are localized on a probe brane. These probe degrees of freedom in the bulk are found to be related to the boundary degrees of freedom by the desired field theory duality.

Review of Holography Applied to 3d Bosonization

Let us first briefly review the case of level-rank. Starting with $\mathcal{N} = 4$ SYM one can go to $2 + 1$ dimensions via compactifying the theory on a circle of radius R. With anti-periodic boundary conditions for the fermions in the theory, all fermionic Kaluza Klein modes pick up masses of order $1/R$ and the scalars then pick up masses of the same order via loop corrections. At energies below $1/R$ we are left with pure Yang-Mills in $2 + 1$ dimensions, which is believed to confine. The theory is gapped with gap of order $1/R$. This is not quite yet the theory we want, the IR is trivial rather than a non-trivial Chern-Simons TFT.

To produce the desired Chern-Simons terms we need to introduce the theta angle. Like all coupling constants in the Lagrangian, the theta angle in $3+1$ dimensional gauge theories is usually introduced as a position independent constant, but it can be promoted to a non-trivial background field. What we need here is a theta angle that linearly changes by $2\pi n$ as we walk around the circle once. Since theta is only well defined modulo 2π this is consistent as long as n is an integer. The $\theta F \wedge F$ term in the Lagrangian with constant theta gradient can be integrated by parts to turn into a $2+1$ dimensional Chern-Simons term with level $-n$. So in short, $\mathcal{N} = 4$ SYM with anti-periodic boundary conditions for fermions and a constant theta gradient gives rise to a gapped $2+1$ dimensional theory which, at low energies, is well described by an $SU(N)_{-n}$ Chern-Simons theory.

These deformations are easily repeated in the holographic dual. The compactification with anti-periodic boundary conditions for fermions is dual to the cigar geometry of [118], that is a doubly-Wick rotated planar Schwarzschild black-hole where the compact time direction of the Euclidean black hole plays the role of the compact spatial directions, whereas one of the directions along the planar "horizon" becomes the new time direction. Most importantly, the radial coordinate in this cigar geometry truncates at a finite value $r = r_*$ where the compact circle contracts. Consequently this geometry acts as a finite box and so indeed all supergravity fluctuations exhibit a gapped spectrum [118] with a mass gap of order $1/R$. In order to retain a non-trivial topological sector we still need to implement the spatially varying theta angle. The theta angle is set by the near boundary behavior of the bulk axion field, so we are looking for a supergravity solution where the axion asymptotes to $a \sim ny/R$. Here y denotes the coordinate along the circle direction and $a = ny/R$ is an exact solution to the axion equation of motion in the cigar background. As long as we are only interested in the $n \ll N$ limit we can ignore the backreaction of the axion on the background geometry and $a = ny/R$ appears to be the full solution to the problem. The only remaining issue is that the axion field strength $f_y = \partial_y a = n/R$ in the bulk has to be supported by a source. This source can be introduced by locating n D7 branes, wrapping the entire internal S^5, at the tip of the cigar at $r = r_*$. This stack of D7 brane introduces new degrees of

freedom in the bulk. The scalar fields corresponding to fluctuations of the D7 away from the tip are massive due to the geometry of the cigar. Like all other geometric fluctuations they have mass of order $1/R$. The only other degree of freedom introduced by the n D7 branes is the worldvolume gauge field. The latter acquires a Chern-Simons term of level N from the Wess-Zumino coupling to the N units of background 5-form flux through the S^5. Lo and behold, the low energy description of the holographic bulk dual is simply a $U(n)_N$ Chern-Simons gauge theory living on the D7 branes. Comparing low energy descriptions on both sides, AdS/CFT boiled down to level-rank duality for the emerging TFTs.

The last step in order to derive 3d bosonization rather than level-rank from this construction is to add extra light matter into the theory. This can be easily accomplished using flavor probe branes [74]. In the construction put forward in [66] an extra probe D5 adds fermionic matter localized on $2+1$ dimensional defects in the $3+1$ dimensional theory. These defects live at points in the circle direction, so at low energies they simply become light fermions coupled to the $SU(N)_{-n}$ Chern-Simons gauge fields. The same probe branes can be argued, from the bulk point of view, to add scalar matter to the dual $U(n)_N$ Chern-Simons gauge theory. Instead of simply giving us level-rank, in this case holography, at low energies, reduces to the basic non-Abelian 3d bosonization duality.

Holographic Realization of Theta Walls

To holographically realize the field theory theta domain walls we just reviewed we need to start with a holographic duality for a confining $3+1$ dimensional theory and then simply once again follow the field theory deformation corresponding to turning on theta in the bulk. The simplest realization of a confining $3+1$ gauge theory with a gravity dual is Witten's black hole [118]. This is almost the same construction we employed previously, but lifted one dimension up. We start with a 5d gauge theory, maximally supersymmetric YM with gauge group $SU(N)$, and compactify it on a circle with anti-periodic boundary conditions. The dual geometry has once again the basic shape of a cigar, and the explicit supergravity

solution is given by

$$ds^2 = \left(\frac{u}{L}\right)^{3/2}\left(\eta_{\mu\nu}dx^\mu dx^\nu + f(u)dy^2\right) + \left(\frac{L}{u}\right)^{3/2}\left(\frac{du^2}{f(u)} + u^2 d\Omega_4^2\right),$$
$$e^\phi = g_s\left(\frac{u}{L}\right)^{3/4}, \quad F_4 = dC_3 = \frac{2\pi N}{V_4}\epsilon_4, \quad f(u) = 1 - \frac{u_*^3}{u^3}. \tag{3.61}$$

Here x^μ are the 4 coordinates of $3+1$ dimensional Minkowski space, y is the circle direction we compactified to go from $4+1$ to $3+1$ dimensions. ϕ is the dilaton field, F_4 the RR 4-form field strength. Ω_4 is the internal 4-sphere, with $d\Omega_4^2$, ϵ_4 and $V_4 = 8\pi^2/3$ its line element, volume form and volume respectively. The string coupling g_s and the string length l_s are the parameters of the underlying type IIA super-string theory. L sets the curvature radius of the solution, it is determined by Einstein's equations to be $L^3 = \pi g_s N l_s^3$. Last but not least u_* is the location of the tip of the cigar, it is related to the periodicity $2\pi R$ of the compactification circle by $R = \frac{2}{3}L^{3/2}u_*^{-3/2}$.

The holographic realization of turning on a constant theta angle has been worked out in [120]. The theta angle is dual to the Wilson line of the bulk RR 1-form C_μ along the compact y direction:

$$\int_{S^1} C = \theta + \ldots \tag{3.62}$$

where the ellipses denote terms with negative powers of u, that is terms that vanish near the boundary. The Wilson line is gauge invariant modulo $2\pi\mathbb{Z}$, so theta is indeed an angle. Using Stokes's law, we can rewrite the condition (3.62) as

$$\int_D F = \theta + 2\pi K. \tag{3.63}$$

Here $F = dC$ is the field strength associated with the RR one-form and D is the cigar geometry, which has the topology of a disc. Since $\int_D F$ is a well-defined real number whereas θ is an angle, we have a $2\pi K$ ambiguity in F where K is an integer. For a given theta there is more than one bulk solution for F, characterized by K. This is responsible for the multi-branched structure of the allowed ground states which we expect to find. Physics in any given one of the branches is only periodic in $2\pi N$, the actual periodicity of θ is 2π as it should be. We simply jump to a different branch.

For generic theta it is non-trivial to solve the supergravity solutions subject to the constraint (3.63). But a very simple solution can once more be found [120, 20] in the probe limit $(\theta + 2\pi K) \ll N$, or in other words $K/N \ll 1$. In this limit one can neglect the backreaction of the axion on the background geometry. Newton's constant is of order $1/N^2$ in units where the curvature scale $L = 1$, whereas the axion action and hence its stress tensor is of order 1 in the large N counting. The only non-trivial equation left to solve is Maxwell's equation for C_1 in the background geometry (3.61) subject to the boundary condition (3.63). The solution is

$$C_1 = \frac{f(u)}{2\pi R}(\theta + 2\pi K)dy. \tag{3.64}$$

The integer K is the bulk manifestation of the K-th vacuum. In fact, plugging the solution (3.64) back into the action we find that the vacuum energy density of the K-th vacuum has exactly the expected form from (3.52) with [20]

$$h(\theta/N) = -\frac{2N^2\lambda}{3^7\pi^2 R^4}\left[1 - 3\left(\frac{\lambda}{4\pi^2}\right)^2\left(\frac{\theta + 2\pi K}{N}\right)^2\right] \tag{3.65}$$

where $\lambda = g_{YM}^2 N = 2\pi g_s l_s N/R$ is the 't Hooft coupling.

While it is not obvious to us how to realize interfaces in this setup, the holographic dual for a domain wall has already been proposed in [120]. A jump in vacuum, according to (3.63), requires a jump in $\int_D F$, which in turn requires a source magnetically charged under the RR 1-form. The naturally stringy object carrying the appropriate RR charge is a D6 brane. The D6 brane needs to wrap the entire internal S^4 as well as the 3d Minkowski space spanned by t, x_1 and x_2. It is localized in the x_3 direction as well as on the cigar geometry D. From the induced metric of a D6 sitting at a fixed position u and wrapping $M^{2,1} \times S^4$ is we can infer that the D6 Lagrangian density $e^{-\phi}\sqrt{-g_I}$ reads

$$\mathcal{L} \propto u^{5/2} \tag{3.66}$$

meaning that the D6 brane experience a potential pulling it to smaller values of u: the D6 brane will sink to the tip of the cigar, see Fig. 3.4.

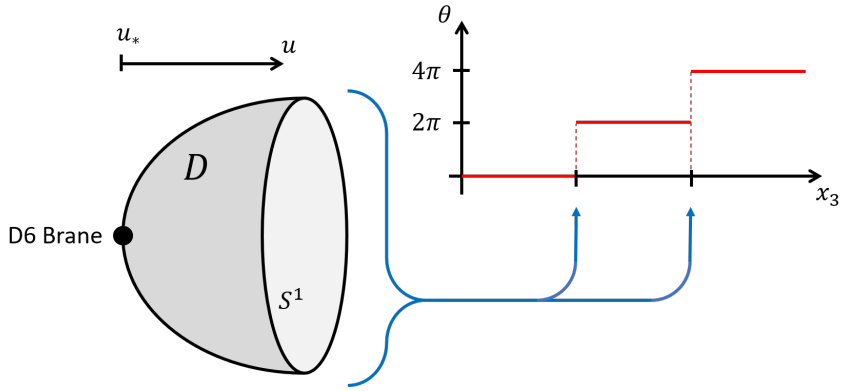

Figure 3.4: Configuration of D6 branes.

Let us first discuss the case of a single D6 brane. Without loss of generality, we can place the D6 at $x_3 = 0$. If we denote by D_- the cigar/disc spanned by (y, u) at a fixed negative x_3 and D_+ the cigar/disc at a fixed positive x_3, then the analog of the magnetic Gauss' law for the D6 brane reads

$$\int_{D_+} F - \int_{D_-} F = 2\pi. \tag{3.67}$$

Comparing with (3.63) we see that this means that $(\theta + 2\pi K)$ jumps by 2π as we cross, in the field theory, the bulk x_3 location of the D6-brane. This also implies that the vacuum energy of the theory jumps across the D6. Furthermore, the D6 brane is clearly dynamical. The x_3 position of the D6 brane is a dynamical field. Since the metric is independent of x_3 the corresponding worldvolume scalar is massless. These facts together clearly identify the D6 brane as the domain wall between the j-th and $(j+1)$-th vacuum [120] at a fixed theta angle. The general wall in which we jump from the j-th vacuum to the $(j+K)$-th simply corresponds to K coincident D6 branes. We can pull apart the stack of K D6 branes to obtain a configuration of walls where the vacuum jumps one unit at a time at well-separated locations in the x_3 direction.

It is fairly straightforward to determine the low energy physics in the bulk. The background geometry once more truncates at a finite radial position, $u = u_*$. Correspondingly

all supergravity modes are gapped. The only degrees of freedom surviving are the ones localized on the D6 branes. For a stack of n coincident D6 branes, these worldvolume degrees of freedom are a $U(n)$ gauge field as well as 3 adjoint scalars corresponding to motion of the stack into the u, y and x_3 direction. The u and y fluctuations are massive due to the cigar geometry just as we reviewed above in section 3.3.2. The x_3 scalar, however, is massless. The worldvolume gauge field picks up a Chern-Simons term of level N from the Wess-Zumino coupling of the worldvolume gauge field to the N units of 4-form flux. So the low energy dynamics in the bulk is governed by a $U(n)_N$ gauge theory with a single massless adjoint representation scalar. Holographic duality implies that this is an equivalent representation of the quiver gauge theory with the additional $n-1$ translational modes associated with the domain walls at least in the large N limit.

Note that this way we almost landed on the duality (3.4). There is however a small difference. On the quiver side, we have the extra light modes corresponding to the translational motion of the domain walls. As we argued before, we expect these to be present at large N. At any finite N the domain walls would no longer be static. The phases of the quiver theory are still given by (3.55) as long as one accounts for the extra decoupled translational modes. The analogous statement on the U side of the duality is that the adjoint scalar governing the position of the stack of probe branes this time corresponds to a flat direction. The various phases are still parametrized by the n eigenvalues of the scalar matrix $\langle x_3 \rangle$. But this time instead of having to add deformations to the potential we have a moduli space of vacua where we can freely dial the expectation values of x_3. The eigenvalues of $\langle x_3 \rangle$ simply correspond to D6 positions and the enhanced gauge symmetries we encounter for coincident eigenvalues simply arise from coincident D6 branes. The gauge groups of the various phases once again are given by (3.60), but since the scalar potential was exactly flat this time each gauge group factor comes with an extra massless adjoint. In the generic case where the gauge group is $[U(1)_N]^n$ these extra massless adjoints map exactly to the n translational modes we identified on the quiver side. Surely the exactly flat potential for the probe scalar is also an artifact of the large N limit and any bulk quantum corrections would lift this flat direc-

tion. Furthermore, the phase where the adjoint gets a positive mass squared is not easily realized in the brane picture. Modulo these extra light scalars, matching on both sides, the holographic construction exactly reproduces our conjectured duality (3.4).

3.4 Adding Flavors to Quivers

We now turn our attention to the construction and dualization of *flavored* quiver gauge theories. In analogy to the unflavored quiver gauge theories discussed in the previous sections, these purely $2+1$ dimensional theories will serve as an effective description of interfaces in $3+1$ dimensional QCD when one varies the θ angle along a particular coordinate direction. Interestingly anomaly considerations alone aren't sufficient to pin down the $2+1$ dimensional theory. While it is difficult to prove, it has been argued in [50] that different theories govern the steep versus the shallow interface. Concretely, let us focus on the case where the θ angle experiences a net jump of $2\pi n$ with an integer n. In this case the shallow interface in a $3{+}1$ dimensional gauge theory with gauge group $SU(N)$ is believed to be described by a $2{+}1$ dimensional $[SU(N)_{-1}]^n$ gauge theory, whereas the steep wall is described by a single $SU(N)_{-n}$ theory.

At least for the shallow interface this can easily be argued based on the general expectations for the θ dependence in $SU(N)$ gauge theories, at least at large N, as described in [120]. The vacuum energy in any given vacuum at large N can be shown to be $2\pi N$ periodic. In order to reconcile this with the expected 2π periodicity of QCD one postulates that the theory has N different vacua as depicted in figure 3.5. At any given θ the vacuum energy is lowest in one of the N vacua. As θ increases one finds that whenever it reaches an odd multiple of π two of the vacua are degenerate. Further increasing θ past this point triggers a transition to a different vacuum and by the time we shifted θ by 2π one indeed is back to the same physics, but in a different vacuum.

This allows a very simple description of the shallow interface, where the gradient of θ is small compared to the strong coupling scale of the theory. All the interesting physics is localized at the points where θ passes odd multiples of π. Since the gradient of θ is small,

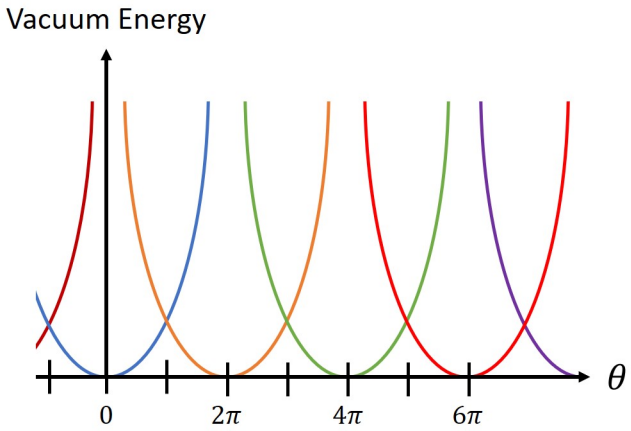

Figure 3.5: Expected behavior of the vacuum energy as a function of θ in a large N gauge theory. Distinct branches are shown in different colors.

these loci are widely separated and we expect the total topological field theory to be simply n copies of the theory living on a single interface, which then can be argued to be $SU(N)_{-1}$ based on anomalies [1, 43]. For a steep interface there is another theory that can carry the correct anomaly – a single $SU(N)_{-n}$. If the transition between the steep and shallow interfaces is second order, it should be described by a conformal field theory. This is the quiver gauge theory of (3.3). If we give all the scalars a large positive mass, we simply remove all bifundamental scalars leaving behind the product gauge group of the shallow interface. On the other hand, giving all the scalars a large negative mass drives the gauge groups into the Higgs phase, breaking them down to the single gauge group of the steep interface. We wish to see how this picture changes with the addition of fundamental fermions.[15] This will require the use of the flavor violated master duality developed in the previous section.

To construct the flavorless quivers, we used the fact that one can identify and gauge the $SU(N_f) \times SU(N_s)$ flavor symmetries of (multiple copies of) the master duality to get bifundamental matter charged under various gauge symmetries. Adding flavors to the nodes

[15]For a discussion on interfaces in QCD_4, see Appendix A of [50].

can be achieved if we only gauge a *part* of the flavor symmetry instead of the entire global flavor symmetry. The leftover global symmetry and the corresponding field components then become additional matter on each node.

We employ the aforementioned procedure in order to engineer a quiver with SU gauge theories and scalar matter on the links. Node-by-node duality in general turns this into an equal length quiver with U gauge theories on the nodes and once again scalar bifundamental matter. We add extra fundamental representation fermions on the original SU side, which we will see necessitate extra scalar matter on the dual U side. Intermediate steps involve theories with bifundamental fermions as well, but they are present neither in the initial nor in the final theory. The U side can be argued to collapse to a single gauge group when the ranks of the gauge groups on all nodes are equal in the original SU type theory. This pattern is what we previously found in the case of the unflavored quivers, and we will see it again once flavors are included.

While we can construct these quiver dualities for generic ranks and levels on the nodes (subject to certain bounds) there are special values of these parameters for which certain nodes confine. While in this case uncontrolled strong coupling dynamics is important, holography suggests that in this case a much simpler duality emerges. We will argue that

$$[SU(N)_{-1+N_F/2}]^n + \text{bifundamental scalars} + N_F \text{ fundamental fermions per site} \tag{3.68}$$

with certain potential terms is dual to

$$U(n)_N + \text{adjoint scalar} + N_F \text{ fundamental scalars.} \tag{3.69}$$

Clearly this is a intuitive generalization of (3.3) and (3.4). Let us justify these results again using node-by-node duality and holography.

However, one runs into difficulty when applying the same methods discussed above for the unflavored case. When applying bosonization dualities to each node, one finds that the flavor bound is always violated for at least one node. To rectify this, we must first extend the master duality [24, 64] beyond the flavor bound, in a manner consistent with the symmetry

breaking scenario of Komargodski and Seiberg [80]. In particular, we map out the phase diagram for the master duality in the regime where $k < N_f < N_*(N,k)$ and $N_s < N$.

3.4.1 Extending the Master Duality

Before diving into the extension of the master duality phase diagram, we will review the construction of [80], i.e. examine the $N_s = 0$ limit. Like the ordinary master duality, the phase diagrams for the $N_s < N$ and $N_s = N$ cases look fairly different due to particular cancellations which occur in the latter case. We will begin with the phase diagram for the more general $N_s < N$ since it is slightly simpler to analyze. The $N = N_s$ case will be considered second and it will be applicable to the quivers we are constructing to model the domain wall behavior of QCD_4. Finally, we will discuss extending the master duality to the double saturated case in Sec. 3.4.3.

Review of QCD_3 Symmetry-Breaking

As was mentioned in the the introduction, the flavor bounds of (**??**) are imposed because when $N_f > k$, the Higgs phase of the U side of the theory becomes a non-linear sigma model. This does not appear to be matched on the SU side, because the corresponding fermion mass deformation simply shifts the Chern-Simons level. Hence the bound $N_f \leq k$ was imposed to avoid the mismatch from the non-linear sigma model phase.

The proposal of [80] is that when $k < N_f < N_*(N,k)$, for small fermion masses, i.e. $|m_\psi| < m_*$, the SU Chern-Simons theory causes the fermions to condense, yielding a non-linear sigma model whose target space is the complex Grassmannian manifold[16]

$$\mathcal{M}(N_f,k) = \frac{U(N_f)}{U(k)\times U(N_f-k)}. \tag{3.70}$$

Said another way, the SU side exhibits "chiral" symmetry breaking, yielding as its low energy "pion" Lagrangian the target space of (3.70). Importantly, it is the number of fermions with

[16]Note, here we are using a slightly different convention than [80] for the levels of the Chern-Simons terms. The SU levels we use do not have the additional $-N_f/2$ shift used in [80] to make the phases look more symmetric.

$|m_\psi| < m_*$ which determines whether or not the associated gauge group confines, resulting in the Grassmannian (3.70). Specifically, the assumption is that if the number of light fermions exceeds the bare level of the gauge group (the level without the η-invariant offset), the fermions still condense. When we construct quivers below we will further split the N_f symmetry into smaller subgroups and individually tune their masses. This can lead to a rich structure with many different Grassmannians, but in this work we will generally be concerned with phases outside of this region. More details on such subtleties of the phase diagram can be found in Refs. [16, 22].

A potential issue with this assumption is that the Grassmannian of the SU side only exists for small mass deformations, see Fig. **??**. This is not matched on the U side if we use the phase diagram of the flavor-bounded duality (**??**), which has a Grassmannian phase for unbounded negative scalar mass deformations. To rectify this, the authors of ref. [80] propose that there are *two* scalar theories dual to the SU end that are patched together to describe the full phase diagram. More explicitly, the duality proposed is

$$SU(N)_{-k+N_f/2} \text{ with } N_f\, \psi \qquad \leftrightarrow \qquad \begin{cases} U(k)_N \text{ with } N_f\, \Phi_1 & m_\psi = -m_* \qquad \text{(blue)} \\ U(N_f-k)_{-N} \text{ with } N_f\, \Phi_2 & m_\psi = m_* \qquad \text{(red)} \end{cases}, \tag{3.71}$$

where the colors in parenthesis correspond to those in Fig. **??** and figures which follow. Note that in both scalars theories, when the mass becomes negative we obtain the same aforementioned Grassmannian manifold of (3.70). Accompanying the Grassmannian is a Wess-Zumino-Witten term with a coefficient that is determined by the level of the Chern-Simons theories on the U side. This is important for matching of the operators across the duality, but will not play an essential role in our story. For more details on this term see [80]. This model is summarized in Fig. **??**.

One feature of this construction that we will see occurs also in the master duality case is that the SU side of the duality does not yield a good description of the quantum phase or the theories which exist at the phase transition. That is, the true IR description on the

SU side is hidden by strong dynamics and so we must pass to the U side to obtain a full description of the phase diagram.

3.4.2 Flavor-Violated Master Duality

We now generalize the analysis of [80] to the master duality. In particular, we are interested in mapping out the phase diagram of

$$SU(N)_{-k+N_f/2} \text{ with } N_f \ \psi \text{ and } N_s \ \phi \tag{3.72}$$

when $N_f > k$ and $N_s \leq N$ as a function of the scalar and fermion masses. We will begin our analysis in the asymptotic regimes where the mass deformations are large compared to the strong scale and we don't expect to see quantum phases. When one or both mass deformations are small, we again expect to find phases that may be described by Grassmannian manifolds.

When we give an asymptotically large positive mass to the scalars, we can integrate them out and they have no effect on the gauge group. The theory we are left with is

$$SU(N)_{-k+N_f/2} \text{ with } N_f \ \psi. \tag{3.73}$$

This is nothing more than the left-hand side of (4.19) and so this portion of the phase diagram is identical to what was found for QCD_3. We can do the same for a large negative mass deformation. Assuming the Higgsing is maximal,the gauge group breaks as $SU(N) \to SU(N - N_s)$. The resulting theory is

$$SU(N - N_s)_{-k+\frac{N_f}{2}} \text{ with } N_f \ \psi \tag{3.74}$$

which again appears to be described by (4.19) so long as $N - N_s > 1$. For now, we are ignoring effects due to the interaction term, but we will return to such considerations when we analyze the Grassmannian regime. We will see such terms make the Grassmannian portion of (3.74) different than that of (4.19) with $N \to N - N_s$.

Since we can match onto (4.19) for the asymptotically large mass phases of the SU side of the master duality, we follow the same reasoning for the U side. We thus assume once more we cannot use a single dual theory to describe all the phases of the U side. This motivates the "flavor-violated master duality" shown in Fig. **??**:

$$SU(N)_{-k+N_f/2} \text{ with } N_f\ \psi \text{ and } N_s\ \phi$$
$$\leftrightarrow \quad \begin{cases} U(k)_{N-N_s/2} \text{ with } N_f\ \Phi_1 \text{ and } N_s\ \Psi_1 & m_\psi = -m_* \text{ (blue)} \\ U(N_f-k)_{-N+N_s/2} \text{ with } N_f\ \Phi_2 \text{ and } N_s\ \Psi_2 & m_\psi = m_* \text{ (red)}. \end{cases} \tag{3.75}$$

As a first consistency check, we make sure all four asymptotic phases match across the duality

$$\text{(I)}: \qquad SU(N)_{-k+N_f} \quad \leftrightarrow \quad U(N_f-k)_{-N}, \tag{3.76a}$$
$$\text{(II)}: \qquad SU(N-N_s)_{-k+N_f} \quad \leftrightarrow \quad U(N_f-k)_{-N+N_s}, \tag{3.76b}$$
$$\text{(III)}: \qquad SU(N-N_s)_{-k} \quad \leftrightarrow \quad U(k)_{N-N_s}, \tag{3.76c}$$
$$\text{(IV)}: \qquad SU(N)_{-k} \quad \leftrightarrow \quad U(k)_N. \tag{3.76d}$$

The levels for both the dynamical and background fields can be fixed by making sure the mass deformations of the two U theories match that of the SU theories for the asymptotically large deformations we have thus far discussed. The details of this analysis as well as explicit Lagrangians are given in Appendix 3.8. Phases I and II follow from the first dual description in (3.75), while phases III and IV correspond to second dual description in (3.75). Note that for $N_f \leq k$, the flavor-bounded master duality instead yields the phases

$$\text{(I')}: \qquad SU(N)_{-k+N_f} \quad \leftrightarrow \quad U(k-N_f)_N, \tag{3.77a}$$
$$\text{(II')}: \qquad SU(N-N_s)_{-k+N_f} \quad \leftrightarrow \quad U(k-N_f)_{N-N_s}, \tag{3.77b}$$

but phases III and IV are the same as the $N_f > k$ case. We will use this fact to save us some work later on.

The mass mappings between the two sides are slightly complicated by the two scalar descriptions of the U side. For $m_\psi < 0$ we have

$$m_\psi + m_* \leftrightarrow -m_{\Phi_1}^2 \qquad m_\phi^2 \leftrightarrow m_{\Psi_1} \tag{3.78}$$

while for $m_\psi > 0$

$$m_\psi - m_* \leftrightarrow m_{\Phi_2}^2 \qquad m_\phi^2 \leftrightarrow -m_{\Psi_2}. \tag{3.79}$$

Once more we see the scalar mass vanishes when the magnitude of the fermion mass is equal to m_*.

Now let us discuss what we expect to occur as we move to smaller mass deformations. Once more, we can use (4.19) as a guiding principle for particular phases. Since phases I and IV precisely correspond to the large mass deformations of (4.19), we expect to find the very same Grassmannian in between them, which we have called phase V. This is indeed consistent with the two U theories of (3.75). The story gets slightly more complicated for other regions of the phase diagram. Let us now analyze the $N_s < N$ and $N_s = N$ cases in turn.

Flavor-Violation for $N > N_s$

Summarizing our results first, the phase diagram of (3.72) and the claimed duals for $N > N_s$ are given in Fig. **??**. As we have learned, many aspects of the phase diagram are better described on the U side, so much of what is drawn on the SU is learned by considering how the two dual U theories can be consistent in the presence of a finite interaction term. Phases I, V, and IV correspond to the three phases of (4.19) conjectured by Ref. [80].

The SU phase diagram contains the following phases

$$\text{(I)}: \quad SU(N)_{-k+N_f} \times [SU(N_f)_N \times SU(N_s)_0 \times J_{\rm I}] \tag{3.80a}$$

$$\text{(II)}: \quad SU(N-N_s)_{-k+N_f} \times \left[SU(N_f)_N \times SU(N_s)_{-k+N_f} \times J_{\rm II}\right] \tag{3.80b}$$

$$\text{(III)}: \quad SU(N-N_s)_{-k} \times [SU(N_f)_0 \times SU(N_s)_{-k} \times J_{\rm III}] \tag{3.80c}$$

$$\text{(IV)}: \quad SU(N)_{-k} \times [SU(N_f)_0 \times SU(N_s)_0 \times J_{\rm IV}] \tag{3.80d}$$

$$\text{(V) to (VIII)}: \quad \text{Better described by } U \text{ side} \tag{3.80e}$$

where the Chern-Simons theories in $[\cdots]$ belong to background gauge fields. Meanwhile,

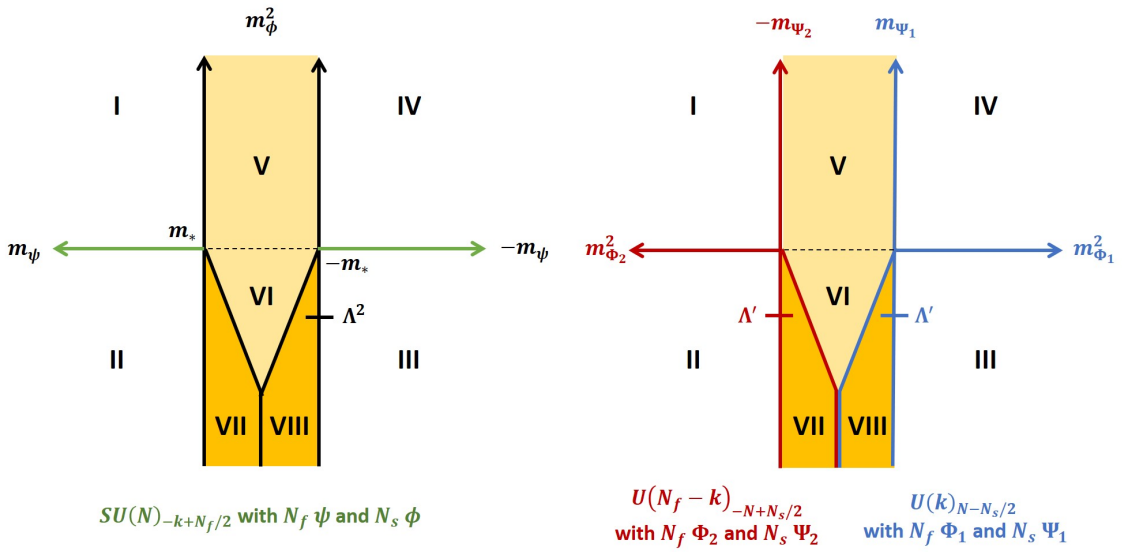

Figure 3.6: SU and U sides of the flavor-violated master duality for $N > N_s$. On the SU side, the critical lines in green are well-described by the corresponding SU theory. The critical lines in black are best described by the U duals.

the U side is given by

$$\text{(I)}: \quad U(N_f-k)_{-N}\times[SU(N_f)_N\times SU(N_s)_0\times J_{\rm I}] \tag{3.81a}$$

$$\text{(II)}: \quad U(N_f-k)_{-N+N_s}\times\left[SU(N_f)_N\times SU(N_s)_{-k+N_f}\times J_{\rm II}\right] \tag{3.81b}$$

$$\text{(III)}: \quad U(k)_{N-N_s}\times[SU(N_f)_0\times SU(N_s)_{-k}\times J_{\rm III}] \tag{3.81c}$$

$$\text{(IV)}: \quad U(k)_N\times[SU(N_f)_0\times SU(N_s)_0\times J_{\rm IV}] \tag{3.81d}$$

$$\text{(V), (VI)}: \quad \mathcal{M}(N_f,k)\times[SU(k)_N\times SU(N_f-k)_0\times SU(N_s)_0\times J_{\rm V,VI}] \tag{3.81e}$$

$$\text{(VII)}: \quad \mathcal{M}(N_f,k)\times\left[SU(k)_N\times SU(N_f-k)_{N_s}\times SU(N_s)_{N_f-k}\times J_{\rm VII}\right] \tag{3.81f}$$

$$\text{(VIII)}: \quad \mathcal{M}(N_f,k)\times[SU(k)_{N-N_s}\times SU(N_f-k)_0\times SU(N_s)_{-k}\times J_{\rm VIII}]\,. \tag{3.81g}$$

We note that phases V and VI are one in the same phase, despite being separated by a dotted line in fig. **??**. This dotted line represents where a phase transition would occur if not for the interaction terms to be discussed below.

We label the critical theories by the two phases which they separate. They are

$$\text{(I-II)}: \quad U(N_f-k)_{-N+N_s/2} \text{ with } N_s\ \Psi_2 \quad \leftrightarrow \quad SU(N)_{-k+N_f} \text{ with } N_s\ \phi \tag{3.82a}$$

$$\text{(III-IV)}: \quad U(k)_{N-N_s/2} \text{ with } N_s\ \Psi_1 \quad \leftrightarrow \quad SU(N)_{-k} \text{ with } N_s\ \phi \tag{3.82b}$$

$$\text{(I-V)}: \quad U(N_f-k)_{-N} \text{ with } N_f\ \Phi_2 \tag{3.82c}$$

$$\text{(IV-V)}: \quad U(k)_N \text{ with } N_f\ \Phi_1 \tag{3.82d}$$

$$\text{(II-VII)}: \quad U(N_f-k)_{-N+N_s} \text{ with } N_f\ \Phi_2 \tag{3.82e}$$

$$\text{(III-VIII)}: \quad U(k)_{N-N_s} \text{ with } N_f\ \Phi_1 \tag{3.82f}$$

$$\text{(VI-VII)}: \quad \mathcal{M}(N_f,k) \text{ with } (N_f-k)N_s\ \psi_s \tag{3.82g}$$

$$\text{(VI-VIII)}: \quad \mathcal{M}(N_f,k) \text{ with } kN_s\ \psi_s' \tag{3.82h}$$

$$\text{(VII-VIII)}: \quad \mathcal{M}(N_f,k) \text{ with } (N_f-k)N_s\ \psi_s \text{ and } kN_s\ \psi_s'. \tag{3.82i}$$

Most of the critical theories are described by U side alone except (I-II) and (III-IV) which have an SU description related by (**??**). As a reminder, ψ_s and ψ_s' denote neutral fermions in the phases where dynamical gauge group is completely broken. By construction, each of the critical theories correctly describes the transition between the two phases which it separates, consistent with anomaly constraints.

The J_i for $i =$ I, II, III, IV are the Abelian Chern-Simons levels of the two $U(1)$ background gauge fields $\tilde{A}_1$ and $\tilde{A}_2$ in the i-th phase. When one enters the Grassmannian phases, the breaking of the $SU(N_f)$ global symmetry yields an additional background $U(1)$ field, which we call $\tilde{A}_3$. We write these $U(1)$ levels as

$$J_i \equiv J_i^{ab} \frac{1}{4\pi} \tilde{A}_a d\tilde{A}_b \tag{3.83}$$

where the J_i^{ab} are[17]

[17] We suppress the third column/row for phases outside of the Grassmannian regime for brevity. For more details on how these terms are calculated, see [64, 24, 13].

$$J^{ab}_{\mathrm{I}} = \begin{pmatrix} N(N_f-k) & 0 \\ 0 & 0 \end{pmatrix} \tag{3.84a}$$

$$J^{ab}_{\mathrm{II}} = \frac{N(N_f-k)}{N-N_s}\begin{pmatrix} N & N_s \\ N_s & N_s \end{pmatrix} \tag{3.84b}$$

$$J^{ab}_{\mathrm{III}} = \frac{-Nk}{N-N_s}\begin{pmatrix} N & N_s \\ N_s & N_s \end{pmatrix} \tag{3.84c}$$

$$J^{ab}_{\mathrm{IV}} = \begin{pmatrix} -Nk & 0 \\ 0 & 0 \end{pmatrix} \tag{3.84d}$$

$$J^{ab}_{\mathrm{V,VI}} = \begin{pmatrix} 0 & 0 & -Nk \\ 0 & 0 & 0 \\ -Nk & 0 & Nk \end{pmatrix} \tag{3.84e}$$

$$J^{ab}_{\mathrm{VII}} = \begin{pmatrix} 0 & 0 & -Nk \\ 0 & N_s(N_f-k) & -N_sk \\ -Nk & -N_sk & \frac{N_sk^2}{N_f-k}+Nk \end{pmatrix} \tag{3.84f}$$

$$J^{ab}_{\mathrm{VIII}} = \begin{pmatrix} 0 & 0 & -Nk \\ 0 & -N_sk & -N_sk \\ -Nk & -N_sk & (N-N_s)k \end{pmatrix}. \tag{3.84g}$$

See Appendix 3.8 for more detailed discussion about the Lagrangian and background fields. We now explain in more detail how we determined these phases and critical lines.

Construction of Flavor-Violated Master Duality As mentioned above, we follow the guiding principle of Ref. [80] to conjecture the phase diagram on the U side of the duality. For Aharony's duality, the natural way of constructing the U side of the flavor-violated phase diagram was to overlay the phase diagram of two scalar theories, which was consistent since both scalar theories exhibited the same non-linear sigma model phase. It follows that as one traverses the quantum phase of the U side one must switch over from one scalar description

to another. This is the same principle by which we have constructed the phase diagram for the master duality.

What complicates the phase diagram description for the flavor-violated master duality is the presence of the interaction term, which leads to an additional splitting of phases. It is straightforward to see the additional critical line from the interaction term is present in what will become the overlapping Grassmannian phases of the U theories. Since phases I, V, and IV should correspond to (4.19), the new critical line should have no effect deep into said regions. One can also verify that the overlapping scalar theories of (3.72) are not consistent outside of phase V without an interaction term. Per these constraints, we conjecture the interaction term's coefficients are chosen such that it splits the Grassmannian region below phase V. Furthermore, since such critical lines cannot simply terminate, at the crossover between the two scalar theories we conjecture the two critical lines merge. Rather remarkably, the merged critical line VII-VIII is precisely the theory needed to be consistent under anomaly constraints given the two phases it separates.

More explicitly, to reach a consistent intermediate phase we require the interaction for the blue theory to have a positive coefficient for its interaction term so as to give the fermions a positive mass when Φ_1 is Higgsed. The interaction takes the form $\mathcal{L}^1_{\text{int}} \supset c'\left(\Phi_1^{\dagger\alpha M}\Psi^1_{\alpha N}\right)\left(\bar{\Psi}_1^{\beta N}\Phi^1_{\beta M}\right)$ with α,β indices for the $U(k)$ gauge field, M an index for the $SU(N_f)$ global symmetry, N index for the $SU(N_s)$ global symmetry, and $c'>0$. We then must give the fermions a negative mass to make the singlets light. This gives kN_s light fermions living on the critical theory between phases VI and VIII. Since the axis of the fermion mass deformation of the red theory is flipped relative to the blue one, it requires a negative coefficient for the interaction term, and so $\mathcal{L}^2_{\text{int}} \supset -c'\left(\Phi_2^{\dagger\alpha M}\Psi^2_{\alpha N}\right)\left(\bar{\Psi}_2^{\beta N}\Phi^2_{\beta M}\right)$ with α,β now $U\left(N_f-k\right)$ indices. This gives $(N_f-k)N_s$ light fermions on the critical line between phases VII and VI. At the crossover between (VI-VII) and (VI-VIII), the two critical theories unite into N_fN_s light fermions, which is consistent with the transition from VII to VIII. This separates the Grassmannian phase into the three different regimes shown in Fig. **??**. These phases all share the same Grassmannian $\mathcal{M}(N_f,k)$, but have distinct non-Abelian

background Chern-Simons terms.[18]

For the rest of the phase diagram, calculating the critical theories is straightforward. As conjectured in [80], the critical lines corresponding to I-V and IV-V, as well as II-VII and III-VIII occur at some finite fermion mass deformation $\pm m_*$. These are obtained by application of (4.19). As such these lines are better described by the U side of the theory. This is different from the I-II and III-IV critical lines, which follow from a straightforward application of (**??**).

Although much of this phase diagram lives in the strong coupling regime, it offers a plausible scenario for the matching of the dynamical and background gauge terms, which we discuss explicitly in Appendix 3.8. The gravitational Chern-Simons terms can also be calculated and are consistent with expectations from level-rank duality.

Flavor-Violation for $N_s = N$

The conjectured phase diagram for $N = N_s$ is shown in Fig. 3.7, with the corresponding phases given in (3.85) and (3.86).

To see why $N = N_s$ needs to be considered separately, we begin by looking at the SU side. In the phase where $m_\phi^2 < 0$, the gauge group is $SU(N - N_s)$ and is thus completely broken when $N = N_s$. Hence for large enough scalar mass, we assume the strong dynamics of the gauge groups which was responsible for the condensation of the fermions is eliminated. If this occurs, the Grassmannian phase cannot persist as we approach $m_\phi^2 \to -\infty$. We will take the termination to occur around $m_\phi^2 \sim \Lambda^2$. When one goes beyond this scale, we assume the gauge bosons of $SU(N)$ pick up too large of a mass (relative to the mass from the Chern-Simons terms) to cause the fermions to condense, meaning the Grassmannian phase terminates as one goes $\left|m_\phi^2\right| \gg \Lambda^2$. Note that this is very different from the $m_\phi^2 > 0$ phase, where the scalars are simply gapped out and the fermion condensate is unaffected.

[18] Also note that phase VII and VIII have a different coefficient of the Wess-Zumino-Witten term from phases V and VI. This comes from the Chern-Simons level of the U gauge theories bordering the Grassmannian phases.

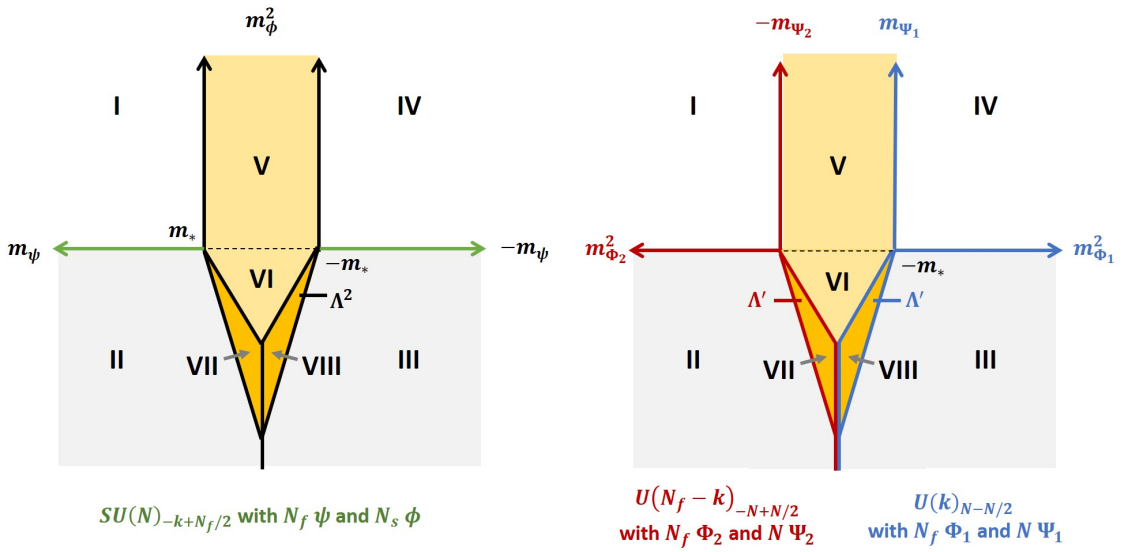

Figure 3.7: SU and U sides of the flavor-violated master duality for $N = N_s$ and $|k| < N_f < N_*$.

This should be mirrored on the U side of the duality for $N = N_s$, where now we have the special case where the level of the U gauge group is zero and thus the gauge bosons are truly massless in the classical theory. Since we are in the strongly coupled regime we can only make conjectures, but we offer a plausible mechanism to match the SU side. Like the SU side, we will make the assumption that the termination comes when the matter, this time the fermion, has a large enough mass (in magnitude) to be integrated out. We conjecture that for large enough fermion mass, the level being $N - N_s = 0$ means the U gauge group is confining and it induces a mass gap for the scalars. This gap is large, but can be cancelled off by an appropriate mass deformation, similar to the singlet fermion picture described above. This allows us to still have a critical theory of light scalars along the II-VII and VIII-III transition that can drive us into the Grassmannian and give a mass to the singlet fermions. Once these theories become degenerate, i.e. when the two lines of light scalar meet in Fig. 3.7 the description breaks down and the Grassmannian terminates, leaving just the singlet fermions on the II-III transition.

The phases of the SU side are[19]

$$\text{(I)}: \quad SU(N)_{-k+N_f} \times [SU(N_f)_N \times SU(N_s)_0 \times J_{\rm I}] \tag{3.85a}$$

$$\text{(II)}: \quad U(1)_0 \times \left[SU(N_f)_N \times SU(N_s)_{-k+N_f} \times U(1)_{N(N_f-k)}\right] \tag{3.85b}$$

$$\text{(III)}: \quad U(1)_0 \times [SU(N_f)_0 \times SU(N_s)_{-k} \times U(1)_{-Nk}] \tag{3.85c}$$

$$\text{(IV)}: \quad SU(N)_{-k} \times [SU(N_f)_0 \times SU(N_s)_0 \times J_{\rm IV}] \tag{3.85d}$$

$$\text{(V) to (VIII)}: \quad \text{Better described by } U \text{ side.} \tag{3.85e}$$

As we saw for Aharony's duality, the U side is a better description for certain phases. Phases of the U side is given by

$$\text{(I)}: \quad U(N_f-k)_{-N} \times [SU(N_f)_N \times SU(N_s)_0 \times J_{\rm I}] \tag{3.86a}$$

$$\text{(II)}: \quad U(1)_0 \times \left[SU(N_f)_N \times SU(N_s)_{-k+N_f} \times U(1)_{N(N_f-k)}\right] \tag{3.86b}$$

$$\text{(III)}: \quad U(1)_0 \times [SU(N_f)_0 \times SU(N_s)_{-k} \times U(1)_{-Nk}] \tag{3.86c}$$

$$\text{(IV)}: \quad U(k)_N \times [SU(N_f)_0 \times SU(N_s)_0 \times J_{\rm IV}] \tag{3.86d}$$

$$\text{(V), (VI)}: \quad \mathcal{M}(N_f,k) \times [SU(k)_N \times SU(N_f-k)_0 \times SU(N_s)_0 \times J_{\rm V}] \tag{3.86e}$$

$$\text{(VII)}: \quad \mathcal{M}(N_f,k) \times \left[SU(k)_N \times SU(N_f-k)_{N_s} \times SU(N_s)_{N_f-k} \times J_{\rm VII}\big|_{N=N_s}\right] \tag{3.86f}$$

$$\text{(VIII)}: \quad \mathcal{M}(N_f,k) \times \left[SU(k)_0 \times SU(N_f-k)_0 \times SU(N_s)_{-k} \times J_{\rm VIII}\big|_{N=N_s}\right]. \tag{3.86g}$$

We now have a single $U(1)$ background gauge field for phases II and III, which is $\tilde{A} \equiv \tilde{A}_1 = -\tilde{A}_2$. This is because the global $U(1)$ baryon/monopole symmetry is spontaneously broken in the phases II and III for $N = N_s$ (see Appendix 3.8 for more details).

[19]Here we use the fact that both the theories $SU(0)$ and $U(k)_0$ lead to a decoupled $U(1)_0$ theory. To see this on the SU side, note the gauge group is completely broken down by the scalar vacuum expectation value, but this leaves a single light degree of freedom which is the Goldstone boson associated with the spontaneous breaking of the $U(1)$ global symmetry. On the U side, the Chern-Simons term disappears and thus we are left with $U(k)$ Yang-Mills in the IR. The $SU(k)$ part of this confines, leaving the Abelian part of the gauge group which has a light photon. The photon is also associated with the spontaneously broken $U(1)$ symmetry corresponding to conserved particle flux (this is easiest to see in the dual photon language). Hence both of these light degrees of freedom can be associated with a spontaneous symmetry breaking of the $U(1)$ global symmetry (i.e. the one associated with $\tilde{B} = \tilde{A}_1 + \tilde{A}_2$).

Finally, critical theories are given by

$$\begin{aligned}
&\text{(I-II)}: && U(N_f-k)_{-N/2} \text{ with } N\ \Psi_2 && \leftrightarrow && SU(N)_{-k+N_f} \text{ with } N\ \phi && \text{(3.87a)}\\
&\text{(III-IV)}: && U(k)_{N/2} \text{ with } N\ \Psi_1 && \leftrightarrow && SU(N)_{-k} \text{ with } N\ \phi && \text{(3.87b)}\\
&\text{(I-V)}: && U(N_f-k)_{-N} \text{ with } N_f\ \Phi_2 && && && \text{(3.87c)}\\
&\text{(IV-V)}: && U(k)_N \text{ with } N_f\ \Phi_1 && && && \text{(3.87d)}\\
&\text{(II-VII)}: && U(N_f-k)_0 \text{ with } N_f\ \Phi_2 && && && \text{(3.87e)}\\
&\text{(III-VIII)}: && U(k)_0 \text{ with } N_f\ \Phi_1 && && && \text{(3.87f)}\\
&\text{(VI-VII)}: && \mathcal{M}(N_f,k) \text{ with } (N_f-k)N\ \psi_s && && && \text{(3.87g)}\\
&\text{(VI-VIII)}: && \mathcal{M}(N_f,k) \text{ with } kN\ \psi_s' && && && \text{(3.87h)}\\
&\text{(VII-VIII)}: && \mathcal{M}(N_f,k) \text{ with } (N_f-k)N\ \psi_s \text{ and } kN\ \psi_s' && && && \text{(3.87i)}\\
&\text{(II-III)}: && U(1)_0 \text{ with decoupled } NN_f\ \tilde{\psi}_s. && && && \text{(3.87j)}
\end{aligned}$$

In the above, ψ_s, ψ_s' and $\tilde{\psi}_s$ denote neutral fermions in the phases where dynamical gauge group is completely broken. Note that in contrast to the $N > N_s$ case, here we have the critical line (II-III) which can only be described by the SU side using semiclassical analysis.

3.4.3 Double Saturated Flavor Bound

We now investigate the validity of the double saturated flavor bound, which will be applicable to the flavored quiver we construct in the next section. That is, can the master duality be extended to also hold for the case $(N_s, N_f) = (N, k)$?

Let us review in more detail why the master duality was invalid in such a limit. In [64]

it is argued that the phases (shown in Fig. **??**) for $N_s = N$ are

$$\text{(I)}: \quad SU(N)_0 \quad \leftrightarrow \quad U(0)_N \tag{3.88a}$$

$$\text{(IIa)}: \quad U(1)_0 \quad \leftrightarrow \quad U(0)_0 \tag{3.88b}$$

$$\text{(IIb)}: \quad SU(0)_0 \quad \leftrightarrow \quad U(0)_0 \tag{3.88c}$$

$$\text{(III)}: \quad U(1)_0 \quad \leftrightarrow \quad U(1)_0 \tag{3.88d}$$

$$\text{(IV)}: \quad SU(N)_{-k} \quad \leftrightarrow \quad U(k)_N \tag{3.88e}$$

with mass mapping $m_\phi^2 \leftrightarrow m_\Psi$ and $m_\psi \leftrightarrow -m_\Phi^2$. Phase I, III, and IV should all match, since these phases reduce to Aharony's dualities, (**??**), and we know the flavor saturated cases pass all tests in those dualities. There appears to be a conflict already in phase I, where one side of the theory is a completely broken $U(0)$ theory, while the other end of the theory is simply $SU(N)$ Yang-Mills with no Chern-Simons term. By assumption, the latter of these confines, so the low energy limit is empty. Meanwhile, in the completely broken theory, the lightest excitations are finite mass vortices. Thus there are no light degrees of freedom in either case, which is consistent. The matching in phase III occurs because each side is described by a decoupled $U(1)_0$, as we saw earlier in the $N = N_s$ flavor violated master.

The conflict in the double saturated master duality then arises in phase IIa and IIb. Let us compare phase IIa to what we had in phase III. On the SU side, we have gone from $SU(0)_{-k}$ to $SU(0)_0$. The breaking and subsequent Goldstone boson which occurred in phase III was irrespective of the Chern-Simons level, so there is no difference in the resulting light degrees of freedom in this phase. Meanwhile on the U side we have gone from $U(k)_0$ to $U(0)_0$. When the rank of the gauge group is reduced to zero, there is no light photon left in the theory. Thus we have a mismatch in the degrees of freedom on either side, leading Refs. [24, 64] to postulate that the master duality no longer holds for such a case.

To summarize the issue: changing the *level* on the SU side has no effect on the theory, but changing the *rank* does affect the light degrees of freedom on the U side of the theory, but only for the case of $N_f = k$ where the rank of the U group is reduced to zero. As we mentioned above, the light degrees of freedom in this phase should be associated with a

spontaneous symmetry breaking of the $U(1)$ global symmetry associated to $\tilde{A}_1$.

To extend the validity of the master duality to the double saturated case is simple – we choose to *explicitly* break the $U(1)$ global symmetry on both sides of the duality. This will eliminate the Goldstone bosons associated with the spontaneous breaking of said symmetry, and thus we will again have a matching in phases IIa and IIb. Note this will also modify the light degrees of freedom in said phases.

Perhaps not by coincidence, we have explicitly broken the same $U(1)$ global symmetry in the construction of the $SU(N)$ Yang-Mills n-node quivers [9]. Specifically, we introduced a $\det(Y_{i,i+1})$ term on the SU side and and appropriate monopole term on the U side to eliminate the $U(1)^{n-1}$ symmetry. It is straightforward to see this will be necessary for our $N_F \geq 1$ quivers as well, since there we would also like to prevent the additional Goldstone bosons arising. Hence, by eliminating these $U(1)$ global symmetries on both sides of the duality, we have also extended the master duality to validity in the $(N_f, N_s) = (k, N)$ case. This allows the master duality to be valid for the $N_F = 1$ quivers, which we construct in the next section.

Note that these determinant terms are going to be present for all our N_F choices so we could think of them simply being a feature of the master duality when $N = N_s$. It does not seem possible to write down the determinant-like term unless $N = N_s$, so this is a nice consistency check.

Thus, we can in fact use the non-flavor extended master duality to derive the $N_F = 1$ quivers. This means the analysis in Sec. 3.4.4 and construction in Fig. 3.8 holds just fine and we need no mass offset to get the desired theories. Furthermore, unlike the $N_F > 1$ theories we only need one theory on the U side of the duality to give the desired dual. The critical theory is then

$$\left[SU(N)_{-1} + \text{fundamental fermion}\right]^n + \text{bifundamental scalars} \qquad \leftrightarrow$$
$$U(n)_N + \text{fundamental scalar} + \text{bifundamental scalars}. \quad (3.89)$$

It is straightforward to analyze how mass deformations behave. It is very interesting that

once more the $N_F = 1$ case is distinct from the $N_F > 1$ case. For QCD_4 this was due to the fact there was an enhanced symmetry when the fermion mass vanished (the axial part of the non-Abelian symmetry), while for $N_F = 1$ the point at which the fermion mass vanished wasn't special. It would be interesting to elaborate on the connection of these two peculiarities.

3.4.4 Node by Node Duality

Before deriving the dual description for flavored quivers, let's remind ourselves of some notation. We will index the nodes by $i = 1, \ldots, n$. The bifundamental scalars between the ith and $(i+1)$th node in the SU and U theories are labeled by $Y_{i,i+1}$ and $X_{i,i+1}$, respectively. The bifundamental fermions of the intermediate theories will be labeled by $\psi_{i,i+1}$. We'll call the flavored fermions belonging to the ith node ψ_i. Meanwhile, the scalar flavor degrees of freedom which are the dualized ψ_i are denoted by ϕ_i. All levels used in these notes are equivalent to the "bare" levels used in [80].

The most general 3-node quiver with flavor degrees of freedom on each node is shown in Fig. 3.8. Its dual can be derived as in Ref. [9] using the master duality and its $N_f = 0$ and $N_s = 0$ limits.[20] In particular, if one gauges the flavor symmetries of the master duality, one arrives at the following two and three-node dualities,

$$SU(N)_{-k} \times [SU(N_s)_0] \quad \leftrightarrow \quad U(k)_{N-N_s/2} \times \left[SU(N_s)_{-k/2}\right] \tag{3.90}$$

$$SU(N)_{-k+N_f/2} \times \left[U(N_f)_{N/2}\right] \quad \leftrightarrow \quad U(k)_N \times [U(N_f)_0] \tag{3.91}$$

$$SU(N)_{-k+N_f/2} \times \left[U(N_f)_{N/2} \times SU(N_s)_0\right] \quad \leftrightarrow \quad U(k)_{N-N_s/2} \times \left[U(N_f)_0 \times SU(N_s)_{-k/2}\right]. \tag{3.92}$$

Each of these is subject to particular flavor bounds, but let us ignore them for a moment. Stepping from Theory A to Theory B we use (3.92) with the $U(N_f)$ symmetry ungauged

[20] In Ref. [9] the $N_F = 0$ quiver was derived with no regard to distinguishing between ordinary and spin_c connections. In Appendix 3.9 we elaborate on how such quivers can be consistently formulated on spin_c manifolds.

(i.e. the master duality with only the $SU(N_s)$ symmetry promoted to be dynamical). From Theory B and Theory C, again use (3.92) but gauge only part of the background flavor symmetry such that the $U(k_1 + F_2)$ background fermion flavor symmetry becomes a $U(k_1)$ gauge symmetry and the remaining $SU(F_2) \times U(1)$ are still global symmetries. Finally, use (3.91) to go from Theory C to Theory D, again with a split flavor symmetry with a part which is gauged and another which is untouched.

It is straightforward to see how this pattern generalize to the n-node quiver. Let N_1, ..., N_n denote the number of colors on the nodes and k_1, ..., k_n the levels of the corresponding Chern-Simons terms. The duality for the n-node quiver reads

$$\left[SU(N_1)_{-k_1+\frac{F_1}{2}} + \text{fund } \psi_1\right] \times \prod_{i=2}^{n} \left[SU(N_i)_{-k_i+\frac{F_i}{2}} + \text{bifund } Y_{i-1,i} + \text{fund } \psi_i\right] \tag{3.93a}$$

$$\leftrightarrow \quad \prod_{i=1}^{n-1} \left[U(K_i)_{N_i - N_{i+1}} + \text{bifund } X_{i-1,i} + \text{fund } \phi_i\right] \times \left[U(K_n)_{N_n} + \text{fund } \phi_n\right]. \tag{3.93b}$$

The ranks of the gauge groups in the U quiver are given by

$$K_n \equiv \sum_{i=1}^{n} k_i. \tag{3.94}$$

This is very similar to the relation as was found in the unflavored case [9]. As in the 3-node case depicted in Fig. 3.8 we can also keep track of the level of the flavor groups. These can always be shifted by an overall background Chern-Simons term added on both sides, but if we chose the levels to be $SU(F_i)_{N_i/2}$ on the SU side, they end up being $SU(F_i)_0$ on the U side.

Now let us specialize to the case where $N_1 = \ldots = N_n = N$, $k_1 = \ldots = k_n = 1$, and $F_1 = \ldots = F_n = N_F$. If, in addition, we add a $\det X_{i,i+1}$ potential term on each link, this is the theory that describes the physics of interfaces in QCD_4. Recall, the determinant term was needed in order to eliminate the additional $U(1)^{n-1}$ global symmetry present on the quivers [9, 50], and its U side equivalent is a monopole operator. It is easy to see that only the $N_F = 0$ case does not violate any flavor bounds. This is because all the levels must satisfy $k_i \geq F_i$ and in addition we must avoid the double-saturation limit of the master

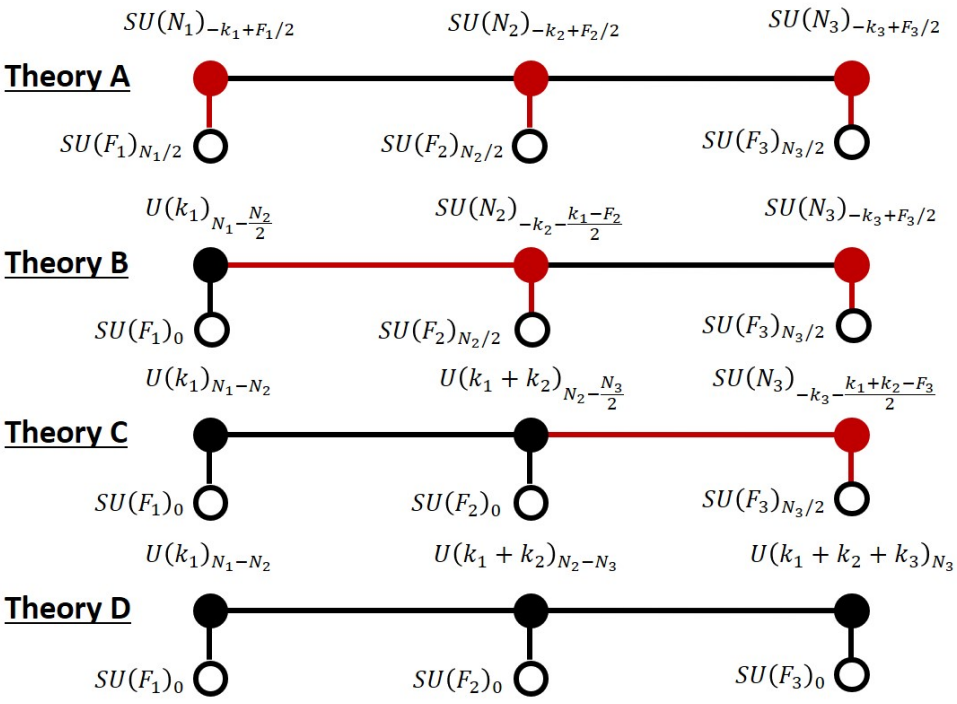

Figure 3.8: Flavored quiver with fermions on the SU side and scalars on the U side. The red/black nodes correspond to U and SU gauge groups, respectively. The red and black links are fermions and scalars. The white nodes are background flavor symmetries.

duality. Since we have already saturated the $N_i \geq N_{i+1}$ flavor bound, $N_F = 0$ is the only way we can avoid violating such bounds.

The flavor-extended master duality and double saturated master we laid out in the previous section allows us to proceed. The $N_F = 1$ case corresponds to use of the double-saturated master duality. As discussed in Sec. 3.4.3, the introduction of the determinant terms allow extend the validity of the master duality to this limit. We will discuss the $N_F > 1$ in detail in what follows below, but let us summarize here the essential points for general $N_F \geq 1$. We saw that for one sign of the mass the flavor extended duality is just the same as we had when the flavor bounds were obeyed (see (3.76c) and (3.76d)) , so we can just continue to use the duality above if we stay in such phases. On the SU side, each of the nodes has a

$$SU(N)_{-1+N_F/2} \text{ with } N_F \ \psi \tag{3.95}$$

theory on it. We also see that in this special case of equal N_i we get a dual quiver on the U side where all but the last node have a level 0 Chern-Simons term. This is once again completely identical to the case of the unflavored quivers considered in [9]. The non-Abelian factors with level 0 confine. Lo and behold, all but the last node disappear from the low energy spectrum. To pin down the remaining charged matter under the last gauge group, we need to make some dynamical assumptions for this confinement mechanism. In [9] it was argued that the only light remnant of the bifundamental matter is an adjoint “meson" made from the bifundamentals on the last link. This assumption gave rise to a duality conjecture that agreed with the holographic construction and passed several non-trivial consistency tests. If we make the same assumption here, we are lead to the duality conjecture of eqs. (3.68) and (3.69). Once again, we will see that this is also what the holographic construction tells us.

Similar dualities can also be derived if the extra flavors on the SU side are taken to be scalars, but the patterns that emerge are more complicated than in the fermionic case and do not appear to yield any simple interesting new dualities.

Constructing the $N_F > 1$ Quiver

Let us now use the flavor extended master duality to construct quivers. This will allow us to extend the validity of our dualities to $N_F > 1$. As we have seen, this will be complicated slightly by the fact one needs two theories to describe the entire phase diagram of the U side. Since there are even more mass deformed phases in the quivers, we should expect the number of theories needed to ultimately describe all possible mass deformations of the U side to be quite large. Every time one uses a flavor violated duality the number of scalar theories needed to describe the entire phase diagram doubles. For our three-node case we can consider $2^3 = 8$ separate theories to capture all possible mass deformations of the original fermionic theory. However, all eight theories should be equivalent descriptions of the same Grassmannian manifold.

In this section we will only consider two of the eight possible descriptions of the U side of the quiver. These will be the cases which are valid when all masses of the quivers are deformed such that we are in phases III and IV or I and II of the flavor-extended master duality. These correspond to the extreme cases in the original SU theory where all the fermions are tuned to large positive and large negative mass, respectively. It is possible construct quivers for mixed phases, but we do not consider them here.

In what follows, we will first apply this general strategy to the special case of $n = 3$ nodes. After considering the three-node case, we will generalize such extreme cases to n-nodes.

$m_{\psi_i} < 0$ *Duality*

The special case where all masses are negative is especially easy since in this case the duality map is formally still given by (3.92). That is, the entire derivation shown in Fig. 3.8 in principle still holds since the initial theory is the same and the extended master/Aharony dualities are also the same. Thus much of the same conclusions we made there can be applied here. The primary difference is that the identification between the two sides of the phase diagrams is shifted from the flavorless case. Following the mass mappings through

the derivation, for the bifundamentals we still have $m^2_{Y_{1,2}} \leftrightarrow m^2_{\psi_{1,2}} \leftrightarrow -m^2_{X_{1,2}}$. For the flavor degrees of freedom we have

$$m_{\psi_i} + m_* \leftrightarrow -m^2_\phi. \tag{3.96}$$

Zero mass for the fermion no longer maps to zero mass for the boson. In particular, the $m_{\psi_i} = 0$ region now corresponds to the $m^2_{\Phi_i} < 0$ region, and this "mass offset" will introduce certain complications.

Let us discuss in detail how the analysis of interfaces changes in the presence of the additional flavors due to this mass offset. Once more we specialize to the values relevant for QCD_4, namely $N_i = N$, $k_i = 1$, and $F_i = N_F > 1$. We'll begin by assuming no deformations of the matter on the SU side, i.e. $m_{\psi_i} = 0$ and $m^2_{X_{i,i+1}} = 0$. First off, note that because $N_F > 1$ each node in the initial SU theory has Grassmannians. Thus, this should ultimately map to something on the U side of the duality which also produces Grassmannians. Since the U side only has scalars, in order to produce said Grassmannians some of said scalars must be in their Higgs phase. This is already very different than the flavorless case where theories with no mass deformations were mapped to one another.

It will be useful to keep in mind which matter is "responsible" for the flavor violation and presence of the Grassmannian description. Recall, per the conjecture of [80], this can occur from either having too many light fermions or too many scalars with a negative mass. The culprit is obvious in the SU theory: without the additional flavors on each node we have the flavorless case which we know meets all flavor bounds. Thus, it is the additional fermions of each node which are responsible.

This is complicated in (say) Theory B, where we now have two subgroups of fermions connected to the second node, corresponding to $SU(F_2)$ and $SU(k_1)$ (see Fig.3.8). The former are the additional flavors that were on that node to begin with, the latter are the bifundamental fermions which were previously scalars. If all such fermions were light for the portion of the phase diagrams we are interested in, the Grassmannian manifold of the second node may have changed, and this would be problematic since we claim it is dual to Theory A.

To resolve this issue, first note that in Theory B the flavor degrees of freedom on the first node have been converted into scalars, and because the mass offset these scalars have a negative mass. This is consistent with there being a Grassmannian on the first node. What we have neglected are the interactions introduced by using the master duality that are now present in Theory B. Since the scalar flavors on the first node are now Higgsed, the interactions cause the $\psi_{1,2}$ fermions to be gapped. Meanwhile, the ψ_2 remain light. Hence the only light fermionic degrees of freedom are those which were already present in Theory A, so the Grassmannian on the second node also remains the same.

Generalizing this argument down the quiver, we see that it is always either the ψ_i or ϕ_i (i.e. the flavor degrees of freedom on each node) which break the nodes down to Grassmannian descriptions. This might have been expected, since these are the new ingredients relative to the flavorless case, but it is nice that the quivers get it right.

As in Ref. [9], the phase corresponding to $m^2_{X_{i,i+1}} < 0$ causes a breaking of the Chern-Simons terms in the theory to $[U(1)_N]^3$. Thus on the U side of the theory we ultimately end up with

$$U(1)_N \text{ with } N_F \ \phi_i \tag{3.97}$$

on each node, with $m^2_{\phi_i} < 0$, as we would have expected.

Critical Theory Formally the duality map (3.75) is only valid when we tune the fermion mass to its critical value, the scalar mass to zero and apply the map (3.78). In this case the dualized scalars ϕ_i are massless and the interactions terms introduced through the master duality do nothing to the mass of the fermions. This is okay since we would not expect Grassmannians at this location in phase space. Additionally, since the number of bifundamental fermions is less than the level of the corresponding node, we do not get any Grassmannians. The duality thus states

$$\begin{aligned}[SU(N)_{-1} + N_F \text{ fundamental fermions with } m_{\psi_i} = -m_*]^n + \text{bifundamental scalars} \\ \leftrightarrow \qquad U(n)_N + N_F \text{ fundamental scalars} + \text{bifundamental scalars.}\end{aligned} \tag{3.98}$$

It is interesting to consider deformations of the bifundamentals in this phase. Luckily, almost all of the analysis performed in [9] holds here as well. That is, on the SU side gapping the bifundamentals simply removes them from the spectrum. Higgsing the bifundamentals leaves the gauge transformations which transform two adjacent nodes equally unbroken. This causes the levels of the two nodes to add. The mass identifications of the bifundamentals on the U side are still opposite of those on the SU side. Thus for gapped scalars on the SU side we have Higgsing of the U groups down to $U(1)$. Meanwhile, the first $n-1$ nodes on the U side are confining for full Higgsing on the SU side.

Let us consider this latter case in a little more detail. Consider sitting at the critical point where all $m_{\psi_i} = -m_*$ and all $m^2_{Y_{i,i+1}} = 0$. Now give all $Y_{i,i+1}$ a negative mass, so the Chern-Simons term on the SU side is $SU(N)_{-n}$. All bifundamentals are gapped on the U side, and the only non-confining node is all the way on the right, given by a $U(n)_N$ Chern-Simons theory. Now consider tuning the masses of the flavor degrees of freedom. Move the fermion on the last node, ψ_n, to a slightly larger mass (but smaller in magnitude), $-m_* + \epsilon$, which causes us to get a $\mathcal{M}(N_F, n)$ Grassmannian. On the U side this causes the dual scalar ϕ_n to acquire a negative mass, breaking down the node flavor symmetry to $\mathcal{M}(N_F, n)$. Thus both sides are consistent.

One needs to be slightly more careful when tuning the masses of any other matter, say ψ_j for $j < n$. Moving to a larger mass $m_{\psi_j} = -m_* + \epsilon$ again causes the corresponding ϕ_j scalar to get a negative mass, which due to interaction terms present on the U side gives the $X_{j,j+1}$ bifundamental a *negative* mass. Although the interactions are finite, we will only focus on the case when they are stronger than mass deformations. The scalar then breaks the corresponding the $U(j+1)_0$ gauge group and this propagates down the quiver similar to the flavorless case. Ultimately this causes a breaking of $U(n)_N \to U(n-j)_N \times U(j)_N$. On the SU side of things this is reflected in the fermion condensing, causing a breaking of the gauge group and a $\mathcal{M}(N_f, j)$ Grassmannian on the jth node, and a leftover $SU(N)_{-n+j}$. This is consistent since the breaking from the negative mass bifundamental scalar, $Y_{j,j+1}$, is inconsequential for corresponding node since it is instead now broken by the fermion condensate. To summarize,

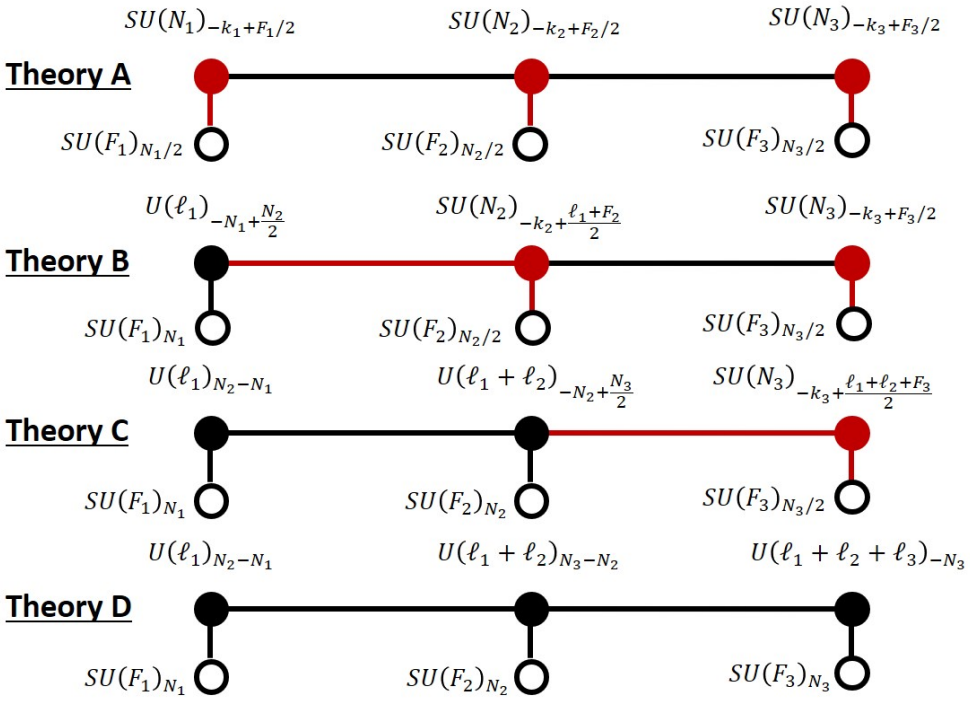

Figure 3.9: Flavored quiver with fermions on the SU side and scalars on the U side. This is an alternate theory in the flavor extended case. Here we have introduced the notation $\ell_i \equiv F_i - k_i$.

tuning the masses of flavor degrees of freedom on nodes $j < n$ undoes the effects of Higgsing the bifundamental scalars on the SU side/gapping the bifundamental scalars on the U side.

$m_{\psi_i} > 0$ *Duality*

Now let us instead look at the case where all masses are positive. In this case we need to use the $m_\psi = m_*$ theory of (3.75), which is spelled out explicitly in (3.164), to derive the flavor extended quiver. We consider again the three node quiver for the most general set of parameters. It will be useful to introduce a new notation $\ell_i \equiv F_i - k_i$. The derivation is shown in Fig. 3.9.

Note since we are using the $m_\psi = m_*$ duality, the interaction in this phase is slightly

different. Namely, the interactions are now in the $m_\Phi^2 < 0$ and $m_\Psi > 0$ phase and prevent the fermions from getting a positive mass. That means that the interaction term comes with a negative sign out front.

3.4.5 Holographic Construction

Having generalized the node-by-node construction in order to motivate the duality between (3.68) and (3.69), let us now turn to the holographic derivation. The holographic construction used in [9] is in spirit similar to the one first introduced in [66] for the study of 2+1 dimensional bosonization dualities, which is based on the even earlier holographic realization of level/rank duality in [47]. The key idea here is to embed the Chern-Simons matter theory of interest inside a larger gauge theory with a known holographic dual. In the UV we have the full set of degrees of freedom of the larger gauge theory, dual to a theory of gravity in the bulk. Upon suitable deformation on both sides the gauge theory and its gravitational dual develop a gap for most degrees of freedom, only a small subset survives in the infrared. The original field theory is engineered to reduce to a Chern-Simons matter theory in 2+1 dimensions. In the bulk most degrees of freedom are gapped out as well, including all the fluctuations of the graviton and its superpartners. The only degrees of freedom that survive are localized on a probe D-brane.

More specifically, in [66] the basic bosonization dualities were reproduced by compactifying $\mathcal{N} = 4$ super Yang-Mills on a circle with antiperiodic boundary conditions for the fermions and a θ angle wrapping non-trivially around the circle direction. The low energy theory yielded a gapped Chern-Simons theory, with extra light matter added via probe branes. In order to obtain quiver gauge theories one needs to start with a slightly more complicated construction. Fortunately, most of this framework has been laid out in [120] in the context of the simplest holographic dual for a confining gauge theory: Witten's black hole [118]. Witten's black hole describes the gravitational dual of $4 + 1$ dimensional super Yang-Mills compactified on a circle with anti-periodic boundary conditions for the fermions. This procedure gives masses to all matter fields and so, at low energies, one is left with

pure Yang-Mills in $3+1$ dimensions, which itself is gapped. Topologically Witten's black hole solution is $\mathbb{R}^{3,1} \times D_2 \times S^4$, where the first factor is $3+1$ dimensional Minkowski space and the disc or "cigar" D_2 contains the radial direction of the holographic dual as well as a compact circle direction which smoothly shrinks to zero size at a critical value r_* of the radial coordinate. The relevant holographic dual for the interfaces we are seeking are D6 branes sitting at the bottom of the cigar, wrapping all of the internal S^4 and being localized in one of the three spatial directions of the $\mathbb{R}^{3,1}$ factor.

One subtlety here is that the D6 branes were argued in [120] to be dual to a domain walls between two vacua at a fixed θ rather than a θ interface. At a given θ we still have N vacua, with all but one of them being only meta-stable. The energy difference between vacua however is of order 1 in the large N counting, whereas the tension of the domain wall is of order N. So in the large N limit these domain walls are long lived and approximately stationary. To truly describe an interface, we should turn on a θ gradient in addition to the D6 branes, which corresponds to a RR 1-form in the bulk that depends on the radial direction in the bulk as well as the spatial direction orthogonal to the domain walls, call it x. The simplest such supergravity solution is an RR 1-form that grows linearly along x. In this case the RR 1-form equation of motion is solved without giving the 1-form any dependence on the holographic radial coordinate. This solution as it stands corresponds to increasing θ along a spatial direction without adjusting vacua, but instead staying on a meta-stable branch. This is clearly not the physical vacuum of the theory. In order to truly correspond to the interfaces of [50] we need to still include D6 branes in addition to the spatially varying theta angle in order to ensure that the field theory always is living in the locally true vacuum. At least in the simple case of a linearly varying θ angle it is easy to see that the D6 branes experience a potential that will automatically localize them where θ crosses odd multiples of π. To see that this is the case, recall that the backreaction of the D6 branes induces an RR 1-form field $\sim (\theta + 2\pi K)$ which gives rise to an energy density of order $(\theta + 2\pi K)^2$. Here K labels the different vacua. Let us look at a spatial region in which θ varies over a 2π range. Let us chose this range to be 0 to 2π with $K = 0$. This can always be done by the way we

label vacua in terms of K. Let us assume that the change is θ is taking place over an interval of length L with $\theta = 2\pi x/L$. There is a single D6 brane located at x_0 with $0 \leq x_0 \leq L$ across which the vacuum jumps to $K = -1$. The vacuum energy associated to this configuration is

$$E \sim \int_0^l dx \, (\frac{2\pi}{L} x - \Theta(x - x_0) 2\pi)^2 = \frac{4\pi^2 (L^2 - 3Lx_0 + 3x_0^2)}{3L} \tag{3.99}$$

where Θ is the step function that is 1 when its argument is positive and 0 otherwise. Minimizing with respect to x_0 we indeed find $x_0 = L/2$. The D6 brane wants to sit at the middle of the interval where $\theta = \pi$. Note that these energies are all of order 1 in the large N counting. This is due to the fact that they involve the brane backreaction. When determining the leading order in N physics on the brane, we can neglect these potentials. The upshot is that irrespective on whether we describe interfaces or domain walls, the holographic dual description is given in terms of a stack of n D6 branes at the bottom of the cigar as long as we jump n vacua across the co-dimension one object.

Interestingly, this holographic dual at low energies does not give back the quiver gauge theory (3.3), but its dual incarnation (3.4): the theory on a stack of n D6 branes is a $U(n)$ super-symmetric gauge theory. Due to the Wess-Zumino terms on the worldvolume coupling to the 4-form flux supporting Witten's black hole the gauge field picks up a Chern-Simons term of level N. The worldvolume fermions get mass from the compactification on the internal S^4. The worldvolume scalars correspond to geometric fluctuations of the D6 branes. The two scalars corresponding to fluctuations of the D6 on the disc are massive due to the warped geometry of the spacetime: there is a non-vanishing potential energy cost associated with fluctuating up the cigar. The only light matter on the D6 branes is a single massless adjoint scalar corresponding to the fluctuations in the x directions. To leading order in N it is massless, even though we've already seen above that a non-trivial potential will surely be generated at order 1. Lo and behold, the gauge theory on the D6 branes exactly realizes (3.4) as advertised.

The inclusion of extra flavors is now conceptually straightforward but the details are somewhat daunting. Many aspects of this construction have been discussed nicely in [15].

On the field theory side, our flavored quiver gauge theory from (3.68) indeed already appeared in the study of interfaces alongside its flavorless cousin. If instead of studying θ interfaces in pure Yang-Mills one studies them in a confining $SU(N)$ gauge theory with fundamental fermions, the correct gauge theory on the domain walls is exactly the flavored quiver [50]. In the holographic dual, we need to augment Witten's black hole with N_F flavor D8 branes in order to describe holographic QCD [99]. The D8 branes are localized on the compact circle but their worldvolume extends in all other directions. In particular, the D6 branes dual to the domain walls are entirely embedded inside the D8 worldvolume. That is, the D6/D8 system constitutes a Dp/Dp+2 brane system with 2ND directions. Correspondingly, the 6-8 strings connecting the two gives rise to extra scalar matter in the fundamental representation of the $U(n)_N$ gauge theory on the D6 worldvolume. Indeed we have found that the flavored quiver of (3.68) has a holographic dual description in terms of the theory in (3.69). When asking more detailed questions, lots of open problems emerge. The scalar at a 2ND brane intersection is tachyonic. So in order to find the CFT dual to the flavored quiver, we need to let the scalars condense. The result is outside of the range of perturbative string theory, so the outcome is somewhat inspired guesswork. The fact that this condensation is happening is presumably related to the fact that in the field theory we passed the flavor bound. The extension of the duality into this regime moved occurrence of the conformal field theory in the phase diagram from zero mass to the edge of the chirally broken regime with its Grassmannian pion Lagrangian as already argued in [15]. So qualitatively holography supports our duality conjecture.

3.4.6 Phase Matching

As a final check we want to confirm that the possible phases match in the duality of (3.68) and (3.69). Recall how the matching of phases worked in the flavor-less case. On the SU side the bifundamental scalars could either acquire an expectation value or a mass. In the latter case they just disappear from the low energy spectrum, in the former they break two neighboring nodes to the diagonal subgroup. The corresponding levels add. The allowed

phases were hence given by partitions $\{n_I\}$ of n, that is integers n_I with $\sum_I n_I = n$. Each n_I specified how many consecutive nodes were broken down to the diagonal subgroup before encountering a scalar that became massive. So $n_1 = n$ corresponds to the case were all bifundamentals acquired an expectation value, whereas $n_I = 1$ for $I = 1, \ldots, n$ is the case where all bifundamentals get a mass. The generic partition led to a phase governed by a topological field theory based on a gauge group

$$\prod_I SU(N)_{-n_I}. \tag{3.100}$$

The phases of the $U(N)_n$ gauge theory were parametrized by the expectation values of the adjoint scalar. Latter can always be diagonalized, so we have to specify N eigenvalues. Enhanced unbroken gauge groups arise whenever eigenvalues coincide. Using again the partition $\{n_I\}$ to denote to multiplicities of repeated eigenvalues the phases of the $U(N)_n$ plus adjoint theory gave

$$\prod_I U(n_I)_N. \tag{3.101}$$

Eqs. (3.100) and (3.101) are level-rank duals, so both sides have the same phase diagram.

Now let us see what happens in the presence of flavors. Let us first take a look at the U side of the duality. Under the gauge symmetry breaking of (3.101) triggered by the adjoint scalar the fundamental matter multiplets decompose into fundamental matter under each of the product factors, so that we obtain a theory

$$\prod_I \left[U(n_I)_N + N_F \text{ fund scalars}\right]. \tag{3.102}$$

For each gauge group factor we now can, as usual, drive the fundamental scalars to condense or to become heavy and decouple. We know that the dual description of all these phases is captured by:

$$\prod_I \left[SU(N)_{-n_I+N_F/2} + N_F \text{ fund fermions}\right]. \tag{3.103}$$

This is indeed a theory we can get out of the flavored quiver, but it requires a non-trivial potential. Note that in the quiver without potential we would find that whenever two nodes

with their $SU(N)_{-1+N_F/2}$ gauge groups and N_F fundamental fermions each get broken down to their diagonal subgroup, we would get a $SU(N)_{-2+N_F}$ and $2N_F$ fundamental fermions and an enhanced flavor symmetry. In order to get (3.103) we need a quartic potential which gives one of the two sets of N_F flavors a negative mass so they decouple and shift the Chern-Simons level back to $N_F/2$. Generally, when we break down n_I nodes to their diagonal factor, we need $n_I - 1$ sets of N_F flavors to get a negative mass from the $n_I - 1$ bifundamentals. This can be accomplished by the appropriate quartic potential, but it is crucial that this is included. Apparently the limit of no interactions on the SU side that we have mostly been working with in the flavorless case is inconsistent with the confinement scenario where we are left with the theory of (3.69) on the U side.

3.4.7 Enhanced Flavor Symmetries

A crucial feature of the new flavor-violated master duality is the presence of finite interactions on the SU side of the duality. These interactions ensure that when one Higgses the bifundamental scalars they give a gap to all but the very last node's flavor degrees of freedom. Explicitly, the interactions enter in the form[21]

$$\mathcal{L} \subset c' \sum_{i=1}^{n-1} \left(Y^{\dagger}_{i,i+1} \psi_i \right) \left(\bar{\psi}_i Y_{i,i+1} \right). \tag{3.104}$$

Thus, when we Higgs the $Y_{i,i+1}$ bifundamentals, the ψ_j for $j = 1, \ldots, n-1$ all acquire a finite positive mass. Since only the ψ_n remains light, we effectively have an $SU(N)_{-n+N_F/2}$ theory coupled to only N_F fermions. If these interaction terms were not present, all ψ_i would remain light. This would lead to an $SU(N)_{-n+N_F/2}$ theory coupled to nN_F fermion, which gives a Grassmannian which does not agree with the pure $3+1$ dimensional analysis [50].

Although the ψ_j acquire a mass from interaction terms, this can be canceled by an *explicit* mass deformation for all the ψ_j. This is what occurs on critical lines corresponding to II-III,

[21] For consistency we must also include finite interactions for scalars on adjacent links, however we are only focusing on the part of phase space where these interactions are small compared to any given mass scalar mass deformation. We leave a full mapping of the phase diagram with finite interactions for future work.

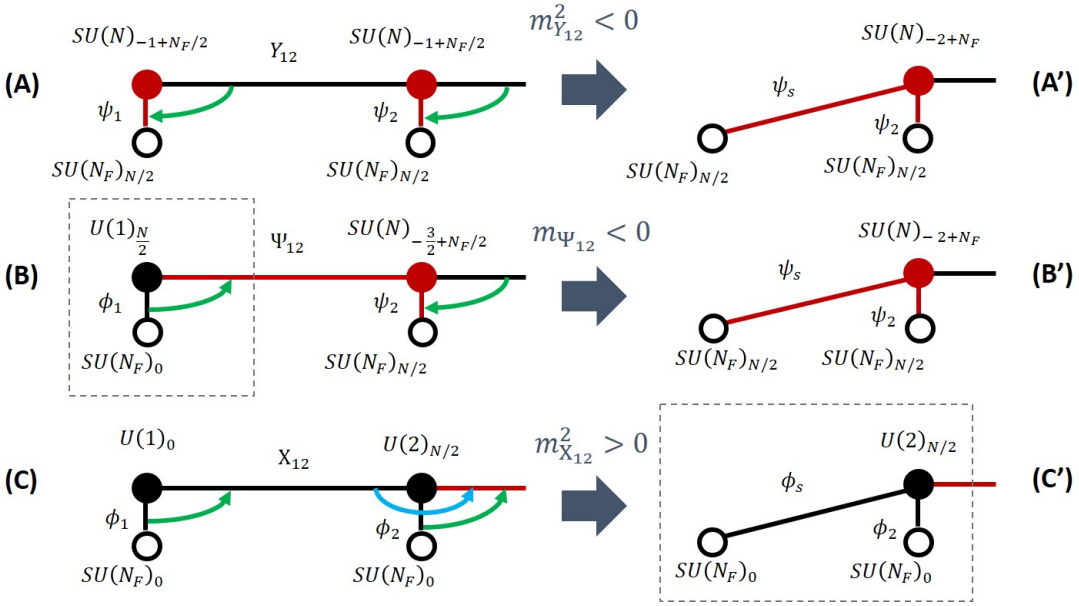

Figure 3.10: Explanation of interaction and enhanced flavor symmetries which arise due to the flavor-violated master duality and its finite interaction terms. We are using green/blue arrows to denote the (unidirectional) interactions. The green arrows represent finite interactions between the flavor degrees of freedom and adjacent bifundamentals. The light blue arrows represent interactions between bifundamental scalars, which were also present in the pure YM case of [9]. We assume they take the very same form they did there. The right-hand side shows how one arrives at enhanced flavor symmetries on the adjacent node at each step of the duality.

II-VI, and III-VI. If this is done for all ψ_j, then we once more have nN_F light fermions, which can lead to enhanced symmetries and strange looking Grassmannians. For consistency, these flavor enhanced Grassmannians should be present on the U side of the duality as well. This is indeed what occurs. The procedure is summarized in Fig. 3.10.

First let us review what occurs in the fully SU theory, denoted by A in Fig. 3.10. When one Higgses the Y_{12} bifundamental, this effectively ties the gauge theories of the first and second node together. We have denoted this mass deformation in A' by representing said nodes as a single node. From the point of view of Fig. 3.7, this corresponds to moving along the II-III critical line. Now, when one gauges the $SU(N_s)$ global symmetry, one gets a Grassmannian around where this line was previously. This is because the non-Abelian background terms have Chern-Simons levels which violate the flavor bounds. This Grassmannian will be $\mathcal{M}(2N_F, 2)$, where the $2N_F$ comes from the N_F fermion flavors which were already tied to the second node, and another N_F flavors which previously belonged to the first node.

Now let us discuss how this is matched in B of Fig. 3.10. To do so, it is helpful to reference what occurs in Fig. 3.7 along the II-III critical line when the $SU(N_s)$ global symmetry is gauged. Note that, prior to the gauging of said symmetry, we also get $N_s N_f$ light fermions along said line, which we will call ${\psi_s}$[22]. From Fig. 3.7, we get the same behavior when we give Ψ_{12} a negative mass deformation. The ψ_s lead to an enhanced flavor symmetry on the second node, shown in B' of Fig. 3.10. If we took the ψ_s and ψ_2 to be light, we would again arrive at the Grassmannian $\mathcal{M}(2N_F, 2)$. Everything seems consistent so far, which shouldn't be too surprising since we have only used the flavor-violated master duality once, and it can be confirmed this is consistent when gauging the $SU(N_s)$ symmetry.

In moving from B to C we have used the flavor-violated master duality on the second node. This changes the fermions Ψ_{12} and ψ_2 to scalars. Strictly looking at C and gapping

[22] As a quick aside, notice that it is difficult to see from the point of view of just the blue scalar theory where these light fermions come from (as opposed to the III-VI critical line, where all kN_s fermions modes are simply light). Said light fermions are needed to explain the change in background Chern-Simons terms between phases II-III, which gives us confidence their number is correct. Abstractly, they can be viewed as the two critical lines II-VI and III-VI merging together, but these singlet fermions are described by the two distinct scalar theories (i.e. the red and blue ones).

the X_{12} scalars, which via mass mapping is analogous to Higgsing the Y_{12}, it is difficult to see how we again get the enhanced flavor symmetry on the second node. This isn't too surprising, because even in moving from B to B' it was difficult to explain where the $N_s N_f$ ψ_s came from. Instead, consider applying the master duality to B' (i.e. B with Ψ_{12} already deformed to large negative mass). This would change the N_F light ψ_2 and N_F light ψ_s to corresponding light scalars in C'. Thus from this point of view, it makes sense that we get N_F light ϕ_2, but also N_F light ϕ_s, leading once more to an enhanced flavor symmetry. Similar to ψ_s, the we can conjecture the ϕ_s are light by some cancellation between the interaction terms and the explicit mass deformations. Since we now have $2N_F$ light scalars, if we take them to negative mass we once more find the $\mathcal{M}(2N_F, 2)$ Grassmannian.

To see this continues to occur as we move to more general quivers, note that we can continue to use these very same arguments used above to see enhanced flavor symmetries in U theories. In particular, in Fig. 3.10, the part of the quiver in the dashed box of C' is identical to that of B, except for the fact the former has $2N_F$ light scalars instead of only N_F light scalars. Thus, repeating the very same arguments used in moving from B to B' above, we come to the conclusion that as one takes Ψ_{23} to negative mass, we should again get light ψ_s fermions bifundamentally charged under the scalar and fermion flavor symmetries. However, now those symmetries are $SU(N_s) \times SU(2N_F)$. This would then lead to an $SU(3N_F)$ symmetry on the third node.

Lastly, let us propose where the extra light ψ_s and ϕ_s we saw above in theories B' and C' arise. There are very natural bound states which have the exact quantum numbers to match these bifundamentals, namely

$$\psi_s = \phi_1 \Psi_{12}, \qquad \phi_s = \phi_1 X_{12}. \tag{3.105}$$

Furthermore, the corresponding U node under which each component of these bound states is charged (i.e. node one) is confining. Thus we conjecture that some combination of confinement and mass deformations somehow makes said bound states light. This procedure generalizes as one moves down the quiver. For example, the additional light scalars one gets

on the third node for certain mass deformations could correspond to bound states $\phi_1 X_{12} X_{23}$ and $\phi_2 X_{23}$. Along with ϕ_3, said scalars can lead to an enhanced flavor symmetry.

3.5 Orthogonal and Symplectic Gauge Groups

3.5.1 Node-by-node

We can generalize the duality for quiver gauge theories to the case of symplectic and orthogonal gauge groups. The node-by-node construction generalizes in a straightforward fashion. According to [3] the basic bosonization dualities in this case are

$$SO(N)_k + N_f \text{ real scalars} \quad \leftrightarrow \quad SO(k)_{-N+N_f/2} + N_f \text{ real fermions} \tag{3.106a}$$

$$Sp(N)_k + N_f \text{ real scalars} \quad \leftrightarrow \quad Sp(k)_{-N+N_f/2} + N_f \text{ real fermions.} \tag{3.106b}$$

Both of these can be extended to the case of "master dualities" with fermions and scalars on both sides [24, 64]; in any case, note that the assignments of the matrix size (which is now twice the rank) as well as the levels on the dual side exactly match the corresponding assignments in the unitary group. So going through the exercise of dualizing node by node we get exactly the same answers as in the unitary case, except for the fact that SU and U both get replaced with all SO or all Sp respectively. Let us focus here for simplicity on the case of unflavored quivers, the flavored case follows straightforwardly. We get the following two dualities in direct analogy with the unitary case:

$$\prod_{i=1}^{n} SO(N_i)_{-k_i} \qquad \text{is dual to} \qquad \left[\prod_{i=1}^{n-1} SO(K_i)_{N_i - N_{i+1}}\right] \times SO(K_n)_{N_n} \tag{3.107}$$

and

$$\prod_{i=1}^{n} Sp(N_i)_{-k_i} \qquad \text{is dual to} \qquad \left[\prod_{i=1}^{n-1} Sp(K_i)_{N_i - N_{i+1}}\right] \times Sp(K_n)_{N_n}. \tag{3.108}$$

Once again we can use these node-by node duality chains to argue for the special case that all $N_i = N$ and all ranks are $k_i = 1$. In this case the original theories become quivers with equal rank and level nodes analogous to 3.3. In the dual theory we get all but the last node to be at level 0. Appealing to a confinement scenario as in the unitary case, we would argue

that the last bifundamental gets replaced by a meson gauge invariant under the second to last node. This is a symmetric combination in the case of orthogonal gauge groups and an anti-symmetric combination in the symplectic case. Correspondingly we should conclude that

$$[SO(N)_{-1}]^n + \text{bifundamental scalars} \qquad \leftrightarrow \tag{3.109a}$$

$$SO(n)_N + \text{symmetric rank-2 scalar} \tag{3.109b}$$

and

$$[Sp(N)_{-1}]^n + \text{bifundamental scalars} \qquad \leftrightarrow \tag{3.110a}$$

$$Sp(n)_N + \text{antisymmetric rank-2 scalar.} \tag{3.110b}$$

When we add flavors, we face same the complications as the unitary case. Fortunately these dualities can be extended into the flavor violated regime in exactly the same manner as the SU theories. The main difference is the Grassmannians become

$$\frac{SO(N_f)}{SO(k) \times SO(N_f - k)} \qquad \text{and} \qquad \frac{Sp(N_f)}{Sp(k) \times Sp(N_f - k)}. \tag{3.111}$$

These changes introduces a whole slew of interesting physics which is discussed in great detail in [80]. For our purposes, we simply note that the story of flavored quivers goes through in the same manner as in the SU case.

3.5.2 Phase Matching

The phase matching in the symplectic and orthogonal cases also directly mimics their unitary counterparts. Let us focus first on the orthogonal case. In the quiver we can once again express the phases by partitions of n, determining whether the bifundamental scalars get positive or negative mass squareds. The generic phase of the quiver is given by

$$\prod_i SO(N)_{-n_i} \tag{3.112}$$

in direct analogy with (3.100) of the SU quiver. The phases of the $U(N)_n$ gauge theory were parametrized by the expectation values of the adjoint scalar, a hermitian matrix that we were able to diagonalize with the unitary gauge transformation. This time we are having a scalar in a symmetric matrix, exactly the object that can be diagonalized by our orthogonal gauge transformations. So once again the phases of the dual theory can be parametrized by the eigenvalues of the matrix and enhanced unbroken gauge groups arise whenever eigenvalues coincide. The phases of the dual theory hence become

$$\prod_i SO(n_i)_N, \tag{3.113}$$

indeed a level/rank dual representation of (3.112). In the symplectic case the antisymmetric matrix plays exactly the role of the symmetric matrix in the orthogonal case. It can be brought into normal form by symplectic transformations, breaking the gauge group down into products of smaller symplectic groups.

3.5.3 Holographic Construction

Holographic QCD was generalized to the orthogonal and symplectic case in [59]. An orientifold O6 plane is introduced into the D4/D8 system in order to project the original unitary group down to either an orthogonal or symplectic subgroup. Both O6 and D8 are localized on the circle; if both are present they need to be offset from each other by an angle $\pi/4$ so that the stack of D8 branes gets mirrored onto the antipodal stack of anti-D8 branes by the orientifold projection. The two options for the gauge group are distinguished by exactly what type of O6 we add, the two options are usually denoted $O6^-$ for orthogonal and $O6^+$ for symplectic groups, the superscript indicating the sign of the RR charge associated with the orientifold plane. The full brane content both in the flat embedding space picture as well as in the dual geometry is enumerated in Tables 3.3a and 3.3b. Included in Table 3.3b is also the D6 brane that acts as the domain wall.

In order to understand the theory in the bulk, we simply need to determine the effect of the O6 plane on the gauge theory living on the domain wall D6s. As is apparent from

	0	1	2	3	4	5	6	7	8	9
D4	**x**	**x**	**x**	**x**	**x**	o	o	o	o	o
D8	**x**	**x**	**x**	**x**	o	**x**	**x**	**x**	**x**	**x**
O6	**x**	**x**	**x**	**x**	o	**x**	**x**	**x**	o	o

(a) Brane realization of the gauge theory in 10d flat space. X_4 is a compact direction.

	0	1	2	3	r	θ	S^4
D8	**x**	**x**	**x**	**x**	**x**	o	S^4
O6	**x**	**x**	**x**	**x**	**x**	o	S^2
D6	**x**	**x**	**x**	o	o	o	S^4

(b) Embedding of the probe branes in Witten's black hole.

Table 3.3: Brane realization of holographic QCD with symplectic or orthogonal gauge group. In a) N color D4 branes intersect an orientifold O6 to project to a real gauge group. In b) the same branes are embedded in the dual $\mathbb{R}^{3,1} \times D_2 \times S^4$ geometry, together with D6 branes dual to the θ-interfaces. Also indicated are flavor D8 branes that would be needed to add additional flavors. t, $x_{1,2,3}$ are the coordinates on $\mathbb{R}^{3,1}$, and r and θ the coordinates on D_2.

Tables 3.3a and 3.3b the O6 planes have 4 relative ND directions with both the D4s of the flat space embedding and the D6s in the black hole geometry. What this means is that the worldvolume theory on both D4s and D6s experience the same type of projection: the gauge groups are either orthogonal on both or symplectic on both. This is exactly as we would expect from our node-by-node procedure.

Last but not least we need to determine what happens to the formerly adjoint scalar corresponding to motion of the stack of D6s in the x_3 direction. Let us start with the case of an orthogonal gauge group. For a scalar describing motion transverse to the orientifold one finds that branes have to move off in mirror pairs, with a $U(1)$ gauge theory on each pair that can enhance to $U(n_i)$ for n_i coincident branes on one side. This is the breaking pattern we would expect from an antisymmetric rank 2 tensor. On the other hand, a scalar corresponding to motion inside the orientifold allows the stack of n branes to completely separate into n individual branes - since they are inside the orientifold they need no mirror partner. Each brane has an $SO(1)$ gauge group on its worldvolume that can get enhanced

to $SO(n_i)$ for coincident eigenvalues. Since the motion of the D6s into the x_3 direction is inside the O6, this corresponds to a symmetric rank-2 tensor. Reassuringly this is exactly what we are supposed to find according to our duality conjecture in (3.109b). For symplectic gauge groups, the role of symmetric and antisymmetric rank-2 tensors is reversed. So the bulk physics yields indeed (3.110b) in that case.

In order to fully realize our dualities we would need to find (3.109a) and (3.110a) to be the corresponding field theories living on the boundary. For the case of symplectic gauge groups this appears indeed to be the obvious guess for the theory on the domain walls of a confining $Sp(N)$ gauge theory generalizing the discussion of [50] in the unitary case. In the orthogonal case this is certainly incorrect for the case of $SO(N)$ gauge groups, but it appears reasonable if the gauge group is instead $Spin(N)$. Since the stringy realizations of these gauge groups always involve heavy spinors, it is entirely reasonable to assume that the relevant gauge theories living on the branes were actually $Spin(N)$ groups all along. Unfortunately, these global issues are often not considered carefully in the orientifold literature. Somewhat confusingly, the node-by-node dualization above seems to be literally working with SO groups, not $Spin$ groups. So while a coherent and self-consistent duality story seems to emerge on the symplectic side, a complete understanding of the orthogonal case would require solid control of these global issues.

3.6 Discussion

Here we have developed the methodology for dualizing linear quiver gauge theories with bifundamental scalars and argued that they can be viewed as the non-Abelian generalization of particle/vortex duality. Crucial to this is the interaction terms, which couple scalars living on adjacent links and propagate the symmetry breaking pattern down the quiver in a unidirectional manner. This is required to ensure the mass deformed phases are level-rank dual to each other.

We then specialize this general framework to the study of domain walls that arise in $3+1$ dimensional Yang-Mills theory with a spatially varying theta angle. In addition, we

embed this special case in string theory and study the duality holographically. We find a novel duality between a theory with bifundamental matter and one with adjoint matter, schematically given by (3.4). Let us comment on the similarities and differences between these two approaches.

From the setup in ref. [50], we expect the bifundamental scalars on the SU side of the duality to interpolate between a smoothly varying and a sharp domain wall/interface. However, the pure field theoretic quiver approach of Sec. 3.2.2 makes opaque the geometric interpretation of a physical wall located in space. The complementary geometric approach of Sec. 3.3.2 makes this manifest: Higgsing a bifundamental is literally removing a D6 brane (i.e. domain wall) from a stack and moving it to a different physical location in space. Widely separated D6s correspond to the smoothly varying phase, reinforcing our intuition of the theory at small $|\nabla\theta|$.

It is a nice consistency check that we get adjoint particles even when the U groups are broken down, just like when we separated the branes and get smaller U groups. We can see how one can effectively tune the diagonal vacuum expectation values of the adjoint scalar without introducing interactions terms which explicitly break the $U(n)$ gauge symmetry. This was unclear when we only had the $U(n)$ factor, but can now be made manifest. Namely, one can effectively break the smaller $U(p)$ symmetries (with $p < n$) and then the interaction terms propagate the breaking to the larger gauge groups. The adjustment of effective eigenvalues can be seen from the generalization of (**??**). There is also a natural way to describe the gapping of such modes, which just leaves the $U(n)_N$ TFT untouched.

When the walls on top of one another in the holographic duality we have new light matter one both sides of the duality, but it manifests itself in a very different manner. On the U side the extra matter enhances the gauge symmetry. Meanwhile, on the SU side the bifundamentals just become additional massless scalars. This may seem peculiar given the fact the bifundamental degrees of freedom match quite nicely when the walls are separated (albeit by construction). But this is precisely the behavior we would expect in our 3d bosonization duality. As we learned from the particle-vortex duality generalization, it is

not actually the bifundamental degrees of freedom which should match on either side of the duality but rather particles and vortices. The very same mismatch of particle degrees of freedom is present in the bosonic particle-vortex duality as well.

In fact, the matching of the particle and vortex degrees of freedom is very nicely realized in the holographic duality. The dual of the baryons in the bulk are based on the standard holographic construction of the baryon vertex [119], very similar to what was found in [66]. Namely, they are D4 branes wrapping the S^4 and also extended along the time direction. In order to be neutral, fundamental strings run from the D4 branes to the D6 branes on which they live. Furthermore, the D6 branes dissolve the D4 branes turning them into magnetic flux (it is more energetically favorable and has the same quantum numbers). The attachment of N fundamental strings is analogous to particle/flux attachment. It can be argued that the N fundamental strings cannot end on the same D6 brane. Hence when the D6 branes get separated, the monopoles must also pick up a mass since the fundamental strings must stretch from one D6 brane to another–providing more evidence that lines of flux can end on domain walls. This is also in nice agreement with the behavior which occurs on the SU side where the bifundamentals are interpreted as strings which stretch from one brane to another and thus both acquire a mass proportional to the separation between branes.

Also the holographic system has additional translational degrees of freedom associated with moving the walls. On the SU side this is interpreted as the literal position of the domain walls along the x_3 direction. Meanwhile, on the bulk side this is interpreted as the vacuum expectation values of the adjoint U matrix which are the locations of the D6 branes. Since the nodes of the quiver had no concept of absolute position in space, this was never considered in the 3d bosonization case. This could potentially be resolved by including the Goldstone bosons associated to the broken translational invariance with an appropriate potential.

In the holographic duality, the scalar excitations are always massless, since translations correspond to flat directions for the adjoint scalar excitations. This is in contrast to the adjoints of the quiver duality which are massive except perhaps at very fine tuned locations

in deformation space. This may just be a feature of the large N limit, though, since stringy corrections will generate a Coleman-Weinberg potential for the adjoint.

It seems likely that many of the discrepencies between the two approaches can be attributed to the large N, large λ limit on the holographic side of the duality. For instance, gapping the bifundamentals on the SU side of the duality is dual to seperating the stack of D6 branes in the bulk. Higgsing the bifundamentals, on the other hand, has no dual gravitational description since the CFT occurs when all the D6 branes are on top of each other and the strings stretching between the D6 branes are massless. At finite N, however, tachyonic contributions will become important. There will be some finite seperation of D6 branes where the strings become massless, below which open string excitations are tachyonic and interesting stringy dynamcis occurs. We believe this regime is dual to the Higgs phases of the SU side of the duality. Stated another way, our holographic construction does not probe the whole phase diagram–some phases may not be accesible in the large N limit. This claim could be tested by computing finite N corrections on the gravity side or taking the large N limit of the quiver theories. We leave this to future work.

For instance, there is an uncertainty on the U side of the quiver duality as to whether or not we should treat the particles as adjoint or bifundamentals (this is related to the fact of whether or not we are considering the confinement scale to be greater or smaller than the mass deformation). The issue with considering adjoints is that they do not couple to $U(1)$ factors, and thus cannot seem to yield the correct breaking pattern for negative masses on the U side of the duality. That is, when an adjoint acquires a vacuum expectation value, it will not contribute the appropriate $U(1)$ factor to yield the correct combination of $U(1)_N$ levels. What we need is something charged under the appropriate $U(1)$ factor to acquire a vacuum expectation value in order for the breaking to occur. Since the $U(p)_0$ factors are confining, we can only have gauge singlets under the corresponding gauge groups, and thus we need something analogous to baryons to be light (the adjoints are analogous to mesons).

One may wonder whether our quiver dualities can be useful in the context of deconstruction, following the recent work of [12]. There it was shown that Abelian quiver dualities can

be lifted to dualities in 3+1 dimensions. It would be very interesting to do this in the non-Abelian case. One important ingredient in this construction is the use of "all scale" versions of the duality, following the construction of [72] in the supersymmetric case. We'd like to point out that at least for two node quivers, our method of gauging global flavor symmetries does allow us to give all scale versions of the non-Abelian duality. Say we want a dual for $SU(N)_k$ with N_f fermionic flavors with a finite gauge coupling. Since the gauge coupling is dimensionful we are describing a theory with a non-trivial RG running. It interpolates between a free theory in the UV and a strongly coupled CFT in the IR. We can obtain this theory by starting with NN_f free fermions and gauging a $SU(N)$ subgroup of the global $SU(NN_f)$ flavor symmetry. At this stage we can add both the Chern-Simons as well as the Maxwell kinetic terms. The original theory of NN_f free fermions has dual descriptions in terms of a $U(K)_1$ gauge theory coupled to NN_f scalars. Modulo flavor bounds K is a free parameter. The global flavor symmetry simply rotates the scalar flavors in this dual. Promoting a $SU(N)$ subgroup to be dynamical we end up with a $U(K)_1 \times SU(N)_k$ gauge theory with N_f bi-fundamentals. While the $U(K)$ factor has infinite coupling, the $SU(N)_k$ factor has a finite Maxwell term which maps directly to the Maxwell term of the same $SU(N)_k$ factor on the dual side. This way we did construct a non-Abelian all scale dual to $SU(N)_k$ with fermions. Unfortunately it is not yet clear how to generalize this construction to more interesting quivers. In this work we extended the master duality presented in [64, 24] to the flavor violated regime where $N_f > k$. It is important to keep in mind the general philosophy used in deriving the phase diagrams of Figs. **??** and 3.7: the dynamics in the quantum phase is hidden by strong dynamics in the SU theory. It is only when we pass to the U theory that we can see interesting structure emerge, similar to approached used in [80] as well as in [55, 38, 33, 37]. Like these prior works, our dualities pass all the required consistency checks short of explicit large N calculations. And although it is difficult to prove the existence of these new quantum phases exactly, 3d bosonization gives good evidence that they indeed exist.

We then went on to extend the quiver dualities by using the flavor violated master

duality. We constructed a dual for a flavored quiver with bifundamental scalars on the links and fundamental fermions coupled to each node via node-by-node dualization. Such a theory describes interfaces in $3+1$ dimensional QCD as discussed in Ref. [50]. The resulting dual theories were qualitatively supported by a holographic construction with D6 branes in the Sakai-Sugimoto model. We then extended our work to orthogonal and symplectic gauge groups, both in the node-by-node dualization and in holography. More interesting directions would be exploring other gauge theories with different matter contents. It is widely believed that infrared phase of three-dimensional theories describes effective worldvolume theory of walls/interfaces in corresponding four-dimensional theories [55, 1, 80, 50, 9, 15, 34, 21, 73]. It would be nice to understand what kind of quiver gauge theories with its phase diagram and stringy constructions would emerge when analyzing phase transitions of multiple walls/interfaces in various cases similar to what we've done in the case of QCD_4.

There are some limitations to our approach, however. First, the analysis in Appendix A of [50] seems to indicate a periodicity of the Grassmannian as a function of the number of nodes, n. That is, the most general Grassmannian is not $\mathcal{M}(N_f, n)$ but instead $\mathcal{M}(N_f, n \text{ mod } N_f)$. Our quiver theory seems to indicate that this is not the case – if the number of nodes n is greater than N_f, the full Higgsed regime gives $SU(N)_{-n+\frac{N_f}{2}}$ with N_f ψ. This is flavor bounded and so does not exhibit a quantum regime. The case examined in [50] is valid for $n \leq N_f$. The analysis just seems to point to this periodicity, but an explicit demonstration of it has not yet been completed. Perhaps there is some subtle strong coupling dynamics in the $3+1$ dimensional theory that causes the Grassmannian to disappear. Or maybe our quiver theory is only valid for $n \leq N_f$ and there is some extension of our work that can bring us into the $n > N_f$ regime. We hope to report on this interesting question in future work.

We have also found that the quivers corresponding to $N_F = 1$ and $N_F > 1$ require the use of two very different versions of the master duality – the double-flavor saturated and flavor violated cases, respectively. In Ref. [50], it was found these two cases also separated themselves quite distinctly due to the lack of an enhanced symmetry when the $3+1$-dimensional fermion mass disappeared in the $N_f = 1$ case. It is not obvious to the

authors if these two facts are somehow related.

The inclusion of finite interactions in the flavored and unflavored quiver immensely complicates the phase diagram. This is because it is possible for interactions to give negative mass deformations to links living on adjacent nodes, which propagate symmetry breaking down the entire quiver. However, these negative mass deformations could be undone by a positive mass deformation of a given link. This leads to a whole new variety of critical lines and theories. We are able to explicitly verify the matching of phases for low-node quivers, but a general proof of phase matching for an arbitrary number of nodes is still beyond our reach.

The holographic side of things is ripe with interesting puzzles. For instance, it is still unknown what the exact form of our derived orthogonal duality is. As briefly commented on in the end of Sec. 3.5, the duality derived from the orientifold projection onto the orthogonal subgroup seems to be insensitive to the global properties of the gauge group. That is, we know that there are multiple different types of orthogonal gauge groups in 2+1D that differ by the required background terms and the gauging of various $\mathbb{Z}_2$ global symmetries [38]. Can these global issues be understood in string theory? Moreover, how does one even see a quantum phase in the holographic construction of $SU(N)$ gauge theories with fundamental fermions in holography? We leave these questions for future work.

3.7 Supplementary: Building Non-Abelian Linear Quivers

Here we provide further details of our construction of the non-Abelian linear quivers.

3.7.1 Other Forms of the Duality

The second of Aharony's dualities is given by taking the $N_s = 0$ of the master duality, (3.5), which gives

$$\mathcal{L}_{SU} = i\bar{\psi}\not{D}_{b'+C+\tilde{A}_1}\psi - i\left[\frac{N_f-k}{4\pi}\mathrm{Tr}_N\left(b'db' - i\frac{2}{3}b'^3\right) + \frac{N}{4\pi}\mathrm{Tr}_{N_f}\left(CdC - i\frac{2}{3}C^3\right)\right] - i\left[\frac{N\left(N_f-k\right)}{4\pi}\tilde{A}_1 d\tilde{A}_1\right], \tag{3.114a}$$

$$\mathcal{L}_U = |D_{c+C}\phi|^2 - i\left[\frac{N}{4\pi}\mathrm{Tr}_k\left(cdc - i\frac{2}{3}c^3\right) - \frac{N}{2\pi}\mathrm{Tr}_k\left(c\right)d\tilde{A}_1\right]. \tag{3.114b}$$

Performing the using $\tilde{c} \to \tilde{c} + \tilde{A}_1$ shift, canceling common factors on either side of the duality, and defining $E_\mu \equiv C_\mu + \tilde{A}_{1\mu}$, we end up with

$$\mathcal{L}_{SU} = i\bar{\psi}\not{D}_{b'+E}\psi - i\left[\frac{N_f-k}{4\pi}\mathrm{Tr}_N\left(b'db' - i\frac{2}{3}b'^3\right) + \frac{N}{4\pi}\mathrm{Tr}_{N_f}\left(EdE - i\frac{2}{3}E^3\right)\right] \tag{3.115a}$$

$$\mathcal{L}_U = |D_{c+E}\phi|^2 - i\left[\frac{N}{4\pi}\mathrm{Tr}_k\left(cdc - i\frac{2}{3}c^3\right)\right]. \tag{3.115b}$$

This yields the duality (3.21) which we use in going from theory D to theory E. Note that in promoting $\tilde{A}_1$ into a dynamical field, we again introduce a new global symmetry. We will call the background gauge field associated with said symmetry $\tilde{B}_1$.

Returning to the master duality, in the main text we could have combined the $U(1)$ and $SU(N_f)$ global symmetries into the definition of $E_\mu = C_\mu + \tilde{A}_{1\mu}\mathbb{1}_{N_f}$. For the purposes of deriving the non-Abelian linear quivers, this was not necessary. For completeness, we show the form of the duality here, because it gives the explicit master duality with all background fields in its most succinct form. It is also convenient to define the $U(N_s)$ gauge field $H_\mu \equiv B_\mu + \tilde{A}_{1\mu} + \tilde{A}_{2\mu}$. This leaves us with a duality of the form

$$\mathcal{L}_{SU} = |D_{b'+H}\phi|^2 + i\bar{\psi}\not{D}_{b'+E}\psi + \mathcal{L}_{\mathrm{int}} - i\left[\frac{N_f-k}{4\pi}\mathrm{Tr}_N\left(b'db' - i\frac{2}{3}b'^3\right)\right] - i\left[\frac{N}{4\pi}\mathrm{Tr}_{N_f}\left(EdE - i\frac{2}{3}E^3\right)\right], \tag{3.116a}$$

$$\mathcal{L}_U = |D_{c+E}\Phi|^2 + i\bar{\Psi}\not{D}_{c+H}\Psi + \mathcal{L}'_{\mathrm{int}} - i\left[\frac{N}{4\pi}\mathrm{Tr}_k\left(cdc - i\frac{2}{3}c^3\right)\right]. \tag{3.116b}$$

This makes the $U(N_s) \times U(N_f)$ global symmetry explicit.

3.7.2 Global Symmetries

Here we discuss the matching of the global symmetries across the dualities in more detail.

In our four node example of Sec. 3.2.2, when stepping from theory A to B and subsequently from theory B to C, there is an implicit matching that occurs between the two equivalent Lagrangians we call theory B. To follow the global symmetries all the way through from theory A to E, it is necessary to look at this matching more carefully. This implicit matching also occurs for every intermediate theory as well (i.e. theories C and D for the four node case). We will call these two equivalent descriptions theory B' and B" and use a similar notation to describing the matching of C and D as well.

To start, let us explicitly consider the matching of theory B. Specifically, theory B' is what we get from using (3.20) with theory A. Meanwhile, theory B" is what we would like to apply the master duality in the form of (3.24) to get out what we now call theory C'. When matching these theories to one another, what was the color gauge symmetry of theory B' gets mapped to the (promoted) $U(k_3)$ flavor symmetry of theory B". Meanwhile, the flavor symmetry of theory B' becomes the color symmetry of theory B".

It will be helpful to consider in closer detail how we are matching all the gauge fields to which the fermions couple. The fermion couplings for the two theories are given by

$$(\text{B'}): \qquad i\bar{\Psi}\not{D}_{c+B+\tilde{A}_1}\Psi \tag{3.117}$$

$$(\text{B"}): \qquad i\bar{\psi}\not{D}_{b'+C+\tilde{A}_1-\tilde{A}_2}\psi. \tag{3.118}$$

With a slight abuse of notation, the dynamical/background gauge fields of theory B' and B" denoted above are completely distinct and must be matched. The matching of the gauge fields associated with gauge and global symmetries are shown in Table 3.4. Note the $\tilde{A}_1$ field belonging to Ψ is matched to $\tilde{B}_2$ field of the subsequent node.

This careful matching allows us to focus on how the global $U(1)$ symmetry gets transferred through the dualities. In the duality relating theory A and B', the $U(1)$ global symmetry is associated with $\tilde{A}_1$. For theory A this shows up as a baryon-number symmetry and in theory B' it appears as monopole-like symmetry which couples to the U field flux. From

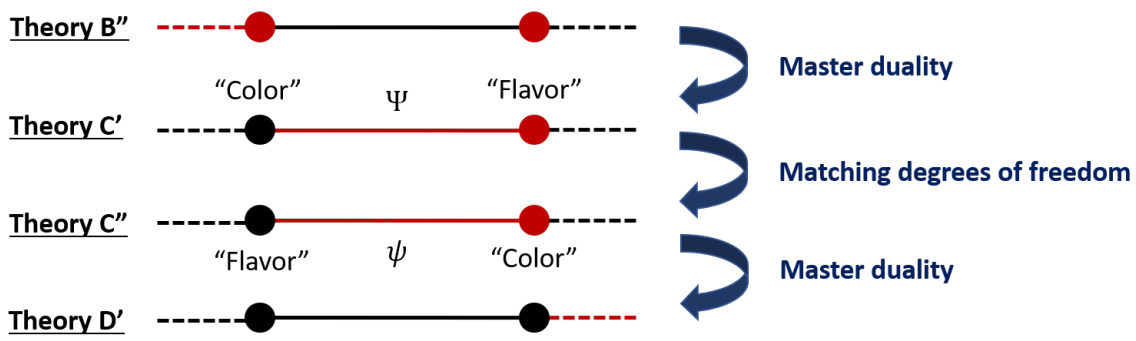

Figure 3.11: How the matching occurs on a generic internal link, which for the purposes of concreteness we have labeled C’ and C".

Table 3.4, we identify this symmetry with the $U(1)$ monopole symmetry of theory B", where the associated background gauge field is $\tilde{B}_2$. Recall, this is the new global $U(1)$ symmetry which couples to the newly gauged $\tilde{A}_2$ field associated with the U symmetry of the first node. Since this new monopole symmetry is the same on both sides of the duality relating B" and C’, when we ultimately arrive at theory C’ we have a monopole-like symmetry which still couples to the newly dynamical $\tilde{A}_2$. From theory C’ onward, the nodes and links associated with such a symmetry are untouched. Thus the $U(1)$ global symmetry which coupled to the $Y_{1,2}$ bifundamental in theory A becomes a monopole symmetry coupled to the Abelian part of the first U node in theory E.

Similarly matching must occur for theory C. Fortunately, we don’t need to work very hard because the matching between C’ and C" is identical to what occurs above for B’ and B" and is schematically shown in Fig. 3.11. The additional global symmetry associated with $\tilde{A}_1$ is identified with the global $U(1)$ symmetry on the next node.

We can again follow a global symmetry through from theory A to E for any of the global $U(1)$ symmetries which couple to bifundamentals higher up the quiver. We find results identical to those of the first node/link above: each $U(1)$ global symmetry which couples to the $Y_{i,i+1}$ bifundamental becomes a $U(1)$ global symmetry associated with monopole number

•	B' Side	B" Side	C' Side	C" Side	D' Side	D" Side
U Node	c	$C - \tilde{A}_2$	c	$C - \tilde{A}_2$	c	$C + \tilde{A}_1$
SU Node	B	b'	B	b'	B	b'
$U(1)_m$ Global Symmetry	$\tilde{A}_1$	$\tilde{B}_2$	$\tilde{A}_1$	$\tilde{B}_2$	$\tilde{A}_1$	$\tilde{B}_1$

Table 3.4: Matching of the intermediate theories. Note the matching of theory B' and B" generalizes for any internal matching, except for the very last. Here, $\tilde{B}_2$ is the background gauge field associated with the new global symmetry we get from gauging $\tilde{A}_2$.

for the ith node.

Finally, consider how the matching occurs for the last node. In going from theory D" to theory E in the example we considered in the main text, we used (3.21). Since for this duality we need to promote the entire $U(k_2)$ flavor symmetry to dynamical, we once more acquired an additional global symmetry which couples to the newly promoted $\tilde{A}_1$ whose associated background field we call $\tilde{B}_1$. The matching of symmetries is slightly different and is shown in Table 3.4. Since Aharony's dualities only have one $U(1)$ global symmetry, there is no monopole-like symmetry associated with the right-most node.

We should also point out a special feature of the global symmetries that occurs for certain mass deformed phases. Note that the $\tilde{A}_1$ coupling of (3.5b) only couples to the unbroken part of the dynamical gauge field c. That is, when the U gauge group is broken down to say $U(k_1 - k_2)$, the coupling changes from $\mathrm{Tr}_{k_1}(c)dA_1 \to \mathrm{Tr}_{k_1-k_2}(c)dA_1$. This is important because when we are in certain mass deformed phases, we must be careful what gauge components are coupled to the $\tilde{A}_1$ charge. Of particular concern in the main text is whether or not vortices couple to certain global symmetries. Since certain finite mass vortices are charged under the broken part of certain gauge fields, they will not couple to particular global symmetries and this will be important for matching excitations.

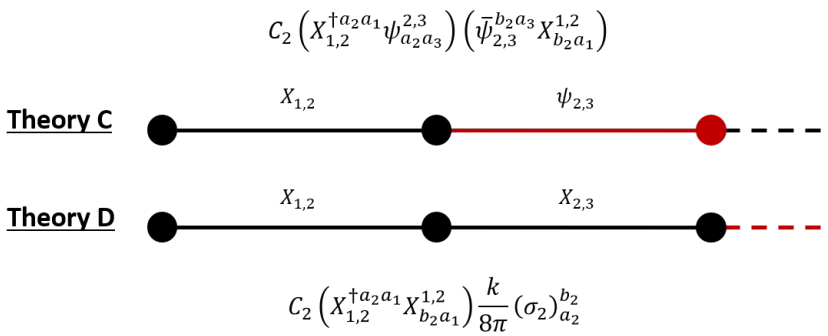

Figure 3.12: Example case of properly dualizing interaction terms. This is for the second node of the four node case considered in the main text in Sec. 3.2.2 and also pictures in Figure 3.3.

3.7.3 Bosonizing Interaction Terms

In this appendix, our goal is to justify the proper mapping of the interaction term present in the master duality. We take as an example what occurs on the second node of our four node example in Sec. 3.2.2, which has a $U(K_2)$ gauge symmetry on it. Specifically, we look at how the interaction term changes when moving from Theory C to Theory D (see Fig. 3.12). With the proper transformation in hand, we will then generalize to interaction terms on the SU and U sides of the duality.

The term from the master duality we would like to apply the duality toward is

$$C_2^{(C)}\left(\bar{\psi}_{2,3}^{a_2 a_3}X_{a_2 a_1}^{1,2}\right)\left(X_{1,2}^{\dagger b_2 a_1}\psi_{b_2 a_3}^{2,3}\right). \tag{3.119}$$

Although we commit to a magnitude for $C_2^{(C)}$ in the main text, to keep this appendix general we only assume $C_2^{(C)} < 0$ in what follows. From the master duality, the purpose of this interaction term is that when the $X_{1,2}$ field obtains a vacuum expectation value this should cause a subset of the fermions to get a mass [24, 64].

One might guess the proper transformation of the term between $\psi_{2,3}$ and $X_{2,3}$ from theory C to theory D is simply a generalization of the $m_\psi\bar{\psi}\psi \leftrightarrow -m_X^2\left|X\right|^2$ mass identification.

Hence a naive generalization and the shorthand used in the main text is

$$C_2^{(C)}\left(\bar{\psi}^{a_2a_3}_{2,3}X^{1,2}_{a_2a_1}\right)\left(X^{\dagger b_2a_1}_{1,2}\psi^{2,3}_{b_2a_3}\right) \quad \leftrightarrow \quad -C_2^{(D)}\left(X^{a_2a_3}_{2,3}X^{1,2}_{a_2a_1}\right)\left(X^{\dagger b_2a_1}_{1,2}X^{2,3}_{b_2a_3}\right). \tag{3.120}$$

This term has the correct behavior when $X_{1,2}$ acquires a vacuum expectation value. Namely, it gives $X_{2,3}$ a color-breaking vacuum expectation value. Unfortunately this suffers from the fact that the reverse procedure can happen as well. That is, when $X_{2,3}$ acquires a vacuum expectation, this gives a mass to $X_{1,2}$. This is because $X_{1,2}$ and $X_{2,3}$ enter on symmetric footing in (3.120), so it is difficult to see where the desired unidirectional behavior that was present in (3.119) will come from. This means the TFT deformations do not match, so we must look for a better generalization.

To do so, it will be helpful to go back to the large N and k studies where the duality map between operators is better established. We will assume such mappings continue to hold for finite values of N and k, at least up to order one factors, which will not affect the results of our analysis.

Ultimately we'd like to find the true bosonic dual of $\bar{\psi}^{a_2a_3}_{2,3}\psi^{2,3}_{b_2a_3}$ with a_2 and b_2 promoted flavor indices. To do so, we'll look for the bosonic dual of $\bar{\psi}\psi$ and assume our results generalize to arbitrary flavor indices. We follow ref. [86] which represents the most general fermion Lagrangian describing the fixed point as,[23]

$$\begin{aligned}\mathcal{L}_F = {} & i\bar{\psi}\not{D}_{b'}\psi - i\left[\frac{N_f-k}{4\pi}\mathrm{Tr}_N\left(b'db' - i\frac{2}{3}b'^3\right)\right] \\ & + \sigma_F\left(\bar{\psi}\psi - y_2^2\frac{N_f-k}{4\pi}\right) - y_4\frac{N_f-k}{4\pi}\sigma_F^2 + y_6\frac{N_f-k}{4\pi}\sigma_F^3.\end{aligned} \tag{3.121}$$

where σ_F is an auxiliary field and y_2^2, y_4, and y_6 are arbitrary coefficients of the relevant and marginal operators of the UV Lagrangian. For the coefficients we choose the values

$$y_4 = x, \qquad y_2^2 = -2xm_\psi, \qquad y_6 = 0. \tag{3.122}$$

Eventually we would like to flow to the deep IR, which amounts to taking $x \to \infty$, where the fermions pick up a finite mass m_ψ, but for now we will assume it to be finite. The dual

[23] We use a different regularization convention for the Chern-Simons-matter theories than that in [86]. See [2] for a nice discussion on the differences in regularization conventions.

of $\mathcal{L}_F$ on the bosonic side is

$$\mathcal{L}_B = |D_c\phi|^2 - i\left[\frac{N}{4\pi}\mathrm{Tr}_k\left(cdc - i\frac{2}{3}c^3\right)\right] + m_B^2\phi^\dagger\phi + b_4\frac{4\pi}{N}\left(\phi^\dagger\phi\right)^2 + x_6\frac{(2\pi)^2}{N^2}\left(\phi^\dagger\phi\right)^3 \tag{3.123}$$

where m_B^2, b_4, and x_6 are coefficient of marginal/relevant operators (the dual of the fermionic parameters) which are then

$$b_4 = x, \qquad m_B^2 = 2x\left(\frac{N-k}{N}\right)m_\phi^2, \qquad x_6 = 0. \tag{3.124}$$

Unfortunately, in the analysis of ref. [86], there is no clear dual to $\bar{\psi}\psi$. We can however express $\bar{\psi}\psi$ in terms of operators which do have a well-defined dual. Integrating out σ_F in S_F enforces the equations of motion

$$x\frac{N_f-k}{2\pi}\sigma_F = \bar{\psi}\psi + x\frac{N_f-k}{2\pi}m_\psi. \tag{3.125}$$

We can rearrange this expression to solve for $\bar{\psi}\psi$,

$$\bar{\psi}\psi = x\frac{N_f-k}{2\pi}\left(\sigma_F - m_\psi\right). \tag{3.126}$$

Fortunately, we know how to dualize the RHS from the maps in [86]. We obtain

$$\bar{\psi}\psi = 2x\frac{N_f-k}{4\pi}\left(\sigma_F - m_\psi\right) \leftrightarrow -2x\left(\phi^\dagger\phi + \frac{N-k}{4\pi}m_\phi^2\right). \tag{3.127}$$

Now let's see how this is implemented for the WF scalar. We know we can rewrite the WF scalar using auxiliary fields, namely, we write the quadratic and quartic terms so that S_B then contains the terms

$$S_B \supset \int d^3x\left[\sigma_B\left(\phi^\dagger\phi + \frac{N-k}{4\pi}m_\phi^2\right) - \frac{N}{16\pi x}\sigma_B^2\right]. \tag{3.128}$$

Again, σ_B is an auxiliary field and its corresponding equation of motion is

$$\phi^\dagger\phi + \frac{N-k}{4\pi}m_\phi^2 = \frac{N}{16\pi x}\sigma_B. \tag{3.129}$$

Notably, the LHS of this expression matches the term on the RHS of (3.127), so we can establish the duality

$$\bar{\psi}\psi \leftrightarrow -\frac{N}{8\pi}\sigma_B. \tag{3.130}$$

Note all factors of x have dropped from this expression.

Hence, under the bosonization of the fermion end of this interaction, a naive generalization of (3.130) for (3.119) would be

$$C_2^{(C)}\left(\bar{\psi}_{2,3}^{a_2a_3}X_{a_2a_1}^{1,2}\right)\left(X_{1,2}^{\dagger b_2a_1}\psi_{b_2a_3}^{2,3}\right) \quad \leftrightarrow \quad -C_2^{(D)}\left(X_{1,2}^{\dagger b_2a_1}X_{a_2a_1}^{1,2}\right)\frac{N}{8\pi}\left(\sigma_{2,3}\right)_{b_2}^{a_2} \tag{3.131}$$

where we have introduced the $K_2 \times K_2$ auxiliary fields $\sigma_{2,3}$. Importantly, there is an inherent asymmetry here because $\sigma_{2,3}$ belongs to the $X_{2,3}$ link. Grouping this together with the other terms linear in $\sigma_{2,3}$ and taking the $x \to \infty$ limit, the bosonic action of the link to the right of the node is a generalization of (3.128) is

$$S_B \supset \int d^3x\ \left(\sigma_{2,3}\right)_{b_2}^{a_2}\left(X_{2,3}^{\dagger b_2a_3}X_{a_2a_3}^{2,3} + \frac{N-k}{4\pi}m_{2,3}^2\delta_{a_2}^{b_2} - C_2^{(D)}\frac{N}{8\pi}X_{1,2}^{\dagger b_2a_1}X_{a_2a_1}^{1,2}\right) \tag{3.132}$$

where we have assumed that we have used the $U(K_2)$ symmetry such that $\left(m^2\right)_{a_2}^{b_2}$ is always diagonal.

Before proceeding, let us briefly comment on the need to introduce $(K_2)^2$ σ fields. Had we introduced only K_2 sigma fields, all self-interactions would have been of the form

$$\sum_{a_2}\left(X_{2,3}^{\dagger a_2a_3}X_{a_2a_3}^{2,3}\right)^2. \tag{3.133}$$

In contrast, (3.132) implies self-interaction terms of the form $\left(X_{2,3}^{\dagger b_2a_3}X_{a_2a_3}^{2,3}\right)^2$ with *no sum* over a_2 and b_2. These can be combined into a perfect square, $\left(\sum_{a_2}X_{2,3}^{\dagger a_2a_3}X_{a_2a_3}^{2,3}\right)^2$. This potential is needed to realize the full "flavor" symmetry, i.e. $SU(N_s)$. Meanwhile, (3.133) only preserves the diagonal $U(1)^{N_s}$ subgroup. For example, in the $N_s = 2$ the two distinct choices for the interaction term are

$$|\phi_1|^4 + |\phi_2|^4 \qquad \text{or} \qquad \left(|\phi_1|^2 + |\phi_2|^2\right)^2. \tag{3.134}$$

The former is invariant under a $U(1)^2$ symmetry while the latter is invariant under $SU(2)$. While it doesn't appear that anyone has been careful enough to distinguish the two possibilities in the context of Non-Abelian 3d bosonization dualities[24], it appears that for symmetry matching of the global flavor symmetries we do need (3.132) with its $(K_2)^2$ auxiliary σ fields.

To analyze the effect of the interaction terms in (3.132) , let us recall how the original WF term without the additional interactions, $\mathcal{L}_B \supset \sigma_B \left(\phi^\dagger \phi + \frac{N-k}{4\pi} m_\phi^2\right)$. We know that we should expect

$$m_\phi^2 > 0 : \qquad \left\langle \phi^\dagger \phi \right\rangle = 0 \tag{3.135a}$$

$$m_\phi^2 < 0 : \qquad \left\langle \phi^\dagger \phi \right\rangle \sim m_\phi^2. \tag{3.135b}$$

We can use this to make conclusions about (3.132). Note that we are assuming the U groups on the nodes are of unequal rank and thus $\left\langle X_{1,2}^{\dagger a_1 a_2} X_{a_1 b_2}^{1,2} \right\rangle = (v_{1,2}^2)_{b_2}^{a_2} \neq v^2 \delta_{b_2}^{a_2}$ as in (3.36) for some constant v. We'll also assume maximal Higgsing so that the a negative deformation of $m_{2,3}^2$ produces a vacuum expectation value of $\left\langle X_{2,3}^{\dagger a_2 a_3} X_{b_2 a_3}^{2,3} \right\rangle = (v_{2,3}^2)_{b_2}^{a_2} \sim \delta_{b_2}^{a_2}$. We then find

$$m_{2,3}^2 > 0, \qquad \left\langle X_{1,2}^{\dagger a_1 a_2} X_{a_1 b_2}^{1,2} \right\rangle > 0 : \qquad \left\langle X_{2,3}^{\dagger a_2 a_3} X_{b_2 a_3}^{2,3} \right\rangle \sim C_2^{(D)} \left(v_{1,2}\right)_{b_2}^{a_2} \tag{3.136a}$$

$$m_{2,3}^2 > 0, \qquad \left\langle X_{1,2}^{\dagger a_1 a_2} X_{a_1 b_2}^{1,2} \right\rangle = 0 : \qquad \left\langle X_{2,3}^{\dagger a_2 a_3} X_{b_2 a_3}^{2,3} \right\rangle = 0 \tag{3.136b}$$

$$m_{2,3}^2 < 0, \qquad \left\langle X_{1,2}^{\dagger a_1 a_2} X_{a_1 b_2}^{1,2} \right\rangle > 0 : \qquad \left\langle X_{2,3}^{\dagger a_2 a_3} X_{b_2 a_3}^{2,3} \right\rangle \sim \left(C_2^{(D)} v_{1,2} + v_{2,3}\right)_{b_2}^{a_2}. \tag{3.136c}$$

$$m_{2,3}^2 < 0, \qquad \left\langle X_{1,2}^{\dagger a_1 a_2} X_{a_1 b_2}^{1,2} \right\rangle = 0 : \qquad \left\langle X_{2,3}^{\dagger a_2 a_3} X_{b_2 a_3}^{2,3} \right\rangle \sim \left(v_{2,3}\right)_{b_2}^{a_2}. \tag{3.136d}$$

This is precisely the behavior that we would expect for a term dual to (3.119). That is, we see that a nonzero vacuum expectation value of the $X_{1,2}$ fields can cause certain components of $X_{2,3}$ to also get a vacuum expectation value. Importantly, if $X_{2,3}$ has a vacuum expectation value but $X_{1,2}$ does not, the interaction term does not work in reverse. To see this, note that the equation of motion for $(\sigma_2)_{b_2}^{a_2}$ would require

$$(v_{2,3}^2)_{b_2}^{a_2} + (N-k)\frac{m_{2,3}^2}{4\pi} = C_2^{(D)} \frac{N}{8\pi} X_{1,2}^{\dagger b_2 a_1} X_{a_2 a_1}^{1,2}. \tag{3.137}$$

[24] In the Abelian case, dualities which differ only by the structure of the quartic interactions have been discussed in [111].

Similar equations of motion hold for the $X_{3,4}$ link, but importantly the $X_{1,2}$ link contains no such interaction term. To determine the vacuum expectation values, one then just needs to consistently solve the three equations of motion. To do so, it is helpful to start with the one corresponding to the $X_{1,2}$ link. Since there is no interaction term for the $X_{1,2}$ link, $X_{2,3}$ has no influence on $v_{1,2}$ and its value follows in a manner completely analogous to (3.135). When $X_{1,2}$ acquires a vacuum expectation value, it then affects the $X_{2,3}$ equation of motion via (3.137). Hence we get our desired unidirectional influence. This behavior was always difficult to achieve using the naive interaction generalization in (3.120) because both the $X_{2,3}$ and $X_{1,2}$ fields appeared in the term symmetrically. Thus the effect of one field acquiring a nonzero vacuum expectation value was always the same as the other field, up to flavor structure.

More generally, for interactions on the U side we have

$$C_I \left(\bar{\psi}^{a_I a_{I+1}}_{I,I+1} X^{I-1,I}_{a_I a_{I-1}}\right)\left(X^{\dagger b_I a_{I-1}}_{I-1,I}\psi^{I,I+1}_{b_I a_{I+1}}\right) \quad \leftrightarrow \quad -C_I \left(X^{\dagger b_I a_{I-1}}_{I-1,I} X^{I-1,I}_{a_I a_{I-1}}\right)\frac{K_{I-1}}{8\pi}\left(\sigma_{I,I+1}\right)^{a_I}_{b_I} \tag{3.138}$$

while for interactions on the SU side, which are unidirectional to the left,

$$C_I \left(\bar{\psi}^{a_{I-1} a_I}_{I-1,I} Y^{I,I+1}_{a_I a_{I+1}}\right)\left(Y^{\dagger b_{I+1} a_I}_{I,I+1}\psi^{I-1,I}_{b_{I+1} a_I}\right) \quad \leftrightarrow \quad -C_I \left(Y^{\dagger b_{I+1} a_I}_{I,I+1} Y^{I,I+1}_{a_{I+1} a_I}\right)\frac{N_I}{8\pi}\left(\sigma_{I-1,I}\right)^{a_I}_{b_I} \tag{3.139}$$

where the $\sigma_{I,I+1}$ are auxiliary fields belonging to the $(I, I+1)$-th bifundamental and I runs over all internal nodes (e.g. $I = 2, 3$ for the four node case).

3.8 Supplementary: Background Terms and Flavor Violation

In this appendix we work out the Lagrangians of the flavor extended master duality coupled to background fields, which provide important consistency checks for the phase diagram of the extended master duality proposed in section 3.4.1. We mostly analyze the case of $N > N_s$ (Fig. **??**) and briefly comment for the case of $N = N_s$ (Fig. 3.7). Finally we discuss gauging of flavor symmetry and description of flavor-violated quivers which are used extensively in the section 3.4.

3.8.1 SU side

First, we discuss the SU side of the duality. The Lagrangian corresponding to the SU side of flavor-violated master duality (3.75) is given by

$$\begin{aligned}\mathcal{L}_{SU} = &\left|D_{b'+B+\tilde{A}_1+\tilde{A}_2}\phi\right|^2 + i\bar{\psi}\not{D}_{b'+C+\tilde{A}_1}\psi + \mathcal{L}_{\text{int}} - i\left[\frac{N_f-k}{4\pi}\text{Tr}_N\left(b'db' - i\frac{2}{3}b'^3\right)\right] \\ &- i\left[\frac{N}{4\pi}\text{Tr}_{N_f}\left(CdC - i\frac{2}{3}C^3\right) + \frac{N(N_f-k)}{4\pi}\tilde{A}_1 d\tilde{A}_1 + 2NN_f\text{CS}_{\text{grav}}\right]\end{aligned} \tag{3.140}$$

which we denote using

$$SU\left(N\right)_{-k+N_f/2} \times \left[SU\left(N_f\right)_{N/2} \times SU\left(N_s\right)_0 \times U\left(1\right)_{N(N_f-k)/2} \times U\left(1\right)_0\right] + N_f\psi + N_s\phi \tag{3.141}$$

where again the terms in the $[\cdots]$ are global symmetries. In the mass deformed regime where $|m_\psi| \gg m_*$, phases are straightforwardly obtained from SU side as follows:[25]

$$\text{(I)}: \qquad SU(N)_{-k+N_f} \times \left[SU\left(N_f\right)_N \times SU\left(N_s\right)_0 \times J_I\right] \tag{3.142a}$$

$$\text{(II)}: \qquad SU(N-N_s)_{-k+N_f} \times \left[SU\left(N_f\right)_N \times SU\left(N_s\right)_{-k+N_f} \times J_{II}\right] \tag{3.142b}$$

$$\text{(III)}: \qquad SU(N-N_s)_{-k} \times \left[SU\left(N_f\right)_0 \times SU\left(N_s\right)_{-k} \times J_{III}\right] \tag{3.142c}$$

$$\text{(IV)}: \qquad SU(N)_{-k} \times \left[SU\left(N_f\right)_0 \times SU\left(N_s\right)_0 \times J_{IV}\right]. \tag{3.142d}$$

where

$$J_i \equiv J_i^{ab}\frac{1}{4\pi}\tilde{A}_a d\tilde{A}_b \tag{3.143}$$

---

[25] We are suppressing gravitational Chern-Simons terms for brevity. They are straightforward to restore using level-rank duality.

is the Chern-Simons term for the Abelian background gauge fields in the ith phase in for $a, b = 1, 2$. For the asymptotic mass phases, the J_i^{ab} are

$$J_{\mathrm{I}}^{ab} = \begin{pmatrix} N(N_f - k) & 0 \\ 0 & 0 \end{pmatrix} \tag{3.144a}$$

$$J_{\mathrm{II}}^{ab} = \frac{N(N_f - k)}{N - N_s} \begin{pmatrix} N & N_s \\ N_s & N_s \end{pmatrix} \tag{3.144b}$$

$$J_{\mathrm{III}}^{ab} = \frac{-Nk}{N - N_s} \begin{pmatrix} N & N_s \\ N_s & N_s \end{pmatrix} \tag{3.144c}$$

$$J_{\mathrm{IV}}^{ab} = \begin{pmatrix} -Nk & 0 \\ 0 & 0 \end{pmatrix}. \tag{3.144d}$$

It is instructive to calculate, say, $\tilde{J}_{\mathrm{III}}^{ab}$. First we only turn on U(1) background fields $\tilde{A}_1$ and $\tilde{A}_2$. Then we express $b' \in SU(N)$ as $U(N) \times U(1)$ with $b \in U(N)$ and $e \in U(1)$. We then couple e to a new background field which we denote $N(\tilde{A}_1 + \tilde{A}_2)$ and add an appropriate counter term. After giving the fermions a large negative mass and integrating them out the Lagrangian becomes:

$$\begin{aligned} \mathcal{L}_{\text{IV-III}} =& (D_{b+B}\phi)^2 + \frac{1}{2\pi}\left(Tr_N(b) - N(\tilde{A}_1 + \tilde{A}_2)\right) de - \frac{Nk}{4\pi}\tilde{A}_1 d\tilde{A}_1 \\ & - \frac{k}{4\pi N} Tr_N(b) dTr_N(b) + \frac{Nk}{4\pi}(\tilde{A}_1 + \tilde{A}_2) d(\tilde{A}_1 + \tilde{A}_2) \end{aligned} \tag{3.145}$$

We then give the scalars a negative mass deformation. This only effects the $Tr_N(b)$ term. We get

$$\begin{aligned} \mathcal{L} =& \frac{1}{2\pi}\left(Tr_{N-N_s}(b) - N(\tilde{A}_1 + \tilde{A}_2)\right) de - \frac{k}{4\pi(N - N_s)} Tr_{N-N_s}(b) dTr_{N-N_s}(b) \\ & - \frac{Nk}{4\pi}\tilde{A}_1 d\tilde{A}_1 + \frac{Nk}{4\pi}(\tilde{A}_1 + \tilde{A}_2) d(\tilde{A}_1 + \tilde{A}_2) \end{aligned} \tag{3.146}$$

Integrating out e, we indeed find

$$J_{\mathrm{III}}^{ab} = \frac{-Nk}{N - N_s} \begin{pmatrix} N & N_s \\ N_s & N_s \end{pmatrix} \tag{3.147}$$

For the region of small fermion mass $|m_\psi| < m_*$, corresponding to phases V to VIII, we are in the quantum regime and flavor symmetry is expected to be spontaneously broken by the non-perturbative fermion condensate,

$$U(N_f) \to U(N_f - k) \times U(k). \tag{3.148}$$

We now move on to the U side of master duality, which describes quantum regime of SU side as well as the semiclassical regimes.

3.8.2 U side

The Lagrangians for the U side of the flavor-violated master duality can be fixed by demanding that they yield the same TFTs and background Chern-Simons terms as the SU case for phases I to IV. As mentioned in the main text, this is achieved via two different scalar theories, one of which is identical to the flavor-bounded case. Explicitly, the Lagrangians corresponding to (3.75) are given by

$$\begin{aligned}
\mathcal{L}_U^{m_\psi<0} &= |D_{c+C}\Phi_1|^2 + i\bar{\Psi}_1 \not{D}_{c+B+\tilde{A}_2}\Psi_1 + \mathcal{L}'^{(1)}_{\text{int}} \\
&\quad - i\left[\frac{N}{4\pi}\text{Tr}_k\left(cdc - i\frac{2}{3}c^3\right) - \frac{N}{2\pi}\text{Tr}_k(c)d\tilde{A}_1 + 2Nk\text{CS}_{\text{grav}}\right] \qquad (3.149a) \\
\mathcal{L}_U^{m_\psi>0} &= |D_{c+C}\Phi_2|^2 + i\bar{\Psi}_2 \not{D}_{c+B-\tilde{A}_2}\Psi_2 + \mathcal{L}'^{(2)}_{\text{int}} \\
&\quad - i\left[\frac{-N+N_s}{4\pi}\text{Tr}_{N_F-k}\left(cdc - i\frac{2}{3}c^3\right) + 2\left(Nk - N_s(N_f-k)\right)\text{CS}_{\text{grav}}\right] \\
&\quad - i\left[\frac{N}{4\pi}\text{Tr}_{N_f}\left(CdC - i\frac{2}{3}C^3\right) + \frac{N_f-k}{4\pi}\text{Tr}_{N_s}\left(BdB - i\frac{2}{3}B^3\right)\right] \\
&\quad - i\left[-\frac{N}{2\pi}\text{Tr}_{N_f-k}(c)\,d\tilde{A}_1 - \frac{N_s}{2\pi}\text{Tr}_{N_f-k}(c)d\tilde{A}_2 + \frac{N_s(N_f-k)}{4\pi}\tilde{A}_2 d\tilde{A}_2\right]. \qquad (3.149b)
\end{aligned}$$

In general, dynamical gauge groups for these two theories are distinct, so the number of degrees of freedom in the matter fields is different. The reason the $m_\psi > 0$ Lagrangian looks significantly more complicated is largely a result of our convention for η-invariant terms (see

footnote 2). Schematically, these theories can be denoted by

$$m_\psi < 0: \quad U(k)_{N-N_s/2} \times \left[SU(N_f)_0 \times SU(N_s)_{-k/2} \times U(1)_{NN_f/2} \times U(1)_{-NN_s/2}\right] + N_s\Psi_1 + N_f\Phi_1 \tag{3.150a}$$

$$m_\psi > 0: \quad U(N_f-k)_{-N+N_s/2} \times \left[SU(N_f)_N \times SU(N_s)_{(-k+N_f)/2} \times U(1)_0 \times U(1)_{NN_s/2}\right] + N_s\Psi_2 + N_f\Phi_2. \tag{3.150b}$$

$$\text{(I)}: \quad m_{\Psi_2} < 0, \quad m^2_{\Phi_2} > 0 \quad \Rightarrow \quad U(N_f-k)_{-N} \times \left[SU(N_f)_N \times SU(N_s)_0 \times \tilde{J}_I\right] \tag{3.151}$$

$$\text{(II)}: \quad m_{\Psi_2} > 0, \quad m^2_{\Phi_2} > 0 \quad \Rightarrow \quad U(N_f-k)_{-N+N_s} \times \left[SU(N_f)_N \times SU(N_s)_{-k+N_f} \times \tilde{J}_{II}\right] \tag{3.152}$$

$$\text{(III)}: \quad m_{\Psi_1} < 0, \quad m^2_{\Phi_1} > 0 \quad \Rightarrow \quad U(k)_{N-N_s} \times \left[SU(N_f)_0 \times SU(N_s)_{-k} \times \tilde{J}_{III}\right] \tag{3.153}$$

$$\text{(IV)}: \quad m_{\Psi_1} > 0, \quad m^2_{\Phi_1} > 0 \quad \Rightarrow \quad U(k)_N \times \left[SU(N_f)_0 \times SU(N_s)_0 \times \tilde{J}_{IV}\right]. \tag{3.154}$$

Reassuringly, the procedure laid out in [64] gives background terms for the asymptotic region which match those from the SU side. The next complication comes in determining the $U(1)$ levels in the quantum phase. On the U side, the monopole current couples to $\tilde{A}_1$ which couples to the Kahler-form w

$$\mathcal{L}_U \supset \frac{N}{2\pi} w d\tilde{A}_1. \tag{3.155}$$

We can then integrate out w in a procedure analogous to the semiclassical regions discussed above.

As mentioned in the main text, moving into the quantum regions we find an additional $U(1)$ background symmetry which was a subgroup of the original $SU(N_f)$ global symmetry. Being careful with said breaking pattern results in the TFTs described in (3.81). For the

mass deformations describes middle region we find

$$(\text{V\&VI}): \qquad m_{\Psi_2}<0, \quad m^2_{\Phi_2}<0 \quad \Rightarrow \quad \mathcal{M}(N_f,k)\times\Big[SU(k)_N\times SU(N_f-k)_0\times SU(N_s)_0\times\tilde{J}_{V,VI}\Big] \tag{3.156}$$

$$(\text{VII}): \qquad m_{\Psi_2}>0, \quad m^2_{\Phi_2}<0 \quad \Rightarrow \quad \mathcal{M}(N_f,k)\times\Big[SU(k)_N\times SU(N_f-k)_{N_s}\times SU(N_s)_{-k+N_f}\times\tilde{J}_{VI} \tag{3.157}$$

$$(\text{VIII}): \qquad m_{\Psi_1}<0, \quad m^2_{\Phi_1}<0 \quad \Rightarrow \quad \mathcal{M}(N_f,k)\times\Big[SU(N_f-k)_0\times SU(k)_{N-N_s}\times SU(N_s)_{-k}\times\tilde{J}_{VIII} \tag{3.158}$$

$$(\text{V\&VI}): \qquad m_{\Psi_1}>0, \quad m^2_{\Phi_1}<0 \quad \Rightarrow \quad \mathcal{M}(N_f,k)\times\Big[SU(N_f-k)_0\times SU(k)_N\times SU(N_s)_0\times\tilde{J}_{V,VI}\Big]. \tag{3.159}$$

with U(1) background terms as

Here again, it is instructive to calculate the background term $\tilde{J}^{ab}_{\text{VII}}$ and $\tilde{J}^{ab}_{\text{VI}}$. Starting from (3.149b), we shift $\tilde{a}\to\tilde{a}-\tilde{A}_1$ and integrate out the fermion and scalar similar to the calculation of $\tilde{J}^{ab}_{\text{III}}$ case above which give:

$$\tilde{J}_{\text{VII}}=\frac{1}{4\pi}(NN_f+(N_f-k)(-N+N_s))\tilde{A}_1d\tilde{A}_1+\frac{1}{4\pi}(N_f-k)N_s\tilde{B}d\tilde{B}-\frac{1}{2\pi}N_s(N_f-k)\tilde{A}_1d\tilde{B} \tag{3.160}$$

Transition from VII to VI involves the $(N_f-k)N$ singlet fermions being negative mass from positive mass. Since these fermions are charged under $\tilde{A}_1+\tilde{B}$, after integrating out the fermion we get the U(1) background term in phase III:

$$\tilde{J}_{\text{VI}}=\frac{1}{4\pi}Nk\tilde{A}_1d\tilde{A}_1 \tag{3.161}$$

]

Notably, exactly parallel analysis of $\tilde{J}_{\text{VIII}}$ and VIII-VI critical line predict the same $\tilde{J}_{\text{VI}}$. Together with the observation $\tilde{J}_{\text{V}}=\tilde{J}_{\text{VI}}$ and the matching of dynamical gauge group and nonabelian background terms support the phase structure of middle region in figure **??**.

3.8.3 $N = N_s$

We remark that all the above analysis of $N > N_s$ case is directly extended to $N = N_s$ with two important differences.

First, in the phases II and III there is a spontaneous breaking of the diagonal $\tilde{A}_1 + \tilde{A}_2$ background field. This is straightforward to see on the SU side where the dynamical gauge symmetry is completely Higgs when $N = N_s$. To see this on the U side, one can move to a dual photon description to make the shift symmetry explicit. The breaking signals the naive divergence of background terms proportional to $\frac{N}{4\pi}(\tilde{A}_1 + \tilde{A}_2)\tilde{d(\tilde{A}_1 + \tilde{A}_2)}$ in (3.144) for $N = N_s$.

Second, as it's clear from the figure 3.7, phases VII and VIII have finite regions in contrast to the $N > N_s$ case. Thus we have extra critical line II-III with $U(1)_0 + NN_f\ \tilde{\psi}_s$, and it is reassuringly consistent with all the background terms calculated in phases II and III.

3.8.4 Quiver description

Since the flavor-violated SU theory is master dual to two different U theories which describe certain patches of the SU phase diagram respectively, it will become useful to adopt a notation similar to (3.90) to denote the appropriate theory located in the common region $m_\psi = 0$ and $m_\phi^2 = 0$ of phase space, corresponding to a Grassmannian manifold. One can choose either of the U theories to describe phases V and VI, which contain the SU theory. Since the two scalar theories are uniquely related to one another, later we will adopt a method for converting from one scalar theory to the other. As such, one should still be able to start with the U theory and determine all mass deformations. Choosing the $m_\psi < 0$ theory, we have a duality between the two theories

$$SU\left(N\right)_{-k+N_f/2} \times \left[SU\left(N_f\right)_{N_f/2} \times SU\left(N_s\right)_0\right] \qquad \leftrightarrow$$
$$U\left(k\right)_{N-N_s/2} \times \left[SU\left(N_f\right)_0 \times SU\left(N_s\right)_{-k/2}\right]. \quad (3.162)$$

As with the flavorless case, it will be useful to have a version of this theory where the

SU side has its fermion flavor symmetry and a $U(1)$ global symmetry combined into a single $U(N_f)$ symmetry. This is achieved by grouping the C and $\tilde{A}_1$ fields together(we do not include the additional $\tilde{B}$ symmetry to make contact with 3.90 in addition to include $N = N_s$). The above duality becomes

$$SU(N)_{-k+N_f/2} \times \left[U(N_f)_{N/2} \times SU(N_s)_0\right] \quad \leftrightarrow \\ U(k)_{N-N_s/2} \times \left[U(N_f)_0 \times SU(N_s)_{-k/2}\right]. \quad (3.163)$$

Immediately note that this duality is identical to that of (3.92).

Alternatively, if we had chosen the $m_\psi > 0$ theory on the U side, we would have arrive at something a little different, namely,

$$SU(N)_{-k+N_f/2} \times \left[U(N_f)_{N/2} \times SU(N_s)_0\right] \quad \leftrightarrow \\ U(N_f-k)_{-N+N_s/2} \times \left[U(N_f)_N \times SU(N_s)_{(-k+N_f)/2}\right]. \quad (3.164)$$

3.9 Supplementary: Quivers and Spin$_c$

In [13] it was discussed how the master duality is consistent with being put on a spin$_c$ manifold. Unfortunately, we weren't particularly careful with ordinary and spin$_c$ connections in [9], so we should clarify the consistency here.

In [9] a modified version of the master duality is used and various shifts were performed. Specifically, a shift on the Abelian portion of c was performed, $\tilde{c} \to \tilde{c} + \tilde{A}_1$ and the common $\tilde{A}_1$ Chern-Simons term was canceled. Being more careful with connections, this is equivalent to redefining a new spin$_c$ gauge field which we will call $\tilde{a} = \tilde{c} - \tilde{A}_1$ and ordinary gauge field $\tilde{B} = \tilde{A}_1 + \tilde{A}_2$, so that the U side is now

$$\mathcal{L}_U = \left|D_{c'+\tilde{a}+\tilde{A}_1+C}\Phi\right|^2 + i\bar{\Psi}\not{D}_{c'+\tilde{a}+B+\tilde{B}}\Psi + \mathcal{L}'_{\text{int}} \\ - i\left[\frac{N}{4\pi}\text{Tr}_k\left(c'dc' - i\frac{2}{3}c'^3\right) + \frac{Nk}{4\pi}\tilde{a}d\tilde{a} + 2Nk\text{CS}_{\text{grav}}\right]. \quad (3.165)$$

We also shifted the $\tilde{A}_2$ fields into the ψ and Φ matter by taking $\tilde{A}_1 \to \tilde{A}_1 - \tilde{A}_2$. Instead, define a new ordinary connection $\tilde{G} = \tilde{A}_1 + \tilde{A}_2$(corresponds to the $\tilde{B}$ in the U side above)

so the SU side of the duality now reads

$$\mathcal{L}_{SU} = \left|D_{b'+B+\tilde{G}}\phi\right|^2 + i\bar{\psi}\not{D}_{b'+C+\tilde{A}_1}\psi + \mathcal{L}_{\text{int}} - i\left[\frac{N_f-k}{4\pi}\text{Tr}_N\left(b'db' - i\frac{2}{3}b'^3\right)\right]$$
$$- i\left[\frac{N}{4\pi}\text{Tr}_{N_f}\left(CdC - i\frac{2}{3}C^3\right) + NN_f\left(\frac{1}{4\pi}\tilde{A}_1 d\tilde{A}_1\right) + 2NN_f\text{CS}_{\text{grav}}\right]. \tag{3.166}$$

This is the same as we have in our paper with the replacements, $\tilde{G} \to \tilde{A}_1$, $\tilde{A}_1 \to \tilde{A}_1 - \tilde{A}_2$, $c' + \tilde{a} \to c$, $\tilde{B} \to \tilde{A}_1$. We also promote the field $\tilde{A}_2$ which introduces a new background symmetry which we call $\tilde{B}_2$. In our new notation this is equivalent to gauging $\tilde{A}_1 \to \tilde{a}_1$, and we will called the new ordinary connection to which it couples $\tilde{B}_1$.

The part we need to be most careful is in the match of the two theories as we move across the quiver construction. This is spelled out in the most detail in Appendix A.3 of [9] become. There we make certain identifications based on fermion interactions which are now equivalent to

$$i\bar{\Psi}\not{D}_{c'+\tilde{a}+B+\tilde{B}}\Psi \qquad \leftrightarrow \qquad i\bar{\psi}\not{D}_{b'+C+\tilde{A}_1}\psi. \tag{3.167}$$

The field level identification which are in Table 3 of [9] become

$$c' + \tilde{a} \qquad \leftrightarrow \qquad C + \tilde{a}_1 \tag{3.168a}$$
$$B \qquad \leftrightarrow \qquad b' \tag{3.168b}$$
$$\tilde{B} \qquad \leftrightarrow \qquad \tilde{B}_1. \tag{3.168c}$$

Since we are matching ordinary connections to ordinary connections and spin$_c$ connections to spin$_c$ connections, everything is consistent and it does appear these quivers are consistent with being put on spin$_c$ manifolds.

Chapter 4

BREAKING THE FLAVOR SYMMETRY

Disclaimer: *This work was conceived and carried out solely by the author*

One aspect of the derivation presented in the previous chapter that has yet to be discussed is the matching of phases at each step of the duality. Indeed, this is a difficult task since an $n+1$ node quiver, there 2^n phases. This is complicated by the fact that in building the quiver one must explicitly break the flavor symmetry by gauging a subgroup of the full flavor group. For example, consider a simple three node quiver with $SU(N)_k$ gauge groups on the nodes, bifundamental scalars on the links and extra fundamental fermions. Upon dualizing the first node, one has two distinct sets of fermions: one group of bifundamentals and one group of fundamentals. Thus, to accurately match the phases at each step of the derivation, one must first map out the phase diagram of an $SU(N)_k$ gauge theory coupled to fermions with a product gauge group of the form $U(f) \times U(N_f - f)$.

In this chapter we will construct the phase diagram of such a gauge theory as a function of two unequal masses. Specifically, we explicitly break the flavor group $U(N_f)$ to $U(f) \times U(N_f - f)$ and then match the resulting theories onto (**??**) or (4.19). We find a rich structure of Grassmannians which disappear and reemerge as we tune F and f relative to k. Our results reduce to that of [80] in the limit where both quark masses are equal. Our phase diagram as a function of f and F is given in Fig. 4.9. In section 4.1 we lay out the phases diagrams as a function of mass for each relevant case. In section 4.2 we describe how to obtain the rich network of Grassmannians from the scalar theories and the necessary potentials needed to obtain this structure. We conclude in section **??**.

As this work was being finalized we learned of [16] which has overlap with this work. Luckily our results are in agreement.

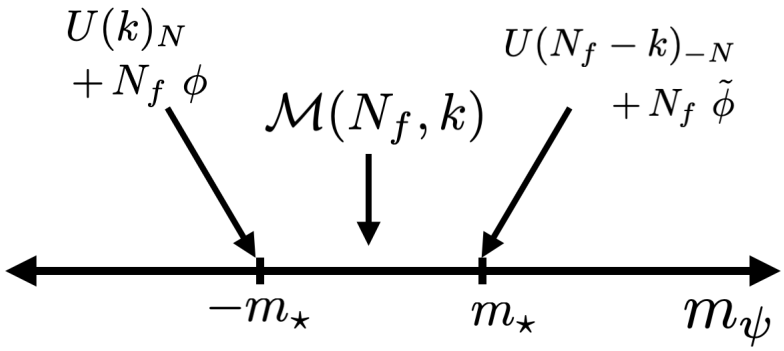

Figure 4.1: Symmetry breaking of QCD_3 according to [80]

4.1 Constructing the Phase Diagram

We start with a flavor group of $U(F) \times U(f)$ with $F + f = N_f$. Without loss of generality, we take $f \leq F$. We denote F fermions by Ψ with mass M and the f fermions by ψ with mass m. We always work with "bare" Chern-Simons level k, explicitly displaying the $\frac{N_f}{2}$ contribution from the η invariant, rather than defining $k_{eff} = k_{bare} - \frac{N_f}{2}$. Moreover, k will always be positive and a negative Chern-Simons level will always come with an explicit minus sign.

4.1.1 Flavor Bounded Case

We start by considering the $f + F \leq k$ case for completeness. We obtain a phase diagram as in Fig. 4.2. Any value of the mass deformation leads to a theory which satisfies the flavor bound. As a result, we have four distinct topological field theories seperated by critial lines hosting light fermions. These lines admit bosonized duals in accordance with [2]. The completely gapped phases give the following TFTs:

$$\text{I)}: \quad SU(N)_{-k+f+F} \;\leftrightarrow\; U(k-f-F)_N \tag{4.1a}$$

$$\text{II)}: \quad SU(N)_{-k+f} \;\leftrightarrow\; U(k-f)_N \tag{4.1b}$$

$$\text{III)}: \quad SU(N)_{-k} \;\leftrightarrow\; U(k)_N \tag{4.1c}$$

$$\text{IV)}: \quad SU(N)_{-k+F} \;\leftrightarrow\; U(k-F)_N \tag{4.1d}$$

while the critical lines host

$$\text{I-II)}: \quad SU(N)_{-k+f+\frac{F}{2}} \text{ with } F\ \Psi \leftrightarrow U(k-f)_N \text{ with } F\ \Phi \tag{4.2a}$$

$$\text{II-III)}: \quad SU(N)_{-k+\frac{f}{2}} \text{ with } f\ \psi \leftrightarrow\ U(k)_N \text{ with } f\ \phi \tag{4.2b}$$

$$\text{III-IV)}: \quad SU(N)_{-k+\frac{F}{2}} \text{ with } F\ \Psi \leftrightarrow U(k)_N \text{ with } F\ \Phi \tag{4.2c}$$

$$\text{IV-I)}: \quad SU(N)_{-k+F+\frac{f}{2}} \text{ with } f\ \psi \leftrightarrow U(k-F)_N \text{ with } f\ \phi. \tag{4.2d}$$

This scenario is relatively straightforward since there are no quantum phases. More structure emerges as we allow violation of the flavor bound. There is also the added complication of a possible $U(f) \times U(F)$ potential on the scalar side. This will not drastically effect the structure of this phase diagram. See Sec. 4.2 for more details.

4.1.2 Flavor Violated Case

We now turn to the case where $k < N_f < N_\star$. Right away we note that if $m = M$ our flavor group is enchanced from $U(f) \times U(F) \to U(f+F)$ and we are back to the case considered in [80]. This will serve as an important benchmark for the complete phase diagram.

For the case of two flavor groups we obtain six separate phase diagrams depending on the relative sizes of f, F and k. These are

i.) $f < k,\ F < k$

ii.) $f < k,\ F > k$

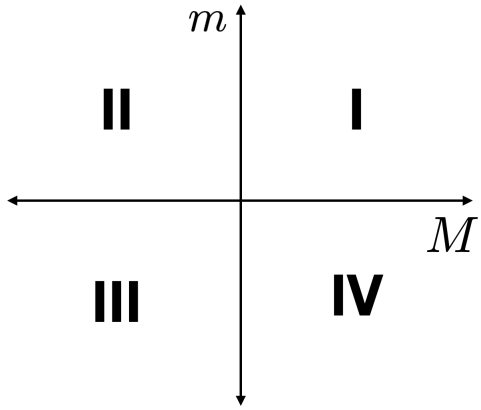

Figure 4.2: Phases when $f + F < k$

iii.) $f > k$, $F > k$

iv.) $f < k$, $F = k$

v.) $f = k$, $F > k$

vi.) $f = k$,$F = k$.

The procedure for mapping out these phase diagrams is identical in all six phases. We start by gapping out all of the matter to determine the asymptotic TFTs. Next, we keep one flavor light and give the other a positive or negative mass deformation. This reduces the problem to a single flavor group with a shifted Chern-Simons level. The resulting asymptotic theory will either satisfy the flavor bound with the new CS level and admit a single scalar dual or violate it and have a quantum phase with two scalar duals. We will assume that $0 < k < f + F < N_\star$.

Before we proceed we would like to highlight one subtlety in the procedure above. When examining the flavor bounds we must take the effective CS level to have opposite sign as the shift coming from the η invariant. This is the convention used throughout the literature and

is necessary for an accurate application of the dualities. As an example say we encounter a situation where the CS level is $k+\frac{f}{2}$. The dualities in [2, 80] say nothing about this situation as written. To apply the dualities correctly, we shift k such that we obtain $k+f-\frac{f}{2}$ and apply the flavor bounds with respect to $k_{eff}=k+f$. This simply corresponds to changing the sign of the η invariant in the path integral [122]. This may look disturbing, since it seems as if we are using different regularizations in separate parts of the phase diagram. However this is not the case. We are simply shifting the levels of the induced CS terms in such a way that it appears as if we are changing the sign of the η invariant, without actually explicitly performing the necessary time-reversal operation to do so. Stated another way–the partition function of an $SU(N)_k$ fermionic theory with a positive η-invariant is equivalent to an $SU(N)_{k+f}$ fermionic theory with a negative η-invariant[1]. Let us now turn to the phase diagrams for these six cases.

$f, F < k$

The phase diagram for this case is given in Fig. 4.3. Explicit mass labels correspond to positive values of the mass deformation. Both flavors of fermions condense. Naively this may not seem possible since both groups of flavors satisfy the flavor bounds. But when compared to the effective CS level induced by integrating out the other group, they become

[1]This is another reason why we choose to work with the bare CS level. This procedure is straightforward to implement in this case. It is obscured by working with the full quantum CS level.

flavor violating. The phases are

$$\text{I}): \quad SU(N)_{-k+f+F} \leftrightarrow U(F+f-k)_{-N} \tag{4.3a}$$

$$\text{II}): \quad SU(N)_{-k+f} \leftrightarrow U(k-f)_{N} \tag{4.3b}$$

$$\text{III}): \quad SU(N)_{-k} \leftrightarrow U(k)_{N} \tag{4.3c}$$

$$\text{IV}): \quad SU(N)_{-k+F} \leftrightarrow U(k-F)_{N} \tag{4.3d}$$

$$\text{V}): \quad \mathcal{M}(f+F,k) + N\,\Gamma \tag{4.3e}$$

$$\text{VI}): \quad \mathcal{M}(F,k-f) + N\,\Gamma \tag{4.3f}$$

$$\text{VII}): \quad \mathcal{M}(f,k-F) + N\,\Gamma \tag{4.3g}$$

while the critical lines (red) host the bosonic theories

$$\text{I-VI}): \quad U(F+f-k)_{-N} \text{ with } F\,\tilde{\Phi} \tag{4.4a}$$

$$\text{VI-II}): \quad U(k-f)_{N} \text{ with } F\,\Phi \tag{4.4b}$$

$$\text{II-III}): \quad U(k)_{N} \text{ with } f\,\phi \tag{4.4c}$$

$$\text{III-IV}): \quad U(k)_{N} \text{ with } F\,\Phi \tag{4.4d}$$

$$\text{IV-VII}): \quad U(k-F)_{N} \text{ with } f\,\phi \tag{4.4e}$$

$$\text{VII-I}): \quad U(F+f-k)_{-N} \text{ with } f\,\tilde{\phi}. \tag{4.4f}$$

The theories sitting at the stars in the third and first quadrant are $U(k)_N$ with $f\,\phi + F\,\Phi$ and $U(F+f-k)_{-N}$ with $f\,\tilde{\phi} + F\,\tilde{\Phi}$ respectivley. These are the scalar theories corresponding to the flavor enchanced case of [80] and will be present in all of the remaining diagrams. Also note that the II-III and III-IV critical lines are dual to massless fermionic theories, while the others are dual to a fermionic theory with a mass offset. As the number of flavors decreases this mass offset should decrease as well, leading to the curvature of the critical lines.

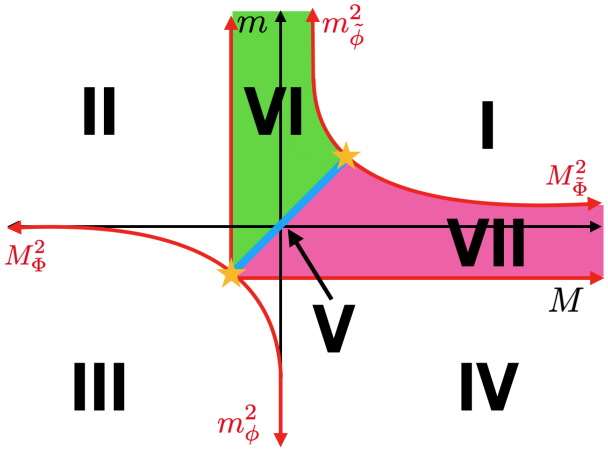

Figure 4.3: Phase diagram for flavor broken QCD_3 with $f, F < k$. The phases are described in Sec. 4.1.2. The stars denote the bosonic duals given in [80].

$f < k,\ F > k$

The phase diagram for this case is given in Fig. 4.4. Here it is always the F fermions which are condensing so long as we are away from the flavor enhanced line. The phases are

$$\text{I}): \quad SU(N)_{-k+f+F} \leftrightarrow U(F+f-k)_{-N} \tag{4.5a}$$

$$\text{II}): \quad SU(N)_{-k+f} \leftrightarrow U(k-f)_{N} \tag{4.5b}$$

$$\text{III}): \quad SU(N)_{-k} \leftrightarrow U(k)_{N} \tag{4.5c}$$

$$\text{IV}): \quad SU(N)_{-k+F} \leftrightarrow U(F-k)_{-N} \tag{4.5d}$$

$$\text{V}): \quad \mathcal{M}(f+F,k) + N\,\Gamma \tag{4.5e}$$

$$\text{VI}): \quad \mathcal{M}(F,k-f) + N\,\Gamma \tag{4.5f}$$

$$\text{VII}): \quad \mathcal{M}(F,k) + N\,\Gamma \tag{4.5g}$$

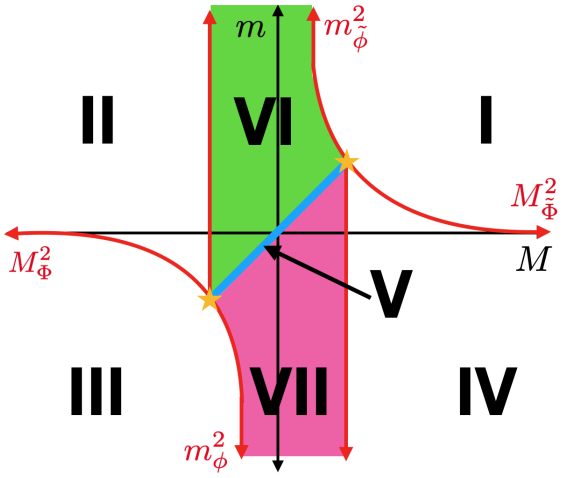

Figure 4.4: Phase diagram for flavor broken QCD$_3$ with $f < k$, $F > k$. These phases are laid out in Sec. 4.1.2.

while the critical lines which separate them are given by the by the following bosonic theories:

$$\text{I-VI}): \quad U(F+f-k)_{-N} \text{ with } F\,\tilde{\Phi} \tag{4.6a}$$

$$\text{VI-II}): \quad U(k-f)_{N} \text{ with } F\,\Phi \tag{4.6b}$$

$$\text{II-III}): \quad U(k)_{N} \text{ with } f\,\phi \tag{4.6c}$$

$$\text{III-VII}): \quad U(k)_{N} \text{ with } F\,\Phi \tag{4.6d}$$

$$\text{VII-IV}): \quad U(F-k)_{-N} \text{ with } F\,\tilde{\Phi} \tag{4.6e}$$

$$\text{VI-I}): \quad U(F+f-k)_{-N} \text{ with } f\,\tilde{\phi}. \tag{4.6f}$$

Once again the theories sitting at the stars in the third and first quadrants are $U(k)_N$ with $f\,\phi\ +\ F\,\Phi$ and $U(F+f-k)_{-N}$ with $f\,\tilde{\phi}\ +\ F\,\tilde{\Phi}$ respectively.

$f, F > k$

The phase diagram for this case is given in Fig. 4.5. Here both sets of fermions are condensing. The phases are

$$\text{I}): \quad SU(N)_{-k+f+F} \leftrightarrow U(F+f-k)_{-N} \tag{4.7a}$$

$$\text{II}): \quad SU(N)_{-k+f} \leftrightarrow U(f-k)_{-N} \tag{4.7b}$$

$$\text{III}): \quad SU(N)_{-k} \leftrightarrow U(k)_{N} \tag{4.7c}$$

$$\text{IV}): \quad SU(N)_{-k+F} \leftrightarrow U(F-k)_{-N} \tag{4.7d}$$

$$\text{V}): \quad \mathcal{M}(f+F,k) + N\,\Gamma \tag{4.7e}$$

$$\text{VI}): \quad \mathcal{M}(f,k) + N\,\Gamma \tag{4.7f}$$

$$\text{VII}): \quad \mathcal{M}(F,k) + N\,\Gamma \tag{4.7g}$$

while the critical lines which separate them are given by the by the following bosonic theories

$$\text{I-II}): \quad U(F+f-k)_{-N} \text{ with } F\,\tilde{\Phi} \tag{4.8a}$$

$$\text{II-VI}): \quad U(f-k)_{N} \text{ with } f\,\tilde{\phi} \tag{4.8b}$$

$$\text{VI-III}): \quad U(k)_{N} \text{ with } f\,\phi \tag{4.8c}$$

$$\text{III-VII}): \quad U(k)_{N} \text{ with } F\,\Phi \tag{4.8d}$$

$$\text{VII-IV}): \quad U(F-k)_{-N} \text{ with } F\,\tilde{\Phi} \tag{4.8e}$$

$$\text{VI-I}): \quad U(F+f-k)_{-N} \text{ with } f\,\tilde{\phi}. \tag{4.8f}$$

We note that this phase can be derived from the $f, F < k$ case of Sec. 4.1.2 by a clever use of time reversal symmetry. This maps the theory with $f, F < k$ to one with $f, F > \tilde{k}$ where $\tilde{k} = F + f - k$. We then have $\mathcal{M}(F, f-k) = \mathcal{M}(F, \tilde{k})$. The action of time reversal also maps $m \to -m$ and so will change the location of this phase as well[2]. This mapping was used in [16] to deduce the form of Fig. 4.5 without explicitly performing the mass deformations.

[2]We thank the authors of [16] for discussion on this mapping.

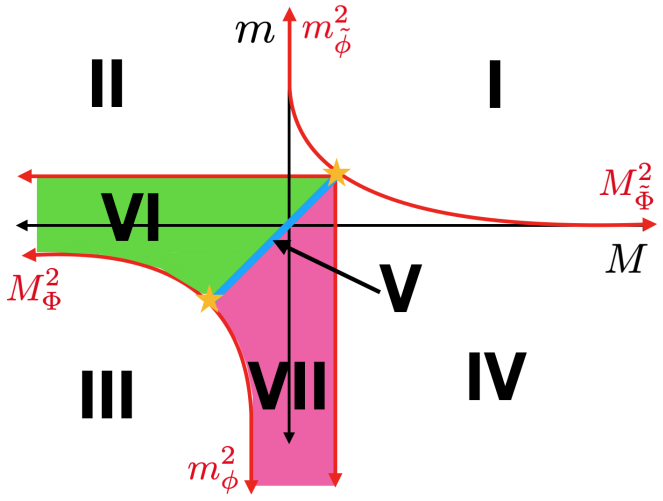

Figure 4.5: Phase diagram for flavor broken QCD$_3$ with $f, F > k$. These phases are laid out in Sec. 4.1.2.

$f < k$, $F = k$

The case when either f or F is equal to k offers a unique challenge. Consider the case at hand, $f < k$ and $F = k$, as shown in Fig. 4.6 . When we integrate out F, we will cancel the CS term completely and the Grassmannian corresponding to phase VII in Fig. 4.3 will disappear. As we increase F further, the Grassmannian will reappear as phase VII in Fig. 4.4. This offers an interesting view of the phase diagram as a function of F and f. As we smoothly change F through k, one of our Grassmannians disappears–we no longer have symmetry breaking in that part of the diagram. The theory is confining, all quarks pick up a mass from some confinement mechanism and the low energy theory is trivial. Moreover, in sharp distinction from the cases where neither f nor F is equal to k, we only have two Grassmannians instead of one. The phases corresponding to VI in Fig. 4.3 remains, however, since the effective CS level from integrating out the f fermions ensures that the flavor bound is violated in this regime. The phases are:

$$\text{I}): \quad SU(N)_f \leftrightarrow U(f)_{-N} \tag{4.9a}$$

$$\text{II}): \quad SU(N)_{-k+f} \leftrightarrow U(k-f)_N \tag{4.9b}$$

$$\text{III}): \quad SU(N)_{-k} \leftrightarrow U(k)_N \tag{4.9c}$$

$$\text{IV}): \quad SU(N)_0 = \text{ trivial} \tag{4.9d}$$

$$\text{V}): \quad \mathcal{M}(f+F,k) + N\,\Gamma \tag{4.9e}$$

$$\text{VI}): \quad \mathcal{M}(k,k-f) + N\,\Gamma \tag{4.9f}$$

$$\tag{4.9g}$$

The resulting scalar theories on the critical lines are

$$\text{I-VI}): \quad U(f)_{-N} \text{ with } k\,\tilde{\Phi} \tag{4.10a}$$

$$\text{VI-II}): \quad U(k-f)_N \text{ with } k\,\Phi \tag{4.10b}$$

$$\text{II-III}): \quad U(k)_N \text{ with } f\,\phi \tag{4.10c}$$

$$\text{III-VII}): \quad U(k)_N \text{ with } k\,\Phi \tag{4.10d}$$

$$\text{IV-I}): \quad U(f)_{-N} \text{ with } f\,\tilde{\phi}. \tag{4.10e}$$

The III-IV and IV-I critical theories are consistent with the above since completely breaking the gauge group will lead to a trivial theory in the IR [24, 64].

$f = k$, $F > k$

This case is similar to the above in that one of the Grassmannian phases disappears while the other persists. This time, however, it is the Grassmannian which corresponds to phase VI in the $f < k, F > k$ (Fig. 4.4) diagram which disappears. This has the same interpretation as the previous case–namely as we smoothly vary f through k the Grassmannian disappears and reappears as phase VI in the $f, F > k$ (Fig. 4.5) phase diagram. At the transition we again only have two Grassmannians. The phase diagram is shown in Fig.4.7. The phases are

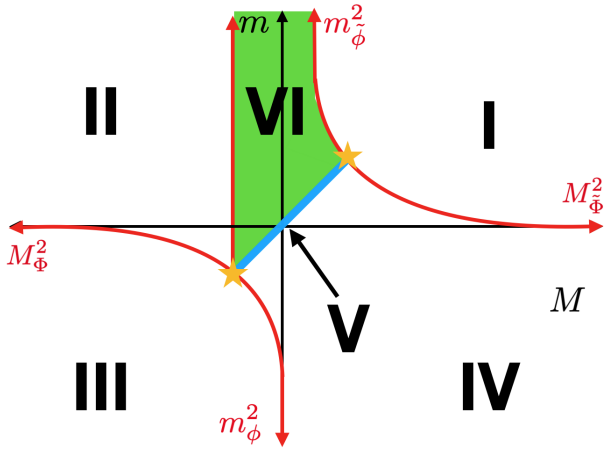

Figure 4.6: Phase diagram for flavor broken QCD_3 with $f < k$, $F = k$. These phases are described in Sec. 4.1.2.

$$\text{I}): \quad SU(N)_F \leftrightarrow U(F)_{-N} \tag{4.11a}$$

$$\text{II}): \quad SU(N)_0 = \text{ trivial} \tag{4.11b}$$

$$\text{III}): \quad SU(N)_{-k} \leftrightarrow U(k)_N \tag{4.11c}$$

$$\text{IV}): \quad SU(N)_F = U(F)_{-N} \tag{4.11d}$$

$$\text{V}): \quad \mathcal{M}(f+F,k) + N\,\Gamma \tag{4.11e}$$

$$\text{VI}): \quad \mathcal{M}(F,k) + N\,\Gamma \tag{4.11f}$$

$$\tag{4.11g}$$

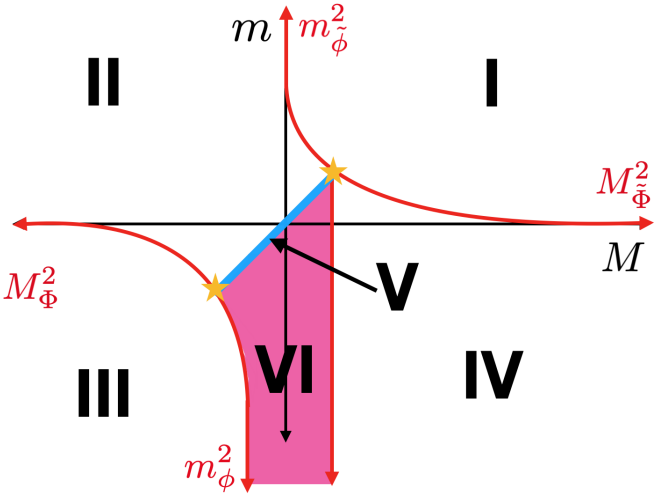

Figure 4.7: Phase diagram for flavor broken QCD_3 with $f = k$, $F > k$. These phases are laid out in Sec. 4.1.2.

while the bosonic theories are

$$\text{I-II}): \quad U(F)_{-N} \text{ with } F\,\tilde{\Phi} \tag{4.12a}$$

$$\text{II-III}): \quad U(k)_{N} \text{ with } k\,\phi \tag{4.12b}$$

$$\text{III-VI}): \quad U(k)_{N} \text{ with } F\,\Phi \tag{4.12c}$$

$$\text{VI-IV}): \quad U(F-k)_{-N} \text{ with } k\,\tilde{\Phi} \tag{4.12d}$$

$$\text{IV-I}): \quad U(F)_{-N} \text{ with } k\,\tilde{\phi}. \tag{4.12e}$$

The III-IV and IV-I critical theories are again consistent as explained in the previous subsection. This diagram can also be deduced from the action of time reversal on Fig. 4.7 as described at the end of Sec. 4.1.2.

$f = k$, $F = k$

Finally we consider the case when both flavor are equal to k. In this case, we only get one Grassmannian phase living on the flavor-enhanced diagonal with two trivially gapped

theories on either side. This case is given in Fig. 4.8

$$\text{I}): \quad SU(N)_k \leftrightarrow U(k)_{-N} \tag{4.13a}$$

$$\text{II}): \quad SU(N)_0 = \text{ trivial} \tag{4.13b}$$

$$\text{III}): \quad SU(N)_{-k} \leftrightarrow U(k)_N \tag{4.13c}$$

$$\text{IV}): \quad SU(N)_0 = \text{ trivial} \tag{4.13d}$$

$$\text{V}): \quad \mathcal{M}(2k,k) + N\,\Gamma \tag{4.13e}$$

$$\tag{4.13f}$$

while the bosonic theories are

$$\text{I-II}): \quad U(k)_{-N} \text{ with } k\,\tilde{\Phi} \tag{4.14a}$$

$$\text{II-III}): \quad U(k)_N \text{ with } k\,\phi \tag{4.14b}$$

$$\text{III-IV}): \quad U(k)_N \text{ with } k\,\Phi \tag{4.14c}$$

$$\text{IV-I}): \quad U(k)_{-N} \text{ with } k\,\tilde{\phi}. \tag{4.14d}$$

This is nothing more than the flavor broken generalization of the symmetry breaking put forward by Vafa and Witten [110]. The Vafa-Witten theorem then says that there can be no further symmetry breaking than what occurs on the flavor-enhanced diagonal. It is a reassuring check that our methods satisfy this theorem.

4.1.3 Adding More Flavor Groups

The next obvious generalization is to give a different mass to a third subset of flavors. This would further break the flavor symmetry to $U(N_f) \to U(f_1) \times U(f_2) \times U(f_3)$. The resulting phase diagram as a function of mass is now three dimensional so we will not try to reproduce it here. However we do have a few comments. Giving equal masses to each flavor will again reduce the problem to the single flavored case considered in [80]. These will lie on the line given by $m_1 = m_2 = m_3$. Now giving an asymptotically large mass to one of the flavors will reduce to one of the cases considered in Sec. 4.1.2. The resulting scalar theories in

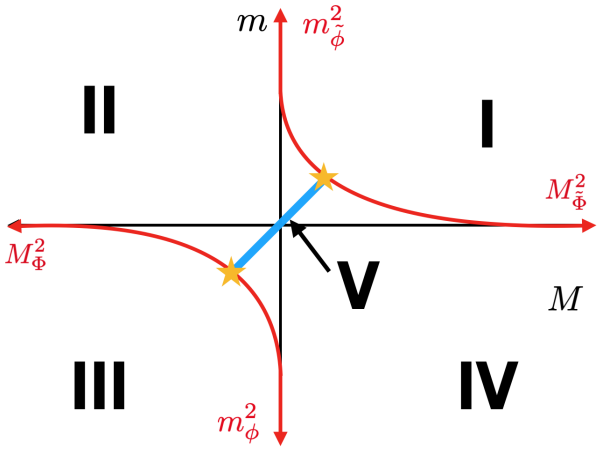

Figure 4.8: Phase diagram for flavor broken QCD_3 with $f = k$, $F = k$. These pahses are described in Sec. 4.1.2. This symmetry breaking pattern was first conjectured by Vafa and Witten [110].

that part of the phase diagram will not be localized on a curve as in Sec. 4.1.2, but on a curved plane embedded in the three dimensional diagram. In between these planes will be the appropriate Grassmannians, if the effective CS level is flavor violating. There will now be a web of Grassmannians of differing dimensions permeating the diagram. As we tune any of the f_i to k, then a corresponding Grassmannian will disappear and one of the TFTs will become trivial, as in the 2-flavor case. In general, the scalar theories will be localized on co-dimension 1 surfaces and there will be a plethora of flavor enhanced critical theories of various codimensionality where the different flavor groups become mass degenerate.

The above procedure is difficult to implement in practice, however. That is because the existence of flavor-violated phases not only relies on the relative sizes of the f_i's, but the size of the pairwise sum of f_i's with respect to k . For example, consider a situation where $f_1 < k$ with $f_1 < f_2 < f_3$. The two-flavor theory we are left with is then $SU(N)_{-k+f_1+\frac{f_2+f_3}{2}}$ with $f_2\,\psi_2$ and $f_3\,\psi_3$. Now give f_2 a negative mass. The existence of a quantum phase then depends on if $f_3 > k - f_1$ or $f_3 + f_1 > k$. The amount of data needed to map out the phase

diagram grows exponentially with the addition of each successive flavor group. Nevertheless this procedure can be implemented inductively as a way to map out the phase diagram as a function of each fermion mass individually.

4.1.4 Summary

If our conjectured phases diagram is correct, the phases of QCD_3 as a function of f and F are given in Fig. 4.9. The black excision from the top right reflects the fact that we have restricted our analysis to $f \leq F$. We can simply reflect the diagram about the diagonal if we are so inclined but the pertinant information is displayed. The solid blue line is again a reduction to the single flavor analysis considered in [80]. The various regions are:

(i): This corresponds to the $f + F < k$ considered in 4.1.1. There are no quantum phases, just four distinct TFTs separated by CFTs with a single scalar dual.

(ii): This corresponds to the $f, F < k$ case considered in Sec. 4.1.2. There are three Grassmannians and four TFTs separated by six scalar theories.

(iii): This corresponds to the $f < k$, $F > k$ case considered in Sec. 4.1.2. There are again are three Grassmannians and four TFTs separated by six scalar theories.

(iv): This corresponds to the $f, F > k$ case considered in Sec. 4.1.2. There are three Grassmannians and four TFTs seperate by six scalar theories

(v): This corresponds to $N_f > N_\star$. There are again four distinct TFTs but no scalar CFTs seperating them.

Sitting on the lines between these phases are

(i)-(ii): This transition marks the beginning of the existence of quantum phases. This line, however, is still captured by the duality in eq. **??**.

(ii)-(iii): This transition corresponds to $f < k, F = k$ case considered in Sec. 4.1.2. Here there are three non-trivial TFTs, one trivial phase and two Grassmannians.

(iii)-(iv): This transition corresponds to $f = k, F < k$ case considered in Sec. 4.1.2. Again there are three non-trivial TFTs, one trivial phase and two Grassmannians.

Finally the yellow dot corresponds to the Vafa-Witten breaking scenario [110]. This lies on the $f = F$ line and is the crux of the entire phase diagram. Indeed, one can derive this entire symemtry breaking scenario from this breaking pattern alone [80].

The emergence, disappearance, and reemergence of various Grassmannians is an incredibly interesting phenomena. We believe this is indication that the phase transition between these phases is first order–the topology of the phase diagram as a function of m and M changes wildly when you tune f and F. This must be taken with a grain of salt since f and F are not continuous parameters and so this is not a bonafide thermodynamic-type phase transition. It is possible that if we analytically continue f and F that the Grassmannians smoothly disappear and reappear as we tune, which would be indication of a second order "phase" transition. The exact structure of the singly-saturated cases considered in Secs. 4.1.2 and 4.1.2 indicate that a smooth transition may be possible. However Grassmannian manifolds with continuous dimensional is not a well-studied subject. Perhaps the answer is hiding in this complicated math. We leave a definitive answer to this important question for future work.

4.2 Comments on Scalar Potentials

Let us briefly comment on the consistency of the scalar theories in our phase diagram. We use the following intuitive picture to guide our construction of the phase diagram: as we follow the RG flow from the UV to the IR, whichever mass deformation we encounter first will dictate the resulting dynamics. For example if we encounter a mass deformation which completely breaks the gauge group, this is will be the first thing to happen. The rest of the

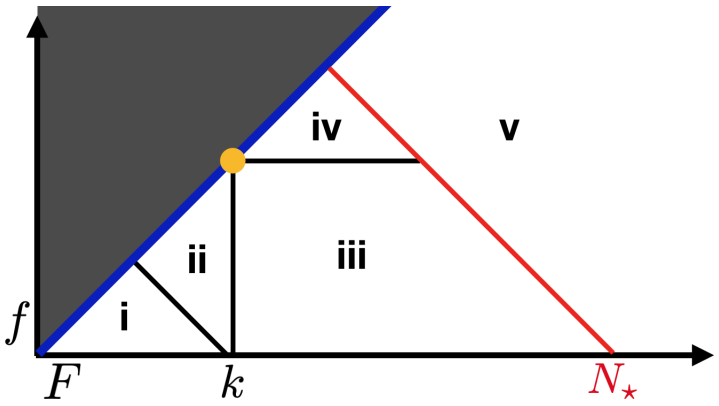

Figure 4.9: Phases as a function of f and F.

story is in the details of the scalar potential. With this picture in mind we can accurately say which scalars condense first in various parts of the phase diagrams.

As with any discussion involving 3d bosonization dualities we are dealing with Wilson-Fisher scalars with a quartic potential tuned to the fixed point. As was recently shown in [16] and [17] this potential includes both single and double trace potentials of the form

$$\left(\mathrm{Tr}\bar{\phi}\phi\right)^2 \text{ and } \mathrm{Tr}\left((\bar{\phi}\phi)^2\right). \tag{4.15}$$

This potential is necessary to generate the maximal Higgsing pattern that has been used throughout the literature[3]. See the aforementioned references for a detailed discussion on how this occurs.

In addition to the quartics (4.15), we will also assume that explicitly breaking the flavor symmetry in the UV will generate a certain $U(f) \times U(F)$ invariant relevant operator as we flow to the IR. This operator has the form

$$\mathcal{O}_4 = c\,\phi^\dagger_{a\,I}\Phi^{a\,J}\Phi^\dagger_{b\,J}\phi^{b\,I} \tag{4.16}$$

where a, b are $SU(N)$ gauge indicies, I is a $U(f)$ flavor index and J is an $U(F)$ flavor index. This operator should be mirrored on the fermionic side as well, although it is not clear what

[3]The large N analysis of [17] indicates that it may be necessary to include sextet terms as well, although it is possible that at finite N the structure simplifies and only the quartics are necessary.

it should be mapped to (for hints on how to do this see appendix A of [9]). For our conjecture to work, we need c to be large and positive. This is similar in spirit to the quartic potential used in the master duality [24, 64] where it was crucial for the correct mapping of the phases. Indeed it performs the same task–when one scalar gets a vev, the other gains a large positive mass deformation for some of the gauge components. In analogy to [24, 64] we call the gauge components which gain a mass from (4.16) "singlet scalars" since they are charged under the broken part of the gauge group. As an example consider the case when $f < k, F > 0$ given in Fig. 4.4. Assuming maximal Higgsing (which we will continue to do from here on out) as we give ϕ a negative mass deformation, the gauge group gets broken down to $U(k-f) \times U(f)$ and ϕ picks a vev which can be written as

$$\langle \phi^{\dagger}_{a\,I} \phi_{b\,I} \rangle = v \begin{pmatrix} I_{f\times f} & 0 \\ 0 & 0 \end{pmatrix}^{a\,b} \tag{4.17}$$

This causes first f gauge components of the Φ scalars to decouple from the unbroken part of the gauge group and obtain a large positive mass. The remaining $k-f$ light components can then drive the unbroken gauge group into the Grassmannian phase. If we considered the case where $f > k$ as well, then all of the components of Φ would get a large positive mass and would not contribute to the low energy dynamics, such as in the third quadrant of Fig. 4.5. When both have the same mass, this does not occur and we again back to the case of [80]. This mechanism nicely explains the Grassmannian structures in Sec. 4.1.2 and why only one flavor can condense at a time independent of the presence of the single trace quartics in (4.15). For consistency we must assume that once this potential is triggered along the RG flow, it no longer has any effect on the physics. That is the action of this potential is unidirectional with respect to whichever scalar get it's vev first. If ϕ gets triggered first, and then Φ, the ϕ vev will give masses to the components of Φ but not vice versa.

Further, there is a possibility that this mass deformation for the singlet scalars can be cancelled off by an explicit negative mass deformation of the Φ's. This would result in extra lines of light singlet scalars within the Grassmannian phases that are decoupled from the dynamics (for a related discussion see [7]). We assume that this is not the case by letting c

be larger than any other scale in the problem. This is, of course, rather artificial. Certainly this coefficient will flow to a specific value along the RG flow. What we are actually doing here is scaling one of the scalar fields relative to the other so that we zoom in to the part of the phase diagram where these interactions dominate[4].

In addition to the induced mass brought on by (4.16), the potential (4.15) can also induce a mass deformation for one of the scalars. For example the double trace term will decompose as

$$\left(|\phi|^2 + |\Phi|^2\right)^2 = |\phi|^4 + |\Phi|^4 + 2|\phi|^2|\Phi|^2 \tag{4.18}$$

Again we get that if one scalar condenses we again have $\langle\phi\rangle \neq 0$ the other flavor gets and induced mass deformation from the cross term in (4.18). This can be compensated for by a suitable shift in the mass of Φ and so should only serve to shift the location of where Φ goes light in the phase diagram. This is different from the case discussed above because it is not various subsets of the gauge components which obtain a mass from this interaction. In other words this interaction does not lead to the existence of singlet scalars. We assume our red scalar theories in Sec. 4.1.2 take this effect into account.

4.3 Taking the Large N Limit

Note: *Here we change notation related to the η invariant. Instead of explicitly displaying the half integer contribution to the level from the Pauli-Villars fields, we will shift the level as $k \to k - \frac{N_f}{2}$*

So far we have been dealing exclusively with gauge theories at finite N. To reiterate, the authors of [80] extended the duality of Aharony past the flavor bound and found the following:

$$SU(N)_k \text{ with } N_f\, \psi \quad \leftrightarrow \quad \begin{cases} U(\frac{N_f}{2}+k)_{-N} \text{ with } N_f\, \phi & m_\psi = m_\star \\ U(\frac{N_f}{2}-k)_{N} \text{ with } N_f\ \tilde{\phi} & m_\psi = -m_\star \end{cases} . \tag{4.19}$$

[4]We thank Andreas Karch for discussion on this point.

Between these critical points exists a NLσM given by the complex Grassmannian:

$$\mathcal{M}(N_f, \frac{N_f}{2} + k) \cong \frac{U(N_f)}{U(\frac{N_f}{2} + k) \times U(\frac{N_f}{2} - k)} \tag{4.20}$$

supplemented by an appropriate WZW type term. This scenario assumes that each of the N_f fermions is given the same mass deformation. The plot thickens when one passes to the large N limit. Large N limits in Chern-Simons matter theories have been studied before (see for instance [86, 51, 6, 5, 61] and references therein) where N/k remains constant. However, this limit does not lead to the Grassmannian (4.20). Instead, the authors or [17] studied a large N limit of Yang-Mills-Chern-Simons theory coupled to fermions with $g^2N = const$, where g is the gauge coupling. In this limit, the distinguished points in the phase diagram where one transitions between the semi-classical phases get resolved into a series of first order phase transitions with Grassmannians of the form $\mathcal{M}(N_f, p)$ as in figure 4.10. Interestingly, this is true when $k = 0$ as well as when $k \geq N_f/2$ and $k < N_f/2$. Additionally, each Grassmannian is accompanied by a decoupled pure Chern-Simons theory of the form $SU(N)_{k+p-N_f/2}$, even when $k = 0$. The phases identified at finite N are distinguished by the fact that their CS theory has zero level.

In these final sections, we extend the analysis of [22, 16] to the large N limit using the techniques laid out in [17]. We find series of first order phase transitions in special locations of the phase diagram consistent with the results of [22, 16] . Interestingly, there exists special places in the diagram where many ($2n$ where $n - 1$ is the number of distinct flavors) Grassmannians become degenerate. Additionally, for odd N_f we find degenerate symmetry broken and symmetry unbroken phases from any value of the mass, not just at special locations where phase transitions occur. We also discuss modifications to the dual scalar potential which will lead to doubly symmetry broken phases. The layout of our paper is as follows: in section 4.4 we review the necessary results of [80, 17, 22, 16] which are used in this work. Next, in section 4.5, we discuss the construction of our phase diagram and perform some consistency checks. In section 4.6 we briefly discuss scalar potentials and modifications which lead to interesting doubly symmetry broken phases. We conclude in

section 4.8. Additionally, we include numerical evidence for the diagram in appendix 4.7.

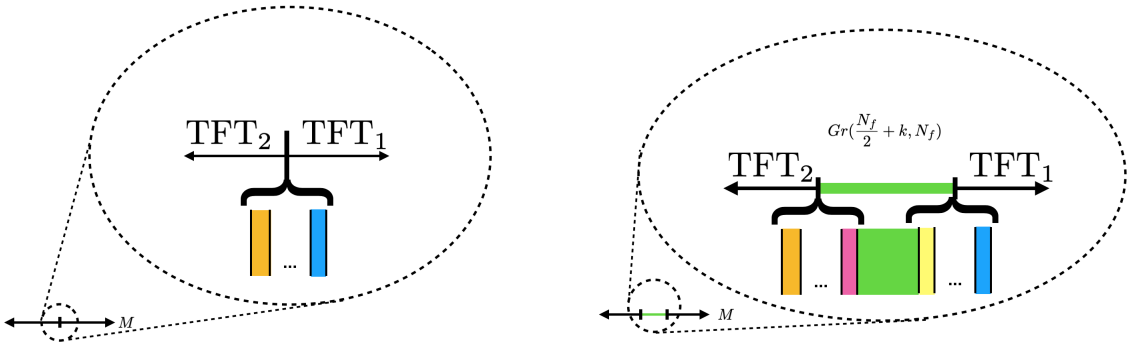

(a) $k > N_f/2$ and $N_f \to \infty$ (b) $k < N_f/2 < N_\star$

Figure 4.10: Resolution of critical points into a series of first order phase transitions. The different colored regions represent distinct Grassmannians

4.4 Symmetry Breaking in QCD$_3$ and Vacuum Structure at Large N

As mentioned in the introduction, the 3d non-Abelian bosonization dualities fail to hold when $k \leq N_f/2 < N_\star$ where $N_\star$ is some yet-to-be-pinned-down function of N_f and k[5]. When the scalars obtain a large negative mass deformation, they obtain a vev of the form

$$\langle \phi \rangle = \left(\mathbb{1}_{\frac{N_f}{2}+k} \; 0_{\frac{N_f}{2}-k} \right) \tag{4.21}$$

which spontaneously breaks the flavor symmetry as

$$U(N_f) \to U(\frac{N_f}{2}+k) \times U(\frac{N_f}{2}-k) \tag{4.22}$$

leading to Goldstone bosons which are valued in the complex Grassmannian[6]

$$\mathcal{M}(N_f, N_f/2+k) \cong \frac{U(N_f)}{U(\frac{N_f}{2}+k) \times U(\frac{N_f}{2}-k)}. \tag{4.23}$$

[5]For an upper bound derived from the f-theorem see [105]

[6]Henceforth we will drop the “complex" for sake of presentation.

A key observation of [80] is that this is not the only scalar theory with this symmetry breaking pattern. One can instead consider the theory

$$U(\frac{N_f}{2}-k)_{-N} \text{ with } N_f \ \tilde{\phi} \tag{4.24}$$

with a large negative mass deformation and find the same symmetry breaking pattern, leading to equivalent low energy dynamics. In addition, positive mass deformations of this scalar theory will land us in the level/rank dual of the TFT corresponding to negative mass deformations of the original fermionic theory. This motivates the duality

$$SU(N)_k \text{ with } N_f \, \psi \quad \leftrightarrow \quad \begin{cases} U(\frac{N_f}{2}+k)_{-N} \text{ with } N_f \, \phi & m_\psi = m_\star \\ U(\frac{N_f}{2}-k)_{N} \text{ with } N_f \ \tilde{\phi} & m_\psi = -m_\star \end{cases} \tag{4.25}$$

and the corresponding phase diagram in figure 4.10. Thus, there is a finite range of masses for which spontaneous symmetry breaking (SSB) occurs and the low energy theory is described by massless Goldstone modes valued in the Grassmannian. In addition to the Lagrangian which describes the NLσM, the action contains a contribution from a Wess-Zumino-Witten term which allows for the existence of skyrmions which play the role of baryons in the symmetry broken phase. The WZW term, however, will not play a crucial role in our discussion.

4.4.1 Symmetry Breaking with Unequal Masses

The above analysis is applicable when one gives equal masses to all N_f of the fermions. A more interesting structure emerges when one gives different mass deformations to separate subsets of the N_f fermions [22, 16]. Namely, we give the first f of the fermion flavors a mass m and the other $N_f - f$ a mass M. Such mass deformations will explicitly break the flavor group as $U(N_f) \to U(f) \times U(N_f - f)$. As a result of this explicit breaking, it will always be either one or the other subset of flavor which will condense to form Grassmannians. The specific Grassmannians and their location in the phase diagram depends on the relative values of $f, N_f - f$ and k. There are 6 possible options:

i.) $f - \frac{N_f}{2} < k,\ \frac{N_f}{2} - f < k$

ii.) $f - \frac{N_f}{2} < k,\ \frac{N_f}{2} - f = k$

iii.) $f - \frac{N_f}{2} < k,\ \frac{N_f}{2} - f > k$

iv.) $f - \frac{N_f}{2} = k,\ \frac{N_f}{2} - f > k$

v.) $f - \frac{N_f}{2} > k,\ \frac{N_f}{2} - f > k$

vi.) $f - \frac{N_f}{2} = k, \frac{N_f}{2} - f = k.$

The structure of the phase diagrams in each case shown in figure 4.11. For each of parameter regime we have the following Grassmannians[7] along the specified axis in the $m - M$ plane.

i.) $M < 0 :\ \mathcal{M}(f, k + f - \frac{N_f}{2},)$
$m < 0 :\ \mathcal{M}(N_f - f, k - f + \frac{N_f}{2})$

ii.) $m < 0 :\ \mathcal{M}(N_f - f, k - f + \frac{N_f}{2})$

iii.) $m > 0 :\ \mathcal{M}(N_f - f, k + \frac{N_f}{2})$
$m < 0 :\ \mathcal{M}(N_f - f, k - f + \frac{N_f}{2})$

iv.) $m > 0 :\ \mathcal{M}(N_f - f, k + \frac{N_f}{2})$

v.) $M > 0 :\ \mathcal{M}(f, k + \frac{N_f}{2},)$
$m > 0 :\ \mathcal{M}(N_f - f, k + \frac{N_f}{2})$

vi.) No additional Grassmannians

Strictly speaking this analysis is applicable when at least one mass deformation is macroscopically large[8]. The massive fermions shift the Chern-Simons level and the problem then

[7]These are in addition to the Grassmannian $\mathcal{M}(N_f, k + \frac{N_f}{2})$ which exists along the diagonal in each regime

[8]By “macroscopically large" we mean larger than the strong scale Λ.

reduces to the analysis of flavor bounds of the light flavors with this shifted level. The behavior when both mass deformations are small is still ambiguous but can be slightly elucidated in the large N limit.

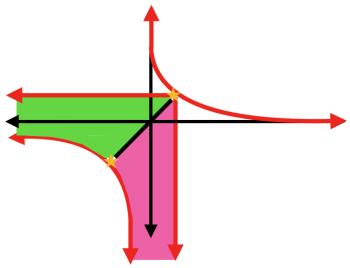

(a) Phase diagram associated to i).

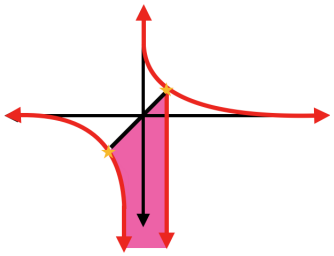

(b) Phase diagram associated to ii).

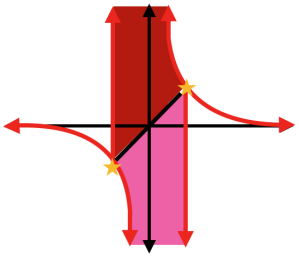

(c) Phase diagram associated to iii).

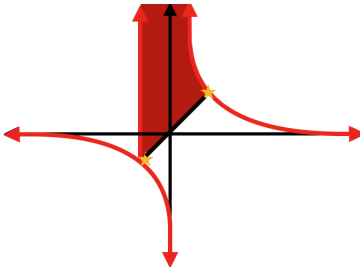

(d) Phase diagram associated to iv).

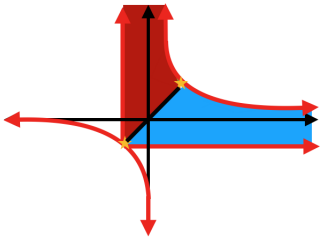

(e) Phase diagram associated to v).

Figure 4.11: Various phase diagrams for the scenarios discussed in sec. 4.4.1, where m is on the y axis and M is on the x-axis.

4.4.2 Vacuum Structure at Large N

One major drawback of the analyses in the previous section is the lack of insight about the nature of the phase transitions. On one hand the fact that they are mediated by scalar theories seems to indicate that these are second order. However they are also strongly coupled and so the presence of light degrees of freedom at the transition point does not

necessarily mean that the transition is second order. In order to probe the nature of these phase transitions, we must pass to some perturbative limit where calculations are possible.

One such perturbative analysis was recently performed in [17] using the "standard" 't Hooft large N limit: $N \to \infty$, $g^2 N$ =fixed. This differs from previous large N calculations in Chern-Simons matter theories where one takes k/N = fixed. As a result, this counting scheme leads to the standard large N counting rules–leading order diagrams are arbitrary planar gluon diagrams, and quark loops are suppressed by a factor of $1/N$.

Since we are interested in the patterns of flavor-symmetry breaking in this limit, the primary observable of interest is the expectation value of the fermion condensate

$$\mathcal{M}_I^J = \frac{1}{N}\langle \bar{\psi}_I \psi^J \rangle \tag{4.26}$$

where $I, J = 1, .., N_f$ are flavor indices. This term is valued in the adjoint representation of the global $SU(N_f) \subset U(N_f)$ flavor symmetry, invariant under the baryonic $U(1) \subset U(N_f)$ and is time-reversal odd. It enters into the Lagrangian via a mass term for the fermions

$$\mathcal{L} \supset -m_I^J \bar{\psi}_J \psi^I = -N\mathrm{tr}(m\mathcal{M}). \tag{4.27}$$

Here we defined m as the matrix with entries m_I^J.

The basic strategy of [17] is to use large N reasoning to derive a general form for the effective potential as a function of $\langle \mathcal{M} \rangle$. Specifically, we are interested in

$$V(\langle \mathcal{M} \rangle) = -W(m) - N\mathrm{tr}(m\mathcal{M}) \tag{4.28}$$

where $W(m) = -i\ln(Z(m))/V_3$ is the sum of all connected correlation functions of $\mathcal{M}$ and V_3 is the spacetime volume. We now review their leading order and next to leading order calculations.

Leading Order

The $\mathcal{O}(N)$ contributions to $W(m)$ (and, by extension, $V(\langle \mathcal{M} \rangle)$) come from diagrams which are topologically a disk with a single fermion loop and an arbitrary number of $\mathcal{M}$'s inserted

on it's boundary as in figure 4.12. The interior of the disk is an arbitrary planar gluon diagram. As a result, $W(m)$ can only take on contributions from single-trace operators. Time reversal symmetry requires that the potential obey $W(-m) = W(m)$ which further constrains the allowed terms. When the dust settles, we can schematically write $W(m)$ as

$$W(m) = N\Lambda^3 \sum_{n=2,4,6..}^{\infty} \frac{C_n}{\Lambda^n} \mathrm{tr}(m^n) \tag{4.29}$$

which leads to a very similar form for the effective potential:

$$V(\langle \mathcal{M} \rangle) = N\Lambda^3 \sum_{n=2,4,6..}^{\infty} \frac{C'_n}{\Lambda^{2n}} \mathrm{tr}(\langle \mathcal{M} \rangle^n). \tag{4.30}$$

We now use an $SU(N_f)$ transformation to diagonalize $\mathcal{M}$ to get

$$\mathcal{M} = \Lambda^3 \mathrm{diag}(x_1, x_2 ... x_{N_f}), \quad x_i \in \mathbb{R} \tag{4.31}$$

which leads to an effective potential of the form

$$V(x_i) = N\Lambda^3 \sum_{i=1}^{N_f} \sum_{n=2,4,6,...}^{\infty} C'_n x_i^n \equiv N\Lambda^3 \sum_{i=1}^{N_f} F(x_i). \tag{4.32}$$

An incredibly crucial assumption of [17] is that $F(x)$ has degenerate minima at some finite $\pm x_\star$ and by a simultaneous rescaling of $\mathcal{M}$ and $F(x)$ we can set $x_\star = 1$[9]. Since the potential is minimized as $x_i = \pm 1$, each eigenvalue must take on either one of those values. This leads to $N_f + 1$ degenerate vacua labeled by the number of positive (or negative) eigenvalues of $\mathcal{M}$. The NLσM that describes the low energy physics is again the Grassmannian

$$\mathcal{M}(N_f, p) \cong \frac{U(N_f)}{U(p) \times U(N_f - p)} \tag{4.33}$$

supplemented by the appropriate WZW term. In addition to the Grassmannian, each of these vacua will contain a non-trivial Chern-Simons TFT of the form $SU(N)_{p-\frac{N_f}{2}+k}$, even when $k = 0$. This is necessary is one assumes that there are no phase transitions as one tunes the mass from small non-zero values to asymptotically large values.

---

[9] Without this assumption the results of [17] would be inconsistent with the Vafa-Witten theorem [110, 109]

One can add a mass term for the fermions which will lift the degeneracy of these vacua. It is not difficult to show that

$$[m, \mathcal{M}] = 0 \tag{4.34}$$

which allows for the simultaneous diagonalization of both m and $\mathcal{M}$. Let m_i be the eigenvalues of m. Then the mass term will add a term to the effective potential of the form

$$V(x_i) \supset N\Lambda \sum_{i=1}^{N_f} m_i x_i. \tag{4.35}$$

Now if we take the first $m_i > 0$ for $i = 1, .., p$ and $m_i < 0$ for $i = p+1, ..., N_f$, the potential will be minimized by taking $x_i = -1$ for $i = 1, .., p$ and $x_i = 1$ for $i = p+1, ..., N_f$. This lifts the degeneracy and singles out $\mathcal{M}(N_f, p)$ as the true ground state.

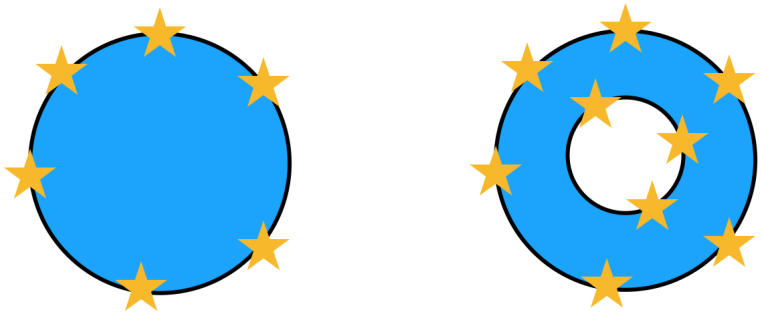

(a) (b)

Figure 4.12: Leading (a) and subleading (b) diagrams in the large N limit. Blue represents arbitrary gluon loops and stars are insertions of $\mathcal{M}$.

Next-To-Leading-Order

In the proceeding section we discussed the vacuum structure of QCD_3 by examining the $\mathcal{O}(N)$ contribution to the effective potential, which stems from the disk diagram of figure 4.12 (a). The $\mathcal{O}(1)$ contribution, on the other hand, comes from the annulus diagram of figure 4.12 (b) and so contains double trace terms such as $\mathrm{tr}(\langle\mathcal{M}\rangle^n)\mathrm{tr}(\langle\mathcal{M}\rangle^{n'})$. Since we are

not interested in any higher order terms in the large N expansion, we can restrict the x_i's to their values which minimize the $\mathcal{O}(N)$ potential. This fact, along with constraints from time-reversal invariance, give the following form for the $\mathcal{O}(1)$ potential

$$V(x_i) \supset \Lambda^3 \Delta \sum_{i,j=1}^{N} x_i x_j. \tag{4.36}$$

The constant Δ is a strictly positive constant whose value is determined from calculation of the diagrams in figure 4.12. It's positivity is required by consistency with the Vafa-Witten theorem–in the absence of mass terms the ground state is given by $\mathcal{M}(N_f, N_f/2)$.

One can add a small singlet mass deformations $m \sim m\delta_{ij}$ to this and examine how the ground state will change as a function of the mass. In addition, we can add a non-zero Chern-Simons term to the action. The contribution from the Chern-Simons term enters in the same form as the mass term and so we can group them together. The potential is then

$$V(x_i) \supset \Lambda^3 \Delta \sum_{i,j=1}^{N_f} x_i x_j + \left(Nm\Lambda^2 + k\Lambda^3\right) \sum_{i=1}^{N_f} x_i. \tag{4.37}$$

Note that this mass deformation is subleading only when m $\mathcal{O}(1/N)$. If $m \sim \mathcal{O}(1)$, then it becomes part of the $\mathcal{O}(N)$ potential. Now we make the ansatz that the first p eigenvalues of $\langle \mathcal{M} \rangle$ are -1 and the remaining $N_f - p$ are 1. Minimizing the effective potential with respect to p gives

$$p = \frac{N_f}{2} + [\![\frac{Nm + \Lambda k}{4\Lambda\Delta}]\!] \tag{4.38}$$

where $[\![x]\!]$ denotes the nearest integer of x. The vacuum which minimizes the effective potential jumps by ± 1 whenever $\frac{Nm+\Lambda k}{4\Lambda\Delta} \in \mathbb{Z} + \frac{1}{2}$. Thus as we tune m we traverse each Grassmannian until we wind up in the asymptotic phases. In other words, one encounters a series of first order phase transitions as a function of m.

4.5 Vacuum Structure With an Explicitly Broken Flavor Group

In the above discussion we gave the fermions a mass deformation of the form $m = m\mathbb{1}$ which preserved the global flavor symmetry. In this section we will examine a different scenario in

which

$$\tilde{m} = \text{diag}\left(\underbrace{m,..,m}_{f},\underbrace{M,..,M}_{N_f-f}\right). \tag{4.39}$$

This mass deformation *explicitly* breaks the global flavor symmetry as $U(N_f) \to U(f) \times U(N_f - f)$. As a result, we will distinguish the corresponding eigenvalues of our condensate:

$$\langle \mathcal{M} \rangle = \frac{1}{N}\text{diag}\left(x_1,..,x_f,y_1,...,y_{N_f-f}\right). \tag{4.40}$$

We may then ask if these subgroups get broken down any further by the resulting fermion condensate. The purpose of this section is to determine the circumstances under which these subgroups get spontaneously broken.

4.5.1 Leading Order

We start by assuming $M = 0$. The full $\mathcal{O}(N)$ potential including the mass deformation is

$$V(x_i) = N\Lambda^3 \sum_{i=1}^{N_f} F(x_i) + m\sum_{i=1}^{f} x_i. \tag{4.41}$$

The mass term fixes all the x's to be -1 but places no such restriction on the $y's$. Thus each y can be ± 1 which again leads to a degeneracy. Assuming the first p of the y eigenvalues are 1, our symmetry group will spontaneously break as

$$U(f) \times U(N_f - f) \to U(f) \times U(p) \times U(N_f - f - p) \tag{4.42}$$

which leads to the coset

$$\frac{U(f) \times U(N_f - f)}{U(f) \times U(p) \times U(N_f - f - p)} = \frac{U(N_f - f)}{U(p) \times U(N_f - f - p)} \cong \mathcal{M}(N_f - f, p). \tag{4.43}$$

Thus there are $N_f - f + 1$ degenerate vacua, one for each choice of p, each one accompanied by a Chern-Simons TFT.

If we take $M \neq 0$, then the corresponding eigenvalues will also be fixed and, in general, no SSB will occur.

4.5.2 Next-To-Leading Order

The story becomes much more interesting at $\mathcal{O}(1)$ due to the asymmetry in the mass term. The full $\mathcal{O}(1)$ potential including, including the Chern-Simons term and an $\mathcal{O}(1/N)$ mass deformation, can be written as

$$V = \Delta\Lambda^3 \left(\sum_{i=1}^{f} x_i + \sum_{i=1}^{N_f - f} y_i \right)^2 + k\Lambda^3 \left(\sum_{i=1}^{f} x_i + \sum_{i=1}^{N_f - f} y_i \right) + Nm\Lambda^2 \sum_{i=1}^{f} x_i + NM\Lambda^2 \sum_{i=1}^{f} y_i. \tag{4.44}$$

As in the flavor symmetric case the eigenvalues of $\mathcal{M}$ take on their $\mathcal{O}(N)$ values in the $\mathcal{O}(1)$ potential since we are not considering terms which are higher order. The general structure of the phase diagram will also be uneffected by the Chern-Simons term and so the bulk of our analysis will be concerned with the $k = 0$ case. Adding non-zero k will only serve to shift the locations of various phases in the phase diagram, rather than change it's structure.

We start this section by demonstrating a lack of double condensation of the fermions when $m \neq M$. That is, it is forbidden to have SSB in both groups of fermions simultaneously. The resulting scenarios can then be broken up into three cases–one where symmetry breaking happens in the upper left $f \times f$ block of $\mathcal{M}$, one that happens in the lower right $(N_f - f) \times (N_f - f)$ block, and one where no symmetry breaking occurs. We then identify the regions of the phase diagram where these symmetry breaking scenarios occur by examining the relative values of the effective potential. We then use the fact that $\mathcal{M}(N, M)$ does not exist unless $0 \leq M \leq N$ to further refine our diagram.

A Lack of Double Condensation

We start by looking for a solution in which both groups of fermions undergoes spontaneous symmetry breaking. That implies the formation of a condensate of the form

$$N\langle\mathcal{M}\rangle = \text{diag}(\underbrace{1, ..., 1}_{p}, \underbrace{-1, ..., -1}_{f-p}, \underbrace{1, ..., 1}_{q}, \underbrace{-1..., -1}_{N_f - f - q}) \tag{4.45}$$

leading to the double coset

$$\mathcal{M}(f,p)\times\mathcal{M}(N_f-f,q). \tag{4.46}$$

The integers p and q are bounded below by zero and above by the number of fermion flavors in that block. In other words, p and q takes integer values in the domain $\mathcal{D}=[0,f]\times[0,N_f-f]$. If, for general m and M, the effective potential admits a minimum on $\text{int}(\mathcal{D})$ then double condensation can occur. Otherwise, the minimum must occur on $\partial\mathcal{D}$ and only one group of flavors undergoes SSB. Plugging (4.45) into (4.44) gives

$$\frac{V}{\Delta\Lambda^3}=(2p+2q-N_f)^2+\left(\frac{mN}{\Lambda\Delta}+\frac{k}{\Delta}\right)(2p-f)+\left(\frac{MN}{\Lambda\Delta}+\frac{k}{\Delta}\right)(2q-N_f+f)\,. \tag{4.47}$$

To find extrema, we extend p and q to the real numbers and solve the system of equations:

$$\frac{\partial V}{\partial p}=4(2p+2q-N_f)+2\left(\frac{mN}{\Lambda\Delta}+\frac{k}{\Delta}\right)=0 \tag{4.48}$$

$$\frac{\partial V}{\partial q}=4(2p+2q-N_f)+2\left(\frac{MN}{\Lambda\Delta}+\frac{k}{\Delta}\right)=0. \tag{4.49}$$

To simplify this, rewrite it as a matrix equation:

$$\begin{pmatrix}8&8\\8&8\end{pmatrix}\begin{pmatrix}p\\q\end{pmatrix}=\begin{pmatrix}4N_f-2\left(\frac{mN}{\Lambda\Delta}+\frac{k}{\Delta}\right)\\4N_f-2\left(\frac{MN}{\Lambda\Delta}+\frac{k}{\Delta}\right)\end{pmatrix}. \tag{4.50}$$

Clearly the coefficient matrix $\begin{pmatrix}8&8\\8&8\end{pmatrix}$ has determinant zero and is therefore not invertible. This system of equations has no solutions and the extrema must occur on $\partial\mathcal{D}$. Explicit numerics demonstrating the same conclusion are given in Appendix A.

At finite N, one can show that double condensation is forbidden by explicitly minimizing the potential on the scalar side, as was done in [16, 17]. There the authors included both a single and double flavor trace quartic potentials and minimized with respect to the eigenvalues. Positivity constraints show that there is no double condensation outside of the flavor enhanced $m=M$ line. However, this same reasoning can not be applied to large N QCD_3, since the proposed form of the (finely tuned) *sextic* potential on the scalar side does not include double trace deformations at leading order. Since the leading order solution

determines the eigenvalues of the condensate, there is no *a priori* reason to expect a lack of double condensation. We will discuss some modifications to the potential that could allow for such double condensation in section 4.6 below.

Single Massive Flavor

We start by examining what happens when we give the first f flavors a mass $m > 0$ while leaving the other $N_f - f$ light. The situation is slightly different when $f \leq \frac{N_f}{2}$ and $f \geq \frac{N_f}{2}$. We examine these in turn. The potential is the same in either case. We start by taking $k = 0$. We have

$$V = \Delta\Lambda^3 \left(\sum_{i=1}^{f} x_i + \sum_{i=1}^{N_f - f} y_i \right)^2 + Nm\Lambda^2 \sum_{i=1}^{f} x_i. \tag{4.51}$$

First, consider giving $f < \frac{N_f}{2}$ a mass m. In this scenario, we can take all the x's to be -1. Now, since there are more $y's$ than there are x's, we can entirely cancel off the contribution from the x's in the quadratic term by taking f of the $y's$ to be equal to $+1$. Of the remaining $N_f - 2f$ y's, we take half to be positive and half to be negative so that they cancel among themselves. If N_f is even, this works perfectly. If N_f is odd, then we will be left with one unpaired eigenvalue. This eigenvalue can be either $+1$ or -1 and since it's only contribution to the effective potential is in the quadratic term, these scenarios have the same value of the effective potential and so are degenerate. When the dust settles our condensate looks like

$$\begin{aligned} N\mathcal{M} &= \text{diag}\left(\underbrace{-1, \ldots -1}_{f}, \underbrace{1, \ldots, 1}_{\frac{N_f}{2}} \underbrace{-1, \ldots, -1}_{\frac{N_f}{2} - f} \right) \quad \text{for } N_f \text{ even} \\ &= \text{diag}\left(\underbrace{-1, \ldots -1}_{f}, \underbrace{1, \ldots, 1}_{\frac{N_f \pm 1}{2}} \underbrace{-1, \ldots, -1}_{\frac{N_f \mp 1}{2} - f} \right) \quad \text{for } N_f \text{ odd} \end{aligned} \tag{4.52}$$

which leads to the Grassmannians

$$\begin{aligned}\mathcal{M}(N_f - f, \frac{N_f}{2}) &\cong \mathcal{M}(N_f - f, \frac{N_f}{2} - f) \quad \text{for } N_f \text{ even} \\ \mathcal{M}(N_f - f, \frac{N_f \pm 1}{2}) &\cong \mathcal{M}(N_f - f, \frac{N_f \mp 1}{2} - f) \quad \text{for } N_f \text{ odd}\end{aligned} \tag{4.53}$$

with effective potentials given by

$$\begin{aligned}V &= -Nm\Lambda^2 f, \quad \text{for } N_f \text{ even} \\ &= 1 - Nm\Lambda^2 f, \quad \text{for } N_f \text{ odd.}\end{aligned} \tag{4.54}$$

These only occur, however, when

$$\begin{aligned}\frac{N_f}{2} - f &\geq 1 \quad \text{for } N_f \text{ even} \\ \frac{N_f \mp 1}{2} - f &\geq 1 \quad \text{for } N_f \text{ odd.}\end{aligned} \tag{4.55}$$

Otherwise, the Grassmannians (4.53) do not exist. If (4.55) is not satisfied, then we simply have some Chern-Simons matter theory with $N_f - f$ massless fermions.

When $f = \frac{N_f}{2}$, we get no spontaneous symmetry breaking when N_f is even. This is because all of the y's can perfectly cancel all the x's. We wind up with a condensate of the form:

$$N\langle\mathcal{M}\rangle = \text{diag}\left(\underbrace{-1, \ldots -1}_{N_f/2}, \underbrace{1, \ldots, 1}_{N_f/2}\right). \tag{4.56}$$

When N_f is odd, we have two choices, since not all of the y's can cancel off the x's. We are left with one unpaired y eigenvalue which can take either sign. Since this eigenvalue enters in eq. (4.51) in the quadratic term, both choices have the same value of the effective potential and we again have a twofold degeneracy as in eq. (4.53). This leads to the following condensates:

$$\begin{aligned}N\langle\mathcal{M}\rangle &= \text{diag}\left(\underbrace{-1, \ldots -1}_{(N_f-1)/2}, \underbrace{1, \ldots, 1}_{(N_f+1)/2}\right) \implies \text{no SSB} \\ N\langle\mathcal{M}\rangle &= \text{diag}\left(\underbrace{-1, \ldots -1}_{(N_f-1)/2}, \underbrace{1, \ldots, 1}_{(N_f-1)/2}, -1\right) \implies \text{SSB with } Gr\left(1, \frac{N_f+1}{2}\right).\end{aligned} \tag{4.57}$$

Already we can see some novelties of the flavor broken case as opposed to the flavor symmetric one. Namely that one does not encounter a series of first order phase transitions as you dial m–you simply stay in the same Grassmannian until you reach the asymptotic regime. Also we see that for odd N_f there exists two degenerate Grassmannians for any value of m. When $f = (N_f - 1)/2$, this degeneracy is between a phase where SSB occurs and one where it does not.

When $f > N_f/2$ the y's can not fully cancel off all of the x's. As a result, we will have some excess energy in either the quadratic term or the linear term. To proceed we calculate the extrema of the effective potential in both cases and compare the values of V to see which scenario is preferred. Proceeding in this way, we find that having excess in the linear term is energetically favorable. This leads to a condensate of the form

$$N\langle\mathcal{M}\rangle = \text{diag}\left(\underbrace{-1,...-1}_{f-q},\underbrace{1,...,1}_{q}\underbrace{1,1,...1}_{N_f-f}\right) \tag{4.58}$$

where

$$q = f - \frac{N_f}{2} - [\![\frac{Nm}{4\Lambda\Delta}]\!]. \tag{4.59}$$

In contrast to the $f \leq N_f/2$ case, we do encounter a series of phase transitions as we tune the mass, albeit a reduced number of them.

Double Massive Flavors

The diagram become much richer when we give the other set of flavor a mass. The potential is

$$V = \Delta\Lambda^3\left(\sum_{i=1}^{f} x_i + \sum_{i=1}^{N_f-f} y_i\right)^2 + Nm\Lambda^2\sum_{i=1}^{f} x_i + NM\Lambda^2\sum_{i=1}^{N_f-f} y_i. \tag{4.60}$$

Now, we must carefully examine the values of the effective potential on the boundary of our $p-q$ domain. The full domain is given by

$$\mathcal{D} = [0, f] \times [0, N_f - f] \tag{4.61}$$

with boundary $\partial\mathcal{D} = \partial\mathcal{D}_1 \cup \partial\mathcal{D}_2 \cup \partial\mathcal{D}_3 \cup \partial\mathcal{D}_4$ where

$$\begin{aligned}
\partial\mathcal{D}_1 &= [0, f] \times \{0\} \\
\partial\mathcal{D}_2 &= [0, f] \times \{N_f - f\} \\
\partial\mathcal{D}_3 &= \{0\} \times [0, N_f - f] \\
\partial\mathcal{D}_4 &= \{f\} \times [0, N_f - f]
\end{aligned} \tag{4.62}$$

Let $\tilde{m} = \frac{mN}{\Lambda\Delta}$ and similarly for $\tilde{M}$. The minimum occur at:

$$\begin{aligned}
&\partial\mathcal{D}_1 : p = \frac{N_f}{2} - [\![\frac{\tilde{m}}{4}]\!],\ q = 0 \text{ with } V_1 = -\frac{\tilde{m}^2}{4} + (\tilde{m} - \tilde{M})(N_f - f) \\
&\partial\mathcal{D}_2 : p = f - \frac{N_f}{2} - [\![\frac{\tilde{m}}{4}]\!],\ q = N_f - f \text{ with } V_2 = -\frac{\tilde{m}^2}{4} - (\tilde{m} - \tilde{M})(N_f - f) \\
&\partial\mathcal{D}_3 : p = 0,\ q = \frac{N_f}{2} - [\![\frac{\tilde{M}}{4}]\!] \text{ with } V_3 = -\frac{\tilde{M}^2}{4} - (\tilde{m} - \tilde{M})f \\
&\partial\mathcal{D}_4 : p = f,\ q = \frac{N_f}{2} - f - [\![\frac{\tilde{M}}{4}]\!] \text{ with } V_4 = -\frac{\tilde{M}^2}{4} + (\tilde{m} - \tilde{M})f
\end{aligned} \tag{4.63}$$

where p and q are subject to

$$0 \le p \le f, \text{ and } 0 \le q \le N_f - f. \tag{4.64}$$

Plugging eq. (4.63) into eq. (4.64) gives the following mass ranges for which we remain on $\partial\mathcal{D}$:

$$\begin{aligned}
\partial\mathcal{D}_1 &: \frac{\tilde{m}}{4} \in \mathcal{I}_1 \equiv \left[\frac{N_f}{2} - f, \frac{N_f}{2}\right] \\
\partial\mathcal{D}_2 &: \frac{\tilde{m}}{4} \in \mathcal{I}_2 \equiv \left[-\frac{N_f}{2}, f - \frac{N_f}{2}\right] \\
\partial\mathcal{D}_3 &: \frac{\tilde{M}}{4} \in \mathcal{I}_3 \equiv \left[f - \frac{N_f}{2}, \frac{N_f}{2}\right] \\
\partial\mathcal{D}_4 &: \frac{\tilde{M}}{4} \in \mathcal{I}_4 \equiv \left[-\frac{N_f}{2}, \frac{N_f}{2} - f\right].
\end{aligned} \tag{4.65}$$

These intervals have the property that $\mathcal{I}_1 \cap \mathcal{I}_2$ and $\mathcal{I}_3 \cap \mathcal{I}_4$ can not both be non-zero. If $f > \frac{N_f}{2}$, the former is non-empty while the latter is empty and vice versa for $f \le \frac{N_f}{2}$. For

regions where these mass intervals overlap, the preferred symmetry breaking scenario is the one which minimizes the effective potential. From eq. (4.63) it is easy to see that if $m < M$ then

$$V_1 < V_2 \text{ and } V_4 < V_3$$

while if $m > M$ we have the opposite. If $m = M$ the flavor group is no longer broken and we return to the phase diagram of [80].

To proceed let us assume $m < M$. The regions in the $\tilde{m} - \tilde{M}$ plane for which symmetry breaking of either type will occur is (up to a factor of 4) are given by $\mathcal{I}_1 \times \mathbb{R}^{m<M}$ and $\mathbb{R}^{m<M} \times \mathcal{I}_4$, respectively, where we defined

$$\mathbb{R}^{m<M} \equiv \{(M, m) \in \mathbb{R}^2 \,|\, m < M\}.$$

One can see that for $\tilde{M}/4 \in \mathcal{I}_4$, we have $\tilde{M} < 0$ except for some small interval $[0, N_f/2 - f]$ if $f < N_f/2$. Similarly, if $\tilde{m}/4 \in \mathcal{I}_1$, then $\tilde{m} > 0$ except for some small interval $[N_f/2 - f, 0]$ if $f > N_f/2$. This shows that *most* of the region where the f fermions condense are for positive values of $\tilde{m}$ while the regions where the other $N_f - f$ fermions condense are for negative values of $\tilde{M}$! And since we restrict our attention to the regions $m < M$, we know that in the first quadrant, we get Grassmannians of the form $\mathcal{M}(f, p)$ and in the third quadrant, we get Grassmannians of the form $\mathcal{M}(N_f - f, q)$. In both cases, as you tune $\tilde{m}$ or $\tilde{M}$, you encounter a series of first order phase transitions which bring you through each Grassmannian until you wind up in the asymptotic, topological phase as in [80]. We can repeat the analysis for $M > m$ and find a similar phenomenon, except now we get Grassmannians of the form $\mathcal{M}(f, p)$ for negative values of $\tilde{m}$ and Grassmannians of the form $\mathcal{M}(N_f - f, q)$ for positive values of $\tilde{M}$.

The resulting phase diagram is given in figure 4.13 Each line represents a transition between Grassmannians, and they are colored according to the component of $\partial\mathcal{D}$ on which the transitions occur. Namely, blue corresponds to $\partial\mathcal{D}_1$, pink to $\partial\mathcal{D}_4$, green to $\partial\mathcal{D}_2$ and red to $\partial\mathcal{D}_3$. The low energy theory in each region is

$$\begin{aligned}
\text{Blue:} \quad & \mathcal{M}(f,p)\otimes SU(N)_{\frac{N_f}{2}-p} \text{ with } p=\frac{N_f}{2}-[\![\frac{\tilde{m}}{4}]\!] \\
\text{Pink:} \quad & \mathcal{M}(N_f-f,q)\otimes SU(N)_{N_f/2-f-q} \text{ with } q=\frac{N_f}{2}-f-[\![\frac{\tilde{M}}{4}]\!] \\
\text{Green:} \quad & \mathcal{M}(f,p)\otimes SU(N)_{f-\frac{N_f}{2}-p} \text{ with } p=f-\frac{N_f}{2}-[\![\frac{\tilde{m}}{4}]\!] \\
\text{Red:} \quad & \mathcal{M}(N_f-f,q)\otimes SU(N)_{N_f/2-q} \text{ with } q=\frac{N_f}{2}-[\![\frac{\tilde{M}}{4}]\!].
\end{aligned} \tag{4.66}$$

These are subject to the isomorphism $\mathcal{M}(N,M)\simeq\mathcal{M}(N,N-M)$. Since we have chosen p and q to represent the number of $+1$ eigenvalues of our condensate, this isomorphism simply puts things in terms of the number of -1 eigenvalues. Physically these are equivalent. The black diagonal represents the flavor symmetric case studied in [80] where the stars represent the phase transitions along that line. In the flavor symmetric case, these were special points where two Grassmannian phases become degenerate. Now, they are phases where six different Grassmannians become degenerate. The vacuum one winds up in depends on the direction in the $M-m$ plane that you approach this point. For instance, if you tune along the $m<M$ from above or below, you wind up in a vacuum of the form $\mathcal{M}(f,p)$, while if you tune along the $m=M$ from above or below you wind up in in $\mathcal{M}(N_f,p)$. In general, if we have n different masses there will be $2n$ degenerate vacua at these special values of the mass.

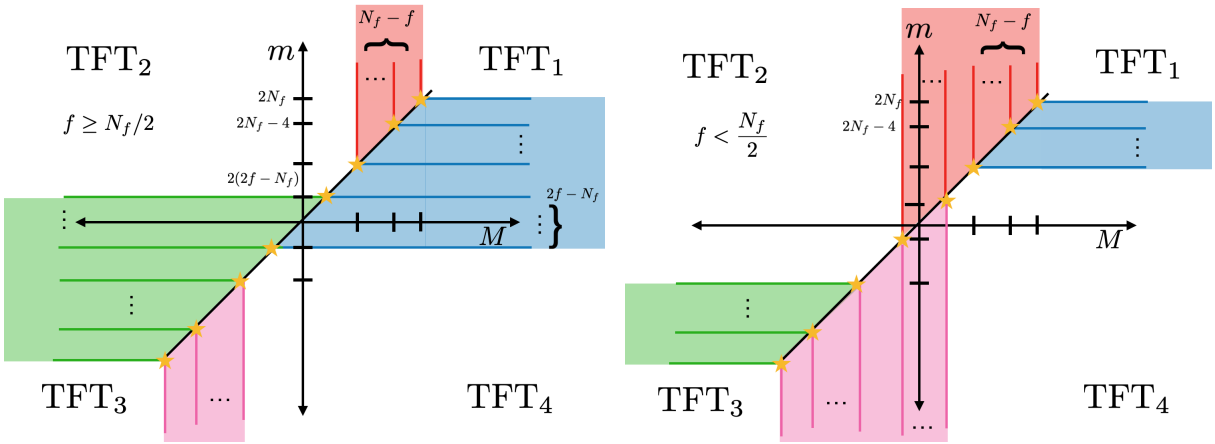

(a) Phase diagram for $f < N_f/2$

(b) Phase diagram for $f \geq N_f/2$

Figure 4.13: Phase diagrams for QCD_3 with an explicitly broken flavor symmetry. The various TFTs shown are $SU(N)$ Chern-Simons gauge theory with level $k + \frac{1}{2}(\text{sgn}(m)f + \text{sgn}(M)(N_f - f))$. The shaded regions represent the Grassmannians as explained in eq. (4.67)

One interesting part of the phase diagram in figure 4.13 is the part where $\mathcal{I}_1 \cap \mathcal{I}_2 \neq \emptyset$ (or $\mathcal{I}_3 \cap \mathcal{I}_4 \neq \emptyset$ if $f < N_f/2$). As we mentioned previously, these low energy theories are determined by which mass is larger. Interestingly, although perhaps not surprisingly, these theories are not equivalent and are related by a time-reversal-symmetry transformation. To see this note that the in the region of overlap, the blue Grassmannians are of the form $\mathcal{M}(f, f-p) \otimes SU(N)_{N_f/2-f+p}$ while the green Grassmannians are of the form $\mathcal{M}(f, p) \otimes SU(N)_{f-N_f/2-p}$. The Grassmannians are equivalent due to the isomorphism we discussed above, but the the Chern-Simons TFTs are related to each other by a time reversal operation! Thus, as one smoothly varies m from $M-\epsilon$ to $m+\epsilon$, one should encounter a domain wall with extra light matter, even though the massless degrees of freedom on both sides are equivalent. Constructing such domain wall solutions is interesting but is beyond the scope of this work. If one includes a non-zero Chern-Simons level, then the TFTs are no longer related by a time reversal symmetry, but one should get a domain wall solution regardless.

In addition to this analytic derivation, we also include some numerical evidence for a specific choice of N_f and f. We find perfect agreement with our analysis in this particular case, as well as for numerous other choices. For brevity we only include the one.

Matching Onto the Finite N Solution

As a check, we would like to match onto the flavor broken phase diagram of [22, 16]. This is not entirely possible, however, due to the fact that the adding a Chern-Simons term does not alter the shape of the phase diagram, only the location in the plane where the transitions occurs. However, as noted in [17] the finite N symmetry broken phase is still present in the large N solution and is distinguished by the fact that it is the phase which has vanishing Chern-Simons level for it's decoupled TFT. When $k = 0$, this occurs at $p = N_f/2$ giving the symmetry broken phase first discussed in [110, 109]. At non-zero k, this occurs when $p = k+N_f/2$, giving the phase discussed in [80]. Thus, one consistency check we can perform is to see if the classical flavor-broken Grassmannians discussed in [22, 16] (and shown in 4.11) are accompanied by $SU(N)_0$ for the relevant parameter regimes.

To proceed, we find for what values of p or q the Chern-Simons level vanish, and find the values of k for which this confining theory exists. We get:

$$\begin{aligned}
\text{Blue: } & p = k + \frac{N_f}{2} \text{ exists when } -\frac{N_f}{2} \leq k \leq f - \frac{N_f}{2} \\
\text{Pink: } & q = k + \frac{N_f}{2} - f \text{ exists when } f - \frac{N_f}{2} \leq k \leq \frac{N_f}{2} \\
\text{Green: } & p = k + f - \frac{N_f}{2} \text{ exists when } \frac{N_f}{2} - f \leq k \leq \frac{N_f}{2} \\
\text{Red: } & q = k + \frac{N_f}{2} - f \text{ exists when } -\frac{N_f}{2} \leq k \leq \frac{N_f}{2} - f.
\end{aligned} \tag{4.67}$$

Comparing these ranges to those discussed in section 4.4.1, we find the following:

i.) $f - \frac{N_f}{2} < k$, $\frac{N_f}{2} - f < k$— Green+ Pink

ii.) $f - \frac{N_f}{2} < k$, $\frac{N_f}{2} - f = k$—Pink only

iii.) $f - \frac{N_f}{2} < k$, $\frac{N_f}{2} - f > k$—Pink+Red

iv.) $f - \frac{N_f}{2} = k,\ \frac{N_f}{2} - f > k$—Red Only

v.) $f - \frac{N_f}{2} > k,\ \frac{N_f}{2} - f > k$—Blue + Red

vi.) $f - \frac{N_f}{2} = k, \frac{N_f}{2} - f = k$—None

As you can see, this perfectly matches with the phase diagrams in [22, 16] and figure 4.11.

4.6 Scalar Potentials and Double Condensation

When we pass to the scalar side of the large N QCD duality we encounter a number of difficulties. Specifically, the authors of [17] have argued that the usual quartic potential at finite N will not accurately capture the phase structure of large N QCD_3. They go on to construct a sextic potential at $\mathcal{O}(N)$ and $\mathcal{O}(1)$ which can reproduce the desired effects:

$$V_{\mathcal{O}(N)} \sim \sum_i y_i^2 (y_i^2 - 1)^2 \tag{4.68}$$

$$V_{\mathcal{O}(1)} \sim \sum_{i,j} (2y_i^2 - 1)(2y_j^2 - 1) \tag{4.69}$$

where y_i is the eigenvalue for the scalar vacuum expectation value. However, as was argued in [17], the coupling constants associated with eqs. (4.68) and (4.69) must be fine tuned to ensure consistency with the fermionic side. This is an unfortunate artifact, but the fact that it can be done for some choice of coefficients is reassuring.

When we break the flavor symmetry to the $U(f) \times U(N_f - f)$ subgroup we generally expect to operators which respect this new symmetry to be generated along the RG flow. On the fermion side of the duality, it is not clear *a priori* what these would be, since quartic potentials are classically irrelevant in 2+1D. For this we turn to the scalar side to see these effects. For simplicity we stick to $U(f) \times U(N_f - f)$ quartic potentials.

Let ϕ_1 represent the first f scalars and ϕ_2 the remaining $N_f - f$. Then, the two quartic

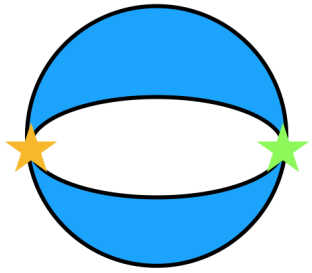

Figure 4.14: Diagram associated to the $U(f) \times U(N_f - f)$ invariant term discussed in section 4.6

$U(f) \times U(N_f - f)$ invariant potentials are

$$\mathcal{L} \supset \lambda \phi_{1I}^{\dagger b} \phi_{1I}^{a} \phi_{2J}^{\dagger a} \phi_{2J}^{b} \tag{4.70}$$

$$\supset \gamma \phi_{1I}^{\dagger a} \phi_{1I}^{a} \phi_{2J}^{\dagger b} \phi_{2J}^{b}. \tag{4.71}$$

Both of these involve double traces over the flavor indicies, while eq. (4.70) has a single trace over the gauge indicies. The index structure of eq. (4.71) indicates it should be part of the $\mathcal{O}(1)$ potential, since it involves separate gauge and flavor traces. Diagrams with this interaction will be included in the annulus diagram as discussed in section 4.4.

The more interesting term is eq. (4.70). Terms of this type have been discussed before in [9, 22]. Heuristically this term behaves as follows: when one set of scalars gets a vev from a negative mass deformation this term induces a mass for some of the components of the other group of scalars. In [22] it was argued that if this term is large enough it could prevent double condensation, since any negative mass deformation could not cancel the off the contribution from the induced mass. The gauge and flavor index structure makes it difficult to determine at which order this type of term should enter since diagrams containing this interaction are neither disk or annulus diagrams but instead are “eyeball" type diagrams as in figure 4.14. Since these are, in a sense, “ in between" a disk and annulus, we examine the effect of including this term at order N and order 1.

Consider the following forms of the vevs for the scalars. If the rank of the gauge group

is larger than the (broken) flavor group, the vev will look like:

$$\phi_1^{aI} = \begin{pmatrix} diag(x_1, ..., x_f) \\ 0 \end{pmatrix}, \ \phi_2^{aI} = \begin{pmatrix} diag(y_1, ..., y_{N_f - f}) \\ 0 \end{pmatrix}. \tag{4.72}$$

When this is multiplied out according to (4.70), we wind up with a term in the effective potential which looks like

$$V \supset \ \lambda \sum_{i=1}^{F} x_i^2 y_i^2 \tag{4.73}$$

where $F \equiv \min(f, N_f - f)$. If we include this term in the $O(1)$ potential, then we would be looking for the optimal configuration of 0's and 1's along the diagonal. This would add a term like $\lambda \min(p, q)$, where now p and q refer to the number of 1's on the diagonals of (4.72). to the minimization problem we have discussed. Again, there is no minimum in the interior of our domain in the $p - q$ plane and the absolute minimum must live on the boundary. On the components of the boundary where either p or q are zero, this term disappears and the analysis is the same as it was without the term. If we are on the other two boundaries, this term becomes something like λp or λq and will serve to simply shift the mass by $\tilde{m} \to \tilde{m} + \lambda/2$. Evidently, in either case the analysis is identical to the inclusion of a Chern-Simons term.

The more interesting case is when we include this term in the $\mathcal{O}(N)$ potential. In which case, we must minimize

$$V_{\mathcal{O}(N)} \sim \sum_{i=1}^{f} y_i^2 (y_i^2 - 1)^2 + \sum_{i=1}^{N_f - f} x_i^2 (x_i^2 - 1)^2 + \lambda \sum_{i=1}^{min(f, N_f - f)} y_i^2 x_i^2. \tag{4.74}$$

Again there are minimum at $x_,y_i = 0, 1$ however the eigenvalues are now correlated. For generic λ the minimum of eq. (4.74) occur at $(x_i, y_i) = (0, 1), (1, 0)$ and $(0, 0)$. Thus, if we choose the first p of the x's to be 1, we must take the first p of the y's to be 0. However, if we choose the first p x's to be 0, then we can choose the corresponding y's to be 0 or 1. Without adding any mass deformations, we thus have many degenerate Grassmannians which, generically, are of the form

$$\mathcal{M}(f, p) \times \mathcal{M}(N_f - f, q) \tag{4.75}$$

where $N_f - f - p \leq q \leq N_f - f$. If q does not fall within this range, we wind up with single condensation. Also, if we give ϕ_1 a positive mass deformation, it forces all the y's to 0 and we wind up with degenerate vacua as in section 4.5. If we give them a negative mass deformation, we force all the y's to be 1. This then restricts the allowed range of q and we do not have as many degenerate vacua.

One could further ask what happens if we include eq. (4.71) at $\mathcal{O}(1)$ in addition to eq. (4.70) at $\mathcal{O}(N)$. This gets messy and so we will not perform a full analysis here, but we do note that for generic values of λ the minimum again occurs on the boundary of the $p - q$ plane. However, there do exist regions of the $m - M$ phase diagram where double condensation at $\mathcal{O}(1)$ can occur for finely tuned values of γ. This is true with or without the inclusion of the λ term—the λ term only serves to restrict the number of Grassmannians one is allowed to traverse due to the correlation of the scalar vev eigenvalues. So again, we could engineer phases on the scalar side of the theory where double condensation can occur in the phase diagram. It is difficult to know if this symmetry breaking actually occurs for QCD_3 unless we can accurately calculate the anomalous dimensions of γ and λ. For now, we only note that with the inclusion of these symmetry breaking potentials, it is possible for both flavors of fermions to condense simultaneously.

4.7 Numerical Evidence for the Phase Diagram

Here we present a subset of numerical results which corroborate the phase diagram discussed in the main text. For simplicity, we choose $N_f = 6$ and $f = 4$ and $k = 0$. We stress that these choices do not impact the qualitative results, only the location and number of phase transitions, as well as the level of the accompanying Chern-Simons TFT. To demonstrate the lack of double condensation, we fix one mass and tune the other. This brings us along the three trajectories shown in figure 4.15. Note that as we tune the mass, the minimum value of the effective potential remains along the boundary of the table. This corresponds to values of p or q which exist along the boundary of the domain $\mathcal{D}$. The trajectories along fixed, positive $\tilde{m} \equiv \frac{mN}{4\Lambda\Delta}$ and $\tilde{M} \equiv \frac{MN}{4\Lambda\Delta}$ are related to those trajectories along fixed negative

$\tilde{m}$ and $\tilde{M}$ by a time reversal transformation. This maps $p \to f - p$ and $q \to N_f - f - q$, which serves to invert the rows and reverse the columns of tables 4.1,4.2 and 4.3

	$q=0$	1	2
$p=0$	-18	-32	-38
1	-14	-20	-18
2	-2	0	10
3	18	28	46
4	46	64	90

(a) $\tilde{M} = 3$ with vacuum $SU(N)_1$

	$q=0$	1	2
$p=0$	-26	-32	-30
1	-22	-20	-10
2	-10	0	18
3	10	28	54
4	38	64	98

(b) $\tilde{M} = 7$ with vacuum $\mathcal{M}(2,1) \otimes SU(N)_2$

	$q=0$	1	2
$p=0$	-34	-32	-22
1	-30	-20	-2
2	-18	0	26
3	2	28	62
4	30	64	106

(c) $\tilde{M} = 11$ with vacuum $SU(N)_3$

Table 4.1: Various values of the effective potential with $\tilde{m} = 12$. This follows trajectory 1 as shown in 4.15. The minimum is shown in red.

4.8 Discussion

In this chapter we have mapped out the phases of QCD_3 with a product flavor group of the form $U(f) \times U(N_f - f)$. We have found a rich structure which involves multiple complex Grassmannians in different regions of the (m, M) plane bounded by various Wilson-Fisher scalar theories. As f and F are tuned through k, some of these Grassmanians disappear and reappear in a different part of the (m, M) plane. We also showed how a certain $U(f) \times U(N_f - f)$ invariant potential, which is expected to be generated along the RG flow, leads to this rich structure on the scalar side. This discussion can be straightforwardly generalized to symplectic and orthogonal gauge groups, since their breaking pattern is qualitatively the same, albeit with different Grassmannians.

Recent work on the "standard" large N limit of QCD_3 has revealed an even richer quantum phase structure than previously imagined [17]. In short, the phase transitions between TFTs

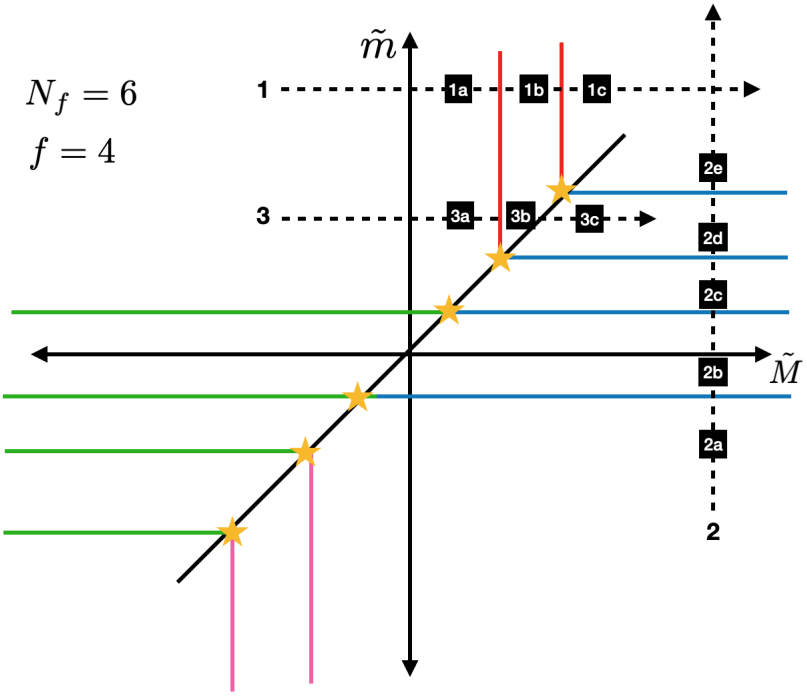

Figure 4.15: Phase diagram for $N_f = 6, f = 4$ with $k = 0$. Various effective potential at the indicated points along trajectories 1,2 and 3 shown are given in tables 4.1, 4.2 and 4.3.

and quantum phases gets resolved into a series of first order phase transitions as you dial the mass. It would be interesting to see the emergence and reemergence of various Grassmannians in this limit and see whether these transitions still occur or not.

One glaring unanswered question is how exactly we can see the transition between Grassmannians in the NLSM phase without mentioning the scalars. Indeed it should be the case that fermion mass deformations can be incorporated by adding a mass term for the fundamental fields of the Grassmannians, as was proposed in [80]. Upon first attempt this procedure looked promising, but it lacked a crucial ingredient unique to 2+1D fermionic theories: the difference in positive and negative mass deformations for the fermions and their effect on the Chern-Simons level. Perhaps this point reflects the author's ignorance on the finer points of Grassmannian geometry. Nevertheless this is something that would be

interesting to work out in all gory detail.

There are still a lot of interesting questions to be answered, most pressing is the actual order of the phase transitions. We believe that this can be explored by a large N, k, N_f analysis or by studying the structure of the Grassmannians as a continuous function of the dimension. In addition, perhaps this work can be extended to the case of $U(N)_k$ with fermions by gauging a global $U(1)$ symmetry and bringing it to the other side of (**??**). This will surely change the form of the Grassmannian, but it may allow us to study the duality in the Abelian limit where calculations are slightly easier. We could also imagine coupling our QCD_3 to scalar matter as in [24, 64]. Another interesting question is the lack of double condensation in the Grassmannian regime. While this question has been explored in detail in [16] using the gauged sigma model, it would be interesting to explore this from the fermionic perspective in spirit to the analysis of [110]. In particular, is there a Vafa-Witten like theorem for non-zero Chern-Simons level?

Further, we studied the large N limit of QCD_3 as a function of two distinct masses. We find that there exists multiple Grassmannians separated by a series of first order phase transitions in certain portions of the phase diagram. These are consistent with the phase diagrams at finite N laid out in [22, 16]. We find a plethora of interesting physics, including multiple degenerate Grassmannians at special values on the mass, degenerate symmetric and symmetry broken phases, and lack of double condensation for unmodified scalar potentials. Additionally, we consider the effect of quartic interactions which may possibly be generated along the RG flow and find that double condensation is possible for finely tuned values of the interaction strength.

An interesting extension to this work is to find a more rigorous argument for the lack of double condensation without the modified scalar potentials. Perhaps there is a deeper reason for this other than the lack of solution for p and q on the interior of the domain $\mathcal{D}$. It does not seem to be forbidden by an f-theorem or anomaly matching type argument, at least not that the author can work out. The generation of $U(f) \times U(N_f - f)$ terms in the scalar potential may be indication that no such general argument exists. Still, it might be

worth investigating further. Additionally, it would be interesting to attempt to compute the anomalous dimensions of these extra terms in the scalar potential to determine if they even get generated along the RG flow. If not, this could be further indication of a more fundamental reason for lack of double condensation.

The rich structure of this phase diagram lends itself nicely to the study of domain walls between Grassmannians. For instance, fix the magnitude of the mass of $f-1$ of the flavors and tuning the mass of the remaining fermion from $m \to M$, we encounter a domain wall with extra light matter living on it. What is the nature of this matter? Does it couple to the Grassmannians? These are questions which are beyond the scope of this work but seem interesting enough to warrant further investigation.

	$q=0$	1	2
$p=0$	26	36	54
1	-4	14	40
2	-26	0	34
3	-40	-6	36
4	-46	-4	46

(a) $\tilde{m} = -5$ with vacuum $SU(N)_{-1}$

	$q=0$	1	2
$p=0$	10	20	38
1	-12	6	32
2	-26	0	34
3	-32	2	44
4	-30	12	62

(b) $\tilde{m} = -1$ with vacuum $\mathcal{M}(4,3) \otimes SU(N)_0$

	$q=0$	1	2
$p=0$	-6	4	22
1	-20	-2	24
2	-26	0	34
3	-24	10	52
4	-14	28	78

(c) $\tilde{m} = 3$ with vacuum $\mathcal{M}(4,2) \otimes SU(N)_1$

	$q=0$	1	2
$p=0$	-22	-12	6
1	-28	-10	16
2	-26	0	34
3	-16	18	60
4	2	44	94

(d) $\tilde{m} = 7$ with vacuum $\mathcal{M}(4,1) \otimes SU(N)_2$

	$q=0$	1	2
$p=0$	-38	-28	-10
1	-36	-18	8
2	-26	0	34
3	-8	26	68
4	18	60	110

(e) $\tilde{m} = 11$ with vacuum $SU(N)_3$

Table 4.2: Various values of the effective potential with $\tilde{M} = 15$. This follows trajectory 2 as shown in 4.15. The minimum is shown in red.

	$q=0$	1	2
$p=0$	-2	-16	-22
1	-6	-12	-10
2	-2	0	10
3	10	20	38
4	30	48	74

(a) $\tilde{M}=3$ with vacuum $SU(N)_1$

	$q=0$	1	2
$p=0$	-10	-16	-14
1	-14	-12	-2
2	-10	0	18
3	2	20	46
4	22	48	82

(b) $\tilde{M}=7$ with vacuum $\mathcal{M}(2,1)\otimes SU(N)_2$

	$q=0$	1	2
$p=0$	-18	-16	-6
1	-22	-12	6
2	-18	0	26
3	-6	20	54
4	14	48	90

(c) $\tilde{M}=11$ with vacuum $\mathcal{M}(4,1)\otimes SU(N)_2$

Table 4.3: Various values of the effective potential with $\tilde{m}=11$. This follows trajectory 3 as shown in figure 4.15. The minimum is shown in red.

Chapter 5

CONCLUSION

In this work we examined the dynamics and phases of 2+1 dimensional gauge theories using a variety of tools from particle and string theory. At the heart of these explorations was a set of dualities relating the dynamics of non-Abelian gauge theories with fermions to those with scalars. These dualities map non-perturbative excitations in one of the theories to baryonic degrees of freedom in the other.

In chapter 2 we explored the behavior of boundary degrees of freedom under the duality map. For this we focused on the Abelian limit of the bosonization dualities, while the non-Abelian story was worked out by collaborators of the author in [13]. An important part of this story was the behavior of i) dual boundary conditions and ii) edge modes associated to non-dynamical Chern-Simons terms. To address these issues, we examine how boundary conditions for the matter fields and dynamical gauge fields map across the duality. Boundary conditions for fermions and scalars are rather different. The latter admits the usual Neumann and Dirichlet boundary conditions, while the former sets one or the other components of the fermions to zero. In all cases, that is for the fermion+flux=scalar and scalar+flux=fermion seed dualities, the scalar must have Dirichlet boundary conditions. The fermion, on the hand, changes it's boundary conditions depending on the seed duality. Additionally the gauge fields undergo the analogous "Neumann" conditions for a gauge field, when gauge flux can flow off perpendicular to the boundary.

In addition to the explicit boundary conditions for the matter fields, we must also shift the perspective on how we view the background Chern-Simons terms in the action. Based on the discussion in chapter 1, these fields can come from the integrating out of massive fermions. We found this perspective to be necessary when accounting for the edge modes on

either side of the duality, since, a priori, chiral edge modes are not possible for pure scalar theories. These “fiducial fermions" account for how the edge modes behave under the duality. They are also necessary for the non-Abelian master duality boundary conditions explored in [13].

In chapter 3 we use both bosonization dualities and holography to derive a family of dualities between quiver gauge theories. These exotic gauge theories arise in the study of domain walls in 3+1 d Yang-Mills and QCD when studying anomalies associated to a spatially varying theta angle. Depending on the size of the gradient of this angle, these domain walls could be stacked almost on top of one another or separated at distinct locations in space. The resulting 2+1D field theories which live on these walls can then be described by a quiver gauge theory, where the mass deformations of the bifundamental scalars determine the exact theories on the walls. Our dualities, however, are more general than the ones that arise in this particular application.

Two important technical points come from the dicussions in 3.2.1 and 3.4.1. In the former, we argued that these non-Abelian quiver dualities should be viewed as non-Abelian generalizations of the well known Abelian particle/vortex duality [95, 42]. As discussed around eq. (3.16), this interpretation simply comes from deriving the Abelian particle/vortex duality from the Abelian seed dualities and performing an analogous computation in the non-Abelian generalizations. Doing so, and keeping careful account of the global Abelian symmetries, shows that indeed the two node non-Abelian quiver and it's bosonized dual behave analogously to the Abelian particle/vortex duality.

The other important technical achievement comes from 3.4.1. There, we studied a 2+1D $SU(N)_k$ gauge theory coupled to fermions and scalars and extended the number of fermions beyond the flavor bound. The result was a rich phase diagram which can be considered as a natural extension of the master duality beyond one of its flavor bounds. An interesting part of this story is the emergence of several critical lines, where singlet fermions become massless in the symmetry broken phases. The result is a set of massless bosons stemming from spontaneous symmetry breaking, and decoupled massless fermions which shift the levels

of background Chern-Simons terms. Further, there are two such lines of singlet fermions, although they combine into one in the center of the phase diagram.

Finally, in chapter 4 we studied the symmetry breaking scenarios of QCD_3 beyond the flavor bound with a product flavor group. Such a product flavor group can be constructed in many ways, such as coupling two sets of identical fermions to differing background $U(1)$ fields, or giving each group of fermions a distinct mass. The result was a rich phase diagram which depends heavily on the differing sizes of the two groups of fermions and their relation to the level. For generic values of the size of the groups, there are three coexisting Grassmannian regions in differing parts of the phase diagrams. As the size of the groups change the Grassmannian regions will disappear and reappear in a different part of the phase diagram.

We then extended the flavor broken analysis to the large N limit as in [17]. Our results were not only consistent with theirs, but also agree with the finite N flavor broken phase diagram. This is owed to the fact that there has been a secret, decoupled Chern-Simons gauge theory sitting with the Grassmannians in the finite N case. In the finite N picture, however, we do not resolve these decoupled Chern-Simons terms since their level is vanishing and thus confining. The would-be low energy degrees of freedom then get gapped out and the resulting theory is trivial. In the large N story, these decoupled CS theories play an important role, since one traverses each possible Grassmannian as one tunes the value of the mass. The important part of this is the fact that the finite N Grassmannians are precisely the ones for which those decoupled CS theories vanish, which makes sense why they are unimportant and nearly impossible to detect in the finite N analysis alone.

Common to all these works is their pertinence to the world of 2+1D gauge theories. As of right now these can be considered purely theoretical works, with the possible exception of the Abelian gauge theories of chapter 2. However, as experimentalists continue to engineer exotic 2d materials with interesting properties, we hope that our results can be realized in a controlled laboratory setting to test their validity. Already there exist a number of interesting such materials which realize emergent gauge fields as their low energy description. It is the author's hope that non-Abelian gauge fields can be engineered in a similar way, and our

dualities can be used to derive useful properties for them.

Still, as with any theoretical pursuit, we mostly hope that this work will be useful and inspiring to others taking up the task of analyzing and discovering exciting new properties of 2+1D gauge theories. Our work, while not at all exhaustive, is now part of the pantheon of 2+1 bosonization dualities and their applications.

BIBLIOGRAPHY

[1] Bobby Samir Acharya and Cumrun Vafa. On domain walls of N=1 supersymmetric Yang-Mills in four-dimensions. 2001.

[2] Ofer Aharony. Baryons, monopoles and dualities in Chern-Simons-matter theories. *JHEP*, 02:093, 2016.

[3] Ofer Aharony, Francesco Benini, Po-Shen Hsin, and Nathan Seiberg. Chern-Simons-matter dualities with SO and USp gauge groups. *JHEP*, 02:072, 2017.

[4] Ofer Aharony, Oren Bergman, Daniel Louis Jafferis, and Juan Maldacena. N=6 superconformal Chern-Simons-matter theories, M2-branes and their gravity duals. *JHEP*, 10:091, 2008.

[5] Ofer Aharony, Guy Gur-Ari, and Ran Yacoby. Correlation Functions of Large N Chern-Simons-Matter Theories and Bosonization in Three Dimensions. *JHEP*, 12:028, 2012.

[6] Ofer Aharony, Guy Gur-Ari, and Ran Yacoby. d=3 Bosonic Vector Models Coupled to Chern-Simons Gauge Theories. *JHEP*, 03:037, 2012.

[7] Kyle Aitken, Andrew Baumgartner, Changha Choi, and Andreas Karch. Generalization of QCD_3 Symmetry Breaking and Flavored Quiver Dualities. *In preperation.*

[8] Kyle Aitken, Andrew Baumgartner, Changha Choi, and Andreas Karch. Generalization of QCD_3 symmetry-breaking and flavored quiver dualities. *JHEP*, 02:060, 2020.

[9] Kyle Aitken, Andrew Baumgartner, and Andreas Karch. Novel 3d bosonic dualities from bosonization and holography. *JHEP*, 09:003, 2018.

[10] Kyle Aitken, Andrew Baumgartner, Andreas Karch, and Brandon Robinson. 3d Abelian Dualities with Boundaries. *JHEP*, 03:053, 2018.

[11] Kyle Aitken, Changha Choi, and Andreas Karch. New and Old Fermionic Dualities from 3d Bosonization. *JHEP*, 01:035, 2020.

[12] Kyle Aitken, Andreas Karch, and Brandon Robinson. Deconstructing S-Duality. *SciPost Phys.*, 4:032, 2018.

[13] Kyle Aitken, Andreas Karch, and Brandon Robinson. Master 3d Bosonization Duality with Boundaries. 2018.

[14] Thomas Appelquist and Daniel Nash. Critical Behavior in (2+1)-dimensional QCD. *Phys. Rev. Lett.*, 64:721, 1990.

[15] Riccardo Argurio, Matteo Bertolini, Francesco Bigazzi, Aldo L. Cotrone, and Pierluigi Niro. QCD domain walls, Chern-Simons theories and holography. 2018.

[16] Riccardo Argurio, Matteo Bertolini, Francesco Mignosa, and Pierluigi Niro. Charting the phase diagram of $\mathrm{QCD}_{\mathbf{3}}$. 2019.

[17] Adi Armoni, Thomas T. Dumitrescu, Guido Festuccia, and Zohar Komargodski. Metastable Vacua in Large-N QCD_3. 2019.

[18] Adi Armoni and Vasilis Niarchos. QCD_3 with two-index quarks, mirror symmetry, and fivebrane anti-BIons near orientifolds. *Phys. Rev. D*, 98(11):114009, 2018.

[19] M. Atiyah, R. Bott, and V. K. Patodi. On the heat equation and the index theorem. *Inventiones mathematicae*, 19(4):279–330, Dec 1973.

[20] Lorenzo Bartolini, Francesco Bigazzi, Stefano Bolognesi, Aldo L. Cotrone, and Andrea Manenti. Theta dependence in Holographic QCD. *JHEP*, 02:029, 2017.

[21] Vladimir Bashmakov, Francesco Benini, Sergio Benvenuti, and Matteo Bertolini. Living on the walls of super-QCD. 2018.

[22] Andrew Baumgartner. Phases of Flavor Broken QCD_3. 2019.

[23] Andrew Baumgartner and Brandon Robinson. *Work in progress*, 2017.

[24] Francesco Benini. Three-dimensional dualities with bosons and fermions. *JHEP*, 02:068, 2018.

[25] Francesco Benini, Po-Shen Hsin, and Nathan Seiberg. Comments on global symmetries, anomalies, and duality in (2 + 1)d. *JHEP*, 04:135, 2017.

[26] Curtis G. Callan, Jr. and Jeffrey A. Harvey. Anomalies and Fermion Zero Modes on Strings and Domain Walls. *Nucl. Phys.*, B250:427–436, 1985.

[27] Jing-Yuan Chen, Jun Ho Son, Chao Wang, and S. Raghu. Exact Boson-Fermion Duality on a 3D Euclidean Lattice. 2017.

[28] Jing-Yuan Chen and Max Zimet. Strong-Weak Chern-Simons-Matter Dualities from a Lattice Construction. 2018.

[29] Wei Chen, Matthew P. A. Fisher, and Yong-Shi Wu. Mott transition in an anyon gas. *Phys. Rev.*, B48:13749–13761, 1993.

[30] Yu-An Chen, Anton Kapustin, and Đorđe Radičević. Exact bosonization in two spatial dimensions and a new class of lattice gauge theories. *Annals of Physics*, 393:234 – 253, 2018.

[31] Shai M. Chester, Luca V. Iliesiu, Mark Mezei, and Silviu S. Pufu. Monopole Operators in $U(1)$ Chern-Simons-Matter Theories. *JHEP*, 05:157, 2018.

[32] Changha Choi. Phases of Two Adjoints QCD_3 And a Duality Chain. *JHEP*, 04:006, 2020.

[33] Changha Choi, Diego Delmastro, Jaume Gomis, and Zohar Komargodski. Dynamics of QCD_3 with Rank-Two Quarks And Duality. 2018.

[34] Changha Choi, Martin Rocek, and Adar Sharon. Dualities and Phases of $3DN = 1$ SQCD. *JHEP*, 10:105, 2018.

[35] Chong-Sun Chu and Douglas J. Smith. Multiple Self-Dual Strings on M5-Branes. *JHEP*, 01:001, 2010.

[36] Sidney R. Coleman. The Quantum Sine-Gordon Equation as the Massive Thirring Model. *Phys. Rev.*, D11:2088, 1975.

[37] Clay Cordova, Po-Shen Hsin, and Kantaro Ohmori. Exceptional Chern-Simons-Matter Dualities. 2018.

[38] Clay Cordova, Po-Shen Hsin, and Nathan Seiberg. Global Symmetries, Counterterms, and Duality in Chern-Simons Matter Theories with Orthogonal Gauge Groups. *SciPost Phys.*, 4(4):021, 2018.

[39] Csaba Csaki, Christophe Grojean, Jay Hubisz, Yuri Shirman, and John Terning. Fermions on an interval: Quark and lepton masses without a Higgs. *Phys. Rev.*, D70:015012, 2004.

[40] Csaba Csaki, Christophe Grojean, Hitoshi Murayama, Luigi Pilo, and John Terning. Gauge theories on an interval: Unitarity without a Higgs. *Phys. Rev.*, D69:055006, 2004.

[41] Clay Córdova, Po-Shen Hsin, and Nathan Seiberg. Time-Reversal Symmetry, Anomalies, and Dualities in $(2+1)d$. *SciPost Phys.*, 5(1):006, 2018.

[42] C. Dasgupta and B. I. Halperin. Phase Transition in a Lattice Model of Superconductivity. *Phys. Rev. Lett.*, 47:1556–1560, 1981.

[43] Markus Dierigl and Alexander Pritzel. Topological Model for Domain Walls in (Super-)Yang-Mills Theories. *Phys. Rev.*, D90(10):105008, 2014.

[44] Gerald V. Dunne. Aspects of Chern-Simons theory. In *Les Houches Summer School in Theoretical Physics, Session 69: Topological Aspects of Low-dimensional Systems*, 7 1998.

[45] Eduardo H. Fradkin. Field Theories of Condensed Matter Physics. *Front. Phys.*, 82:1–852, 2013.

[46] Eduardo H. Fradkin and Fidel A. Schaposnik. The Fermion - boson mapping in three-dimensional quantum field theory. *Phys. Lett.*, B338:253–258, 1994.

[47] Mitsutoshi Fujita, Wei Li, Shinsei Ryu, and Tadashi Takayanagi. Fractional Quantum Hall Effect via Holography: Chern-Simons, Edge States, and Hierarchy. *JHEP*, 06:066, 2009.

[48] Davide Gaiotto. Boundaries, interfaces and dualities. *talk at Natifest, Princeton, September 2016.*

[49] Davide Gaiotto, Anton Kapustin, Zohar Komargodski, and Nathan Seiberg. Theta, Time Reversal, and Temperature. *JHEP*, 05:091, 2017.

[50] Davide Gaiotto, Zohar Komargodski, and Nathan Seiberg. Time-reversal breaking in QCD_4, walls, and dualities in 2 + 1 dimensions. *JHEP*, 01:110, 2018.

[51] Simone Giombi, Shiraz Minwalla, Shiroman Prakash, Sandip P. Trivedi, Spenta R. Wadia, and Xi Yin. Chern-Simons Theory with Vector Fermion Matter. *Eur. Phys. J.*, C72:2112, 2012.

[52] Simone Giombi and Xi Yin. Higher Spin Gauge Theory and Holography: The Three-Point Functions. *JHEP*, 09:115, 2010.

[53] Simone Giombi and Xi Yin. The Higher Spin/Vector Model Duality. *J. Phys.*, A46:214003, 2013.

[54] Maarten F. L. Golterman, Karl Jansen, and David B. Kaplan. Chern-Simons currents and chiral fermions on the lattice. *Phys. Lett.*, B301:219–223, 1993.

[55] Jaume Gomis, Zohar Komargodski, and Nathan Seiberg. Phases Of Adjoint QCD_3 And Dualities. *SciPost Phys.*, 5(1):007, 2018.

[56] Guy Gur-Ari, Sean A. Hartnoll, and Raghu Mahajan. Transport in Chern-Simons-Matter Theories. *JHEP*, 07:090, 2016.

[57] Guy Gur-Ari and Ran Yacoby. Three Dimensional Bosonization From Supersymmetry. *JHEP*, 11:013, 2015.

[58] Po-Shen Hsin and Nathan Seiberg. Level/rank Duality and Chern-Simons-Matter Theories. *JHEP*, 09:095, 2016.

[59] Toshiya Imoto, Tadakatsu Sakai, and Shigeki Sugimoto. O(N(c)) and USp(N(c)) QCD from String Theory. *Prog. Theor. Phys.*, 122:1433–1453, 2010.

[60] Karthik Inbasekar, Sachin Jain, Subhajit Mazumdar, Shiraz Minwalla, V. Umesh, and Shuichi Yokoyama. Unitarity, crossing symmetry and duality in the scattering of $\mathcal{N} = 1$ susy matter Chern-Simons theories. *JHEP*, 10:176, 2015.

[61] Sachin Jain, Mangesh Mandlik, Shiraz Minwalla, Tomohisa Takimi, Spenta R. Wadia, and Shuichi Yokoyama. Unitarity, Crossing Symmetry and Duality of the S-matrix in large N Chern-Simons theories with fundamental matter. *JHEP*, 04:129, 2015.

[62] Sachin Jain, Shiraz Minwalla, and Shuichi Yokoyama. Chern Simons duality with a fundamental boson and fermion. *JHEP*, 11:037, 2013.

[63] Karl Jansen and Martin Schmaltz. Critical momenta of lattice chiral fermions. *Phys. Lett.*, B296:374–378, 1992.

[64] Kristan Jensen. A master bosonization duality. *JHEP*, 01:031, 2018.

[65] Kristan Jensen and Andreas Karch. Bosonizing three-dimensional quiver gauge theories. *JHEP*, 11:018, 2017.

[66] Kristan Jensen and Andreas Karch. Embedding three-dimensional bosonization dualities into string theory. *JHEP*, 12:031, 2017.

[67] Chao-Ming Jian, Zhen Bi, and Yi-Zhuang You. Lattice Construction of Duality with Non-Abelian Gauge Fields in 2+1D. 2018.

[68] Shamit Kachru, Michael Mulligan, Gonzalo Torroba, and Huajia Wang. Bosonization and Mirror Symmetry. *Phys. Rev.*, D94(8):085009, 2016.

[69] Shamit Kachru, Michael Mulligan, Gonzalo Torroba, and Huajia Wang. Nonsupersymmetric dualities from mirror symmetry. *Phys. Rev. Lett.*, 118(1):011602, 2017.

[70] David B. Kaplan. A Method for simulating chiral fermions on the lattice. *Phys. Lett.*, B288:342–347, 1992.

[71] David B. Kaplan. Chiral Symmetry and Lattice Fermions. In *Modern perspectives in lattice QCD: Quantum field theory and high performance computing. Proceedings, International School, 93rd Session, Les Houches, France, August 3-28, 2009*, pages 223–272, 2009.

[72] Anton Kapustin and Matthew J. Strassler. On mirror symmetry in three-dimensional Abelian gauge theories. *JHEP*, 04:021, 1999.

[73] Avner Karasik and Zohar Komargodski. The Bi-Fundamental Gauge Theory in 3+1 Dimensions: The Vacuum Structure and a Cascade. 2019.

[74] Andreas Karch and Emanuel Katz. Adding flavor to AdS / CFT. *JHEP*, 06:043, 2002.

[75] Andreas Karch, Brandon Robinson, and David Tong. More Abelian Dualities in 2+1 Dimensions. *JHEP*, 01:017, 2017.

[76] Andreas Karch and David Tong. Particle-Vortex Duality from 3d Bosonization. *Phys. Rev.*, X6(3):031043, 2016.

[77] Andreas Karch, David Tong, and Carl Turner. Mirror Symmetry and Bosonization in 2d and 3d. *JHEP*, 07:059, 2018.

[78] Abdullah Khalil and Radu Tatar. Phases of QCD_3 with three families of fundamental flavours. 1 2020.

[79] K. v. Klitzing, G. Dorda, and M. Pepper. New method for high-accuracy determination of the fine-structure constant based on quantized hall resistance. *Phys. Rev. Lett.*, 45:494–497, Aug 1980.

[80] Zohar Komargodski and Nathan Seiberg. A symmetry breaking scenario for QCD_3. *JHEP*, 01:109, 2018.

[81] Pedro Liendo, Leonardo Rastelli, and Balt C. van Rees. The Bootstrap Program for Boundary CFT_d. *JHEP*, 07:113, 2013.

[82] Martin Luscher. The Schrodinger functional in lattice QCD with exact chiral symmetry. *JHEP*, 05:042, 2006.

[83] Juan Martin Maldacena. The Large N limit of superconformal field theories and supergravity. *Int. J. Theor. Phys.*, 38:1113–1133, 1999. [Adv. Theor. Math. Phys.2,231(1998)].

[84] Max A. Metlitski. S-duality of $u(1)$ gauge theory with $\theta = \pi$ on non-orientable manifolds: Applications to topological insulators and superconductors. 2015.

[85] Max A. Metlitski and Ashvin Vishwanath. Particle-vortex duality of two-dimensional Dirac fermion from electric-magnetic duality of three-dimensional topological insulators. *Phys. Rev.*, B93(24):245151, 2016.

[86] Shiraz Minwalla and Shuichi Yokoyama. Chern Simons Bosonization along RG Flows. *JHEP*, 02:103, 2016.

[87] Gregory W. Moore and Nathan Seiberg. Taming the Conformal Zoo. *Phys. Lett. B*, 220:422–430, 1989.

[88] David F Mross, Jason Alicea, and Olexei I Motrunich. Explicit derivation of duality between a free dirac cone and quantum electrodynamics in (2+ 1) dimensions. *Physical review letters*, 117(1):016802, 2016.

[89] David F. Mross, Jason Alicea, and Olexei I. Motrunich. Explicit derivation of duality between a free Dirac cone and quantum electrodynamics in (2+1) dimensions. *Phys. Rev. Lett.*, 117(1):016802, 2016.

[90] David F. Mross, Jason Alicea, and Olexei I. Motrunich. Symmetry and duality in bosonization of two-dimensional Dirac fermions. 2017.

[91] Jeff Murugan and Horatiu Nastase. Particle-vortex duality in topological insulators and superconductors. 2016.

[92] Werner Müller. Eta invariants and manifolds with boundary. *J. Differential Geom.*, 40(2):311–377, 1994.

[93] M. Nakahara. *Geometry, topology and physics*. 2003.

[94] Tadashi Okazaki and Satoshi Yamaguchi. Supersymmetric boundary conditions in three-dimensional N=2 theories. *Phys. Rev.*, D87(12):125005, 2013.

[95] Michael E. Peskin. Mandelstam 't Hooft Duality in Abelian Lattice Models. *Annals Phys.*, 113:122, 1978.

[96] Alexander M. Polyakov. Fermi-Bose Transmutations Induced by Gauge Fields. *Mod. Phys. Lett.*, A3:325, 1988.

[97] A.M. Polyakov. Quark confinement and topology of gauge theories. *Nuclear Physics B*, 120(3):429 – 458, 1977.

[98] Subir Sachdev, Harley D. Scammell, Mathias S. Scheurer, and Grigory Tarnopolsky. Gauge theory for the cuprates near optimal doping. *Phys. Rev. B*, 99(5):054516, 2019.

[99] Tadakatsu Sakai and Shigeki Sugimoto. Low energy hadron physics in holographic QCD. *Prog. Theor. Phys.*, 113:843–882, 2005.

[100] Julian Schwinger. Gauge invariance and mass. ii. *Phys. Rev.*, 128:2425–2429, Dec 1962.

[101] Nathan Seiberg, T. Senthil, Chong Wang, and Edward Witten. A Duality Web in 2+1 Dimensions and Condensed Matter Physics. *Annals Phys.*, 374:395–433, 2016.

[102] Nathan Seiberg and Edward Witten. Gapped Boundary Phases of Topological Insulators via Weak Coupling. *PTEP*, 2016(12):12C101, 2016.

[103] N. Shaji, R. Shankar, and M. Sivakumar. On Bose-fermi Equivalence in a U(1) Gauge Theory With Chern-Simons Action. *Mod. Phys. Lett.*, A5:593, 1990.

[104] Yigal Shamir. Chiral fermions from lattice boundaries. *Nucl. Phys.*, B406:90–106, 1993.

[105] Adar Sharon. QCD_3 dualities and the F-theorem. *JHEP*, 08:078, 2018.

[106] Stefan Sint. On the Schrodinger functional in QCD. *Nucl. Phys.*, B421:135–158, 1994.

[107] Dam Thanh Son. Is the Composite Fermion a Dirac Particle? *Phys. Rev.*, X5(3):031027, 2015.

[108] Jun Ho Son, Jing-Yuan Chen, and S. Raghu. Duality Web on a 3D Euclidean Lattice and Manifestation of Hidden Symmetries. 2018.

[109] C. Vafa and Edward Witten. Restrictions on Symmetry Breaking in Vector-Like Gauge Theories. *Nucl. Phys. B*, 234:173–188, 1984.

[110] Cumrun Vafa and Edward Witten. Eigenvalue Inequalities for Fermions in Gauge Theories. *Commun. Math. Phys.*, 95:257, 1984.

[111] Chong Wang, Adam Nahum, Max A. Metlitski, Cenke Xu, and T. Senthil. Deconfined quantum critical points: symmetries and dualities. *Phys. Rev.*, X7(3):031051, 2017.

[112] Chong Wang and T. Senthil. Dual Dirac Liquid on the Surface of the Electron Topological Insulator. *Phys. Rev.*, X5(4):041031, 2015.

[113] Chong Wang and T Senthil. Dual dirac liquid on the surface of the electron topological insulator. *Physical Review X*, 5(4):041031, 2015.

[114] Chong Wang and T. Senthil. Half-filled Landau level, topological insulator surfaces, and three-dimensional quantum spin liquids. *Phys.Rev.*, B93(8):085110, 2016.

[115] Edward Witten. Large N Chiral Dynamics. *Annals Phys.*, 128:363, 1980.

[116] Edward Witten. Non-abelian bosonization in two dimensions. *Communications in Mathematical Physics*, 92(4):455–472, Dec 1984.

[117] Edward Witten. Quantum Field Theory and the Jones Polynomial. *Commun. Math. Phys.*, 121:351–399, 1989.

[118] Edward Witten. Anti-de Sitter space, thermal phase transition, and confinement in gauge theories. *Adv. Theor. Math. Phys.*, 2:505–532, 1998.

[119] Edward Witten. Baryons and branes in anti-de Sitter space. *JHEP*, 07:006, 1998.

[120] Edward Witten. Theta dependence in the large N limit of four-dimensional gauge theories. *Phys. Rev. Lett.*, 81:2862–2865, 1998.

[121] Edward Witten. Sl (2, z) action on three-dimensional conformal field theories with abelian symmetry. *arXiv preprint hep-th/0307041*, 2003.

[122] Edward Witten. Fermion Path Integrals And Topological Phases. *Rev. Mod. Phys.*, 88(3):035001, 2016.

[123] Edward Witten. Three Lectures On Topological Phases Of Matter. *Riv. Nuovo Cim.*, 39(7):313–370, 2016.

VITA

Andrew Baumgartner is a theoretical physicist from Bethel, Connecticut. He is currently either listening to loud music or taking a nap.